PREDICTING MICROALGAL SPECIFIC GROWTH RATES IN RESPONSE TO TEMPERATURE AND LIGHT: A MULTI-SPECIES APPROACH

Thesis submitted in accordance with the requirements of the University of Liverpool for the degree of Doctor in Philosophy

by

Jan E. Bissinger

September 2008

Predicting microalgal specific growth rates in response to temperature and light: a multi-species approach

Jan E. Bissinger

ABSTRACT

Temperature and light are key determinants of microalgal specific growth rates (μ) and hence also influence aquatic ecosystem dynamics. Despite this importance there is no clear consensus on the functions that should be used to model the effects of these environmental variables on within- and across-species microalgal growth rates. Therefore examining the biological basis and statistical fits of existing functions, and deriving new ones, comprise the main objective of this thesis. Using quantile regression, and information theory I have compared existing functions and derived new ones that describe microalgal maximum specific growth rates (μ_{max}) in response to temperature, photon-flux density (PFD), daylength, and PFD, and daylength combined. The main findings are outlined in (i) to (v), below. (i) A comparison of the μ_{max} temperature function derived here to the function of Eppley (1972), suggested that the Eppley curve intercept is too low and that models that incorporate the Eppley function may underestimate primary production by ~ 30%. (ii) My non-linear general model of microalgal growth in response to daylength will be useful in comparative studies to normalise growth rates to a standard daylength. Extrapolation, using an assumed linear relationship, from short daylengths to 24 h can lead to growth overestimates of as much as 65%. Thus, this thesis recommends accounting for the non-linearity of this relationship in calculations of primary production. (iii) The applicability of using the daily light-dose (DLD = PFD x daylength) to describe the specific growth rate response of the freshwater flagellate *Cryptomonas* sp. across a range of DLDs was examined experimentally, and revealed that the DLD concept may not always be reliable because the shape of the growth response to DLD depends on the ratio of PFD to daylength. (iv) I tested the universality of the metabolic theory of ecology (MTE) as applied to microalgal specific growth rates, both within- and across-species, and found that the temperature dependency (expressed as an activation energy, E_a) of microalgal specific growth rates (0.48 eV) is higher than the value predicted by the MTE for processes controlled by photosynthesis in C3 plants. This study also found no significant difference between the thermal sensitivity of the microalgal acclimatory growth rate response and the evolutionary response. This result differs from that predicted by an evolutionary trade-off hypothesis. In addition the allometric exponent was significantly and substantially different from the value of -0.25 predicted by the MTE and suggests that microalgal specific growth rates may not conform to the quarter-power size-scaling relationship predicted by the MTE. (v) The most appropriate temperature function to model microalgal specific growth rates was addressed within- and across-species, and over regions of the response that both included and excluded temperature extremes. When temperature extremes were excluded the within-species relationship was best described by the linear function whereas the across-species μ_{max} relationship was best described by the Arrhenius (1889) model, suggesting little justification for the continued use of exponential functions, such as the widely used Q_{10} relationship. Over the full thermal range the within-species relationship was well described by a Gaussian function whereas the Sharpe-Schoolfield function was the most appropriate model of the across-species μ_{max} relationship.

CONTENTS

APPENDIX 1: Taxa and data sources used in the Liverpool phytoplankton database.

APPENDIX 2: Taxa, specific growth rate, daylength, and data sources used in the analysis of the general microalgal growth response to daylength.

APPENDIX 3: Taxa, daylength, photon flux density (PFD), and sources of data used in the meta-analysis of microalgal μ_{max} as a function of PFD and daylength.

APPENDIX 4: Taxa and data sources used in analyses of the temperature dependency of microalgal μ_{max}.

APPENDIX 5: Taxa and data sources used in the microalgal growth rate thermal response analyses.

APPENDIX 6A: Bissinger, J. E., D. J. S. Montagnes, J. Sharples, and D. Atkinson. 2008. Predicting marine phytoplankton maximum growth rates from temperature: Improving on the Eppley curve using quantile regression. Limnol. Oceanogr. **53:** 487-493.

APPENDIX 6B: Montagnes, D. J. S., G. Morgan, J. E. Bissinger, D. Atkinson, and T. Weisse. 2008. Short-term temperature change may impact freshwater carbon flux: a microbial perspective. Global Change Biol. **14:** 1-16.

FIGURES

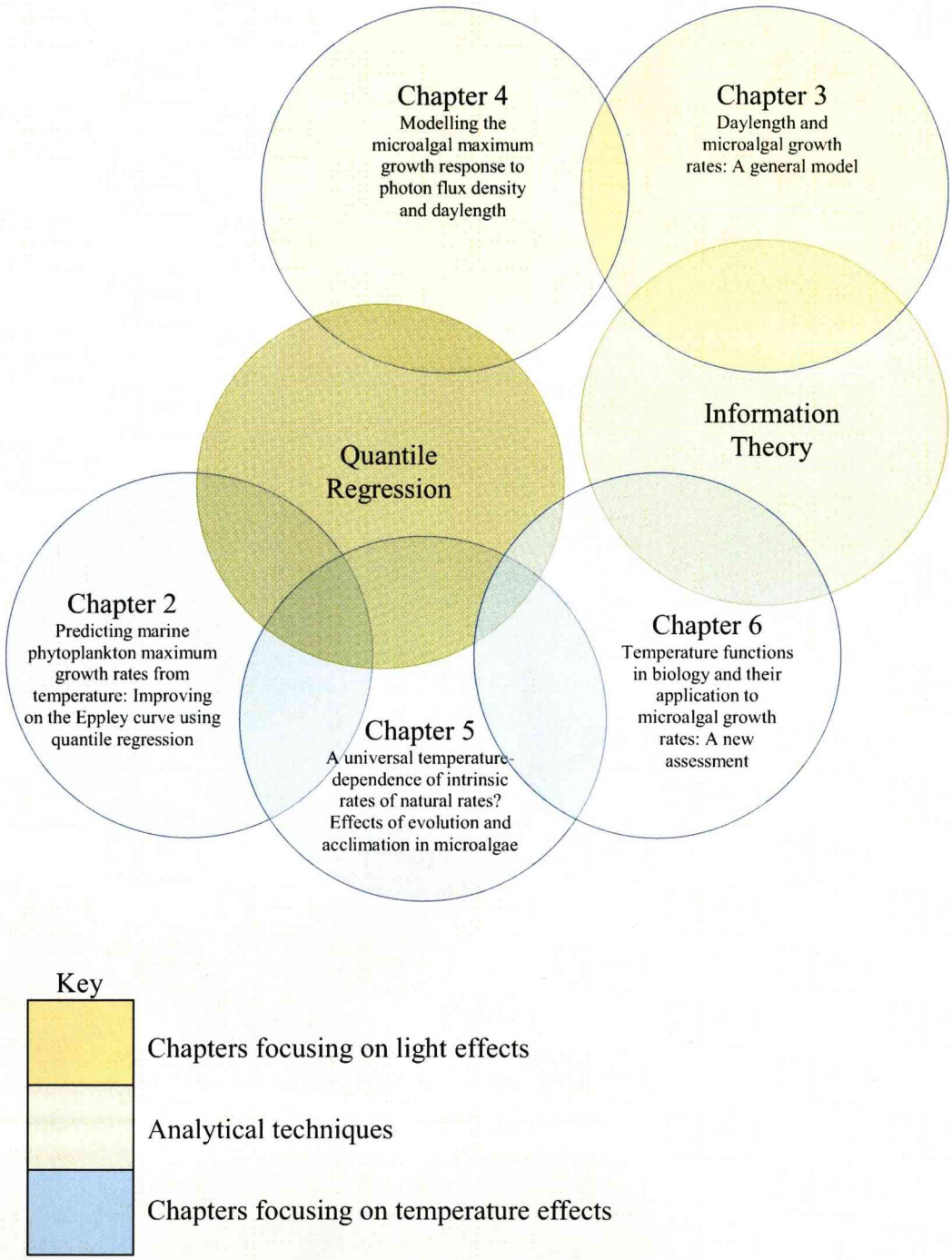

Fig. 1 Venn diagram illustrating thesis structure

PREFACE

I started this endeavour with the aim of making a contribution to the existing scientific understanding of the effects of climate change on biological processes. I had originally, rather loftily, hoped that after four years hard work that this thesis might represent some sort of final word on this subject as applied to microalgae. Now, of course, I realise that research is an iterative process but maybe for me I can at least say that "This is not the end. It is not even the beginning of the end. But it is, perhaps, the end of the beginning" (Churchill 1942).

The structure of this thesis follows the recommendations of Stanistreet (1996) as "a sequential series of linked chapters, bracketed by a general introduction and a general conclusion". Each chapter was conceived as a paper that follows the style of *Limnology and Oceanography*, a sensible target journal for the subject matter of this thesis. One advantage of this approach is that "it facilitates the preparation of sections of the work for publication" (Stanistreet 1996) so providing training in some of the key academic skills needed by a scientific researcher. In direct support of this argument two published papers have arisen from this thesis: one directly derived from chapter 2 (Bissinger et al. 2008), and another (Montagnes et al. in press) indirectly related to this thesis (see Appendix 6). Furthermore, it is my intention to publish all the remaining chapters as papers. If there is any disadvantage with this approach it is that as each chapter was designed to 'stand alone' there may be some repetition in the methods sections of the chapters when this thesis is read in its entirety.

ACKNOWLEDGEMENTS

I would like to acknowledge the help and encouragement of a number of people over the last four years.

Firstly, a big thank you to my two supervisors David Atkinson and David Montagnes. Throughout my PhD the Davids have provided excellent guidance, and their thoughtful suggestions and feedback have been constant and tireless.

I would also like to thank Chris Lowe, who patiently guided me through the early days of algal culturing and offered support and encouragement when things seemed insurmountable. Big Dave also deserves a special mention as his broad shoulders have also given me support on a number of occasions.

The PhD experience can be lonesome at times but I have been lucky enough to be surrounded by a great group of people over here at Liverpool. It's been fun sharing time with a wide variety of people all linked by the fact that we are inquisitive about some aspect of biology. People that I would like to thank for fun times in the office, and over coffee include: Andy, Wol, Sarah, Costas, Suzanne, Steph, Hannah, Chris, Becky, Becci, Tara, Sandra, Marcus, Tom, Tim, Sam, Andy, Nicky, Naomi, Laura. I'm sure there's many more, so apologies if you're not mentioned here.

A special big thanks goes to Kath and Amy who have kept me sane and provided lots of laughs and cakes over the last four years.

Finally, but most importantly, I couldn't have done any of this without the support, love, and patience of Sue. Thanks for putting up with me and microalgae for the last four years, you've been a star.

CHAPTER 1

General Introduction

The importance of microalgae in aquatic ecosystems

Aquatic unicellular autotrophs or microalgae are thought to account for ~ 45% of global photosynthesis (Falkowski and Raven 2007) so play a key ecological role in aquatic ecosystems. Microalgae include both planktonic and benthic species and in the pelagic realm the phytoplankton are the dominant primary producers, being responsible for fixing between 30 and 50×10^9 tonnes C yr^{-1} (Falkowski 1994). Although the distribution and productivity of benthic microalgae is limited by the depth of the euphotic zone, they are the dominant primary producers in streams, shallow lakes, wetlands, and estuaries (Stevenson 1996). Therefore, as microalgae are such an important component aquatic primary production, the challenges imposed by global climate change (IPCC 2007) mean that there is an imperative to better understand how environmental variables, such as temperature and light, affect these primary producers. Intrinsic rates of natural increase (commonly expressed as specific growth rates, μ, in planktonic ecology) are a major determinant of primary production and a quantification of how μ varies within and across multi-species assemblages is the main focus of this thesis.

A multi-species approach to investigate microalgal specific growth rates

Multi-species analyses facilitate an understanding of how broad-scale environmental variation (e.g., a temperature gradient) can influence physiological traits

in ways that have previously gone unrecognised in small-scale investigations (Chown et al. 2004). For example, differences in metabolic cold adaptation between teleost fish (Clarke and Johnston 1999) and terrestrial insects (Addo-Bediako et al. 2002) suggest evolutionary, and ecological, differences in thermal adaptation between aquatic, and terrestrial environments. Thus, by using interspecific variation in physiological traits, macrophysiological (Chown et al. 2004) approaches facilitate a better understanding of the reasons for variation in physiological characteristics, how they have evolved, and their subsequent ecological implications (Chown et al. 2004). However, in addition to examining broad trends, this study also examines within-species microalgal growth rate responses to daylength (Chapter 3), and temperature (Chapters 5, and 6) over a wide range of species.

When using iterative curve fitting methods, as in this study, the evaluation of a model's goodness of fit is enhanced by maximising the number of independent variable measurements rather than increasing the number of replicates (Johnson 1992; Montagnes and Berges 2004). However, few previous studies have assessed microalgal growth rates over wide ranges of temperatures and light levels. Consequently, in addition to analysing data compiled from the literature, this study also adopts an experimental approach (e.g., Chapters 3, 4, and 6) when the collection of high quality growth rate data, over wide ranges of light levels and temperatures, facilitates model parameterisation.

Strategies for analysing multi-species data

One concern when modelling multi-species responses (e.g., specific growth rates) to a single limiting factor, such as temperature, is that the relationship will be confounded by unmeasured variables in the data. For example, size (Savage et al. 2004a), taxonomic affiliation (Banse 1982), and light (e.g., López-Urrutia et al. 2006) may also explain much of the variation in microalgal specific growth rates. When further information is available regarding these other possible limiting factors, and there is a known mathematical relationship between the factor and the response variable, the effects of these other factors can be controlled either by normalising the data or accounting for the relationship in the statistical analysis (López-Urrutia et al. 2006). This is the approach adopted in Chapter 5 of this thesis. However, as this approach requires further information regarding these other factors, which may not always be available, this may limit the sample size and thus possibly limit the statistical power of the analysis. Consequently, another way to quantify the effects of a factor on specific growth rate is to use all the available data and concentrate on the maximum response (μ_{max}) to the environmental factor i.e., the upper envelope of a scatter graph (Scharf et al. 1998). Below this ceiling other unmeasured factors may be the active limiting constraint so the upper edge of the distribution, rather than the centre, gives the best estimate of the effect of the limiting factor in question on the response variable (Kaiser et al. 1994; Cade et al. 1999). This approach is used to derive functions describing microalgal μ_{max} in response to temperature (Chapters 2, 5, and 6), and both daylength, and photon flux density (PFD) (Chapter 4).

Quantile regression

Quantile regression (Koenker and Bassett 1978) is a statistical technique that can objectively determine a relationship at the upper edge of a scatter graph (Cade et al. 1999). The τ^{th} quantile represents the situation where τ proportion of the observations are below and 1- τ proportion of the observations are above the linear estimate, for example the 99th quantile describes a line below which are found 99% of the observations. Quantile regression is based on minimising the sum of the weighted absolute residuals, which is achieved by the inclusion of a check function that gives differing weights to positive and negative residuals. The minimisation problem can then be solved using linear programming methods. In addition to estimating maximum, or minimum, responses quantile regression has many other advantages compared to ordinary least squares (OLS) regression. For example, it is more robust to outliers than OLS regression, makes no assumptions about the error distribution in the model and retains its statistical properties under any linear or non-linear monotonic transformation (Cade and Noon 2003). Consequently, this method has the added benefit that it is possible to use a non-linear transformation (e.g., logarithmic) to estimate the regression quantiles and then back-transform the estimates without loss of information (Cade and Noon 2003). Furthermore, estimation of the edge of a scatter graph using quantile regression is not burdened by arbitrary decisions about data partitioning and the numbers or width of size classes (Scharf et al. 1998), as is the case when binning approaches are used (e.g., Blackburn et al. 1992; Rose and Caron 2007). In this thesis quantile regression is used to derive μ_{max} functions in Chapters 2, 4, 5, and 6.

Model selection procedures

Throughout this study an information-theoretic approach (Burnham and Anderson 2002) is used to facilitate the selection of the most appropriate model of the microalgal growth rate response to temperature or light. This approach is adopted as it explicitly accounts for the tendency of models with more parameters to over-fit the data (Angilletta 2006) and, furthermore, a comparison of the Akaike weights (Burnham and Anderson 2002) associated with each model allows the relative strength of evidence for each to be assessed. In this procedure models are iteratively fit (SigmaPlot v.10, SPSS Inc., Chicago, USA) to the data then, following Burnham and Anderson (2002), the residual sum of squares (*RSS*) from each fit is used to determine the maximised log-likelihood value $\left(\log L\left(\hat{\theta}|y\right)\right)$ of the parameters (Eq. 1.1). This is then applied to calculate the Akaike information criterion (AIC) (Eq. 1.2) for each model:

$$\log L\left(\hat{\theta}|y\right) = \log\left(\frac{RSS}{N}\right)\frac{-N}{2} \tag{1.1}$$

$$\text{AIC} = -2\log L\left(\hat{\theta}|y\right)+2P \tag{1.2}$$

where $\left(\hat{\theta}|y\right)$ represents the parameters $\hat{\theta}$ given the data y, N is the sample size and P is the number of parameters (including the error term). In this thesis the corrected AIC (AIC_C) (Eq. 1.3) is used in favour of the AIC when the sample size is small compared to the number of estimated parameters (Burnham and Anderson 2002).

$$\text{AIC}_\text{C} = -2\log L\left(\hat{\theta}|y\right)+2P+\frac{2P\left(P+1\right)}{N-P-1} \tag{1.3}$$

As the AIC_c estimates the information lost when using a particular model to describe the data (Burnham and Anderson 2002), the most likely model is that with the lowest AIC_c.

The Akaike weights (Eq. 1.5) can then be calculated from the likelihood of each model (Eq. 1.4), as a proportion of the total likelihoods of all the candidate models.

$$L\left(g_i|x\right) \propto \mathrm{e}^{\left(-\frac{1}{2}\Delta_i\right)} \tag{1.4}$$

$$w_i = \frac{\mathrm{e}^{\left(-\frac{1}{2}\Delta_i\right)}}{\sum_{r=1}^{R} \mathrm{e}^{\left(-\frac{1}{2}\Delta_r\right)}} \tag{1.5}$$

where $L\left(g_i|x\right)$ is the likelihood of the model g_i, given the data x; Δ_i is the difference between a given model's AIC_C and that of the lowest AIC_C; and R is the set of candidate models. In this thesis information theory is used in Chapters 3, and 6.

The influence of temperature on microalgal specific growth rates

Temperatures vary spatially and temporally in the aquatic environment and may impact microalgal growth chemically by changes in enzyme kinetics (Johnson et al. 1974) or physically through changes in water viscosity (Bělehrádek 1935) or the solubilities of CO_2 and O_2 (Brown et al. 1995). Temperature is a key determinant of microalgal physiological processes (Raven and Geider 1988), with most biological processes increasing between temperature extremes (Cossins and Bowler 1987). As climate change is predicted to increase global temperatures by 0.3 - 6.4°C over the next century (IPCC 2007), there is a need to better understand how these rising temperatures will impact future aquatic primary productivity. Whilst general multi-species relationships between temperature and metabolism have long been observed (Krogh 1914), and advances have been made in understanding the ecological patterns and evolutionary forces driving temperature adaptation in multi-species assemblages of

teleost fish (Clarke et al. 2004), the effect of temperature on growth rates of microalgae across species has not progressed greatly since the analysis of Eppley (1972). The Eppley curve describes an exponential function that defines the maximum attainable daily growth rate of marine phytoplankton as a function of temperature. As there are concerns that the intercept of the Eppley curve is too low (Brush et al. 2002), and may not be accurate because it was originally fitted by eye, Eppley's data is re-analysed and a new function derived in Chapter 2. As the aim of Chapter 2 is to adopt the same approach as used by Eppley (1972) an exponential function is applied. However, the suitability of the exponential function (and other functions) to describe microalgal growth rates in response to temperature is addressed in Chapter 6.

The metabolic theory of ecology

The metabolic theory of ecology (Gillooly et al. 2001; Brown et al. 2004) states that much of the variation among organisms, including life history traits and ecological roles, is constrained by body sizes, operating temperatures, and chemical compositions. Moreover, the joint effects of body size, M, and temperature T (K) on individual metabolic rate have been combined into one function that is capable of describing the metabolism of all organisms (Gillooly et al. 2001; Brown et al. 2004):

$$B = i_0 M^{3/4} e^{-Ea/kT} \quad (1.6)$$

where B represents metabolic rate, E_a is the activation energy, k is Boltzmann's constant (8.62×10^{-5} eV K^{-1}), and i_0 is a normalisation constant independent of body size and temperature. It is argued that the quarter-power scaling exponent adopted in this model

is based on the fractal geometric design of the surfaces of internal transport networks Savage et al. (2004b). Whereas, the adoption of the Arrhenius (1889) term (Eq. 1.7)

$$e^{-Ea/kT} \tag{1.7}$$

in Eq.1.6 is based on the assumption that metabolic rates increase exponentially with temperature. Chapter 5 compares the thermal sensitivity (expressed as an activation energy) of microalgal specific growth rates with that predicted by the MTE (Allen et al. 2005) and investigates whether there are differences in thermal sensitivity between microalgal acclimatory (within-species), and evolutionary (across-species) growth responses. Then the suitability of the Arrhenius function to describe the thermal sensitivity of microalgal specific growth rates is assessed in Chapter 6.

The influence of light on microalgal specific growth rates

Light is a key variable influencing aquatic primary production, with the availability of light varying across a range of spatial and temporal scales (Falkowski and Raven 2007). Microalgal photosynthesis depends both on daylength and photon flux density (PFD, μmol photons m^{-2} s^{-1}). Daylength varies seasonally and these variations are most noticeable at high latitudes where there can be 24 h of daylight in the summer months. In contrast, PFD varies both diurnally, and throughout the day because of changes in cloud cover. With a clear sky the maximum PFD at the surface of a water body can reach ~ 2000 μmol photons m^{-2} s^{-1}, although this varies with the angle of the sun (Lalli and Parsons 2002). In addition to these effects, both the quality, and intensity

of light is affected by its passage through the water column (Kirk 1994). There being an exponential decrease in light intensity with depth, with different wavelengths of the visible spectrum penetrating to different depths, until eventually the compensation depth is reached when photosynthetic production is balanced by respiratory losses (Kirk 1994).

Chapter 3 derives a non-linear general model of microalgal growth in response to daylength and illustrates that assuming a linear one-to-one relationship (i.e., growth at 24 h being double that at 12 h) when extrapolating from growth at one daylength to another (e.g., Brush et al. 2002; Kiørboe 1997; Landry et al. 2000) can lead to large over- and underestimates. Chapter 4 initially assesses the applicability of combining PFD and daylength measurements into one daily light-dose (DLD, mol photons m^{-2} d^{-1}), and then derives functions of μ_{max} in response to PFD, daylength, and PFD and daylength combined.

CHAPTER 2

Predicting marine phytoplankton maximum growth rates from temperature: Improving on the Eppley curve using quantile regression

Introduction

Models of aquatic primary production are useful tools to predict global biogeochemical fluxes and better inform those involved in aquatic resource management. Marine phytoplankton are a key component of many of these models both because of their carbon assimilation (Behrenfeld et al. 2001) and because of their effect on other ecosystem components (Ryther 1969). Because the utility of such models hinges on the quality of the parameters, we need to be confident in their reliability. Thus, in this study a statistical technique is applied to assess the reliability of a parameter, relating phytoplankton maximum growth rates to temperature, which is a key component of numerous aquatic production models (e.g., Tett et al. 1985). Furthermore, the difference between this relationship and the growth-rate response of heterotrophic protists to temperature has been implicated in the formation of algal blooms in high-latitude ecosystems (Rose and Caron 2007). Thus, the consequences of correctly interpreting the data are considerable.

In dynamic ecosystem production models a temperature function is often used to set the upper limit of phytoplankton growth rates. From this theoretical maximum, growth rates are then reduced by applying coefficients relating to environmental limiting factors such as day-length, photon flux density, and nutrients (Bowie et al. 1985). One temperature function commonly used is that developed by Eppley (1972):

$$\mu_{max} = 0.59e^{0.0633T} \quad (2.1)$$

This exponential relationship defines the maximum attainable daily growth rate (μ_{max}, d^{-1}) of phytoplankton as a function of temperature (T, °C) and has the advantage over more complex functions of being able to generate predictions in the absence of other data, such as community composition or phytoplankton size. The relationship was formulated from a compilation of data from laboratory culture studies in which light and nutrients were considered replete. Eppley (1972) indicated that the data fell within an upper envelope and drew a line by eye that defined the maximum expected growth at any given temperature between 0 and 40°C (Fig. 2.1).

The citation history (> 800) of Eppley (1972) suggests that its strong influence is as pronounced today as it was over 30 years ago (Fig. 2.2). In a sample of 450 papers that cite Eppley (1972), 103 incorporate some aspect of the Eppley formulation in a model i.e., either the function itself (e.g., Cugier et al. 2005) or the Q_{10} of 1.88 derived from the Eppley function (e.g. Tett et al. 1985). Another 85 studies compare their results to the theoretical maximum expected from the curve (e.g., Durbin 1974; Admiraal 1977); of these, 62 had results similar to or below the curve, and 15 had results that exceeded the theoretical maximum (e.g., Brush et al. 2002). In addition, some studies suggest that an exponential function is not the most appropriate model of the relationship across a wide range of temperatures (Moisan et al. 2002). Recognition of these discrepancies throws doubt on the applicability of the Eppley function and thus also on predictions of aquatic primary production.

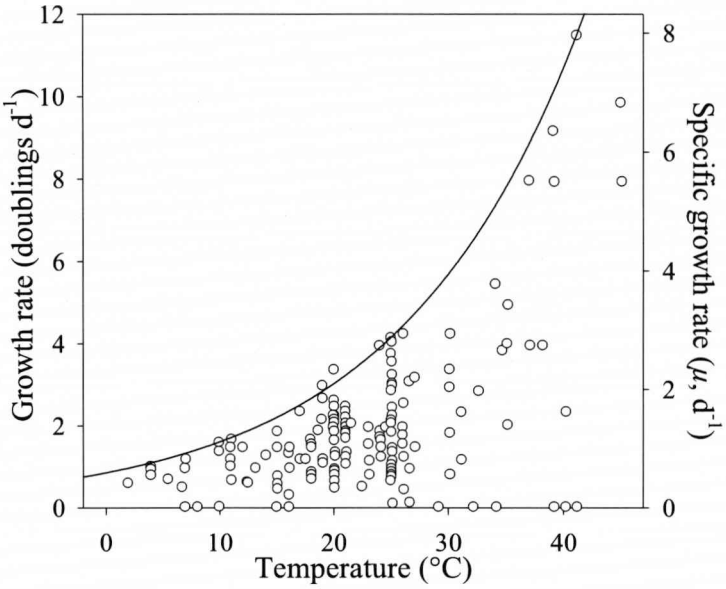

Fig. 2.1 'Variation in the specific growth rate μ of photoautotrophic unicellular algae with temperature'. Redrawn from Fig. 1 of Eppley (1972).

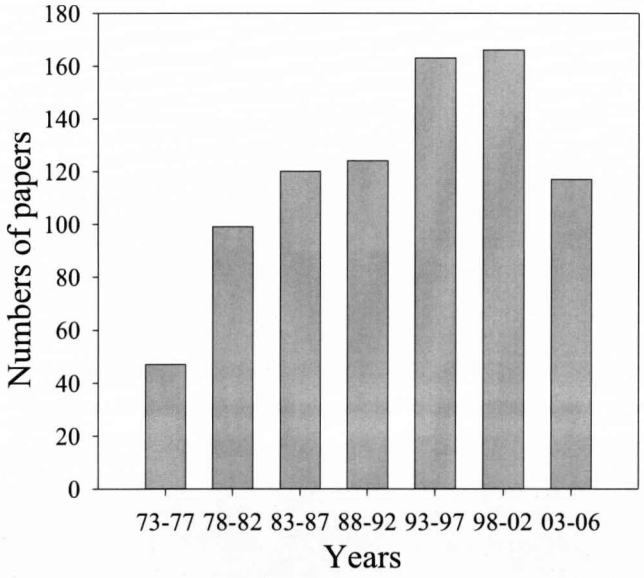

Fig. 2.2 Citation history (http://wok.mimas.ac.uk/) of 'Temperature and phytoplankton growth in the sea' (Eppley 1972). Total number of citations = 835.

Here this study focuses on the exponential portion of the response, as Eppley (1972) did, and explores the outcome of a statistical approach that objectively defines the upper edge of a scatter graph, providing a quantitative measure of the reliability of the estimate obtained. Problems with fitting a line of maximum growth by eye include the subjectivity of the method, especially the risk that the relationship may be disproportionately affected by outliers, and the impossibility of quantitatively measuring the precision of the model parameter estimates. In the Eppley (1972) function an estimate of μ_{max} was inferred from a small sample (n = 162) without any measure of the confidence in that estimate. Furthermore, since Eppley (1972) produced his curve, numerous growth-rate studies have been published with data suitable for incorporation into a new analysis. Therefore, if we plan to use Eppley-like functions in modern aquatic ecosystem models a quantitative assessment of the reliability of this relationship is needed.

Quantile regression (Koenker and Bassett 1978) can be used to infer relationships from the edges of scatter graphs (e.g., the upper edge of the Eppley (1972) data set, Fig. 2.1); for example the 99th quantile describes a line below which are found 99% of the observations. This approach has already been applied to other problems in the aquatic sciences (e.g., the study of maximum bathymetric body size gradients in gastropods carried out by McClain and Rex 2001; and the investigation of opportunistic predation in tuna by Menard et al. 2006). Briefly, quantile regression is based on least absolute deviations (LAD) regression, which uses the median rather than the mean, and therefore is less sensitive to extreme outlying values than ordinary least squares (OLS) regression. The quantile of interest (τ) is estimated using an optimisation function that

minimises the sum of weighted absolute deviations (Koenker and Bassett 1978; Koenker and d'Orey 1987) and the solution to the minimisation problem is achieved using an algorithm such as the simplex method (Cade and Noon 2003). Typically, like most modern statistics, these algorithms are available in computer packages e.g., *R* v. 2.4.1. (http://www.r-project.org).

Regression quantiles, unlike OLS regression, make no assumptions about the error distribution in the model and retain their statistical properties under any linear or non-linear monotonic transformation (Cade and Noon 2003). Consequently, this method has the added benefit that it is possible to use a non-linear transformation (e.g., logarithmic) to estimate the regression quantiles and then back-transform the estimates without loss of information (Cade and Noon 2003). Furthermore, estimation of the edges of scatter graphs using quantile regression is not burdened by arbitrary decisions about data partitioning and the numbers of size classes (Scharf et al. 1998), as is the case when binning approaches are used (e.g., Blackburn et al. 1992; Rose and Caron 2007). As calculation of the standard error for the quantile of interest is dependent on variance in the sample distribution around this quantile (Cade et al. 1999), it is not possible to calculate an upper CI for a 100% quantile ($\tau = 1.0$). Therefore, the most reliable estimate of the edge of the data is that defined by the highest (i.e., nearest to 100%) quantile regression line with confidence intervals that do not include zero (Cade et al. 1999). Thus, in this type of analysis there is often a trade-off between the maximum regression quantile (τ) that can be estimated and the confidence in that estimate.

In this study five issues are addressed: i) the data compiled by Eppley (1972) is re-analysed using quantile regression and the statistics associated with the 99th quantile

examined; ii) following the approach of Eppley (1972), all suitable available data are used to compile a large (n = 1501), database (Liverpool phytoplankton database, LPD) and quantile regression is then used to establish a new predictive equation; iii) as diatoms tend to exhibit high specific growth rates (Furnas 1990) the new, comprehensive database is examined to determine whether it produces a biased response, due to a larger proportion of diatoms; iv) the Q_{10} of the observed responses are calculated and compared, as Q_{10} is used regularly to predict primary production (e.g., Tett et al. 1985; Doney et al. 1996); and finally v) the quantile regression parameter estimates are analysed to determine whether they are influenced by growth rate data at high temperatures, as there are indications that the growth rate response should deviate from an exponential response at higher temperatures (Behrenfeld and Falkowski 1997).

Methods

Quantile regression

Here quantile regression is used to estimate the maximum growth rates of phytoplankton at different temperatures together with a quantitative measure of the confidence in that estimate. As linear quantile regression provides estimates of standard errors and confidence intervals (CI), the data were linearised by logarithmic transformation. However, log-transformation of the data to accommodate zero and negative growth values (e.g., log y +1) prevented direct comparison with the Eppley equation, so these few data (< 1 % of the LPD and ~ 5% of the Eppley data set) were not included. Quantiles and associated statistics were calculated using the 'quantreg' (Koenker 2006) package in the statistical language *R* v. 2.4.1. (http://www.r-project.org).

When estimating extreme quantiles with confidence, a large sample size is required to provide a reasonable density of observations near the edge of the data (Cade et al. 1999). To ensure reliable estimates, Rogers (1992) suggests that $n > 5/(1-q)$ (where n is the sample size, and q is the quantile of interest), so to estimate the 99th quantile $n > 500$. In this study the most reliable estimate of the edge of each data set is defined as the quantile that is the highest possible, complies with the sample size-quantile recommendation of Rogers (1992), and has a slope with 95% CI that exclude zero. In the following analyses data sets are identified with subscripts where: $_{(E)}$ signifies the Eppley data, $_{(LPD)}$ signifies the Liverpool phytoplankton database, and $_{(43\%\,D)}$ signifies the subset of the LPD data where diatoms constitute 43% of the total (the same proportion as in the Eppley (1972) data set).

Re-analysing Eppley's data

Eppley (1972) compiled phytoplankton growth-rate data from both primary and secondary sources and only included data from cultures that were grown in nutrient-replete conditions under continuous illumination, or at optimum daylength where a continuous photoperiod was detrimental to growth. Data points (n = 153 after zero values were removed) from Fig. 1 of Eppley (1972) were digitised using Grab It! (Raleigh, NC) data capture software and converted (i.e., multiplied by $ln2$) from doublings d^{-1} to specific growth rates (μ, d^{-1}). The 99$^{th}{}_{(E)}$ quantile was calculated as described above and visually compared to the Eppley curve (see Fig. 2.3A), as the sample size was too small for further analysis.

Analysing the Liverpool phytoplankton database

The Liverpool phytoplankton database (LPD, $n = 1501$ growth rates of marine taxa) only includes laboratory studies from the primary literature, i.e., field-based observations and compilations of growth-rate studies were not included. Data presented graphically were digitised using Grab It!, and growth rates expressed as doublings or divisions per day were converted to specific growth rates. Data from species that were originally isolated from the benthos were not included, and where experiments varied salinity, only those growth rates with salinities ≥ 30 were included. Thus, the LPD comprises studies that measured growth rates: at only one temperature and those that collected growth rates over a number of different temperatures; in batch, continuous, and chemostat experiments; and for various daylength and photon flux density combinations. Consequently, the LPD includes data where conditions were not always replete and maximum growth rates were not always achieved. The LPD has been compiled from 51 publications, is ~ 10 times larger than Eppley's data set, and is composed of 92 species or strains from 62 genera (Appendix 1).

The influence of the percentage of diatoms in the data

As regression quantiles are based on the percentage of data above or below the specified quantile, and the fast growth rates of diatoms (Furnas 1990) may mean that there is a greater percentage close to the upper envelope, it was important to investigate whether the larger proportion of diatoms in the LPD (68% compared to ~ 43% in the Eppley data set) biased this analysis. This was achieved by randomly sub-sampling ($n = 828$) the LPD to create 30 sub sets in each of which diatoms constituted 43% of the total.

For each sub set the $99^{th}_{(43\% D)}$ quantile with ±95% CI was calculated, and the mean of these was then compared to the Eppley curve and $99^{th}_{(LPD)}$ quantile. To determine if differences existed between the slopes and intercepts of the log-transformed Eppley curve, $99^{th}_{(LPD)}$, and $99^{th}_{(43\% D)}$ quantiles (i.e., 3 comparisons) *t*-tests were applied. To be conservative, these tests were Bonferroni corrected (Sokal and Rohlf 1995) giving an α value of 0.01.

Calculating the Q_{10}

The Q_{10} of the LPD μ_{max}, and that derived from the subsets with 43% diatoms, was calculated using the Q_{10} model of Van't Hoff (1884). This procedure assumed an exponential response and that there was no inhibition of growth rate at high temperatures, following the approach of Eppley (1972).

The influence of growth rates at high temperatures

At higher temperatures (> 29°C, see Fig. 2.3B) data points were fewer and appeared to have maxima below the calculated 99^{th} quantile, so to alleviate any concerns that these high-temperature data may be unduly influencing the parameter estimates from the quantile regression analysis, a reduced data set was created that excluded growth-rate data at temperatures > 29°C. To determine if there were differences between the log-transformed regression parameters from the full and reduced data sets *t*-tests were applied.

Results

Analysis of Eppley's data

Qualitatively, the $99^{th}_{(E)}$ quantile appears similar to the Eppley curve (Fig. 2.3A). However, as only one positive residual point occurs above the $99^{th}_{(E)}$ quantile it was not possible to statistically analyse the differences between the $99^{th}_{(E)}$ quantile, and the Eppley curve. Thus, error estimates were not obtained for the Eppley curve using quantile regression.

Analysis of Liverpool phytoplankton database

As the ± 95% CI of the $99^{th}_{(LPD)}$ quantile slope estimate excluded zero and complied with the minimum size recommended by Rogers (1992) (Table 2.1), this quantile provided the most reliable estimate of the edge of the LPD data set. Back transformation of the parameters from the $99^{th}_{(LPD)}$ quantile yields:

$$\mu_{max} = 0.81e^{0.0631T} \tag{2.2}$$

A comparison of the log-transformed quantile parameters to those of the Eppley curve indicates that the intercept of the $99^{th}_{(LPD)}$ quantile is significantly greater than that of the Eppley curve ($t = 3.20$, df = 1499, $p < 0.01$). Furthermore, at temperatures below 19°C the Eppley curve falls below the lower 95% CI associated with the $99^{th}_{(LPD)}$ quantile (Fig. 2.3B). However, the slope of the $99^{th}_{(LPD)}$ quantile is not significantly different from that of the Eppley curve ($t = 0.53$, df = 1499, $p > 0.01$). The slope and intercept of the $99^{th}_{(43\%\,D)}$ quantile were not significantly different from those of the Eppley curve ($t = 1.05$, df = 826, $p > 0.01$, and $t = 2.08$, df = 826, $p > 0.01$, respectively),

or the $99^{th}_{(LPD)}$ quantile ($t = 0.97$, df = 2325, $p > 0.01$, and $t = 0.66$, df = 2325, $p > 0.01$, respectively).

The Q_{10} value of the $99^{th}_{(LPD)}$ quantile (1.88) was identical to that of the Eppley curve, whereas the Q_{10} value of the $99^{th}_{(43\%\,D)}$ quantile was 1.68. The log-transformed slope and intercept parameter estimates of the reduced ($\leq 29°C$) data set were not significantly different ($t = 0.24$, df = 2953, $p > 0.01$, and $t = 0.18$, df = 2953, $p > 0.01$, respectively) from those of the full data set.

Table 2.1. 99^{th} regression quantile slope parameter estimates and associated statistics for the Liverpool phytoplankton (LPD) data sets. The parameter values are calculated to a confidence level of $\alpha = 0.05$, and $n > 5/(1-q)$ represents the minimum recommended sample size at the specified quantile (Rogers 1992). Note that the 43%D slope estimate and ± 95% CI represent the mean value of 30 sub samples.

data	***n***	$n > 5/(1-q)$	**estimate**	**- 95% CI**	**+ 95% CI**
LPD	1501	500	0.0631	0.0535	0.0721
43%D	828	500	0.0518	0.0259	0.0668

Fig. 2. 3 Marine phytoplankton maximum growth rates (μ_{max}) as a function of temperature. (A) A comparison of the two methodologies used to estimate the upper edge of Eppley's data. The Eppley curve, which was drawn by eye, is compared to the $99^{th}_{(E)}$ regression quantile calculated from Eppley's digitised data (n = 153). (B) The $99^{th}_{(LPD)}$ quantile and associated ± 95% confidence intervals calculated from the Liverpool phytoplankton database (LPD) (n = 1501). The Eppley curve is shown for comparison. (C) Normalization of the LPD data to account for differences in the percentage of diatoms in the data. Lines show the $99^{th}_{(LPD)}$ and $99^{th}_{(43\%\ D)}$ (n = 828) quantiles, with the Eppley curve shown for comparison.

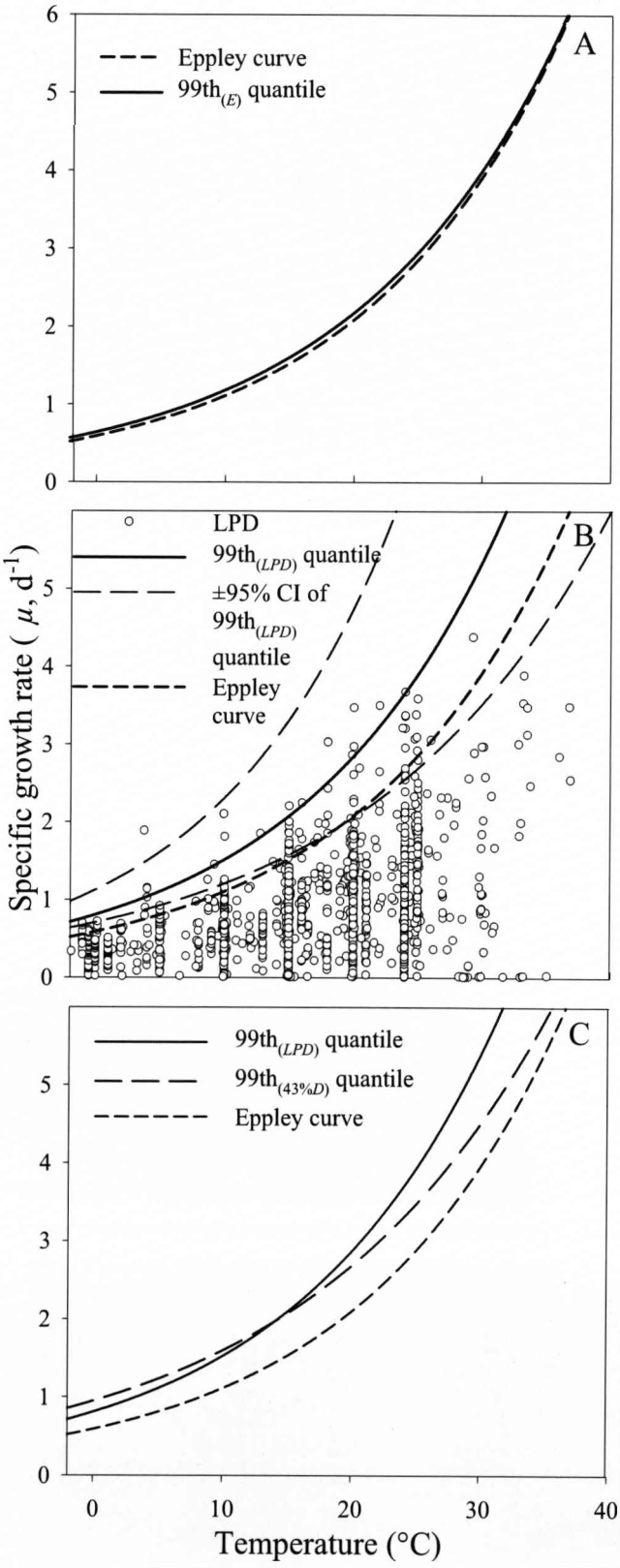
A
Eppley curve
99th(E) quantile
B
LPD
99th(LPD) quantile
±95% CI of 99th(LPD) quantile
Eppley curve
Specific growth rate (μ, d-1)
C
99th(LPD) quantile
99th(43%D) quantile
Eppley curve
Temperature (°C)

Discussion

Using quantile regression this study has recognised that the Eppley curve could be improved upon. To this end, a new exponential function for marine phytoplankton growth rates as a function of temperature has been derived, using the Liverpool phytoplankton database (LPD), and compared to that formulated by Eppley (1972). However, the data set compiled by Eppley (1972) did not fulfil the minimum size recommendations of Rogers (1992) for calculating the 99^{th} quantile with confidence. Calculating extreme quantiles with a small sample size may lead to a limited number of residuals, which renders methods for calculating standard errors unreliable (Koenker, R pers. comm.). Consequently, it was not possible to provide error estimates for the Eppley curve using quantile regression. Nevertheless, the visual fit of the $99^{th}_{(E)}$ quantile to the original Eppley (1972) curve (Fig. 2.3A) suggests that the Eppley curve is a good estimate of the edge of the data. Furthermore, there is no significant difference between the log-transformed slopes of the LPD and the Eppley curve, indicating equivalence in Q_{10} values (1.88) and suggesting that the Eppley curve has been an appropriate estimate of the thermal sensitivity of phytoplankton growth rates. This result should reassure those who have used the Q_{10} value of 1.88 in primary production models over the last 35 yr.

The significant difference between the intercept of the log-transformed $99^{th}_{(LPD)}$ and the Eppley curve supports studies (e.g., Brush et al. 2002) that suggest that the intercept of the Eppley curve is too low. However, in the new relationship (Eq. 2.2) the intercept value (0.81) is lower than the value (0.97) derived by Brush et al. (2002). This discrepancy may be due to the different methodologies adopted in defining the edge of

the upper envelope. In their analysis Brush et al. (2002) adopted the same slope value as Eppley (1972) and determined the upper edge of their data by eye. As this study has discussed earlier, in relation to Eppley (1972), there are possible problems with this approach, e.g., the subjectivity involved and the lack of quantitative measures of reliability.

Construction of the LPD sub set containing 43% diatoms, i.e., an equivalent proportion to that of Eppley (1972), allowed a further investigation of whether differences between the LPD envelope and the Eppley curve could be attributed to the greater percentage of diatoms in the LPD, as diatoms typically have disproportionately high growth rates (Furnas 1990). However, as there were no significant differences between the intercepts of the $99^{th}_{(43\%\ D)}$ quantile and the $99^{th}_{(LPD)}$ quantile, the dissimilarities between the Eppley curve and the $99^{th}_{(LPD)}$ quantile cannot be solely attributable to differing proportions of diatoms in the two data sets. Consequently, the LPD function (Eq. 2.2) is an appropriate model when a single theoretical maximum function is required, e.g., when the only data available are biomass, or Chl *a* and temperature.

A good example of where a single temperature function has been repeatedly employed is in pelagic ecosystem models (e.g., Antoine et al. 1996; Balch and Byrne 1994; Sharples et al. 2006). To assess the extent to which the LPD function may alter model results, the output of one temperate shelf-sea ecosystem model (Sharples et al. 2006) using the new function was compared to the output of one that incorporated the Eppley (1972) function. This simple analysis suggests that models that incorporate the Eppley function may underestimate primary production in cooler temperate waters by ~

30%. This underestimate applied to both the $99^{th}_{(LPD)}$ quantile and the $99^{th}_{(43\% D)}$ quantile, as at lower temperatures these two responses are similar (Fig. 2.3C). Consequently, assessments of the thermal influence of primary production on ecosystem services such as oxygen production, carbon sequestration, and biogeochemical cycling may also require revision.

The analysis of the influence of diatom percentage abundance on the upper envelope, and in particular the differences in slope parameter estimates between the $99^{th}_{(43\%D)}$ quantile and the $99^{th}_{(LPD)}$ quantile (Table 2.1), indicates how other variables may be incorporated into a more accurate model. Size (Savage et al. 2004a), and taxonomic affiliation (Banse 1982), for example, may explain much of the remaining variation in μ_{max} among phytoplankton. Building on the revised general growth rate-temperature relationship outlined here, Chapter 5 develops models that control for the effects of body size in a multi-species analysis of microalgal μ_{max}.

Finally, this study has concentrated on producing a relationship that is directly comparable to the Eppley curve. However, it is important to acknowledge that there are limitations with the applicability of this function in warm or oligotrophic oceanic areas, where the maximum growth rates of phytoplankton may always be limited by factors other than temperature. Furthermore, this analysis has highlighted two issues that need to be addressed in the future. First, while the analysis of the reduced data set (≤ 29°C) indicates that the use of the full data set to determine the upper envelope is valid, as the relationship is not exponential at very high temperatures, caution should be applied when using Eq. 2.2 at temperatures > 29°C. The μ_{max} response across the full thermal range is addressed in Chapter 5 of this thesis. Second, a Q_{10} of 1.88 is somewhat higher

than predicted by the metabolic theory of ecology (Brown et al. 2004; Allen et al. 2005) which gives a Q_{10} of between 1.62 (for 0 – 10°C) and 1.52 (for 20 – 30°C), derived from their predicted activation energy of 0.32 eV for rates controlled by photosynthesis (Allen et al. 2005). This discrepancy clearly merits further scrutiny and is addressed in Chapter 5.

In conclusion, whilst recognising the utility and robustness of the Eppley curve over the last 35 yr, the quantitative measures of reliability associated with the new LPD function (Eq. 2.2) should give users greater confidence in its value and suitability in situations where a single exponential growth rate relationship is sought.

CHAPTER 3

Daylength and microalgal growth: A general model

Introduction

Light is a key variable influencing aquatic primary production, with the availability of light varying across a range of spatial and temporal scales (Falkowski and Raven 2007). At mid and high latitudes daylength exerts a strong influence on the seasonal variation in microalgal specific growth rates (μ) (Kirk 1994), but despite the undoubted importance of this relationship in the aquatic sciences (e.g., Blackford et al. 2004; Kirk 1994; Parsons et al. 1977) there is no consensus on the general shape of the microalgal specific growth response to daylength.

Commonly microalgal specific growth rates increase with increasing daylength (Castenholz 1964; Foy and Gibson 1993; Paasche 1967), although continuous (24 h) light may be detrimental to some species (Brand and Guillard 1981; Sicko-Goad and Andresen 1991). There are also numerous reports of non-linearity in the responses of microalgal specific growth to daylength (Foy and Gibson 1993; Paasche 1967; Thompson 1999), and it has been suggested that a rectangular hyperbolic (Michaelis-Menten type) function may be the most appropriate model of this relationship (Gilstad and Sakshaug 1990; Tang and Vincent 2000).

Despite this reported lack of proportionality in the relationship between μ and daylength, several studies have assumed a linear one-to-one relationship (i.e., growth at 24 h being double that at 12 h) when extrapolating from growth at one daylength to another (e.g., Brush et al. 2002; Kiørboe 1997; Landry et al. 2000). These types of

extrapolations are often necessary when comparing growth rates between studies conducted at different daylengths. For example, the Eppley (1972) curve, which defines the maximum attainable daily growth rate of marine phytoplankton as a function of temperature, is often used as an upper benchmark against which observed microalgal growth rates are compared. As the growth rates used by Eppley (1972) to derive his model were collected in continuous light, observed specific growth rates are often corrected to 24 h to facilitate comparison of the data (e.g., Brush et al. 2002). At present, there is no suitable alternative model of the relationship between microalgal μ and daylength so studies generally assume a linear-one to-one relationship when making these corrections (e.g., Brush et al. 2002; Kiørboe 1997; Landry et al. 2000). Furthermore, other studies have incorporated a linear relationship between daylength and microalgal specific growth rates into primary production models (Geider et al. 1997; Gnanadesikan et al. 2002; Kameda and Ishizaka 2005). However, as will be shown in this Chapter, assuming a linear relationship may be an oversimplification of this relationship and could lead to over- or underestimates of microalgal specific growth rates. Consequently, to check for potentially large errors in estimates of μ, and to ensure that the most appropriate function is incorporated into models, the shape of this response clearly requires clarification.

When using nonlinear curve-fitting methods, as in this study, the ability to evaluate a model's goodness of fit is enhanced by maximising the number of independent variable measurements (e.g., daylength), rather than increasing the number of replicates at fewer daylengths (Johnson 1992; Montagnes and Berges 2004). However, few previous studies of the relationship between daylength and microalgal

specific growth assessed trends over a wide range of daylengths. Consequently, here an experimental approach is used initially to examine the specific growth rate response of a freshwater microalgal species (*Cryptomonas* sp.) to a wide range of daylengths. Then the generality of this response is assessed by combining the *Cryptomonas* sp. specific growth rate data with a multi-species data set of microalgal specific growth rate responses, compiled from the literature.

To assess the linearity of this response two rectangular hyperbolic (Michaelis-Menten type) models are compared with the linear model. Following the approach of others (Gilstad and Sakshaug 1990; Tang and Vincent 2000) a 2-parameter rectangular hyperbolic model (which assumes a zero abscissa intercept, Eq. 3.1) was used.

$$\mu = \frac{\mu_{max} D}{K_D + D} \tag{3.1}$$

where μ_{max} represents the maximum specific growth rate (d^{-1}), D the daylength, and K_D a constant. This 2-parameter model is then compared with a modified 3-parameter rectangular hyperbolic model (Eq. 3.2) which, by allowing for a non-zero abscissa intercept facilitates estimation of the threshold daylength (i.e., daylength when $\mu = 0$), and has been used to model the numerical response in microzooplankton (Montagnes 1996).

$$\mu = \frac{\mu_{max}(D\text{-}a)}{K_D + (D\text{-}a)} \tag{3.2}$$

where a is the abscissa intercept. Undoubtedly there are other possible models of this relationship, but a comparison of these three parsimonious models allows an assessment to be made of both the suitability of the linear model, and the importance of including a threshold term in a model of this relationship.

To compare these models an information-theoretic approach (Burnham and Anderson 2002) is adopted. This approach is appropriate as it explicitly accounts for the tendency of models with more parameters to over-fit the data (Angilletta 2006) and, furthermore, a comparison of the Akaike weights (Burnham and Anderson 2002) associated with each model allows the relative strength of evidence for each to be assessed.

This study will show, that for both *Cryptomonas* sp. and the multi-species assemblage of responses, the modified 3-parameter hyperbolic model describes the specific growth response to daylength better than both the linear model and the 2-parameter hyperbolic model. Therefore, the modified 3-parameter hyperbolic model is subsequently used to derive a general equation describing the microalgal growth response to daylength.

Thus the aims of this study are to: use an information-theoretic approach to identify the most-likely model to describe the specific growth vs. daylength response in *Cryptomonas* sp. across a wide range of daylengths; incorporate the *Cryptomonas* sp. response data into a large multi-species data set of microalgal specific growth rate responses and use information theory to identify the most-likely model of this relationship; use this most-likely model to derive a general equation of the relationship between microalgal μ and daylength.

Methods

Specific growth response of Cryptomonas sp. to daylength

The freshwater flagellate *Cryptomonas* sp. (strain 26.8, Culture Collection of Microalgae in Göttingen, Germany) was maintained in modified Woods Hole medium (MWC, Guillard and Lorenzen 1972) at 16°C ± 1°C, in continuous light, at ~ 70 μmol photons m^{-2} s^{-1}. To explore the shape of the relationship between *Cryptomonas* sp. specific growth rate (μ, d^{-1}) and daylength (h), 15 cultures were maintained at daylengths ranging from 0 to 24 h at a constant photon flux density (PFD) of 70 μmol photons m^{-2} s^{-1}. After acclimation (3-4 d) samples were counted daily, at the same time each day, and μ was determined over the exponential growth phase from the slope of the relationship between *ln* abundance vs. time.

Model selection

As one of the aims of this study was to test the linearity of the response, and inclusion of negative growth (i.e., net mortality) at low daylengths skewed the data towards a non-linear response, a conservative approach was adopted and only positive growth rates (n = 12) were modelled. The non-linear models (Eqs. 3.1, and 3.2), and the linear model, were iteratively fit (SigmaPlot v.10, SPSS Inc., Chicago, USA) to the *Cryptomonas* sp. specific growth vs. daylength data, and parameters determined. To determine the most-likely model using an information-theoretic approach it was necessary to calculate the corrected Akaike information criterion (AIC_C, AIC corrected for small sample size) (Burnham and Anderson, 2002) of each model. These were determined by using the residual sum of squares (*RSS*) associated with each model to

compute the maximised log-likelihood (Angilletta 2006). Using this approach the most-likely model is that with the lowest AIC_C and the largest Akaike weight (Burnham and Anderson, 2002).

The generality of a non-linear specific growth response to daylength

Experimentally derived microalgal specific growth rate daylength responses (54 responses, 239 data points, Appendix 2) were collected from the literature. Data were included where: growth was not negative (i.e., no net mortality); there were at least four data points in each response; and growth was at a maximum at 24 h. This last criterion obviated the problems of growth inhibition at high daylengths, but resulted in a smaller data set as ~30% of available data were not suitable for inclusion because growth was at a maximum at intermediate daylengths. Data presented graphically were digitised, and growth rates expressed as doublings or divisions day^{-1} were converted to μ. The data were compiled from studies on marine, freshwater, benthic, and pelagic species, under a variety of experimental conditions, that employed various temperature, and PFD combinations. To circumvent the problem of variability in the data caused by diverse experimental conditions, and produce a model that could be applied to other data sets, the responses were scaled to a proportion of the maximum specific growth rate within that response (i.e., growth rates measured at 24 h daylength were given a value of 1). The same candidate models (see Table 3.1) as fit to the *Cryptomonas* sp. μ vs. daylength data were then iteratively fit to this data set. The most-likely model was identified using the same information-theoretic methods described above. Although the scaling

transformation meant that the data were heteroscedastic, this did not preclude the computation of the regression coefficients (Zar, 1999).

A general model of microalgal specific growth in response to daylength

The aim here was to use the model determined in the model selection procedure (i.e., the modified 3-parameter hyperbolic model) to derive a general model of the microalgal specific growth response to daylength. In this analysis there were no concerns about negative growth rates skewing the response towards non-linearity so it was appropriate to include mortality data ($n = 3$) to facilitate correct parameter estimation (Montagnes and Berges 2004). Thus, the modified 3-parameter hyperbolic model was iteratively fit to this data set ($n = 242$, Appendix 2), and parameters were determined.

Results

Specific growth response of Cryptomonas sp. to daylength

The linear model was a poor predictor of the specific growth response in *Cryptomonas* sp. (Table 3.1), and the model that best described the specific growth response of *Cryptomonas* sp. to daylength was the modified 3-parameter rectangular hyperbolic model (Eq. 3.2, Fig. 3.1).

Table 3.1. Summary of candidate model selection statistics of *Cryptomonas* sp. specific growth rate (μ, d^{-1}) as a function of daylength (h), modelled on positive growth rates only. *P* represents the number of parameters in each model (including the error term), AIC_C is the corrected Akaike information criterion, Δ_i is the AIC_C difference, and w_i is the Akaike weight. In the equations μ_{max} represents the maximum specific growth rate (d^{-1}), D the daylength, a the abscissa intercept, K_D a constant, μ_0 the ordinate intercept, and b the gradient of the slope.

model	**source**	**equation**	***P***	**AIC_C**	Δ_i	w_i
modified 3-parameter rectangular hyperbola	Montagnes (1996)	$\mu = \frac{\mu_{max}(D-a)}{K_D+(D-a)}$	4	-63.23	0	0.68
2-parameter rectangular hyperbola	Tang and Vincent (2000)	$\mu = \frac{\mu_{max} D}{K_D+D}$	3	-61.72	1.51	0.32
linear	e.g., Geider et al. (1997)	$\mu = \mu_0 + bD$	3	-50.50	12.73	0.00

Table 3.2. Summary of candidate model selection statistics of the general microalgal specific growth rate response to daylength (n = 239), modelled on positive growth rates only. (See Table 3.1 for definitions of: μ_{max}, D, a, K_D, μ_0, b, P, AIC_C, Δ_i, and w_i).

model	**source**	**equation**	***P***	**AIC_C**	Δ_i	w_i
modified 3-parameter rectangular hyperbola	Montagnes (1996)	$\mu = \frac{\mu_{max}(D-a)}{K_D+(D-a)}$	4	-976.70	0	0.76
2-parameter rectangular hyperbola	Tang and Vincent (2000)	$\mu = \frac{\mu_{max} D}{K_D+D}$	3	-974.44	2.27	0.24
linear	e.g., Geider et al. (1997)	$\mu = \mu_0 + bD$	3	-942.46	34.24	0.00

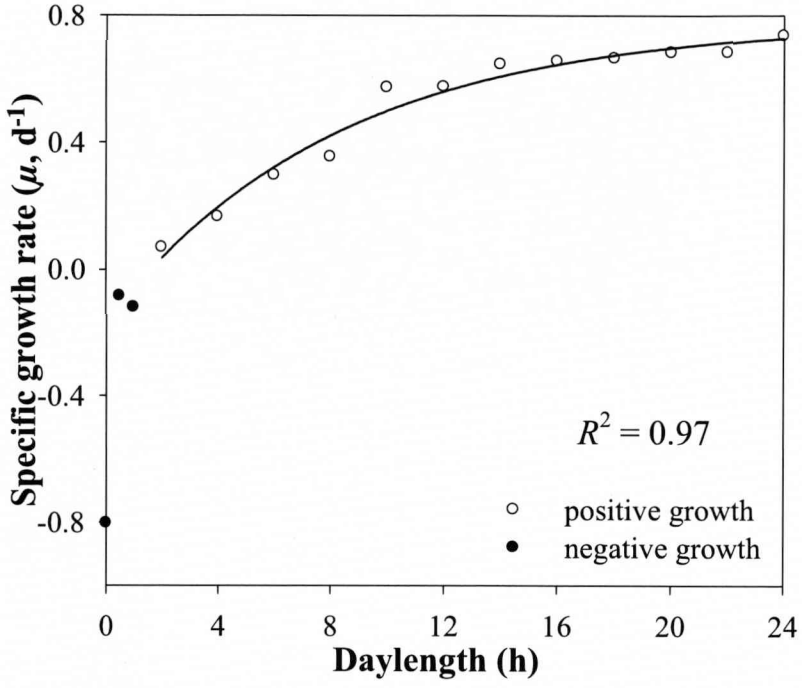

Fig. 3.1 Specific growth rate (μ, d^{-1}) of *Cryptomonas* sp. as a function of daylength (h). Line shows the modified 3-parameter rectangular hyperbolic model (Eq. 3.2) fit to the positive *Cryptomonas* sp. specific growth rates.

The generality of a non-linear specific growth response to daylength

The linear model was a poor predictor of the specific growth response (Table 3.2) and the Akaike weights associated with the modified 3-parameter rectangular hyperbolic model (Table 3.2) indicated that this model described the data considerably better than the other candidate models.

General microalgal specific growth response to daylength

The modified 3-parameter rectangular hyperbolic model (Eq. 3.3, Fig. 3.2B) provided a good fit (R^2 = 0.80) to the multi-species data set (n = 242) that included microalgal net mortality:

$$\mu_G = \frac{1.39(D - 2.4)}{8.4 + (D - 2.4)} \tag{3.3}$$

where μ_G represents the general specific growth rate response to daylength, as a proportion of that at 24 h.

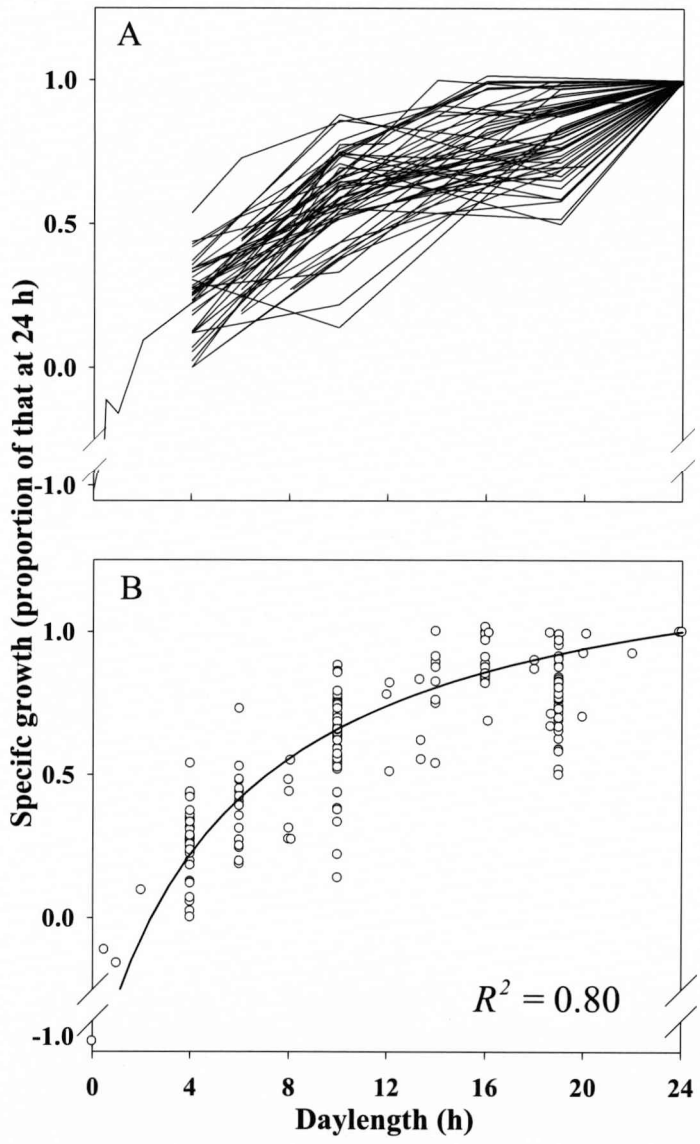

Fig. 3.2 The general microalgal specific growth response to daylength (h). (A) Microalgal specific growth rates (μ, d^{-1}), scaled as a decimal fraction of that at 24 h for each of 54 responses, where each response contains at least 4 data points. B) Same data as (A), but shown as individual data points (n = 242). Line shows least squares regression of the modified 3-parameter rectangular hyperbolic model (Eq. 3.3) fit to the data.

Discussion

The shape of the microalgal growth rate response to daylength has been examined, both at the individual species level (*Cryptomonas* sp.) and in a multi-species assemblage (54 responses). In both analyses, the most-likely model was the modified 3-parameter rectangular hyperbolic model. Furthermore, in both cases the linear model (see Introduction) was a poor predictor of the data. The results from the present study support others that have used a non-linear model of this relationship (Gilstad and Sakshaug 1990; Tang and Vincent 2000) and suggest that a linear model may be an oversimplification of this response.

To explore the consequences of assuming a directly proportional relationship (i.e., assuming 24 h as 100% and 12 h as 50%) between growth rates and daylength, linear one-to-one extrapolations were examined. The general microalgal daylength growth model (Eq. 3.3) was used to estimate the relative specific growth (μ as a proportion of that at 24 h) at daylengths from 1-23 h. These values were then multiplied by the appropriate multiplier (e.g., growth at 12 h multiplied by 2) to extrapolate to 24 h daylength (Fig. 3.3A). The over/underestimate (Fig. 3.3B) was then calculated as the difference between this value and that predicted by the model at 24 h (i.e., 1). This analysis suggests that linear extrapolation from daylengths >4 h to 24 h can lead to growth overestimates of as much as 65%. Applying the same logic, and extrapolating back from growth at 24 h to that at shorter daylengths (>4 h), growth could be underestimated by as much as 40% (Fig. 3.3C). Extrapolations to, or from, very short daylengths (< 4 h) will lead to even larger over/underestimates (see Fig. 3.3B). These results indicate that linear extrapolations of μ from one daylength to another, or

erroneous inclusion of growth over/underestimates such as these in models, will clearly lead to inaccuracies in predictions of primary production. Thus, the recommendation of this study is that it is essential to account for the non-linearity of this relationship in such calculations.

As this analysis focused on responses where growth was at a maximum at 24 h, species that are inhibited by long daylengths were not included in this analysis. Consequently, this criterion may have biased the types of species included in the data set. For example, species originally isolated in tropical or sub-tropical regions will be adapted to a non-varying photoperiod, whereas those from higher latitudes will be adapted to a seasonally varying photoperiod. Thus, species from low latitudes may be expected to be more likely to experience growth inhibition when exposed to long daylengths. Of the species included in the general microalgal growth daylength analysis the range of latitudinal provenances was from 51.4° to 75°. Therefore, this data set may represent a sub-set of species adapted to a seasonally varying daylength. However, the recognition that other species exhibit growth inhibition at long daylengths serves to reinforce the findings of this study regarding the shape of this response i.e., that the microalgal specific growth rate response to daylength is non-linear.

These results illustrate the superiority of the 3-parameter hyperbolic function compared to the 2-parameter hyperbolic function when modelling microalgal μ vs. daylength. This finding highlights the importance of including a non-zero abscissa intercept when modelling this relationship (Montagnes and Berges 2004) and suggests that 2.4 h is the threshold daylength for microalgal specific growth rates as a proportion of the growth at 24 h.

Although numerous studies have demonstrated that the shape of the specific growth rate response to daylength is highly species specific (e.g., Brand and Guillard 1981; Foy and Gibson 1993), this study has shown that, when microalgal specific growth rates are not inhibited by long daylengths, the general interspecific growth response to daylength is well described by a 3-parameter rectangular hyperbolic function. This function will be useful in comparative studies where there is a need to normalise growth rates to a standard daylength, and is preferable to adopting the linear relationship, which will lead to over/underestimates when extrapolating from one daylength to another.

Fig. 3.3 Linear extrapolation of specific growth rates (assuming 24 h as 100%, 12h as 50%) from the modified 3-parameter rectangular hyperbolic model (Eq. 3.3) leads to over/underestimation of microalgal specific growth rate predictions. (A) Extrapolation from 12 h daylength to 24 h (dashed line) and from 24 h to 12 h (dotted line). To calculate the percentage overestimate the model (Eq. 3.3) was used to estimate the growth at daylengths from 1-23 h and multiplied by the appropriate multiplier (e.g., in this example for 12 h multiply by 2) to extrapolate to a 24 h daylength. This value was then subtracted from 1 (the proportion at 24 h in the model) to calculate the percentage overestimate. To calculate the percentage underestimate the value from the model at 24 h (i.e., 1) was divided by the appropriate multiplier (e.g., in this example for 12 h divide by 2). This value was then subtracted from the value of the model at that daylength to calculate the percentage underestimate. (B) Over/underestimation of specific growth rates when extrapolating to a 24 h daylength from shorter daylengths (dashed line), or from 24 h to shorter daylengths (dotted line). (C) The same as B but focusing on over/underestimates at daylengths between 4 and 22 h. (Note the different scales on the *y* axes).

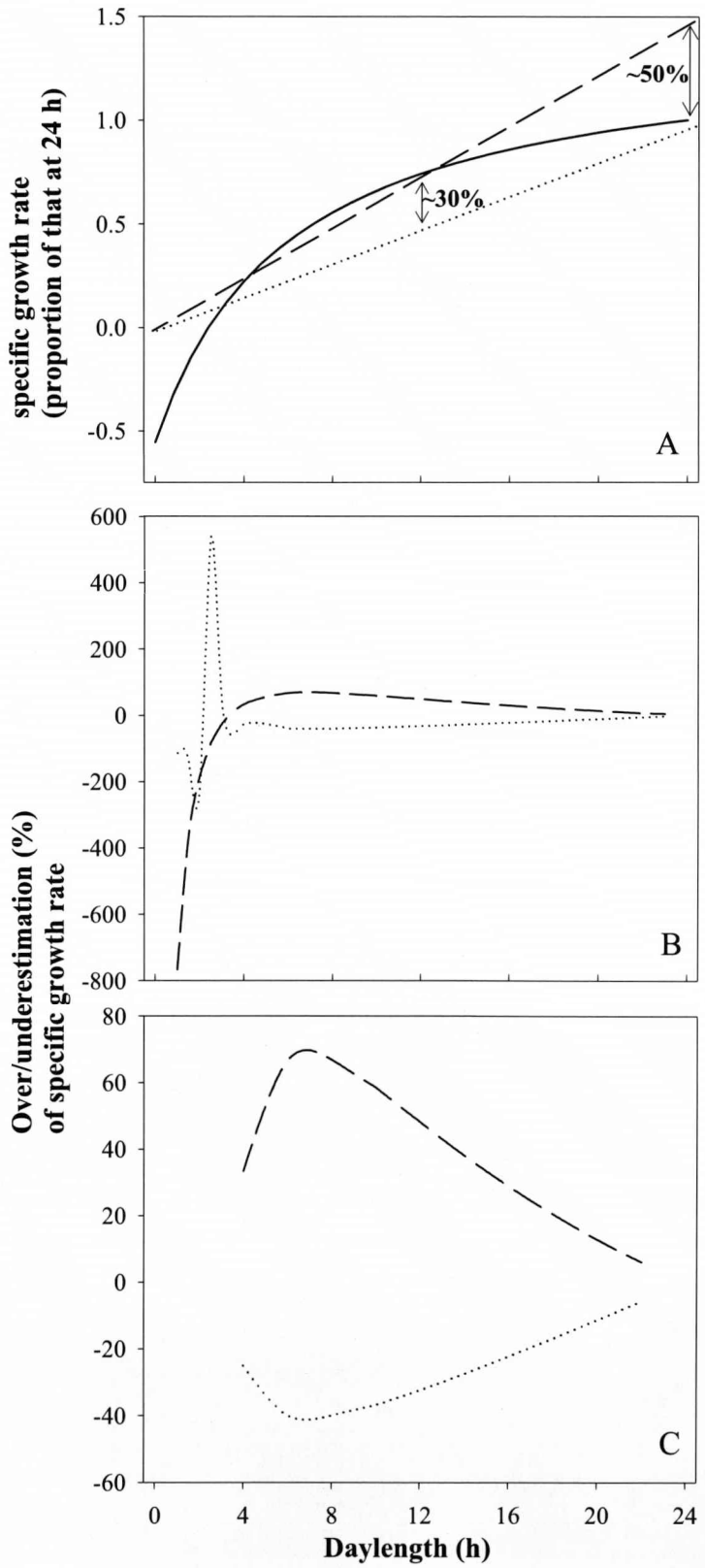
specific growth rate
(proportion of that at 24 h)
1.5
1.0
0.5
0.0
-0.5
~50%
~30%
A
600
400
200
0
-200
-400
-600
-800
B
Over/underestimation (%)
of specific growth rate
80
60
40
20
0
-20
-40
-60
C
0
4
8
12
16
20
24
Daylength (h)

CHAPTER 4

Modelling the microalgal maximum growth response to photon flux density and daylength

Introduction

Accurate models of macrophysiological (Chown et al. 2004) relationships are prerequisites for predicting and simulating large-scale aquatic ecosystem processes. As microalgal specific growth rates (μ) are a key physiological determinant of aquatic primary production (Falkowski and Raven 2007), to better understand these large-scale processes, there is a need to investigate microalgal growth using multi-species assemblages across broad environmental gradients.

Light, because of its influence on photosynthesis, is a key limiting variable influencing microalgal growth rates, across a range of spatial and temporal scales (Falkowski and Raven 2007). However, at any one time, microalgal μ may be limited by environmental factors other than photon flux density (PFD, μmol photons m^{-2} s^{-1}), and daylength (h) (e.g., nutrients, and temperature). Furthermore, when considering a multi-species assemblage, as in this study, taxonomic affiliation and body size (Banse 1982; Tang 1995) are also key determinants of specific growth rates. Such an array of possible variables suggests that any attempt to model μ in response to a single limiting factor, such as PFD or daylength, will be confounded by other unmeasured variables.

One approach to overcome this problem is to concentrate on the maximum specific growth response (μ_{max}) i.e., the upper envelope of a scatter graph (Scharf et al. 1998). Below this ceiling other, possibly unmeasured, factors may be the active limiting

constraint and so responses near the edges, rather than at the centre of distributions, give a better estimate of the effect of the limiting factor on the response variable (Kaiser et al. 1994; Cade et al. 1999). Thus, this study concentrates on the relationship at the upper edge (μ_{max}) of a multi-species assemblage of microalgal specific growth rates in response to PFD and /or daylength. This approach has previously been applied successfully to examine relationships between μ_{max} and temperature (Bissinger et al. 2008) and has numerous applications in dynamic ecosystem production models (e.g., Bowie et al. 1985; Brush et al. 2002).

Prior to modelling these maximum specific growth responses, another important issue addressed in this study is the applicability of combining PFD and daylength measurements into one daily light-dose (DLD, mol photons m^{-2} d^{-1}). Daily light-dose has been widely applied in studies of microalgal growth (Gibson and Foy 1983; Sommer 1994; Tang and Vincent 2000) and is an appealing concept as it allows the two components of the light field to be combined into one, thus facilitating model outputs. However, the non-linearity of the photosynthesis vs. PFD curve (e.g., Jassby and Platt 1976) suggests that there may be problems with this concept. For example, when the saturation point in the μ vs. PFD curve is reached there is no capacity in the system to compensate for a possible subsequent reduction in daylength (Sommer 1994).

Below the PFD saturation point microalgal growth is suggested to be proportional to the DLD (Gibson and Foy 1983, Foy and Gibson 1993). Thus, it would be expected that, below the PFD saturation point, and given the same total DLD, μ would be independent of the ratio of PFD to daylength. Although numerous studies have measured microalgal μ with various combinations of PFD and daylength (e.g.,

Thompson 1999; Verity 1982), none has examined the equivalence of μ when the ratio of PFD to daylength is manipulated, whilst maintaining the same total DLD.

This study will show, using one rigorous experimental investigation of specific growth in a freshwater microalga (*Cryptomonas* sp.) that, below light saturation, microalgal μ may be differentially sensitive to PFD and daylength across a range of DLDs. Therefore, as the DLD may not be a reliable concept, the two components of the light regime are considered separately when using meta-data to derive general functions describing microalgal μ_{max} in response to light.

Thus, the issues addressed in this study are the applicability of using DLD to describe the specific growth rate response of *Cryptomonas* sp. across a range of DLDs and the derivation of equations describing microalgal μ_{max} as a function of PFD, daylength, and PFD and daylength combined.

Methods

Equivalence of daily light-dose components

The aim here was to compare the specific growth rates (μ) of the freshwater flagellate *Cryptomonas* sp. (strain 26.8, Culture Collection of Microalgae in Göttingen, Germany) under a varying photon flux density (PFD, μmol photons m^{-2} s^{-1}) regime with those previously observed under a variable daylength regime (Chapter 3), whilst maintaining the same total daily light-dose (DLD, mol photons m^{-2} d^{-1}). To achieve this 19 cultures were maintained in modified Woods Hole medium (MWC, Guillard and Lorenzen 1972) at 16°C ± 1°C, in continuous light, at PFDs ranging from 0 to 70 μmol photons m^{-2} s^{-1}. These PFDs were achieved by shading each flask with filters and were

chosen so that the total daily light-dose (DLD) of 12 of the cultures was identical to that experienced by 12 cultures in the daylength experiment of Chapter 3, whilst the other cultures allowed the collection of data to increase the power of the regression analysis. After acclimation (3-4 d) samples (2 ml) were counted daily, at the same time each day, and μ was determined over the exponential growth phase from the slope of the relationship between *ln* abundance vs. time.

Unlike the analysis in Chapter 3, where the aim was to assess the degree of linearity in the specific growth response of *Cryptomonas* sp. to daylength, the aim of the present study was to assess the similarity between the specific growth rate response of *Cryptomonas* sp. under a varying PFD regime to that observed under a varying daylength regime, whilst maintaining the same total DLD. Therefore, as there were no concerns about the negative growth at low PFDs and/or short daylengths skewing the data towards non-linearity, it was appropriate to use the data for all DLDs, including those of net mortality, in this analysis. A modified 3-parameter hyperbolic model (Eq. 4.1) (see Chapter 3) was fit to the specific growth rate data:

$$\mu = \frac{\mu_{max}(DLD - a)}{K_{DLD} + (DLD - a)} \tag{4.1}$$

where μ_{max} represents the maximum specific growth rate (d^{-1}), *DLD* represents the product of daylength (h) and PFD (mol photons m^{-2} d^{-1}), a is the abscissa intercept, and K_{DLD} is a constant,

The initial slope, α, of the growth vs. daily light-dose curve provides a measure of growth efficiency (Foy and Gibson 1993). Here, α was estimated from the expression

μ_{max}/K_{DLD} (Rothhaupt, 1990), and differences between the PFD-varying and daylength-varying relationships were investigated by comparing α (*t*-test).

Microalgal μ_{max}: data manipulation and analysis

To determine the microalgal maximum specific growth rate responses data (n = 2178) were compiled from the literature where: studies were laboratory-based; μ was not negative; and both daylength and PFD were measured. Irradiance measurements presented in units other than μmol photons m^{-2} s^{-1}, were approximated using conversion factors (Yoder 1979). This data set is composed of marine/brackish (126 species or strains from 71 genera) and freshwater (37 species or strains from 27 genera) species from 71 publications (Appendix 3). As the studies encompassed a wide range of temperatures (-1.9 - 40.6°C) the specific growth rates were normalised to 20°C using a Q_{10} of 1.88 (Bissinger et al. 2008). A plot of the data revealed that the specific growth rates peaked at ~ 29°C, and as the Q_{10} is based on the assumption of a monotonic rate response to temperature, growth rates determined at temperatures > 29°C were not included (Bissinger et al. 2008).

For each function quantile regression (Koenker and Bassett 1978) was used to objectively define the upper edge of the data (Scharf et al. 1998) and, as this data set was large (n = 2178), it was possible to estimate the 99th quantile for each of the functions (Rogers 1992). The 99th quantiles were modelled using the 'quantreg' package (Koenker 2006) in the statistical language *R* v. 2.6.1. (http://www.r-project.org).

Microalgal μ_{max} as a function of PFD

It is well established that the photosynthesis vs. irradiance relationship follows a non-linear relationship and that high irradiances inhibit microalgal specific growth rates (Falkowski and Raven 2007). However, previous models of the photosynthesis vs. irradiance relationship assume no photoinhibition (e.g., Jassby and Platt 1976), and as in this data set specific growth rates appeared to decline after ~ 230 μmol photons m^{-2} s^{-1} (see Results), a similar approach was followed and only those growth rates where PFD was < 230 μmol photons m^{-2} s^{-1} were considered. When the data were modelled with a modified 3-parameter rectangular hyperbolic model (Eq. 4.1) the intercept was not significantly different from zero ($t = 0.50$, df = 2176, $p > 0.05$). Consequently, the mathematically simple 2-parameter rectangular hyperbolic function (Huisman et al. 2006; López-Urrutia et al. 2006) was chosen to model μ_{max} as a function of PFD (Eq. 4.2):

$$\mu_{max\,20°C(PFD)} = \frac{\mu_{max(PFD)} PFD}{K_{PFD} + PFD} \tag{4.2}$$

where $\mu_{max\,20°C(PFD)}$ is the maximum specific growth rate corrected to 20°C as a function of PFD, and $\mu_{max(PFD)}$ and K_{PFD} are constants.

Microalgal μ_{max} as a function of daylength

Here, the same model (i.e., the modified 3-parameter rectangular hyperbolic model) as used in the daily light-dose analysis (Eq. 4.1) was applied.

Microalgal μ_{max} as a function of PFD and daylength combined

To provide a function that allows microalgal μ_{max} to be modelled in those situations where both PFD and daylength data are available, a third model representing the product of the PFD and daylength μ_{max} functions was established. Unlike the previous two mechanistic μ_{max} functions, this combined model is phenomenological (Eq. 4.3):

$$\mu_{max\,20°C(C)} = \left(\frac{\mu_{max(C)} PFD}{K_{PFD(C)}}\right)\left(\frac{\mu_{max(C)}\left(D - a_2\right)}{K_{D(C)} + \left(D - a_2\right)}\right) \tag{4.3}$$

where $\mu_{max\,20°C(C)}$ is the maximum specific growth rate corrected to 20°C as a function of PFD and daylength combined, D represents daylength (h), and $\mu_{max(C)}$, a_2, $K_{PFD(C)}$, and $K_{D(C)}$ are constants.

Results

Equivalence of daily light-dose components

At low DLDs, the specific growth response of *Cryptomonas* sp. was significantly more sensitive to an increase in PFD than to daylength (α = 5.1 and 0.85 mol photons^{-1} m^2 respectively, t = 2.70, df = 30, $p < 0.05$, Fig. 4.1).

Microalgal μ_{max} as a function of PFD

The statistics associated with the parameters (Table 4.1) from the 99th quantile of the 2-parameter rectangular hyperbolic function suggest that the model (Eq. 4.4, Fig. 4.2) described the data very well:

$$\mu_{max\,20°C(PFD)} = \frac{3.03PFD}{14.11+PFD} \tag{4.4}$$

Microalgal μ_{max} as a function of daylength

The statistics (see Table 4.1, Fig. 4.3) associated with the modified 3-parameter rectangular hyperbolic function suggest that this model described the data reasonably well:

$$\mu_{max\,20°C(D)} = \frac{3.3(D-1.8)}{4.1+(D-1.8)} \tag{4.5}$$

where $\mu_{max20°C(D)}$ is the maximum specific growth rate corrected to 20°C as a function of daylength.

Microalgal μ_{max} as a function of PFD and daylength combined

The combined 4-parameter rectangular hyperbolic function was a good model of the data (Eq. 4.6, Table 4.1, Fig. 4.4):

$$\mu_{max\,20°C(C)} = \left(\frac{1.90PFD}{11.56+PFD}\right)\left(\frac{1.90(D-2.21)}{2.89+(D-2.21)}\right) \tag{4.6}$$

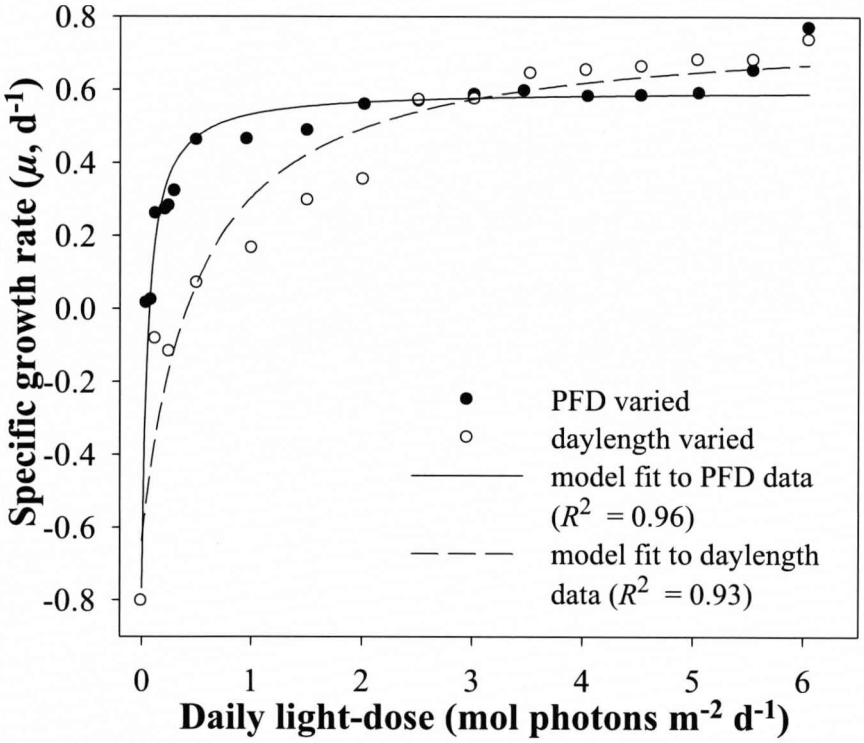

Fig. 4.1 Specific growth response of *Cryptomonas* sp. to daily light-dose (DLD, mol photons m^{-2} d^{-1}), where the ratio of PFD to daylength was varied, whilst maintaining the same DLD, across a range of DLDs. Lines show the modified 3-parameter rectangular hyperbolic models fit to the data.

Table 4.1. Regression coefficients and associated statistics from the analyses of microalgal maximum specific growth (μ_{max}, d^{-1}) as a function of photon flux density (PFD, μmol photons m^{-2} s^{-1}), daylength (h), and the product of PFD and daylength. In the models D represents daylength, a_1 and a_2 are the abscissa intercepts, $\mu_{max(PFD)}$, $\mu_{max(D)}$, $\mu_{max(C)}$, $K_{PFD(C)}$, and $K_{D(C)}$,are all constants. (Note, the units of the coefficients a_1, a_2 and K_D are h, while those of K_{PFD} are μmol photons m^{-2} s^{-1}).

coefficient	**estimate**	**std. error**	***t***	***p***
PFD model				
$\mu_{max(PFD)}$	3.03	0.1669	8.1612	<0.001
K_{PFD}	14.11	4.7508	2.9708	<0.05
Daylength model				
$\mu_{max(D)}$	3.30	0.5569	5.9253	<0.001
a_1	1.80	0.9237	1.9488	0.0515
K_D	4.10	3.4447	1.1902	0.2341
Daylength and PFD combined				
$\mu_{max(C)}$	1.90	0.1439	13.2015	<0.001
a_2	2.21	0.6049	3.6538	<0.001
$K_{PFD(C)}$	11.56	3.6346	3.1805	<0.05
$K_{D(C)}$	2.89	2.3859	1.2113	0.2259

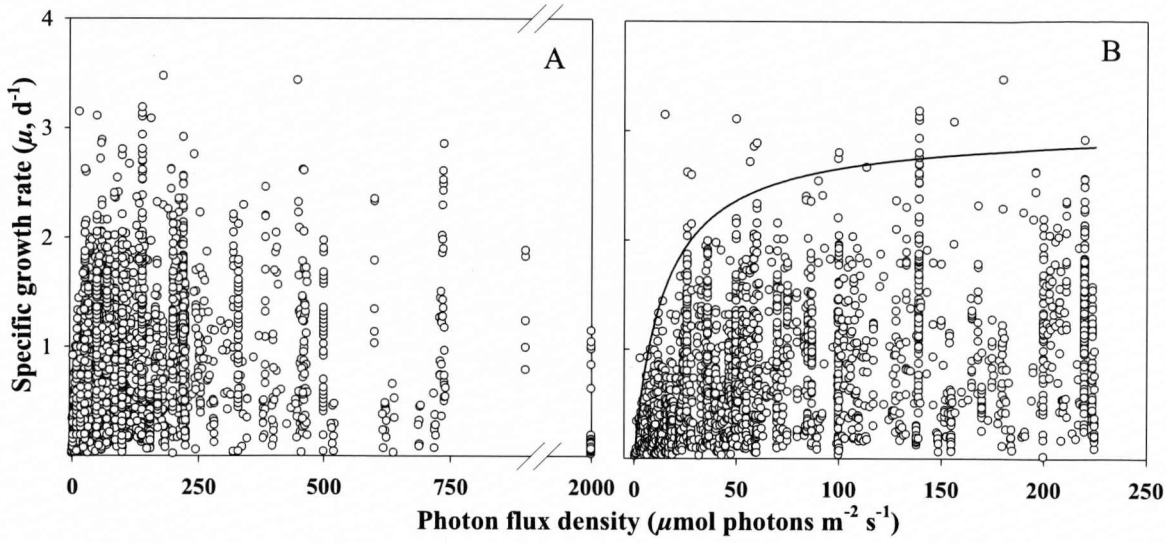

Fig. 4.2 Temperature corrected (normalised to 20°C using a Q_{10} of 1.88) microalgal maximum growth rates as a function of photon flux density (PFD, μmol photons m^{-2} s^{-1}). (A) Full data set (n = 2592) showing the inhibition of growth at photon flux densities > 230 μ mol photons m^{-2} s^{-1}. (B) Line shows the 99th quantile of the 2-parameter rectangular hyperbolic model (Eq. 4.4) fit to the data (n = 2178, limited to growth rates determined at temperatures ≤ 29°C and PFDs < 230 μmol photons m^{-2} s^{-1}) used in modelling the response.

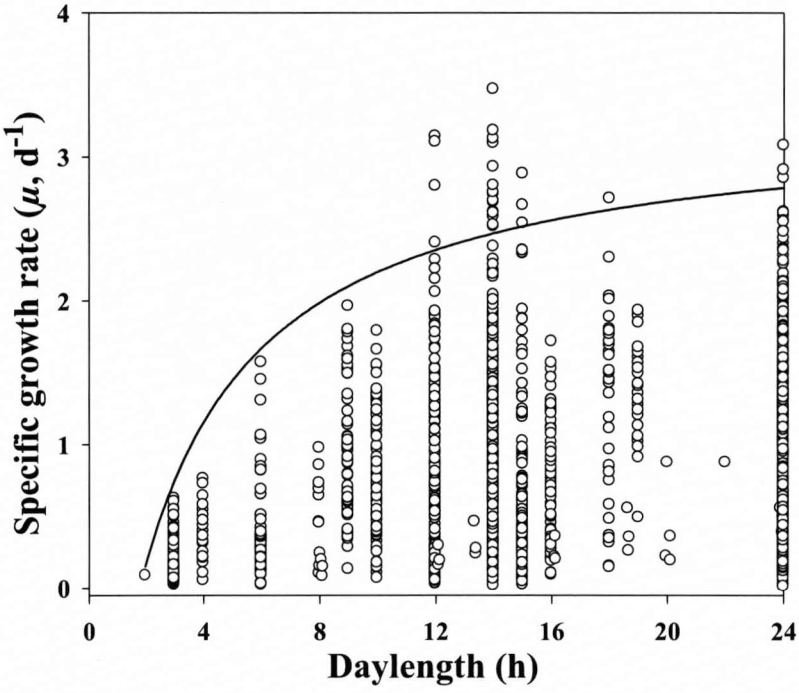

Fig. 4.3 Temperature corrected (normalised to 20°C using a Q_{10} of 1.88) microalgal maximum specific growth rates as a function of daylength (n = 2178, limited to specific growth rates determined at temperatures ≤ 29°C and PFDs < 230 μmol photons m^{-2} s^{-1}). Line shows 99th quantile of modified 3-parameter rectangular hyperbolic model (Eq. 4.5) fit to the data.

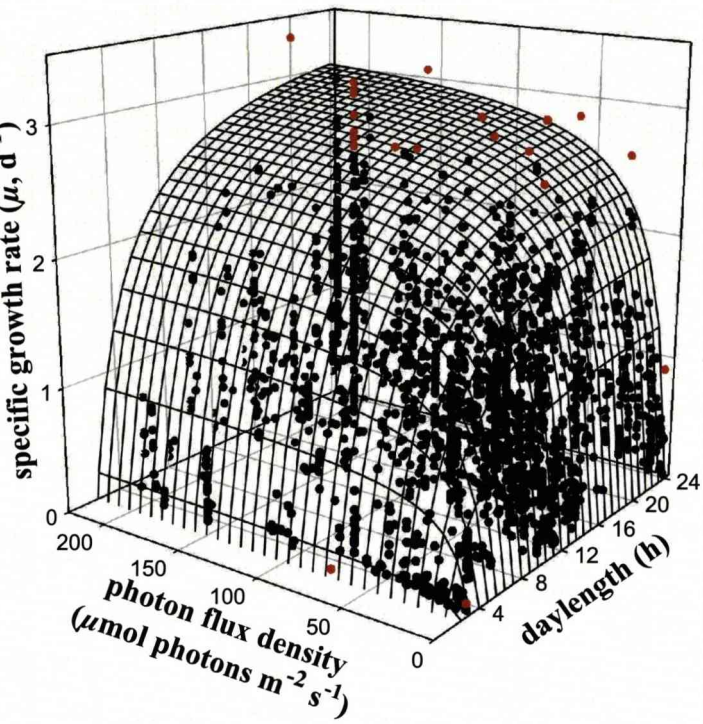

Fig. 4.4 Temperature corrected (normalised to 20°C using a Q_{10} of 1.88) microalgal maximum specific growth rates as a function of photon flux density and daylength combined (n = 2178, limited to specific growth rates determined at temperatures ≤ 29°C, and PFDs < 230 μmol photons m^{-2} s^{-1}). Response surface shows the 99th quantile of the combined model (Eq. 4.6) of specific growth as a function of PFD and daylength and points above the response surface are shown in red.

Discussion

Equivalence of daily light-dose components

The results of the investigation of the *Cryptomonas* sp. specific growth rate (μ) response to daily light-dose (DLD, mol photons m^{-2} d^{-1}), in which the ratio of daylength (h) to photon flux density (PFD, μmol photons m^{-2} s^{-1}) was varied, suggests that the shape of the response to DLD depends on the ratio of PFD to daylength. (Fig. 4.1). In the present study the initial slope, α, of the growth vs. DLD curve was greater when the ratio of PFD to daylength was high than when it was low (5.1 and 0.85 mol photons^{-1} respectively). These results suggest that at low DLDs growth under a high ratio of PFD to daylength is more efficient than one where the PFD to daylength ratio is lower. This result differs from that found by Gibson and Foy (1983), where the slope of the initial response between specific growth rate and DLD was independent of the ratio between PFD and daylength. However, the result in the present study is not directly comparable with the observation of Gibson and Foy (1983), because the equivalence in the initial slope observed by Gibson and Foy (1983) was in an experimental system where DLD was not maintained constant when the effects of daylength and PFD were compared. Thus, the results of the present study suggest that using DLD as a composite of PFD and daylength may not always be reliable and as a consequence these two variables should be modelled separately.

Microalgal μ_{max} as a function of PFD, daylength, and PFD and daylength combined

The proposed models of μ_{max} are a good fit to the data (Table 4.1). As the 2-parameter hyperbolic function used to model maximum growth in response to PFD does

not have an intercept term, one criticism that could be applied to it is that it does not allow for an estimate of the irradiance at which mortality is just balanced (compensated) by growth. However, when modelling the upper edge of the data the intercept term is estimated with low accuracy and, in any case, it has been shown that the irradiance at which growth is approximately equal to respiration is very near zero (Thompson 1999; Foy 1983; Gibson and Foy 1983).

One caveat that applies to these μ_{max} models, is their restriction to those situations where growth is not inhibited by high irradiance levels (< 230 μmol photons m^{-2} s^{-1}) or high temperatures (< 29°C). However, even though the PFD received at the earth's surface can vary between 200-2000 μmol photons m^{-2} s^{-1}, as the depth of the euphotic zone is considered to extend down to 1% of the surface irradiance (Reynolds 2006, and references within) the scales over which these models are applicable are ecologically realistic. Generally, most sea surface temperatures are below 30°C (Lalli and Parsons 2002) so even with the restriction of these models to temperatures ≤ 29°C they can nevertheless be applied to a wide range of environments.

This study has produced models of μ_{max} that will allow estimations of microalgal maximum specific growth rates to be made when either irradiance and/or daylength data are available. In dynamic ecosystem models a function (most commonly a temperature function) is often used to set the upper limit of microalgal specific growth rates, and from this theoretical maximum, growth rates are then reduced by applying coefficients relating to other environmental limiting factors, such as nutrients (Bowie et al. 1985). The μ_{max} models that have been derived here allow for PFD and/or daylength

to set the upper limit of growth, and so they will facilitate alternative approaches to modelling primary production across large spatial and temporal scales.

CHAPTER 5

A Universal temperature-dependence of intrinsic rates of increase? Effects of evolution and acclimation in microalgae

Introduction

General relationships between temperature and metabolism (Krogh 1914), and body size and metabolism (Kleiber 1947) have long been observed. The undoubted ecological importance of these variables has stimulated investigations in which the combined metabolic effects of body size and temperature have been studied in diverse taxa (Gillooly et al. 2001; Robinson et al. 1983). Recently, the proponents of the metabolic theory of ecology (MTE) have suggested that a combined function of temperature and body size is capable of describe the metabolism of all organisms (Gillooly et al. 2001; Brown et al. 2004):

$$B = i_0 M^{3/4} e^{-Ea/kT} \tag{5.1}$$

where B represents metabolic rate, M is body mass, E_a is the activation energy (defined by Gillooly et al. (2001) as an average for the rate-limiting enzyme-catalysed biochemical reactions of metabolism), T is the absolute temperature (K), k is Boltzmann's constant (8.62×10^{-5} eV K^{-1}), and i_0 is a normalisation constant independent of body size and temperature.

The MTE predicts that processes driven by heterotrophic respiration and those driven by photosynthesis will exhibit different temperature dependencies (expressed as an activation energy, E_a) and that the E_a associated with photosynthesis will be 0.32 eV (Allen et al. 2005). Although this prediction was based on photosynthesis in terrestrial

C3 plants (Farquhar 1980), it has been suggested that photosynthesis in marine phytoplankton has a similar temperature dependency (López-Urrutia et al. 2006), thereby suggesting that the predicted temperature dependency of 0.32 eV may be equally valid for phylogenetically distant autotrophs across wide-ranging environments. A universal thermal sensitivity of rates derived from photosynthesis, including specific growth rate (Savage et al. 2004a), implies that there have been no effects of adaptation to different thermal environments on thermal sensitivity or any divergence by different phylogenetic groups. Such concepts pose potential challenges to a universal thermal sensitivity of biological rates and will be examined in this Chapter.

Intrinsic rates of natural increase also scale with temperature and body size

Whilst the MTE initially focused on metabolic rates, its applicability to intrinsic rates of natural increase (or specific growth rates, μ, as commonly used in planktonic ecology) was developed (Savage et al. 2004a) after it had been shown that time to first reproduction, α, is related to mass and temperature in the same way that metabolism is (Gillooly et al. 2002). For unicellular organisms (e.g., microalgae), which have discrete reproduction and reproduce by fission, $\alpha = G$, the generation time, and so:

$$\alpha \propto G \propto M^{1/4} e^{Ea/kT} \tag{5.2}$$

As μ is inversely related to G (May 1976) the exponential growth model (Eq. 5.3) was used to derive an expression for the average number of offspring per individual per generation (R_0)

$$N_t = N_0 e^{\mu t} \tag{5.3}$$

where the size of the population N at time t is a function of the initial population size N_0, and the specific growth rate. The term t is then equivalent to the generation time G, and after taking logs and re-arranging this becomes:

$$\mu = \frac{ln R_0}{G} \approx N_C M^{-1/4} e^{-Ea/kT} \tag{5.4}$$

where N_C is a taxon- and environment-independent normalisation constant. Savage et al. (2004a) state that for unicellular organisms R_0 approximates 2 so $ln\ R_0$ is a slowly varying function, and consequently it is treated as a constant. Thus the majority of the mass and temperature dependence of μ is explained by the variation in G (Savage et al. 2004a).

Challenges to the universality of temperature-dependent metabolism

One criticism of the MTE is its assertion that metabolism is driven by biochemical kinetics i.e., higher temperatures automatically lead to kinetically determined higher metabolic rates (Clarke and Fraser 2004). In contrast, the evolutionary trade-off hypothesis (Clarke 2004) argues that, rather than representing a purely kinetic response to temperature, the resting metabolic rate represents the energetic cost of evolutionary adaptation to a particular temperature and lifestyle. Clarke (2004) argues that the MTE makes no provision for any mechanistic differences between the acute response, laboratory acclimation, field acclimatisation, and evolutionary adaptation, other than by a change in E_a, which then becomes an empirical variable, and thus invalidates the derivation of the theory (Eq. 5.1) from first principles (Clarke 2004).

Furthermore, Clarke (2004) argues that, although increases in metabolic rate with temperature are seen universally within species, the extrapolation of the theory underpinning this to across-species relationships is untenable: because across-species relationships represent statistical populations of individual thermal optimisations they cannot be explained by the same underlying thermodynamic mechanisms. Consequently (Clarke and Fraser 2004) argue that a graphical examination (see Fig. 5.1A and B) of the within- and across-species responses suggests that the thermal sensitivity of the across-species response will be less than that of the within-species response. However, Gillooly et al. (2006) have countered these arguments from Clarke (2004), and Clarke and Fraser (2004) by stating that any differences due to acclimation or adaptation between the within- and across-species responses will be expressed in the normalisation constant i_0 (see Eq. 5.1) rather than the activation energy i.e., the activation energy will be invariant (e.g., Fig. 5.1C). Consequently, this Chapter addresses these points and investigates whether there are differences in thermal sensitivity between microalgal acclimatory (within-species), and evolutionary (across-species) specific growth responses.

Approaches to examine temperature sensitivity across species

In this study two approaches are used to determine the temperature sensitivity of microalgal growth across species, as there are methodological and theoretical advantages and disadvantages associated with each. The first approach uses quantile regression (Koenker and Bassett 1978) to determine the E_a at the top of the envelope of a data set (corrected for size, photon flux density, and daylength) of microalgal specific growth

rates in response to temperature, where the responses are not inhibited by high temperatures (See Fig. 5.1A). This first approach has the advantage that the inclusion criteria associated with it allow for a relatively large data set to be compiled, so increasing the power of the analysis. However, potential biases arising from this approach include the possibility that: i) some responses in the data set may have greater weight if they have both their μ_{max} and other high μ values near the top of the envelope, whereas ii) other responses may have less weight if they have not reached their μ_{max}, because of other unmeasured factors (e.g., nutrients).

The second approach to determine the across-species thermal-sensitivity from a data set (corrected for size, photon flux density, and daylength) is to first compile μ_{max} values of individual species responses to temperature where the specific growth rate peaked at an optimum temperature (T_{opt}) for growth (i.e., the temperature where microalgal μ is at a maximum), and then calculate the E_a across these μ_{max} values for the different species at their respective optimum temperatures (see Fig. 5.1B and C). Because this approach focuses on the peak values of each response, it yields a more accurate measure of the maximum growth response to temperature across species, and thus equates to an approximation of evolutionary growth temperature (Clarke 2003). However, because of the relative scarcity of responses that meet the inclusion criteria, and the large variation in μ_{max} between phyla, the statistical power of this method is reduced when compared to the across-species analysis using quantile regression. Consequently, because of these differences in μ_{max} between phyla, the temperature dependency (E_a) of specific growth rates (μ) in Bacillariophyta (diatoms) are determined separately in addition to those for all microalgae. Diatoms were chosen because they

were the most abundant group in this data set and have distinctively high growth rates when compared to other taxa (Furnas 1990). As this study will show, despite the differences in their assumptions, both approaches to investigating E_a across species produce similar estimates of thermal sensitivity. Moreover, employing two different approaches to address the thermal sensitivities of these across-species relationships adds robustness to the general findings of this study (Levins 1966).

Determination of size-scaling exponent

The mechanistic explanation for the inclusion of the ¼ power size-scaling exponent within the MTE also remains somewhat controversial (Chown et al. 2007), as does the universality of the size-scaling exponent (Bokma 2004; Dodds et al. 2001; White et al. 2007). Consequently, here, rather than impose an allometric exponent *a priori*, multiple regression is used to determine an empirically derived allometric exponent from the data (Downs et al. 2008; López-Urrutia et al. 2006).

Using the approaches outlined above, this study will determine whether the thermal sensitivities (expressed as an activation energy, E_a), and size-dependence, of microalgal specific growth rates are the same as that predicted by the MTE and whether there are differences in thermal sensitivity between microalgal acclimatory (within-species), and evolutionary (across-species) specific growth responses.

Fig. 5.1 Conceptual diagram showing the hypothetical acclimatory (within-species) and evolutionary (across-species) thermal sensitivity of microalgal specific growth rates together with the two different methodologies used to examine the across-species response. In each graph the thin solid line represents the upper envelope across species. (A) Quantile regression is used to objectively define the upper envelope of microalgal μ_{max} across species, where the dotted lines represent individual responses. (B) The μ_{max} values obtained from the individual peak (at T_{opt}) thermal growth responses (thick solid and dashed lines) used to estimate the across-species response. Both (A) and (B) show the prediction of Clarke and Fraser (2004) i.e., the thermal sensitivity of the across-species response is less than that of the within-species response. (C) Shows an alternative scenario where the thermal sensitivities of the within- (thick solid lines) and across-species growth responses are invariant.

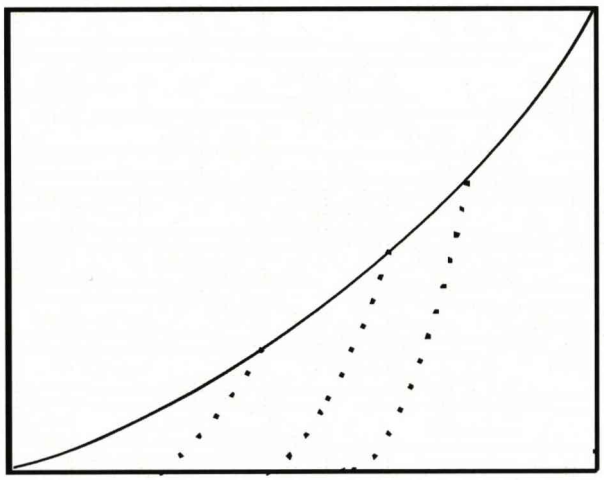

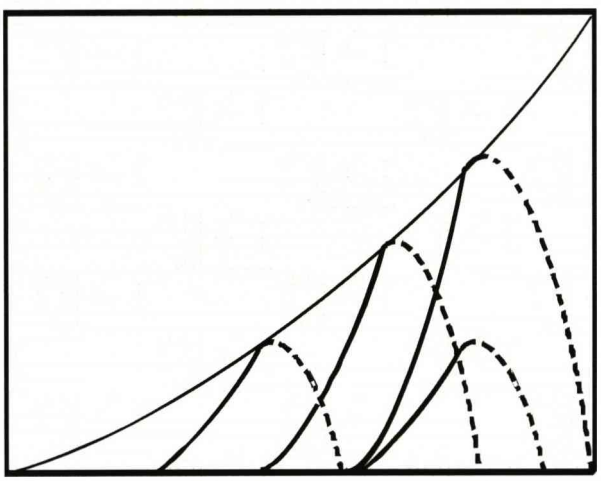

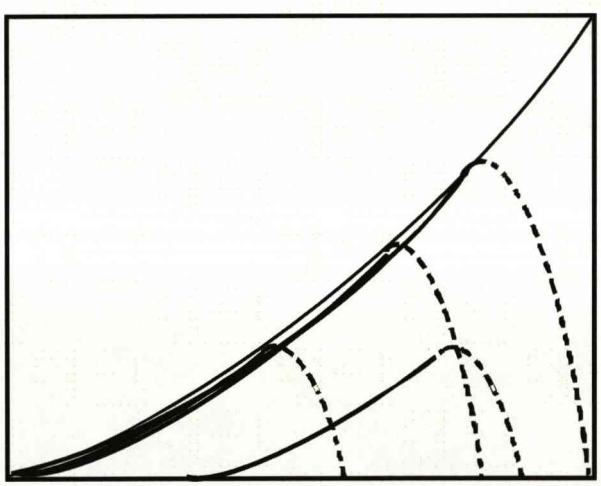

Methods

Within-species microalgal thermal sensitivity

To determine the mean temperature-dependence (E_a) of the within-species microalgal specific growth rate response, a comprehensive data set (Appendix 4A) of microalgal specific growth rate responses to temperature was compiled from the literature. Data were extracted from tables or digitised from figures, and responses were only included when there were ≥ 3 data points in each temperature response. The data set (n =138) comprised 30 responses from 8 phyla (27 species, 3 strains) and 17 studies, the range of cell volumes covered five orders of magnitude and the temperature range was ~30°C. The Arrhenius (1889) equation (Eq. 5.6), adopted in this study to model the temperature dependency of μ, is only applicable over that region of the response where rates are not inhibited by high temperatures.

$$\mu = e^{-Ea/kT} \tag{5.6}$$

Consequently, when specific growth rates peaked (at a T_{opt}) growth rates at temperatures higher than T_{opt} were not included in this analysis. To avoid bias arising from uneven numbers of species, each species was only represented by a single study, and within studies only one response of each species was included. The criteria for selection here were firstly, the response with the largest number of data points followed by that with the widest range of temperatures. The Arrhenius model (Eq. 5.6) was then iteratively fit (SigmaPlot v.10, SPSS Inc., Chicago, USA) to each of the responses, and the weighted mean E_a (to account for numbers of data points in each response) was calculated from

the model parameters. As this data set included eight phyla, an analysis of variance (ANOVA) was applied to test for differences in their thermal sensitivities.

Within-species diatom thermal sensitivity

Using the data set compiled for the within-species analysis of microalgal thermal sensitivity (see above) a subset of diatom specific growth rates responses was compiled (Appendix 4B). This data set ($n = 52$) comprised 11 responses (9 species, 2 strains) from six studies, the range of cell volumes covered three orders of magnitude and the temperature range was ~ 25°C. The Arrhenius equation (Eq. 5.6) was fit to each response, using the same methods as above, and from the model parameters the weighted mean E_a was calculated.

Across-species thermal sensitivity and size-scaling of microalgal μ_{max} using quantile regression

To estimate the across-species temperature dependencies (E_a) of microalgal maximum specific growth rates (μ_{max}) the same data set (Appendix 4A) that was used in the within-species analysis of microalgal thermal sensitivity was used here. Cell size was incorporated into this analysis by adopting the traditional allometric scaling term V^b, where V represents cell volume (μm^2) and b is the allometric scaling exponent. To allow the size and temperature coefficients to be estimated from the data, rather than imposed on the model these variables were incorporated into a multiple regression framework (Eq. 5.7):

$$ln\,\mu_{max} = ln(N_{C1}) + b \times ln(V) - E_a \times \left(\frac{1}{kT}\right) + ln\left(\frac{PFD}{K_{PFD} + PFD}\right) \qquad (5.7)$$

where N_{C1}, and K_{PFD} are constants, and PFD is photon flux density (mol photons m^{-2} d^{-1}). Thus, within this model the temperature dependence of μ_{max} was estimated using the Arrhenius term (see Eq. 5.6) and following the approach of Chapter 4 and López-Urrutia et al. (2006), the light dependency of μ_{max} was estimated using a parsimonious 2-parameter rectangular hyperbolic term. Irradiance measurements presented in units other than mol photons m^{-2} d^{-1}, were approximated using conversion factors (Yoder 1979). To avoid collinearity between daylength and PFD in the multiple regression (i.e., long daylengths were associated with high PFDs), daylengths were normalised to 24 h by applying the general microalgal daylength model (Chapter 3; Eq. 5.8) to the growth rate data prior to the regression analysis.

$$\mu_G = \frac{1.39(D - 2.4)}{8.4 + (D - 2.4)} \qquad (5.8)$$

where μ_G represents the general microalgal specific growth response to daylength (D) as a proportion of that at 24 h. To allow consistent comparisons of the temperature sensitivity and size-scaling exponents between the two types of across-species analyses, rather than apply model simplification to some of the analyses, values from the full model (Eq. 5.7) were always used.

Quantile regression (Koenker and Bassett 1978) was used to objectively define the upper edge of the data (Scharf et al. 1998), and because of the size of this data set (n = 138), the most reliable estimate of the edge of the data was obtained with the 96th

quantile (Rogers 1992). This analysis used the 'quantreg' package (Koenker 2006) in the statistical language *R* v.2.6.1. (http://www.r-project.org).

Across-species thermal sensitivity and size-scaling of diatom μ_{max} using quantile regression

This analysis used the same data set (Appendix 4B) that was compiled for the analysis of diatom thermal sensitivity within species. The same methods as used in the quantile regression analysis of microalgal μ_{max} (see above) were used to compile and analyse this data set of diatom μ_{max} in response to temperature. However, because of the relatively small size of this data set (n = 52), the most reliable estimate of the edge of the data was obtained using the 90th quantile (Rogers 1992).

Across-species thermal sensitivity and size-scaling of microalgal μ_{max} using peak growth at T_{opt}

To determine the temperature dependency (E_a) of microalgal μ_{max} across species using the peak values at the optimum temperatures for growth (T_{opt}, see Fig. 5.1B and C), a data set (Appendix 4C) was compiled of individual microalgal specific growth rate thermal responses ($\geq$ 6 data points) where the growth responses peaked at T_{opt}. This data set (n = 16) comprised 13 species and 3 strains, the range of cell volumes covered three orders of magnitude and the temperature range was ~ 20°C. Variation in cell size, PFD, and daylength were accounted for using the multiple regression model (Eq. 5.7, see above), but in this analysis ordinary least squares regression, rather than quantile

regression, was used to estimate the thermal sensitivity (E_a), and allometric (b) coefficients.

Across-species thermal sensitivity and size-scaling of diatom μ_{max} using peak growth at T_{opt}

This analysis used the same data set that was compiled for the analysis of thermal sensitivity of diatom specific growth within species (Appendix 4B). The same methods as used in the analysis of microalgal μ_{max} at T_{opt} across species (see above) were used to analyse this data set. Thus, as they are based on the same data, a comparison of the activation energies from this analysis with the mean E_a determined for diatoms within species is a more robust test of the difference between acclimatory and evolutionary temperature dependence, and represents the situation seen in the conceptual model (Figs. 5.1B, and C).

Data analysis

The activation energies, and allometric exponents from all of the analyses were compared (t -tests) with the values predicted by the MTE i.e., 0.32eV and -0.25 respectively (Allen et al. 2005; Gillooly et al. 2001), and with each other (see Fig. 5.2). To be conservative, all t-tests were Bonferroni corrected (Sokal and Rohlf 1995), giving alpha values for 2 and 3 comparisons of 0.025 and 0.016 respectively.

Results

Within-species microalgal thermal sensitivity

Analysis of variance indicated that there was no significant difference in E_a among phyla ($F_{7, 22} = 0.45$, $p = 0.862$). The weighted mean activation energy of these responses (Fig. 5.2A) of 0.46 eV (SE = 0.032) was significantly different from the E_a of 0.32 eV predicted by MTE ($t = 4.38$, df = 28, $p < 0.001$).

Within-species diatom thermal sensitivity

The weighted mean activation energy (0.53 eV, SE = 0.137) of the diatom μ_{max} thermal response (Fig. 5.2B) was not significantly different from that of 0.32 eV predicted by MTE ($t = 1.54$, df = 9, $p = 0.158$) or the 0.46 eV estimated for all microalgae within species ($t = 0.07$, df = 37, $p = 0.941$).

Fig. 5.2 A comparison of the results from the within-and across-species analyses of the temperature dependencies (activation energies, E_a) of microalgal, and diatom specific growth rates. (A) Frequency histogram of microalgal activation energies within species (30 responses). The dotted horizontal line represents the weighted mean ± 2SE, the solid line is the E_a ± 2SE from the 96th quantile of the multiple regression (Eq. 5.7) of microalgal μ_{max} (n = 138) across-species analysis, and the dashed line shows the E_a ± 2SE from the ordinary least squares regression (Eq. 5.7) of microalgal μ_{max} at T_{opt} (n = 16). (B) Frequency histogram of diatom activation energies within species (n = 11). Here the dotted horizontal line represents the weighted mean ± 2SE, the solid line is the E_a ± 2SE from the 90th quantile of the multiple regression (Eq. 5.7) of diatom μ_{max} (n = 52) across species, and the dashed line shows the E_a ± 2SE from the ordinary least squares regression (Eq. 5.7) of diatom μ_{max} at T_{opt} (n = 11). In both graphs the arrow marks the activation energy of 0.32 eV predicted by the MTE.

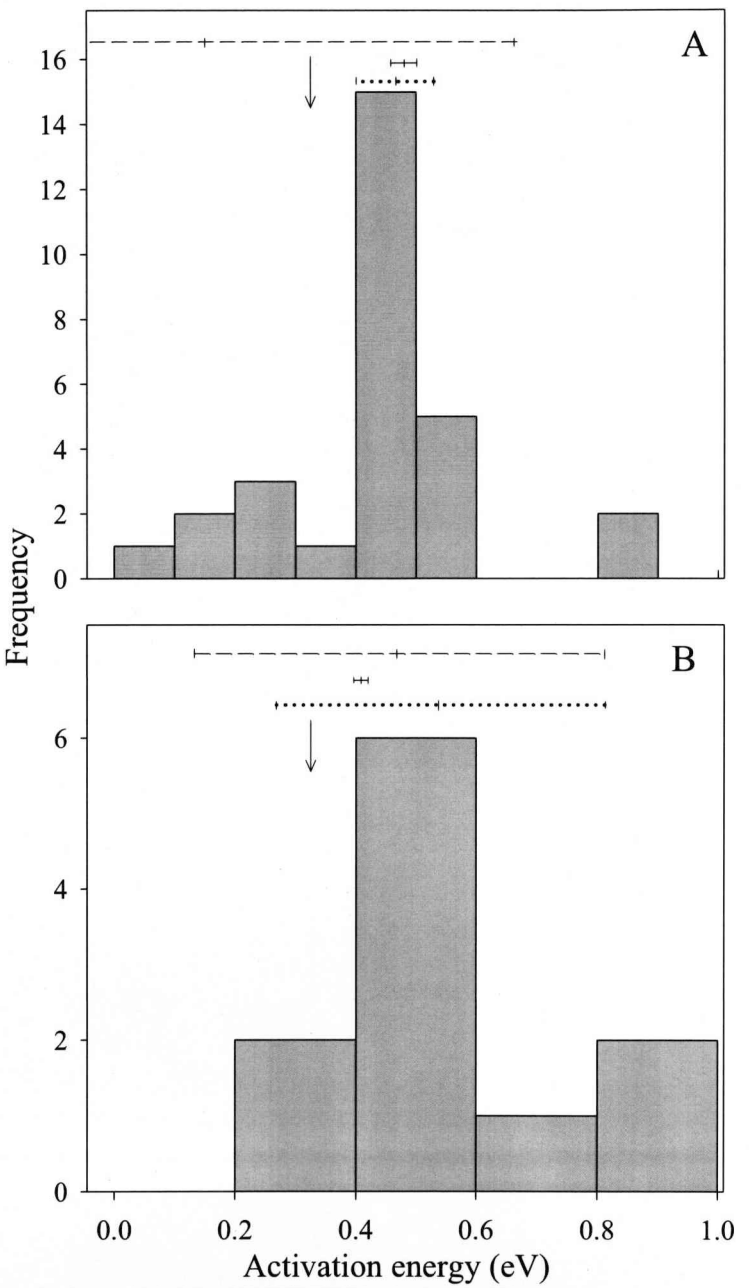
A
B
Frequency
16
14
12
10
8
6
4
2
0
6
4
2
0
0.0
0.2
0.4
0.6
0.8
1.0
Activation energy (eV)

Across-species thermal sensitivity and size-scaling of microalgal μ_{max} using quantile regression

The activation energy of 0.48 eV determined using the 96th quantile (Table 5.1, Figs. 5.2A, 5.3A) was significantly different from the 0.32 eV predicted by MTE (t = 16.43, df = 136, $p < 0.001$) but not significantly different from the 0.46 eV estimated in the within-species analysis of microalgal μ_{max} (t = 0.576, df = 164, p = 0.565). The allometric exponent of 0.15 determined using the 96th quantile (Table 5.1) was significantly different from the value of -0.25 predicted by the MTE (t = 31.59, df = 136, $p < 0.001$).

Across-species thermal sensitivity and size-scaling of diatom μ_{max} using quantile regression

The E_a of 0.41 eV determined from the 90th quantile (Table 5.2, Figs. 5.2B, 5.3B) was significantly different from the 0.32 eV predicted by the MTE (t = 17.22, df = 50, $p < 0.001$), and the across-species microalgal E_a determined using quantile regression (t = 6.55, df = 186, $p < 0.001$), but not significantly different from the mean within-species diatom E_a (t = 0.89, df = 186, p = 0.373). The allometric exponent of 0.19 (Table 5.2) was significantly different from: that of -0.25 predicted by the MTE (t = 73.48, df = 50, $p <0.001$), and that of 0.15 determined in the across-species analysis of microalgal μ_{max} (t = 3.69, df = 186, $p < 0.001$).

Across-species thermal sensitivity and size-scaling of microalgal μ_{max} using peak growth at T_{opt}

In the analysis of this data set none of the model parameters was significantly different from zero (Table 5.3, Fig. 5.2A), so no comparisons were made.

Across-species thermal sensitivity and size-scaling of diatom μ_{max} using peak growth at T_{opt}

The across-species diatom E_a of 0.47 eV determined using peak growth at T_{opt} (Table 5.4, Figs. 5.2B and 5.3C) was not significantly different from: the value of 0.32 eV predicted by MTE ($t = 0.86$, df = 9, $p = 0.410$), the within-species diatom E_a ($t = 0.34$, df = 18, $p = 0.741$), or the across-species diatom E_a determined using quantile regression ($t = 0.346$, df = 59, $p = 0.731$). The allometric exponent of 0.25 (Table 5.4) was significantly different from that of -0.25 predicted by MTE ($t = 3.55$, df = 9, $p < 0.05$) but not significantly different from that of 0.19 in the quantile regression analysis of diatom E_a across species ($t = 0.748$, df = 59, $p = 0.457$) or that of 0.15 in the quantile regression analysis of microalgal E_a across species ($t = 1.29$, df = 145, $p = 0.199$).

Table 5.1. Parameters and associated statistics of the 96th quantile from the across-species multiple regression (Eq. 5.7) of microalgal μ_{max} (n = 138). N_{C96th} is the normalisation constant (d^{-1}), b_{96th} is the allometric exponent, E_{a96th} is the activation energy (eV), and $K_{PFD96th}$ is a constant (mol photons m^{-2} d^{-1}).

parameter	**estimate**	**std. error**	***t***	***p***
lnN_{C96th}	19.47	0.38	51.12	<0.001
b_{96th}	0.15	0.01	18.41	<0.001
E_{a96th}	0.48	0.01	49.10	<0.001
$lnK_{PFD96th}$	4.35	0.36	12.25	<0.001

Table 5.2. Parameters and associated statistics of the 90th quantile from the across-species multiple regression (Eq. 5.7) of diatom μ_{max} (n = 52). N_{C90th} is the normalisation constant (d^{-1}), b_{90th} is the allometric exponent, E_{a90th} is the activation energy (eV), and $K_{PFD90th}$ is a constant (mol photons m^{-2} d^{-1}).

parameter	**estimate**	**std. error**	***t***	***p***
lnN_{C90th}	15.42	0.17	89.71	<0.001
b_{90th}	0.19	0.01	32.05	<0.001
E_{a90th}	0.41	0.01	79.63	<0.001
$lnK_{PFD90th}$	-2.22	0.03	87.87	<0.001

Table 5.3. Parameters and associated statistics from the multiple regression (Eq. 5.7) of across-species microalgal μ_{max} using peak growth at T_{opt} (n = 16). N_{Cm} is the normalisation constant (d^{-1}), b_m is the allometric exponent, E_{am} is the activation energy (eV), and K_{PFDm} is a constant (mol photons m^{-2} d^{-1}).

parameter	**estimate**	**std. error**	***t***	***p***
lnN_{Cm}	6.59	9.95	0.66	0.520
b_m	0.29	0.14	2.10	0.057
E_{am}	0.15	0.25	0.59	0.567
lnK_{PFDm}	18.33	33.18	0.55	0.591

Table 5.4. Parameters and associated statistics from the multiple regression (Eq. 5.7) of across-species diatom μ_{max} using peak growth at T_{opt} (n = 11). N_{Cd} is the normalisation constant (d^{-1}), b_d is the allometric exponent, E_{ad} is the activation energy (eV), and K_{PFDd} is a constant (mol photons m^{-2} d^{-1}).

parameter	**estimate**	**std. error**	***t***	***p***
lnN_{Cd}	17.34	6.55	2.65	<0.05
b_d	0.25	0.08	3.35	<0.05
E_{ad}	0.47	0.17	2.74	<0.05
lnK_{PFDd}	-1.05	2.52	0.42	0.690

Fig. 5.3 Thermal sensitivity of microalgal maximum specific growth rates. (A) Size and light-corrected thermal sensitivity of microalgal μ_{max} across species, using quantile regression (n = 138). The line represents the 96th quantile. (B) Size and light-corrected thermal sensitivity of diatom μ_{max} across species, using quantile regression (n = 52). The line represents the 90th quantile. (C) Size-corrected across-species thermal sensitivity of diatom μ_{max} using peak growth rates at T_{opt} (n = 11). Here, the regression line was determined using ordinary least squares. In all three graphs the parameter estimates used for the corrections are from the multiple regression model (Eq. 5.7), whose use is justified in the text and in Tables 5.1, 5.2, and 5.4. $R^1_{(\tau)}$ represents the relative deviance of the model (Koenker and Machado 1999), which is a measure of the goodness of fit of the model to the data at the specified quantile. In the equations y refers to $ln(cell\ volume^{-b}\ (PFD+K_{PFD})/PFD)$ and x refers to $1/kT$.

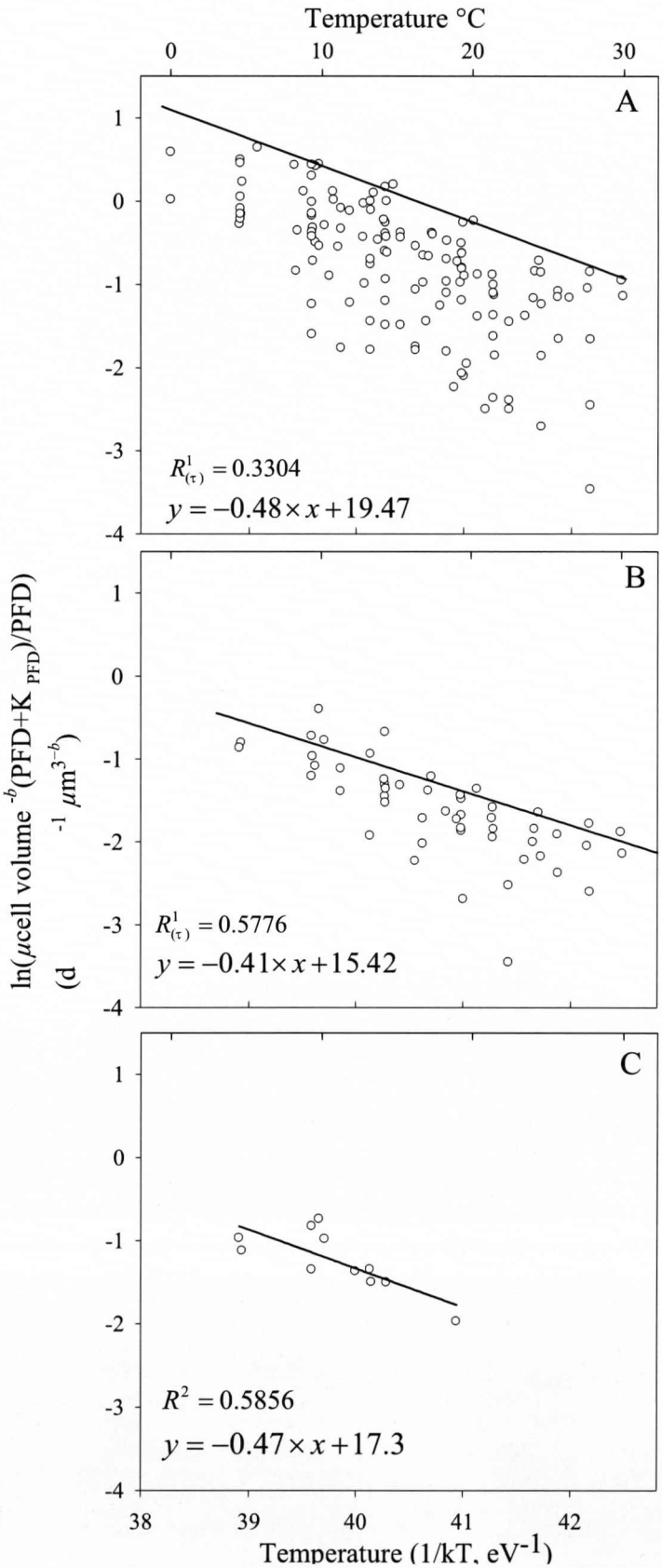
Temperature °C
0
10
20
30
A
B
C
$R^1_{(\tau)} = 0.3304$
$y = -0.48 \times x + 19.47$
$R^1_{(\tau)} = 0.5776$
$y = -0.41 \times x + 15.42$
$R^2 = 0.5856$
$y = -0.47 \times x + 17.3$
ln(μcell volume $^{-b}$(PFD+K $_{PFD}$)/PFD)
(d $^{-1}$ μm^{3-b})
1
0
-1
-2
-3
-4
38
39
40
41
42
Temperature (1/kT, eV^{-1})

Discussion

Thermal sensitivity of microalgae compared to terrestrial plants

This study indicates that the activation energy (E_a) of microalgal specific growth rates is higher than that of 0.32 eV predicted (Allen et al 2005) for processes controlled by photosynthesis in terrestrial C3 plants. The E_a determined in the across-species quantile regressions of microalgal and diatom maximum specific growth rates (μ_{max}), and the mean microalgal within-species E_a, were all significantly higher than 0.32 eV. In the analyses of peak growth at T_{opt}, the activation energies were not significantly different from 0.32 eV, although the statistical power of these analyses may have been reduced by the small sizes of these data sets (n = 9, and 16).

The thermal sensitivity (0.48 eV) of microalgal μ_{max} across species found in the present study also differs (t = 19.49, df = 136, $p < 0.001$) from the thermal sensitivity of net photosynthesis (0.29 eV) observed in marine phytoplankton (López-Urrutia et al. 2006). However, in the across-species analysis of López-Urrutia et al. (2006) the activation energy was based on the mean, rather than the maximum, as in the present study (96th quantile). Consequently, to make a closer comparison of activation energies between studies, the median (50th quantile) E_a of microalgal μ_{max} across species was also determined (0.40 eV, SE 0.0085) and found to be significantly different from the value of 0.32 eV predicted by MTE (t = 9.10, df = 136, $p < 0.001$) and the E_a determined for net photosynthesis by López-Urrutia et al. (2006) (t = 12.65, df = 136, p <0.001). These results suggest that the higher across-species thermal sensitivities of microalgal μ_{max} found in the present study are not due to a different statistical approach. Differences in activation energies between the present study and that of López-Urrutia et

al. (2006) may be explained by the different methodologies used in compiling the data. For example, as López-Urrutia et al. (2006) did not indicate that they excluded any values above T_{opt} prior to compiling their data set, it is possible that their data set includes values where the individual photosynthetic responses were inhibited by high temperatures (i.e., photosynthetic rates beyond those at the peak T_{opt}). The inclusion of such data, that do not comply with the assumption of an exponential relationship between temperature and photosynthesis, would lead to a lower average E_a, and thus may account for the low thermal sensitivities observed in that study. The careful exclusion of data above T_{opt} and use of the μ_{max} response in the present study give greater confidence that the estimates of E_a obtained more closely represent the optimum growth response to temperature, and equate to a better approximation of evolutionary growth temperature (Clarke 2003).

Why might the thermal sensitivity of microalgal growth rates be different from that of terrestrial plants?

The predicted activation energy of 0.32 eV for C3 photosynthesis in terrestrial plants (Allen et al. 2005) was based on the temperature dependence of Rubisco carboxylation (Farquhar 1980), which is sensitive to the respective partial pressures of CO_2 and O_2 within the chloroplast (Falkowski and Raven 2007). However, the partial pressures of CO_2 and O_2 differ between aquatic and terrestrial environments (Brown et al. 1995), and unlike terrestrial plants, microalgae are able to utilise carbonate and bicarbonate ions in addition to CO_2 (Falkowski and Raven 2007). Thus, these environmental and physiological differences may partly explain the higher thermal

sensitivities observed in microalgae. Another possibility is that these differences may represent a mismatch between a theoretically derived relationship and empirical data.

Acclimatory and evolutionary thermal sensitivities of microalgae

The present study has shown that there is no significant difference between the thermal sensitivity of the microalgal acclimatory (within-species) growth rate response and the evolutionary (across-species) response. This supports the argument (Gillooly et al. 2006) that the effects of acclimation, and adaptation are reflected in the normalization constant (i_0 see Eq. 5.1, and Fig. 5.1C) rather than the activation energy. Thus, the results of the present study do not support the evolutionary trade-off hypothesis of Clarke (2004). An explanation for these results is somewhat elusive because they suggest that, in addition to faster growth rates, warm adapted species may also have a broader thermal niche, which is in contrast to theory that predicts a trade off between performance at high and low temperatures regarding the evolution of thermal reaction norms (Huey and Kingsolver 1989). Furthermore, these results also suggest that a single temperature limits the specific growth rates of diverse microalgae (Fig. 5.1C).

Microalgal size-scaling exponent

In all of the analyses in the present study the allometric exponent was significantly different from the value of -0.25 predicted by the MTE. This supports other studies that have found a weak relationship (Banse 1982; Robinson et al. 1983; Sommer 1989; de Castro and Gaedke 2008) between microalgal growth rates and cell size, but differs from other studies (Fenchel 1974; López-Urrutia et al. 2006; Savage et

al. 2004a) that have also found an allometric exponent of -0.25. Such wide-ranging relationships observed between microalgal growth and cell size may arise from alternative life-history strategies that are the result of adaptation to different light and nutrient regimes (Litchman et al. 2007). For example, photosynthetic efficiency in microalgae is affected by the package effect (i.e., chlorophyll is arranged in discrete packages within the cell so increases in chlorophyll content ultimately lead to self-shading) which itself is influenced by the light regime and cell geometry (Kirk 1994; Falkowski and Raven 2007). Furthermore, Litchman et al. (2007) have shown that there is a nutrient affinity/storage trade-off continuum in microalgae such that smaller cells have a high nutrient affinity and hence a competitive advantage at low nutrient concentrations, whereas larger cells (and particularly diatoms with their large storage vacuoles) have a competitive advantage at high nutrient concentration. Consequently, these physiological responses to light and nutrients in microalgae may account for the discrepancies observed in the relationship between size-scaling and growth rates observed in this group (e.g., Fenchel 1974; Banse 1982). However, another possible explanation for these discrepancies may be that the relationship between size and temperature (Atkinson 1994) is causing collinearity in the full model (Eq. 5.7).

As the aim of this study was to assess the applicability of the MTE to microalgal specific growth rates it was appropriate to use the Arrhenius equation to model the temperature dependency of this process. However, it should be noted that this is only one of many possible models (Clarke 2004) that have been used to describe the relationship between microalgal growth and temperature (see Ahlgren 1987), both over that region of the response that excludes temperature extremes, and over the full thermal

range (i.e., including temperatures that exceed the T_{opt}). Consequently, Chapter 6 examines the suitability of these alternative models to mechanistically explain or predict the relationship between temperature and microalgal specific growth rates.

CHAPTER 6

Temperature functions in biology and their application to microalgal growth rates: A new assessment

Introduction

Generally biological responses are left-skewed i.e., rates increase to an optimal temperature and then rapidly decline with further increases in temperature (Frazier et al. 2006; Huey and Berrigan 2001), although there are studies suggesting that the relationship may be well described by a symmetric function e.g., Gaussian (Angilletta 2006). However, as numerous studies (e.g., Gillooly et al. 2001; Gillooly et al. 2002; Savage et al. 2004a) focus only on that region of the response that excludes temperature extremes (i.e., that region where the response is monotonic and increasing) this Chapter initially addresses the microalgal growth response in that region prior to addressing the response across the full thermal range.

Candidate models for the growth rate response with no temperature inhibition

Thermal response functions that have been used to model biological processes over that region of the response that excludes temperature extremes include linear (Montagnes et al. 2003), power (Bělehrádek 1926), and exponential (Arrhenius 1889). The linear model (Eq. 6.1), also known as the degree-day thermal summation rule (Cossins and Bowler 1987; Trudgill et al. 2005), has been widely used in applied entomology and agriculture because of its simplicity and that it often provides a good fit to observed values (Sharpe and DeMichele 1977; Montagnes et al. 2003):

$$\mu_N = \mu_0 + aT \tag{6.1}$$

where μ_N represents microalgal specific growth rates over that region of the response that excludes temperature extremes, T is temperature (°C), μ_0 represents growth at 0°C and a is the slope of μ_N vs. T. The use of the power function (Eq. 6.2, Bělehrádek 1926) was based on the idea that many biological temperature responses are controlled by physical processes (e.g., diffusion and viscosity) that are related to temperature by a power function (Ahlgren 1987):

$$\mu_N = bT^c \tag{6.2}$$

where b, and c are constants. Although not widely adopted in biological studies, this function has been shown to provide a good fit to microalgal growth (e.g., Ahlgren 1987), and invertebrate development (e.g., Lee et al. 2003), in response to temperature. Exponential temperature response functions (Eq. 6.3) form the basis of the well-known Q_{10} relationship which has been widely used in biology as a convenient measure of the effect of temperature on metabolic processes (Cossins and Bowler 1987):

$$\mu_N = \alpha e^{dT} \tag{6.3}$$

where α, and d are constants. However, it has been argued that simple exponential relationships have no clear mechanistic basis and are rarely observed in biological rate processes (Sharpe and DeMichele 1977; Ahlgren 1987). Furthermore, as Q_{10} varies with temperature over the temperature range of most biological processes, comparisons between species can only be made over identical temperature ranges (Cossins and Bowler 1987; Gillooly et al. 2002; Montagnes et al. 2003). This drawback has stimulated interest in temperature functions that aim to explain biological processes in terms of the underlying thermodynamics. The Arrhenius (1889) equation (Eq. 6.4) is also an exponential-type function, but unlike the simple exponential function (Eq. 6.3), it

often provides a good fit to biochemical reactions. However, although it incorporates statistical thermodynamics, the Arrhenius equation is generally considered to be an empirical relationship of the situation seen in ideal gases (Sharpe and DeMichele 1977; Schoolfield et al. 1981; Cossins and Bowler 1987):

$$\mu_N = Ae^{-E_a/RT_{(K)}} \tag{6.4}$$

where A is the pre-exponential factor, E_a is the activation energy (electron volts, eV), R is the universal gas constant (i.e. the Boltzmann constant, 8.62×10^{-5} when expressed in eV K^{-1}), and $T_{(K)}$ is the absolute temperature (K). This study initially investigates which of these functions is the most appropriate model of microalgal specific growth over that region of the response that excludes temperature extremes.

Whilst providing an excellent empirical model of individual biochemical reactions (Cossins and Bowler 1987), the Arrhenius model has also been extended to describe whole organism development time (Gillooly et al. 2002), population growth (Savage et al. 2004a), ecosystem energetics (López-Urrutia et al. 2006), and other biological processes (e.g., Brown et al. 2004). The use of the Arrhenius function to describe complex biological processes remains controversial (Clarke and Fraser 2004; Clarke 2006) and it has been argued that the across-species (i.e., multi-species assemblage) thermal response, as a statistical description of evolutionary optimisations, is fundamentally different from the within-species response (Clarke 2004; Clarke and Fraser 2004, Clarke 2006). This view is in contrast to the use of the Arrhenius term, in the metabolic theory of ecology (MTE) to describe within-and across-species responses (Gillooly et al. 2001; Gillooly et al. 2002; Brown et al. 2004); and the results of Chapter 5. Consequently, there is a need to assess the use of the same temperature functions to

describe within-species thermal responses as those used to model the responses of multi-species assemblages.

However, concentrating only on biological responses over that region of the temperature range that is not inhibited by thermal extremes limits the scope of investigations and can be biologically misleading when this leads to the selection of an inappropriate model of the relationship (Bulté and Blouin-Demers 2006). Consequently, there is a need to examine the metabolic response over the full thermal range, in addition to the region of the response where the metabolic process is inhibited by high and/or low temperatures: this issue is therefore also addressed in this Chapter.

Candidate models for the growth rate response including high temperature inhibition

Where models have been used to model temperature responses over the full thermal range (e.g., Angilletta 2006) these are generally phenomenological rather than based on mechanisms e.g., quadratic, Gaussian, modified Gaussian, Weibull, and modified quadratic (Flinn 1991). However, two functions that attempt to explain biological processes over the full thermal range in terms of the underlying thermodynamics are those of Hinshelwood (1947), and Sharpe and DeMichele (1977). The Hinshelwood (1947) formulation (Eq. 6.5) considers the biological response to temperature to be the result of two opposing processes (synthetic and degradative) both of which are modelled by the Arrhenius equation (Li and Dickie 1987):

$$\mu_I = A_1 e^{\left[\frac{-E_{a1}}{RT_{(K)}}\right]} - A_2 e^{\left[\frac{-E_{a2}}{RT_{(K)}}\right]} \qquad (6.5)$$

where μ_I represents microalgal specific growth rates over the full thermal range, and subscripts *1* and *2* denote the synthetic and degradative processes respectively. *A*, $T_{(K)}$,

and E_a have the same meaning as in the Arrhenius equation (Eq. 6.4), so this model suffers from the same criticisms that can be levelled at the Arrhenius model in terms of lacking a strong theoretical basis.

Recognising the need for a theoretical temperature function that was capable of describing biological rates over a wide range of temperatures (i.e., a model that describes growth inhibition at both temperature extremes) Sharpe and DeMichele (1977) expanded theory embodied in the Eyring (1935) equation (Eq. 6.6) to explain biological processes over the full thermal range:

$$\mu_{(N)} = \frac{k_B T_{(K)}}{h} e^{(\Delta S - \Delta H / T_{(K)})R} \tag{6.6}$$

where k_B is Boltzmann's constant (eV K^{-1}), h is Planck's constant (eV s^{-1}), ΔS is the entropy of activation (eV K^{-1}), and ΔH is the enthalpy of activation (eV). The Eyring (1935) equation, in contrast to the empirical Arrhenius formulation, is based on reaction rate theory and statistical thermodynamics. Thus, by incorporating this theory into their model Sharpe and DeMichele (1977) provided a solid theoretical framework and tool to better understand the underlying processes. Furthermore, Sharpe and DeMichele (1977) also recognised the validity of a linear approximation over that region of the response that excludes temperature extremes (e.g., the degree-day concept) so their full model tends to linearise the response in that mid-temperature region (Fig. 6.1).

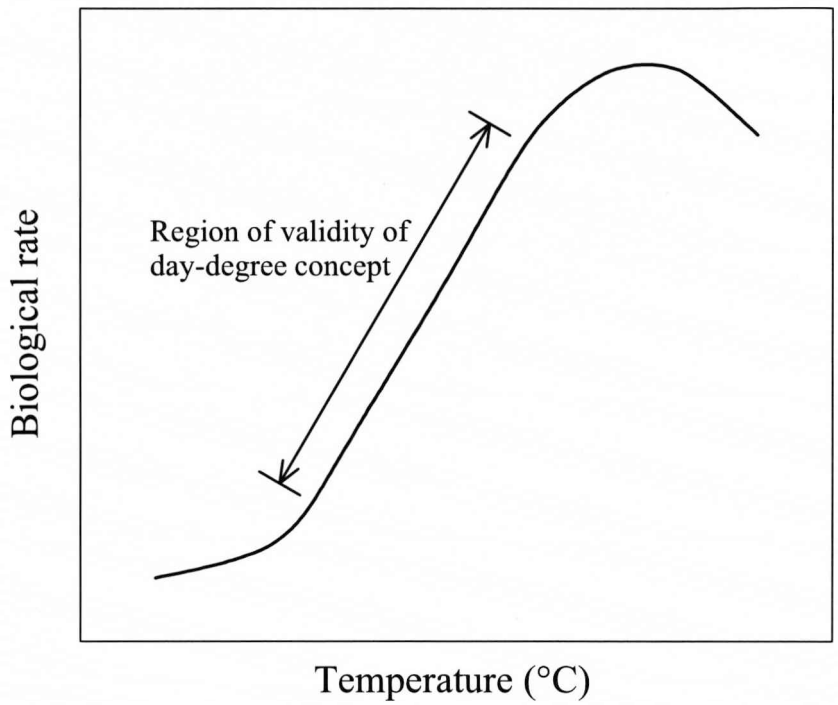

Fig. 6.1 Conceptual relationship between temperature (°C) and a biological rate process, highlighting the linear region of the response. (Redrawn from Sharpe and DeMichele 1977).

In deriving their function Sharpe and DeMichele (1977) made three assumptions: development can be considered to be regulated by a single control enzyme whose reaction rate determines the development of the whole organism; the development rate is proportional to the product of the concentration of the active enzymes and their rate constant; and the control enzyme can exist in two temperature- dependent inactive states well as an active state.

Sharpe and DeMichele (1977) defended the first assumption, by stating that, as enzymes are arranged in series in most biochemical pathways, the overall metabolic process is controlled by strategic control enzymes. They also stated that, in those instances where there are convergent parallel pathways, co-ordination of the overall process means that the rate can be assumed to be limited by a single enzyme. However, the Sharpe and DeMichele (1977) function proved difficult to model using non-linear regression and was subsequently modified by Schoolfield et al. (1981). Consequently, in the present study, the resultant model is referred to as the Sharpe-Schoolfield model (Eq. 6.7):

$$\mu_I = \frac{\rho_{(20°C)}\left(\frac{T_{(K)}}{293.15}\right)e^{\left[\frac{\Delta H_A}{R}\left(\frac{1}{293.15}-\frac{1}{T_{(K)}}\right)\right]}}{1+e^{\left[\frac{\Delta H_L}{R}\left(\frac{1}{T_{(K)1/2L}}-\frac{1}{T_{(K)}}\right)\right]}+e^{\left[\frac{\Delta H_H}{R}\left(\frac{1}{T_{(K)1/2H}}-\frac{1}{T_{(K)}}\right)\right]}} \qquad (6.7)$$

where μ_I represents the specific growth rate at temperature T over the full thermal range, $\rho_{(20°C)}$ is the growth rate at 20°C (= 293.15 K), ΔH_A is the enthalpy of activation of the reaction that is catalysed by the enzyme (eV), $T_{(K)1/2L}$ is the temperature (K) at which the enzyme is half active and half low-temperature inactive, ΔH_L is the change in enthalpy

associated with low temperature inactivation of the enzyme (eV), $T_{(K)1/2H}$ is the temperature (K) at which the enzyme is half active and half high-temperature inactive, ΔH_H is the change in enthalpy associated with high temperature inactivation of the enzyme (eV).

It is argued that the three separate exponential terms in the Sharpe-Schoolfield model allow it to be adapted (Schoolfield 1981; Wagner et al. 1984) to describe thermal response curves with: both high and low temperature inhibition (Eq. 6.1); high temperature inhibition; low temperature inhibition; or no temperature inhibition. For example the removal of both exponential terms in the denominator produces a model suitable for those situations where growth is not inhibited by temperature extremes (see Table 6.1), removal of the first exponential term in the denominator produces a model suitable for describing high temperature inhibition (see Table 6.2), and removal of the second exponential term in the denominator produces a model suitable for describing low temperature inhibition. Thus, in the present study the 2 parameter model (i.e., numerator only, see Table 6.1) is included as a candidate model when examining microalgal specific growth over that region of the response that excludes temperature extremes. However, to examine the microalgal growth response over the full thermal range, the version of this function that also included high temperature inhibition (4 parameters, see Table 6.2) is adopted as a candidate model of that relationship. This version is preferred to the full six-parameter model (Eq. 6.6), that also includes a term for low temperature inhibition, because: the strongest changes in slope are generally observed at the upper end of the thermal range; and the information-theoretic approach adopted in this study requires the number of data points in the response to be P+1

(where P is the number of parameters plus the error term) so use of the full model would limit the number of responses that could be modelled.

Modelling multi-species responses to a single limiting factor

One concern when attempting to model multi-species responses to a single limiting factor, such as temperature, is that the relationship will be confounded by other unmeasured variables in the data. For example, size (Savage et al. 2004a), taxonomic affiliation (Banse 1982), and light (e.g., López-Urrutia et al. 2006; Chapter 3) may also explain much of the variation in microalgal specific growth rates. Here, this problem is overcome by concentrating on the maximum temperature response (μ_{max}) i.e., the upper envelope of a scatter graph (Scharf et al. 1998). Below this ceiling other, possibly unmeasured, factors may be the active limiting constraint and so responses near the edges, rather than at the centre of distributions, give a better estimate of the effect of the limiting factor in question on the response variable (Kaiser et al. 1994; Cade et al. 1999). This type of approach has been adopted in previous studies of temperature and microalgal growth rates (Bissinger et al. 2008; Eppley 1972). However, in both those studies an exponential model was adopted without any assessment of its suitability. Furthermore, Bissinger et al.(2008) noted that the relationship was not exponential at high temperatures (> 29°C) and cautioned against using their model above these higher temperatures. Consequently, this Chapter uses quantile regression (Koenker and Bassett 1978) to objectively determine these μ_{max} multi-species responses over that region of the response that excludes temperature extremes and also over the full thermal range.

Model selection procedures

With such a range of possible temperature models how should we decide which function best describes our data? In this study two approaches are adopted to address this problem: the within-species responses are assessed using information theory (Burnham and Anderson 2002), and the μ_{max} across-species responses are assessed by comparing the quantile relative deviances ($R^1{}_\tau$) (Koenker and Machado 1999). An information-theoretic approach explicitly accounts for the tendency of models with more parameters to over-fit the data (Angilletta 2006) and allows the explanatory power of a range of models to be compared. Furthermore, a comparison of the Akaike weights (Burnham and Anderson 2002) associated with each model allows the relative strength of evidence for each of the models to be assessed. However, at present it is not technically possible to use information-theory with non-linear quantile regression, so here the relative deviance associated with each model is used to compare the across-species μ_{max} models, this being equivalent to the more familiar coefficient of determination used in ordinary least squares regression (Koenker and Machado 1999).

This chapter determines the most-likely model of: the within-species microalgal specific growth rate response over those regions of the response where growth rates both are, and are not, inhibited by high temperatures; the across-species microalgal μ_{max} response over those regions of the response where growth rates both are, and are not, inhibited by high temperatures.

Methods

The within-species growth rate response with no temperature inhibition

The aim here was to determine the most appropriate model to describe the within-species specific growth rate (μ) response of microalgae to temperature, over that region of the response where growth was not inhibited by temperature extremes. To achieve this, experimentally derived microalgal specific growth rate responses to temperature were compiled from the literature (Appendix 5A) where: the responses were not inhibited by temperature extremes; there were at least 5 data points in each response; and daylength, photon flux density, and nutrients were not varied. Candidate models (see Table 6.1) were identified from the literature and from these the most-likely model was selected using an information-theoretic approach (Burnham and Anderson 2002). The shape of these models is illustrated using data from Montagnes et al. (in press) (Fig. 6.2A)

The five candidate models were iteratively fit (SigmaPlot v.10, SPSS Inc., Chicago, USA) to the individual responses, and parameters were determined. Then, following the procedure of Burnham and Anderson (2002), the corrected Akaike Information Criterion (AIC_C) was determined for each model. The AIC_C is used in favour of the AIC when, as in this analysis, the sample size is small compared to the number of estimated parameters (Burnham and Anderson 2002). As AIC_C estimates the information lost when using a particular model to describe the data, the most-likely model is the one with the lowest AIC_C value (Burnham and Anderson, 2002). The total number of times that each model best described the data was calculated and the Akaike weights from these best performing models were summed.

The within-species growth rate response including high temperature inhibition

The aim here was to determine the most-likely model to describe the within-species growth rate response of microalgae to temperature, including that region of the response where there was high temperature inhibition. Experimentally derived microalgal specific growth rate responses to temperature were compiled from the literature (Appendix 5A) where there were at least 7 data points in each response and daylength, photon flux density and nutrients were not varied. Here the candidate models (see Table 6.2) consisted of four 'standard' models (i.e., Gaussian, quadratic, modified Gaussian, Weibull) that have been used, either theoretically or empirically, to describe thermal performance curves (e.g., see Angilletta 2006), and three other models (Flinn 1991; Hinshelwood 1947; Schoolfield et al. 1981) that have been used to describe thermal rate responses in ectotherms (see Table 6.1). Of these models, only those presented by Schoolfield et al. (1981) and Hinshelwood (1947) have some mechanistic basis; the others are phenomenological. The most-likely model was determined using an information-theoretic approach (Burnham and Anderson 2002) using the same methods as in the above analysis.

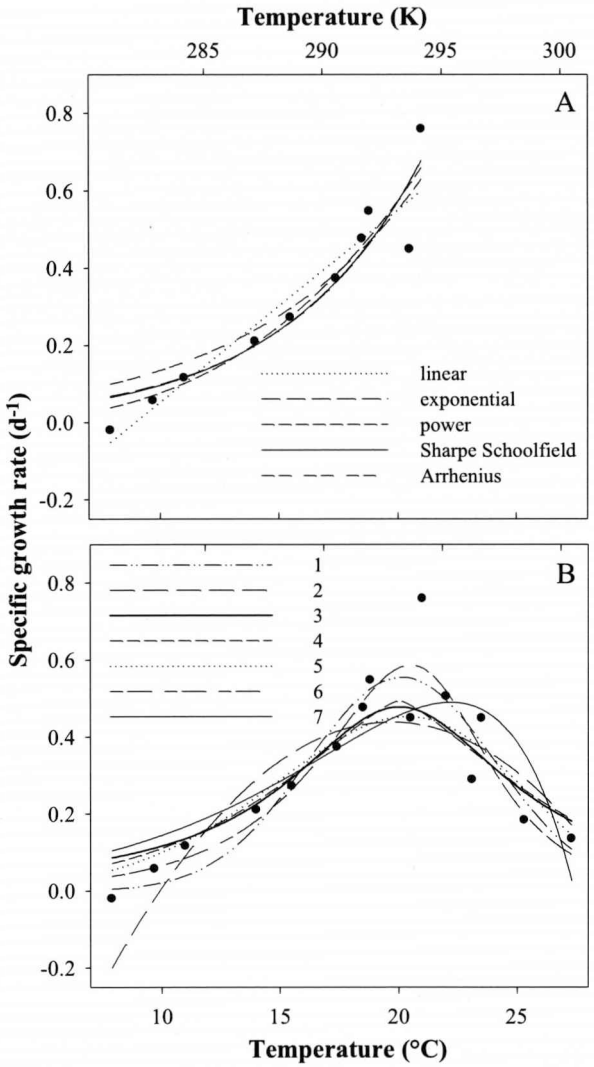

Fig. 6.2 The candidate models (see Tables 6.1, 6.2) fit to *Cryptomonas* sp. specific growth rates as a function of temperature to illustrate the shape of the models. (A) Five candidate models (see Table 6.1) fit to that region of the response where there was no temperature inhibition. (B) Seven candidate models (see Table 6.2) fit to the specific growth rate response including that region where growth was inhibited by high temperatures. Numbers of lines represent: 1) Gaussian, 2) quadratic, 3) Flinn (1991), 4) modified Gaussian, 5) Weibull, 6) Sharpe-Schoolfield, and 7) Hinshelwood (1947). The data were taken from Montagnes et al. (2008).

Across-species μ_{max} with no temperature inhibition

To determine the model that best described across-species microalgal maximum specific growth rates (μ_{max}), over that region of the response where growth is not inhibited by temperature extremes, experimentally derived microalgal specific growth rates were compiled from the literature (Appendix 5B) where growth was positive (i.e., no net mortality). As a plot of the data indicated that μ declined at temperatures >29°C (see Bissinger et al. 2008), only growth rates measured at temperatures ≤ 29°C were included (n = 2504). The same candidate models (see Table 6.1) as applied in the within-species analysis were used in this analysis. For each model quantile regression (Koenker and Bassett 1978) was used to objectively define the upper edge of the data (Scharf et al. 1998) and, as this data set was large (n = 2504), it was possible to estimate the 99th quantile for each of the functions (Rogers 1992). The 99th quantiles were modelled using the 'quantreg' package (Koenker 2006) in the statistical language *R* v.2.6.1. (http://www.r-project.org). The relative deviance, R^1_τ, associated with each model was used as a measure of the goodness of fit associated with that model at the specified quantile (Koenker and Machado 1999).

Across-species μ_{max} including high temperature inhibition

The aim here was to determine the model that best described across-species microalgal μ_{max} including that region of the response that was inhibited by high temperatures. Experimentally derived microalgal specific growth rates (n = 2703) were compiled from the literature (Appendix 5B, and C) and the same candidate models (see Table 6.2) as applied in the within-species analysis including high temperature inhibition

were used in this analysis. In addition, as studies have often used more parsimonious models to describe this relationship (e.g., Bissinger et al. 2008; Eppley 1972) the mathematically simpler models used in the previous analyses, where growth was not inhibited by temperature extremes (see Table 6.1), were also applied here. The 99th quantiles were modelled as in the previous μ_{max} analysis (see above), and the relative deviances $R^1{}_\tau$ from these models were compared.

Results

The within-species growth rate response with no temperature inhibition

The linear model was the most-likely model in the majority of responses (n =23), whereas the Arrhenius model was the most-likely model in only four responses (Table 6.1). For six responses of the 51 in this data set more than one model described the data with equal likelihood. The sum of Akaike weights, Σw_i, shows that in those responses where the linear model was the most likely-model, it described the data considerably better than the other candidate models. The majority (n = 44) of responses comprised < 7 data points and there was no clear pattern between the most-likely model frequency, and the number of data points in the response (Fig. 6.3).

The within-species growth rate response including high temperature inhibition

Of the 35 responses in this data set the Gaussian model was the most-likely model in the majority of responses (Table 6.2). The sum of Akaike weights, Σw_i, indicates that, in those responses where the Gaussian model was the most likely-model, it described the data considerably better than the other candidate models. The majority

(n = 27) of responses contained < 10 data points and there was no clear pattern between the most-likely model frequency and the number of data points in the response (Fig. 6.4).

Across-species μ_{max} with no temperature inhibition

The relative deviance associated with the 99th quantiles (Table 6.3) indicated that the Arrhenius model (Eq. 6.4) described the upper envelope of this data set better than the other models (although only marginally better than the Sharpe-Schoolfield model). The parameters from this analysis yields:

$$\mu_{maxi} = 6.57 \times 10^{7} e^{-0.43/RT_{(K)}} \tag{6.8}$$

where μ_{maxi} represents the maximum specific growth rate when growth is not inhibited by temperature extremes. In this analysis it was not possible to fit the power model to the data.

Across-species μ_{max} including high temperature inhibition

The relative deviance associated with the 99th quantiles (Table 6.4) indicate that the Sharpe-Schoolfield model (Eq. 6.7) described the upper envelope of this data set better than the other models (although only marginally better than the Gaussian model) (Fig. 6.5B). The parameters from this analysis yields:

$$\mu_{max(T)} = \frac{3.01\left(\frac{T_{(K)}}{293.15}\right)e^{\left[\frac{0.50}{R}\left(\frac{1}{293.15}-\frac{1}{T_{(K)}}\right)\right]}}{1+e^{\left[\frac{1.18}{R}\left(\frac{1}{307}-\frac{1}{T_{(K)}}\right)\right]}} \tag{6.9}$$

where $\mu_{max(T)}$ is the maximum specific growth rate over the full thermal range at temperature $T_{(K)}$. In this analysis it was not possible to fit the Flinn (1991), Weibull, modified Gaussian, Hinshelwood (1947) and power functions to the data

Table 6.1. The candidate models to describe the within-species growth rate response with no temperature inhibition. P represents the number of parameters in the model (including the error term), n represents the number of times that model best described the data, and Σw_i is the sum of Akaike weights over n responses. In all models μ_N represents the specific growth rate with no temperature inhibition, T is temperature (°C), $T_{(K)}$ is temperature (K), a, b, μ_0, α, c, and d represent constants. The Sharpe-Schoolfield equation shown here is the reduced model which is suitable for situations where growth is not inhibited by temperature extremes, $\rho_{(20°C)N}$ represents the specific growth rate at 20°C, and ΔH_N is the enthalpy of the activation of the reaction that is catalyzed by the limiting enzyme (eV). In the Arrhenius equation A represents the pre-exponential factor, E_a is the activation energy (eV), and in both the Arrhenius and Sharpe-Schoolfield models R is the universal gas constant (i.e. the Boltzmann constant 8.62×10^{-5} when expressed in eV K^{-1}).

model/ source	**equation**	***P***	***n***	Σw_i
linear	$\mu_N = \mu_0 + aT$	3	25	16.29
exponential	$\mu_N = be^{cT}$	3	8	2.68
power	$\mu_N = \alpha T^d$	3	18	9.01
Sharpe-Schoolfield	$\mu_N = \rho_{(20°C)N}\left(\frac{T_{(K)}}{293.15}\right)e^{\left[\frac{\Delta H_N}{R}\left(\frac{1}{293.15}-\frac{1}{T_{(K)}}\right)\right]}$	3	7	2.12
Arrhenius	$\mu_N = Ae^{-E_a/RT_{(K)}}$	3	3	0.85

Table 6.2. The candidate models used to describe the within-species specific growth rate response with high temperature inhibition. In all models μ_I represents the specific growth rate including high temperature inhibition. In the Sharpe-Schoolfield model $\rho_{(20°C)I}$ represents the specific growth rate at 20°C when there is high temperature inhibition (d^{-1}), ΔH_I is the enthalpy of the activation of the reaction that is catalyzed by the limiting enzyme when there is high temperature inhibition (eV) , ΔH_H is the change in enthalpy associated with high temperature inactivation of the limiting enzyme (eV), $T_{(K)1/2H}$ is the temperature (K) at which the enzyme is half active. In the Hinshelwood (1947) model A_1 and A_2 are the pre-exponential factors, E_{a1} and E_{a2} are activation energies. In the other models letters *a, b, c, d,* and μ_0 represent constants. See Table 6.1 for definitions of T, $T_{(K)}$, R, P, n, and Σw_i.

model/source	**equation**	***P***	***n***	Σw_i
quadratic	$\mu_I = \mu_0 + aT + bT^2$	4	9	5.95
Gaussian	$\mu_I = ae^{\left[-0.5\left(\frac{T-T_0}{b}\right)^2\right]}$	4	11	8.59
Flinn (1991)	$\mu_I = \frac{1}{1+\left(a+bT+cT^2\right)}$	4	7	4.16
Modified Gaussian	$\mu_I = ae^{\left[-0.5\left(\frac{\lvert T-T_0\rvert}{b}\right)^c\right]}$	5	3	1.96
Weibull	$\mu_I = a\left(\frac{d-1}{d}\right)^{1-d/d}\left[\frac{T-b}{c}+\left(\frac{d-1}{d}\right)^{1/d}\right]^{d-1} e^{-\left[(T-b/c)+(d-1/d)^{1/d}\right]_d + \frac{d-1}{d}}$	5	0	0
Sharpe-Schoolfield (High temperature version)	$\mu_I = \frac{\rho_{(20°C)}\left(\frac{T_{(K)}}{293.15}\right)e^{\left[\frac{\Delta H_I}{R}\left(\frac{1}{293.15}-\frac{1}{T_{(K)}}\right)\right]}}{1+e^{\left[\frac{\Delta H_H}{R}\left(\frac{1}{T_{(K)1/2H}}-\frac{1}{T_{(K)}}\right)\right]}}$	5	3	2.71
Hinshelwood (1947)	$\mu_I = A_1 e^{\left[\frac{-E_{a1}}{RT_{(K)}}\right]} - A_2 e^{\left[\frac{-E_{a2}}{RT_{(K)}}\right]}$	5	2	1.56

Table 6.3. The models used to describe the across-species maximum growth response with no temperature inhibition (μ_{maxN}). $R^1{}_\tau$ represents the relative deviance of the 99th quantile and is a measure of the goodness of fit that can be attributed to a model at the specified quantile (Koenker and Machado 1999). See Table 6.1 for definitions of P, parameters, and units.

model/source	**equation**	P	$R^1{}_\tau$
linear	$\mu_{max\,N} = \mu_0 + aT$	3	0.2484
exponential	$\mu_{max\,N} = \alpha e^{dT}$	3	0.2967
Sharpe-Schoolfield	$\mu_{max\,N} = \rho_{(20°C)N}\left(\frac{T_{(K)}}{293.15}\right)e^{\left[\frac{\Delta H_N}{R}\left(\frac{1}{293.15}-\frac{1}{T_{(K)}}\right)\right]}$	3	0.3010
Arrhenius	$\mu_{max\,N} = Ae^{-E_a/RT_{(K)}}$	3	0.3011

Table 6.4. The models used to describe across-species microalgal maximum specific growth rates as a function of temperature including high temperature inhibition (μ_{maxI}). See Tables 6.1and 6.2 for definitions of P, $R^1{}_\tau$, parameters, and units.

model/source	**equation**	***P***	$\boldsymbol{R^I{}_\tau}$
Gaussian	$\mu_{maxI} = ae^{\left[-0.5\left(\frac{T-T_0}{b}\right)^2\right]}$	3	0.3036
quadratic	$\mu_{maxI} = \mu_0 + aT + bT^2$	3	0.2950
Sharpe-Schoolfield (High temperature version)	$\mu_{maxI} = \frac{\rho_{(20°C)I}\left(\frac{T_{(K)}}{293.15}\right)e^{\left[\frac{\Delta H_I}{R}\left(\frac{1}{293.15}-\frac{1}{T_{(K)}}\right)\right]}}{1+e^{\left[\frac{\Delta H_H}{R}\left(\frac{1}{T_{(K)l/2H}}-\frac{1}{T_{(K)}}\right)\right]}}$	4	0.3089
linear	$\mu_{maxI} = \mu_0 + aT$	2	0.2819
exponential	$\mu_{maxI} = ae^{bT}$	2	0.2698
Sharpe-Schoolfield (Reduced version)	$\mu_{maxI} = \rho_{(20°C)I}\left(\frac{T_{(K)}}{293.15}\right)e^{\left[\frac{\Delta H_I}{R}\left(\frac{1}{293.15}-\frac{1}{T_{(K)}}\right)\right]}$	2	0.2767
Arrhenius	$\mu_{maxI} = Ae^{-E_a/RT_{(K)}}$	2	0.2753

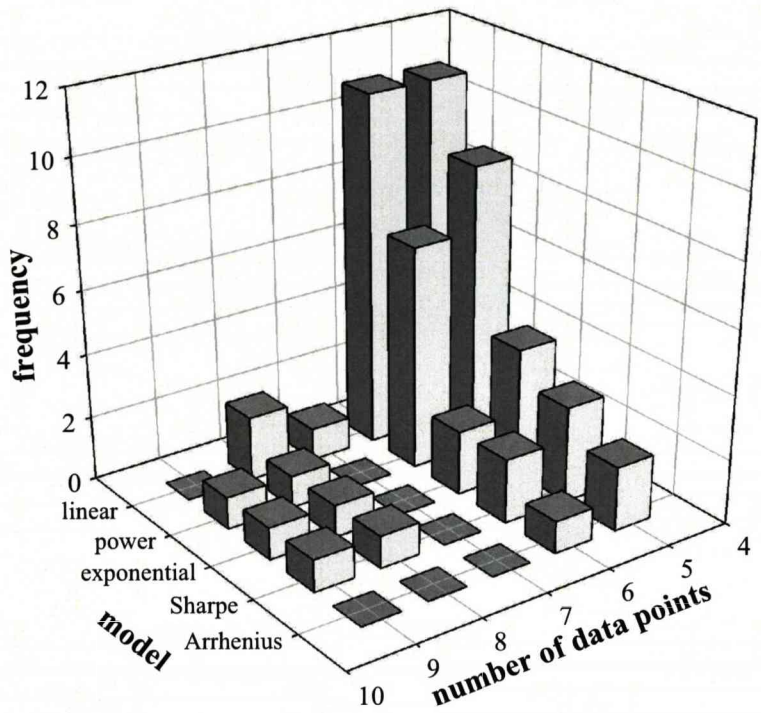

Fig. 6.3 Frequency with which the candidate models (see Table 6.1) were the most-likely fit to the microalgal within-species specific growth rate responses (n = 51), over that region of the response where there was no temperature inhibition.

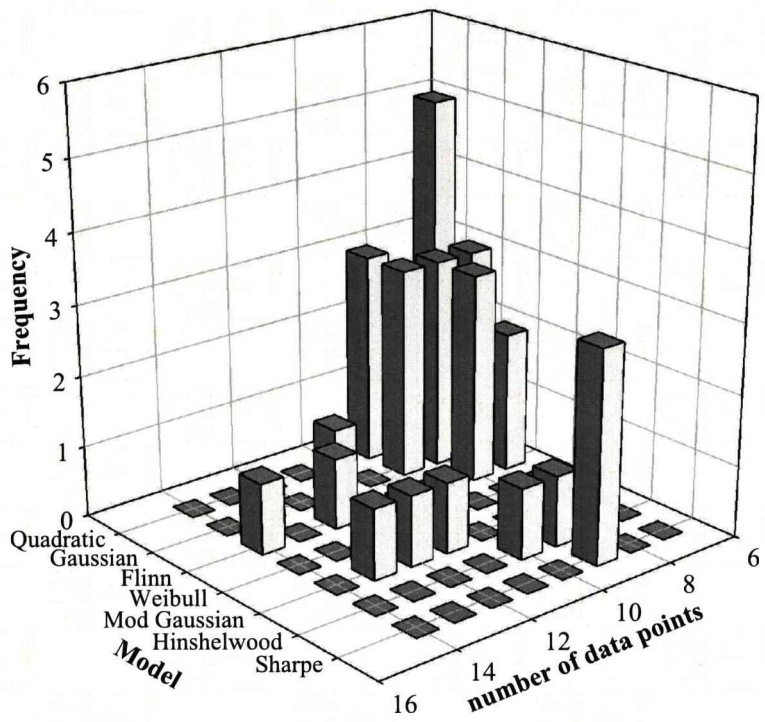

Fig. 6.4 Frequency with which the candidate models (see Table 6.2) were the most-likely fit to the within-species microalgal specific growth rate responses (n = 35) including that region of the response where growth was inhibited by high temperatures.

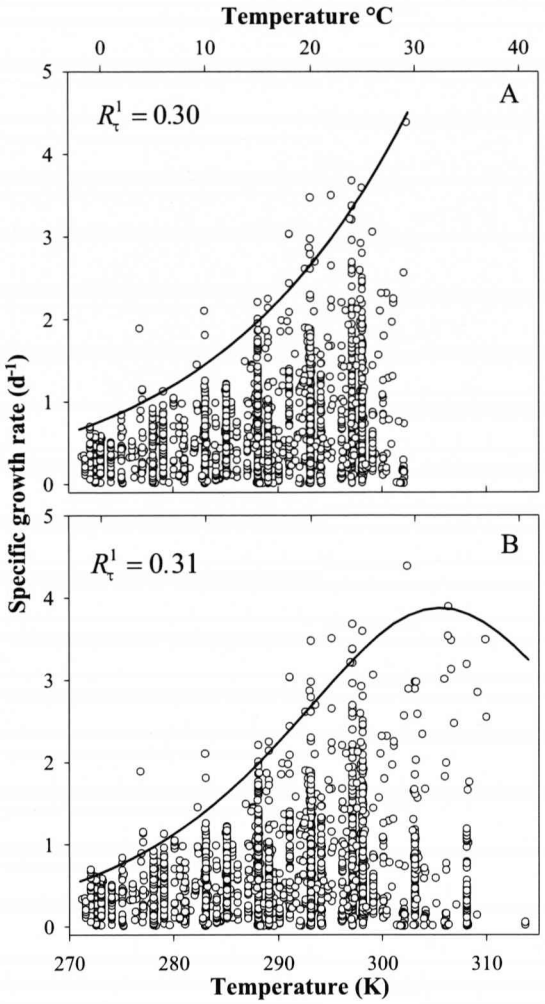

Fig. 6.5 Across-species microalgal maximum specific growth in response to temperature. (A) Line shows the 99th quantile of the Arrhenius model (Table 6.1) fit to microalgal specific growth rates (n = 2504) over that region of the response where growth was not inhibited by high temperatures (≤ 29°C). (B) Line shows the 99th quantile of the Sharpe-Schoolfield model (high temperature version, see Table 6.2) fit to microalgal specific growth rates (n = 2703) over the full thermal response. $R^1{}_\tau$ represents the relative deviance of the quantile, and is a measure of the goodness of fit that can be attributed to the model at the specified quantile (Koenker and Machado 1999) .

Discussion

The within-species growth rate response with no temperature inhibition

This analysis has shown that the response is well described by a linear model. This supports other studies (e.g., see Montagnes and Franklin 2001; Montagnes et al. 2003) that have observed a linear relationship between specific growth rates and temperature in microalgae. In common with other studies (e.g., Ahlgren 1987; Montagnes and Franklin 2001) the present study has demonstrated that the exponential function is a poor model of the data, suggesting that there is little justification for continuing to use the exponential function, such as the Q_{10} relationship, when modelling the within-species microalgal thermal growth response. Consequently, these results indicate that when comparing the within-species thermal sensitivity of microalgal growth between studies, the slope of the linear relationship is a suitable metric. Moreover, these results support the use of the day-degree summation rule to assess biological rate processes (Trudgill et al. 2005).

The reduced Sharpe-Schoolfield and Arrhenius functions were poor models of these microalgal growth rate responses within species, and as these are both 'exponential-type' functions, this again suggests that the shape of the within-species microalgal growth response is not exponential. The validity of a linear response in this region was recognised by Sharpe and DeMichele (1977), and by incorporating enzyme inactivation at temperature extremes, their full model explicitly allows for a linear response in the mid-temperature region i.e., progressive inactivation of enzymes at temperature extremes has the effect of turning down both ends of the reaction curve so diminishing the increasing acceleration effect implied by the exponential region of their

model (Trudgill et al. 2005). However, whilst this logic applies to the full Sharpe-Schoolfield model it is not applicable to the reduced 2-parameter exponential version used in this analysis. This may explain why this function was a poor model of the data here and indicates that the reduced Sharpe-Schoolfield model is not an appropriate model of the within-species thermal growth response over that region where there is no temperature inhibition (Wagner et al. 1984).

In the present study the mean slope of the 25 data sets that were found to be linear was 0.064 ± 0.007 (SE) (d^{-1} $°C^{-1}$), which is not significantly different ($t = 0.70$, df = 100, $p = 0.487$) from the value of 0.07 ± 0.005 (SE) (d^{-1} $°C^{-1}$) found by Montagnes et al. (2003) in their investigation of protist growth rates in response to temperature. The concordance of these results suggests that this may be a general relationship. As the power function was a better fit to the data than the exponential function this gives some support to the suggestion (Bělehrádek 1926) that physical processes, such as viscosity and diffusion, may play a greater role than chemical processes in some biological temperature responses.

The within-species specific growth rate response including high temperature inhibition

This analysis of the within-species microalgal specific growth rate response over the full thermal range indicates that it is well described by a Gaussian function, which is symmetrical around an optimal temperature. This result is surprising as performance curves over the full thermal range are typically assumed to follow a left-skewed distribution i.e., specific growth rates increase to an optimal temperature and then

rapidly decline with further increases in temperature (Frazier et al. 2006; Huey and Berrigan 2001). However, other studies (Angilletta 2006; Huey and Kingsolver 1993) have found that a Gaussian temperature function provides a good phenomenological model of the thermal response over the full thermal range. Angilletta (2006) suggested that, as the calculation of the AIC depends on sample size, small sample sizes may favour less complex models. However, the present study found no clear pattern between model selection frequency and the number of data points in the response, suggesting that the superior likelihood of the Gaussian model in this analysis is not a consequence of small sample size. Another possible explanation for this result lies in the distribution of the specific growth rate measurements along the temperature gradient. It is at the temperature extremes that physiological adaptations become more evident, so to realise the full potential of thermodynamic models, it is necessary to give greater emphasis to measurements at temperature extremes (Sharpe and DeMichele 1977). In the data sets used in this analysis generally most measurements were evenly spread over the temperature gradient, which may have favoured less complex models. Consequently, where researchers aim to use the Sharpe-Schoolfield model, attention needs to be focused on the experimental design to ensure that there will be sufficient measurements at these temperature extremes.

Across-species μ_{max} with no temperature inhibition

The relative deviance associated with the Arrhenius function indicated that this model best described the microalgal across-species maximum growth (μ_{max}) response, although it was only a marginally better fit to the data than the Sharpe-Schoolfield

model. Consequently, as the simple exponential (e.g., Q_{10}) function is not the most appropriate model of these across-species relationships the equation derived here (Eq. 6.8) will be a more accurate model of the microalgal μ_{max} response to temperature than the exponential function derived by Bissinger et al. (2008).

This result also suggests that it may not be appropriate to use the same temperature functions to model the within- and across-species microalgal growth responses. More specifically, whilst the Arrhenius function is a good statistical model of the microalgal μ_{max} response across species, it may not be the most appropriate model of the within-species growth response. Consequently, although the proponents of the metabolic theory of ecology (e.g., Gillooly et al. 2001; Gillooly et al. 2002; Gillooly et al. 2006) state that the Arrhenius model is applicable to within- and across-species analyses, the results of the present study suggest that this is not the case when applied to microalgae. The activation energy of 0.43 eV (SE 0.001) (Eq. 6.8) determined in the across-species analysis is significantly different from the value of 0.32 eV ($t = 220$, df = 2502, $p < 0.001$) predicted by the metabolic theory of ecology for terrestrial C3 plants (Allen et al. 2005), and to the value of 0.29 eV ($t = 3.88$, df = 3563, $p < 0.001$) for marine phytoplankton (López-Urrutia et al. 2006). These results support the general findings of Chapter 5 of this thesis i.e., that microalgal specific growth rates are more sensitive to the thermal environment than are processes associated with photosynthesis in terrestrial C3 plants.

Both Q_{10} and E_a have been used to compare thermal sensitivities in studies of multi-species assemblages when temperature extremes are excluded (e.g., Clarke 2004; Savage et al. 2004a), thus complicating comparisons between studies. As the present

study has shown that it is preferable to use the Arrhenius model, rather than the exponential function, to compare the thermal response in multi-species assemblages, this suggests that E_a may be a more accurate measure of comparative thermal sensitivity than Q_{10} in multi-species studies. This result will also give further credence to the results of those who advocate the use of activation energies as a measure of thermal sensitivity in macrophysiological (Chown et al. 2004) studies (e.g., Gillooly et al. 2001; Gillooly et al 2002; Savage et al. 2004a).

Why is the across-species μ_{max} response with no temperature inhibition non-linear? It is known that life evolved at higher temperatures than are able to sustain life forms today, suggesting that adaptation to cold temperatures has been the main thermal evolutionary driving force for some considerable time (Di Giulio 2000; van de Have 2008). The exponential-type relationship between growth and temperature suggests that the cellular costs (e.g., an increase in mitochondrial density, Clarke 1991) associated with maintaining compensatory growth rates at cooler temperatures (Clarke 2003) have proved to be a significant barrier to microalgal cold temperature adaptation (see Fig. 6.6). A similar exponential-type relationship (i.e., poor cold adaptation) between metabolism and temperature is also seen in teleost fish (Clarke et al. 1999), but not in terrestrial insects (Addo-Bediako et al. 2002), where the relationship indicates that this group is capable of cold temperature adaptation. These differences suggest that, either the costs of adapting to colder environments may be greater, or the evolutionary advantage is less, for fish and microalgae than terrestrial insects. The exponential shape of the microalgal evolutionary growth response to temperature suggests that the costs (vs. benefits) at mid-temperatures appear to be greater than would be expected if

evolutionary temperature adaptation proceeded in a linear fashion, and that the relative costs appear to decrease at very low temperatures (Fig. 6.6). The increasing solubilities of dissolved gases, such as O_2 and CO_2, with a decrease in temperature (Brown et al. 1995), may compensate for the costs of cold temperature adaptation to some degree, and may be one explanation for the shape of this response.

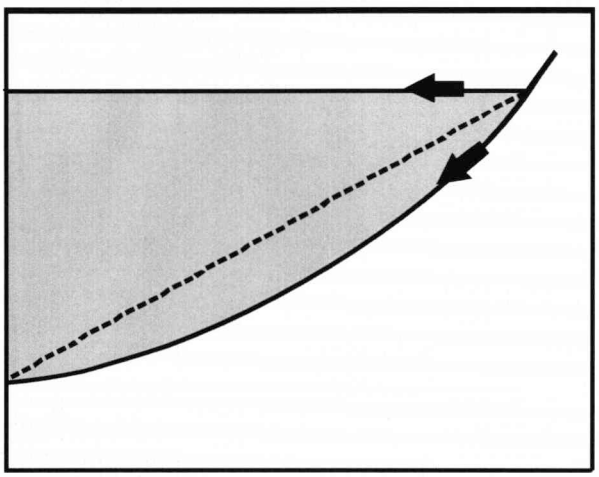

Fig. 6.6 Conceptual diagram showing evolutionary cold temperature adaptation in microalgae. The arrows represent the thermal evolutionary driving force towards growth at colder temperatures; the horizontal solid line represents perfect thermal compensation; the dashed line represents the situation that would be observed if evolutionary temperature adaptation proceeded in a linear fashion; the shaded area represents the evolutionary costs involved in attaining perfect thermal compensation (Clarke 2003).

The across-species μ_{max} response including high temperature inhibition

The Sharpe-Schoolfield function was a good model of the microalgal maximum specific growth response across species, although the relative deviances associated with each model indicates that it was only a marginally better fit to the data than the Gaussian function. A visual comparison of the Sharpe-Schoolfield and Arrhenius models (Fig. 6.5) shows how the Sharpe-Schoolfield model linearises that region of the response where there is no, or negligible, temperature inhibition of growth rates. The relative deviances associated with the more parsimonious functions (e.g., linear and exponential) examined in this analysis suggest that using these mathematically simpler functions is not appropriate when applied to a data set that exhibits high temperature inhibition (e.g., Bissinger et al. 2008). Consequently, the across-species μ_{max} temperature function derived in this study (Eq. 6.9) will provide an accurate model of microalgal maximum growth rates across a wider range of temperatures than is possible with monotonic functions (e.g., Eq. 6.8), and will be useful in those situations for which a single theoretical maximum function is required, and in which data are unavailable to make corrections for size structure or light regime.

The utility of activation energy (E_a) and enthalpy (ΔH) in multi-species comparisons

Graphically, the E_a and ΔH terms in the Arrhenius and Sharpe-Schoolfield equations represent the degree of curvature associated with the region of the thermal response where there is no temperature inhibition (see Fig. 6.5). Thus, comparisons of E_a and ΔH associated with different taxa, functional groups, or similar taxa in different

environments will facilitate a better understanding of the evolutionary pressures associated with temperature adaptation in those groups or environments.

Although many biologists prefer to work with straight line relationships (Clarke 2004), non-linear regression techniques obviate the transformational problems encountered when linearising relationships (Motulsky and Christopoulus 2004) and allow all the data to be used (Bulté and Blouin-Demers 2006). Thus, rather than continuing to use models that concentrate on that region of the thermal response where there is no temperature inhibition, it may be better to use all the available data and model the response over the full thermal range. In the present study the Gaussian equation was a good model of the within-species microalgal growth response to temperature, whereas the Sharpe-Schoolfield equation was a marginally better model of the across-species response. Applying the Sharpe-Schoolfield equation in multi-species analyses would allow the thermal sensitivities, expressed as ΔH, associated with macrophysiological (Chown et al. 2004) processes, to be compared over a wider range of temperatures and environments than is currently possible when applying the Arrhenius model.

CHAPTER 7

General Conclusions

This thesis has examined the effects of temperature and light on microalgal specific growth rates (μ) both within- and across-species. As I shall discuss, this broad approach has facilitated a better description of macroecological patterns (Brown 1995) and the pressures involved in microalgal evolutionary temperature adaptation (Clarke 2003). Here, I summarise the main findings of this study and then outline possible directions for future work.

Summary of main findings

Using a combination of quantile regression (Koenker and Bassett 1978), iterative curve fitting techniques, and information theory (Burnham and Anderson 2002) new functions have been derived describing microalgal maximum specific growth rates (μ_{max}) in response to temperature, photon-flux density (PFD), daylength, and PFD and daylength combined. When compared to the function of Eppley (1972), the μ_{max} temperature function derived in the present study supported others (e.g., Brush et al. 2002) that have suggested that the Eppley curve is too low. Moreover, when the new function was embedded in a temperate shelf-sea ecosystem model (Sharples et al. 2006) the output suggested that models that incorporate the Eppley function may underestimate primary production in cooler temperate waters by ~ 30%. Consequently, this thesis has shown that where the Eppley function has been used to predict the influence of temperature on aquatic primary production these predictions may require revision.

To my knowledge this is the first study to derive functions of μ_{max} vs. PFD, daylength, and PFD and daylength combined. Generally temperature functions have been applied in dynamic ecosystem models to set the upper limit of microalgal specific growth rates (Bowie et al. 1985), thus these new light-based μ_{max} models will provide alternative approaches to modelling primary production across large spatial and temporal scales.

In addition to these μ_{max} functions this study has also derived a general model of microalgal growth in response to daylength that will be useful in comparative studies where there is a need to normalise growth rates to a standard daylength. Furthermore, an exploration of the consequences of assuming a directly proportional relationship (e.g., assuming 24 h as 100% and 12 h as 50%) between growth rates and daylength (Brush et al. 2002; Kiørboe 1997), suggested that linear extrapolation from short daylengths to 24 h can lead to growth overestimates of as much as 65%. Consequently, this study has demonstrated that it is essential to account for the non-linearity of this relationship in calculations of primary production.

The applicability of using the daily light-dose (DLD, PFD x daylength) to describe the specific growth rate response of the freshwater flagellate *Cryptomonas* sp. across a range of DLDs was examined using an experimental approach. However, despite the appeal of integrating the two elements of the light regime into one variable, this thesis has shown that the DLD concept may not always be reliable because the shape of the growth response to DLD depends on the ratio of PFD to daylength.

The universality of the metabolic theory of ecology (MTE) (Gillooly et al. 2001; Gillooly et al. 2002; Brown et al. 2004) as applied to microalgal specific growth rates

has been addressed both within- and across-species. The results of this study indicate that the temperature dependency (expressed as an activation energy, E_a) of microalgal specific growth rates is higher than the 0.32 eV predicted (Allen et al 2005) for processes controlled by photosynthesis in terrestrial C3 plants. I propose that the observed higher thermal sensitivity of growth rates in microalgae may be because of the environmental and physiological differences between terrestrial and aquatic photosynthetic processes.

This study also found that there was no significant difference between the thermal sensitivity of the microalgal acclimatory (within-species) growth rate response and the evolutionary (across-species) response, thus this result does not support the evolutionary trade-off hypothesis (Clarke and Fraser 2004). Although the main focus of Chapter 5 was on the universality of the temperature component of the MTE another key finding was that in all analyses the allometric exponent was significantly different to the value of -0.25 predicted by the MTE. This supports the results of other studies (Banse 1982; Robinson et al. 1983; Sommer 1989; de Castro and Gaedke 2008) and suggests that microalgal specific growth rates may not conform to the quarter-power scaling relationship predicted by the MTE. I suggest that alternative life-history strategies, that are the result of adaptation to different light and nutrient regimes (Litchman et al. 2007), may complicate the relationship between cell size and growth rates in microalgae.

The most appropriate temperature function to model microalgal specific growth rates has been addressed both within- and across-species, and over that region of the response that excludes temperature extremes in addition to the response over the full

thermal range. Over that region of the response that excludes temperature extremes the within-species relationship was well described by the linear function whereas the Arrhenius (1889) function was the most appropriate model of the across-species μ_{max} relationship. This result suggests that there is little justification for continuing to use exponential functions, or the Q_{10} relationship, when modelling the within-species microalgal thermal growth response. More specifically these results indicate that, whilst the Arrhenius function is a good statistical model of the microalgal across-species μ_{max} response, it is not the most appropriate model of the within-species growth response, as has been suggested by the proponents of the MTE (e.g., Gillooly et al. 2001; Gillooly et al. 2002; Gillooly et al. 2006). Over the full thermal range the within-species relationship was well described by a Gaussian function whereas the Sharpe-Schoolfield function was the most appropriate model of the across-species μ_{max} relationship. This analysis also showed that using mathematically parsimonious functions (e.g., linear, exponential) may not be appropriate when applied to a data set that exhibits high-temperature inhibition (e.g., Chapter 2). However, as the aim in Chapter 2 was to facilitate a comparison of the slope and intercept of the Liverpool phytoplankton database (LPD) with the Eppley (1972) exponential model, the use of a parsimonious model was justified there.

This study has argued that using the activation energy (E_a) and enthalpy (ΔH) terms in the Arrhenius (1889) and Sharpe-Schoolfield models in comparative studies of different taxa, functional groups, or similar taxa in different environments will facilitate a better understanding of the evolutionary pressures associated with temperature adaptation in those groups, and may be preferred to comparisons of Q_{10}. Furthermore,

as non-linear regression techniques obviate the transformational problems encountered when linearising relationships (Motulsky and Christopoulus 2004) and allow all the data to be used (Bulté and Blouin-Demers 2006), it may be better to use all the available data and model the response over the full thermal range whenever possible.

Directions for future study

1. There is a need to assess whether the finding that the specific growth response of *Cryptomonas* sp. was more sensitive to an increase in PFD than to daylength, whilst maintaining the same total DLD, is also applicable to other microalgal species. Microalgae from diverse latitudinal provenances, and thus adapted to different daylengths, may show very different responses to this type of manipulation. Such differences in growth rate responses to daylength and PFD would facilitate a better understanding of the possible life-history trade-offs involved in microalgal ecology.
2. The suitability of the Sharpe-Schoolfield model to describe across-species thermal rate responses needs to be assessed over a broad range of taxa and also similar taxa in different environments.
3. Investigations of maximum specific growth rates in response to a single limiting environmental variable are a useful approach in multi-species analyses as they facilitate a better understanding of the nature of the macrophysiological response in question (Cade et al. 1999; Kaiser et al. 1994). However, this type of approach may fail to address much of the detail below the maximum growth envelope, such as the importance of size, taxa, habitat, salinity, and possible

interactions between these variables. Consequently, there is a need to investigate the relative importance of each of these other variables, in addition to temperature and light effects, on the microalgal specific growth rate response. One way of achieving this would be to use multiple regression. However, identifying meaningful ecological patterns from the data may be confounded because of the complex non-linear relationships and interactions between specific growth rates and these variables. Consequently, in addition to multiple regression an analytical method such as regression tree analysis (De'ath and Fabricius 2000), that is capable of handling a broad range of explanatory variable types and non-linear responses, would be an appropriate methodology to assess the importance of these variables.

REFERENCES

Addo-Bediako, A., S. L. Chown, and K. J. Gaston. 2002. Metabolic cold adaptation in insects: a large-scale perspective. Funct. Ecol. **16:** 332-338.

Admiraal, N. 1977. Influence of light and temperature on the growth rate of estuarine diatoms in culture. Mar. Biol. **39:** 1-9.

Ahlgren, G. 1987. Temperature functions in biology and their application to algal growth constants. Oikos **49:** 177-190.

Allen, A.P., J.F. Gillooly, and J.H. Brown. 2005. Linking the global carbon cycle to individual metabolism. Funct. Ecol. **19:** 202-213.

Angilletta, M. J. 2006. Estimating and comparing thermal performance curves. J. Therm. Biol. **31:** 541-545.

Antoine, D., J-M. André, and A. Morel. 1996. Oceanic primary production. Estimation and global scale from satellite (coastal zone colour scanner) chlorophyll. Glob. Biogeochem. Cyc. **10:** 57-69.

Arrhenius, S. 1889. Über die reaktionsgeschwindigkeit bei der inversion von rohrzucker durch säuren. Z. Physik. Chem. **4:** 226-248.

Atkinson, D. 1994. Temperature and organism size-a biological law for ectotherms? Adv. Ecol. Res. **25:** 1-58.

Balch, W. M., and C. F. Byrne. 1994. Factors affecting the estimate of primary production from space. J. Geophys. Res. **99:** 7555-7570.

Banse, K. 1982. Cell volumes, maximal growth rates of unicellular algae and ciliates and the role of ciliates in the marine pelagial. Limnol. Oceanogr. **27:** 1059-1071.

Behrenfeld, M. J., and P. G. Falkowski. 1997. A consumers guide to primary productivity models. Limnol. Oceanogr. **42:** 1479-1491.

Behrenfeld, M. J., J. T. Randerson, C. R. McClain, G. C. Feldman, S. O. Los, C. J. Tucker, P. G. Falkowski, C. B. Field, R. Frouin, W. E. Esaias, D. D. Kolber, and N. H. Pollack. 2001. Biospheric primary production during an ENSO transition. Science **291:** 2594-2597.

Bělehrádek, J. 1926. Influence of temperature on biological processes. Nature **118:** 117-118.

Bělehrádek, J. 1935. Temperature and living matter. Protoplasma-Monographien. Bornträger, Berlin.

Bissinger, J. E., D. J. S. Montagnes, J. Sharples, and D. Atkinson. 2008. Predicting marine phytoplankton maximum growth rates from temperature: Improving on the Eppley curve using quantile regression. Limnol. Oceanogr. **53:** 487-493.

Blackburn, T. M., J. H. Lawton, and J. N. Perry. 1992. A method of estimating the slope of upper bounds of plots of body size and abundance in natural animal assemblages. Oikos **65:** 107-112.

Blackford, J. C., J. I. Allen, and F. J. Gilbert. 2004. Ecosystem dynamics at six contrasting sites: a generic modelling study. J. Marine. Syst. **52:** 191-215.

Bokma, F. 2004. Evidence against universal metabolic allometry. Funct. Ecol. **18:** 184-187.

Bowie, G. L., W. B. Mills, D. B. Porcella, C. L. Campbell, J. R. Pagenkopf, G. L. Rupp, K. M. Johnson, P. W. H. Chan, and S. A. Gehrini. 1985. Rates, constants, and kinetics formulations in surface water quality modelling, 2nd ed. US EPA Environmental Research Laboratory.

Brand, L. E., and R. R. L. Guillard. 1981. The effects of continuous light and light intensity on the reproduction rates of twenty-two species of marine phytoplankton. J. Exp. Mar. Biol. Ecol. **50:** 119-132.

Brown, J., Colling, A., Park, D., Phillips, J., Rothery, D., Wright, J. 1995. Seawater: Its Composition, Properties and Behaviour. Butterworth-Heinemann, Oxford.

Brown, J. H. 1995. Macroecology. Univ. Chicago Press, Chicago.

Brown, J. H., J. F. Gillooly, A. P. Allen, V. M. Savage, and G. B. West. 2004. Toward a metabolic theory of ecology. Ecology **85:** 1771-1789.

Brush, M. J., J. W. Brawley, S. W. Nixon, and J. N. Kremer. 2002. Modelling phytoplankton production: problems with the Eppley curve and an empirical alternative. Mar. Ecol. Prog. Ser. **238:** 31-45.

Bulté, G., and G. Blouin-Demers. 2006. Cautionary notes on the descriptive analysis of performance curves in reptiles. J. Therm. Biol. **31:** 287-291.

Burnham, K. P., and D. M. Anderson. 2002. Model selection and multimodel inference: A practical information-theoretic approach, 2nd ed. Springer, New York.

Cade, B. S., J. W. Terrel, and R. L. Schroeder. 1999. Estimating effects of limiting factors with regression quantiles. Ecology **80:** 311-323.

Cade, B. S., and B. R. Noon. 2003. A gentle introduction to quantile regression for ecologists. Front. Ecol. Environ. **1:** 412-420.

Castenholz, R. W. 1964. The effect of daylength and light intensity on the growth of littoral marine diatoms in culture. Physiol. Plant. **17:** 951-963.

Chown, S. L. A., K. J. Gaston, and D. Robinson. 2004. Macrophysiology: large-scale patterns in physiological traits and their ecological implications. Funct. Ecol. **18:** 159-167.

Chown, S. L., E. Marais, J. S. Terblanche, C. J. Klok, J. R. B. Lighton, and T. M. Blackburn. 2007. Scaling of insect metabolic rate is inconsistent with the nutrient supply network model. Funct. Ecol. **21:** 282-290.

Clarke, A. 1991. What is cold adaptation and how should we measure it? Amer. Zool. **31:** 81-92.

Clarke, A., and N. M. Johnston. 1999. Scaling of metabolic rate with body mass and temperature in teleost fish. J. Anim. Ecol. **68:** 893-905.

Clarke, A. 2003. Costs and consequences of evolutionary temperature adaptation. Trends Ecol. Evol. **18:** 573-581.

Clarke, A. 2004. Is there a universal temperature dependence of metabolism? Funct. Ecol. **18:** 252-256.

Clarke, A., and K. P. P. Fraser. 2004. Why does metabolism scale with temperature? Funct. Ecol. **18:** 243-251.

Clarke, A. 2006. Temperature and the metabolic theory of ecology. Funct. Ecol. **20:** 405-412.

Cossins, A. R., and K. Bowler. 1987. Temperature Biology of Animals. Chapman and Hall, London.

Cugier, P., A. Ménesguen, and F.D. Guillaud. 2005. Three dimensional (3D) ecological modelling of the Bay of Seine (English Channel, France). J. Sea Res. **54:** 104-124.

De'ath, G., and K. E. Fabricius. 2000. Classification and regression trees: A powerful yet simple technique for ecological data analysis. Ecology **81:** 3178-3192.

de Castro, F., and U. Gaedke. 2008. The metabolism of lake plankton does not support the metabolic theory of ecology. Oikos. **117:** 1218-1226.

Di Giulio, M. 2000. The universal ancestor lived in a thermophilic or hyperthermophilic environment. J. Theor. Biol. **203:** 203-213.

Dodds, P. S., D. H. Rothman, and J. S. Weitz. 2001. Re-examination of the "3/4-law" of metabolism. J. Theor. Biol. **209:** 9-27.

Doney, S. C., D. M. Glover, and R. G. Najjar. 1996. A new coupled, one-dimensional biological-physical model for the upper ocean: Applications to the JGOFS Bermuda Atlantic time-series study (BATS) site. Deep-Sea Res. Pt. II. **43:** 591-694.

Downs, C. J., J. P. Hayes, and C. R. Tracy. 2008. Scaling metabolic rate with body mass and inverse body temperature: a test of the Arrhenius fractal supply model. Funct. Ecol. **22:** 239-244.

Durbin, E. G. 1974. Studies on the autecology of the marine diatom *Thalassiosira nordenskioeldii* Cleve.1. The influence of day length, light intensity, and temperature on growth. J. Phycol. **10:** 220-225.

Eppley, R. W. 1972. Temperature and phytoplankton growth in the sea. Fish. Bull. **70:** 1063-1085.

Eyring, H. 1935. The activated complex in chemical reactions. J. Chem. Phys. **3:** 107-115.

Falkowski, P. G. 1994. The role of phytoplankton photosynthesis in global biogeochemical cycles. Photosynth. Res. **39:** 235-258.

Falkowski, P. G., and J. A. Raven. 2007. Aquatic Photosynthesis. Princeton University Press, Princeton.

Farquhar, G. D., S. V. Caemmerer, and J. A. Berry. 1980. A biochemical model of photosynthetic $C0_2$ assimilation in leaves of C3 species. Planta **149:** 78-90.

Fenchel, T. 1974. Intrinsic rate of natural increase: the relationship with body size. Oecologia **14:** 317-326.

Flinn, P. W. 1991. Temperature dependent functional response of the parasitoid *Cephalonomia waterstoni* Gahan (Hymenoptera, Bethylidae) attacking rusty grain beetle larvae (Coleoptera, Cucujidae). Environ. Entomol. **20:** 872-876.

Foy, R. H. 1983. Interaction of temperature and light on the growth rates of two planktonic *Oscillatoria* species under a short photoperiod regime. Br. Phycol. J. **18:** 267-273.

Foy, R. H., and C. E. Gibson. 1993. The influence of irradiance, photoperiod and temperature on the growth kinetics of three planktonic diatoms. Eur. J. Phycol. **28:** 203-212.

Frazier, M. R., R. B. Huey, and D. Berrigan. 2006. Thermodynamic constraints the evolution of insect population growth rates: " Warmer is better". Am. Nat. **168:** 512-520.

Furnas, M. J. 1990. In situ growth rates of marine phytoplankton: approaches to measurement, community and species growth rates. J. Plankton. Res. **12:** 1117-1151.

Geider, R. J., H. L. Macintyre, and T. M. Kana. 1997. Dynamic model of phytoplankton growth and acclimation: responses of the balanced growth rate and the chlorophyll *a*: carbon ratio to light, nutrient-limitation and temperature. Mar. Ecol. Prog. Ser. **148:** 187-200.

Gibson, C. E., and R. H. Foy. 1983. The photosynthesis and growth efficiency of a planktonic blue-green alga, *Oscillatoria redekei*. Br. Phycol. J. **18:** 39-45.

Gillooly, J. F., J. H. Brown, G. B. West, V. M. Savage, and E. L. Charnov. 2001. Effects of size and temperature on metabolic rate. Science **293:** 2248-2251.

Gillooly, J. F., E. L. Charnov, G. B. West, M. Savage Van, and B. J. H. 2002. Effects of size and temperature on developmental time. Nature **417:** 70-73.

Gillooly, J. F., A. P. Allen, V. M. Savage, E. L. Charnov, S. A. West, and J. H. Brown. 2006. Response to Clarke and Fraser: effects of temperature on metabolic rate. Funct. Ecol.**: 20** 400-404.

Gilstad, M., and E. Sakshaug. 1990. Growth rates of ten diatom species from the Barents Sea at different irradiances and day lengths. Mar. Ecol. Prog. Ser. **64:** 169-173.

Gnanadesikan, A., R. D. Slater, N. Gruber, and J. L. Sarmiento. 2002. Oceanic vertical exchange and new production: a comparison between models and observations. Deep Sea Res. Part II **49:** 363-401.

Guillard, R. L., and C. J. Lorenzen. 1972. Yellow-green microalgae with chlorophyllide c. J. Phycol. **8:** 10-14.

Hinshelwood, C. N. 1947. The Chemical Kinetics of The Bacterial Cell. Oxford University Press, Oxford.

Huisman, J., N. N. P. Thi, D. M. Karl, and B. Sommeijer. 2006. Reduced mixing generates oscillations and chaos in the oceanic deep chlorophyll maximum. Nature **439:** 322-325.

Huey, R. B., and J. G. Kingsolver. 1989. Evolution of thermal sensitivity of ectotherm performance. Trends Ecol. Evol. **4:** 131-135.

Huey, R. B., and D. Berrigan. 2001. Temperature, demography, and ectotherm fitness. Am. Nat. **158:** 204-210.

IPCC. 2007. Climate Change 2007: The Physical Science Basis. Contribution of Working Group I to the Fourth Assessment Report of the Intergovernmental Panel on Climate Change [Solomon, S., D. Qin, M. Manning, Z. Chen, M. Marquis, K.B. Averyt, M. Tignor, and H.L. Miller (eds.)]. Cambridge University Press, Cambridge.

Jassby, A. D., and T. Platt. 1976. Mathematical formulation of the relationship between photosynthesis and light for phytoplankton. Limnol. Oceanogr. **21:** 540 - 547.

Johnson, F. H., H. Eyring, and B. J. Stover. 1974. Temperature. The Theory of Rate Processes in Biology and Medicine. Wiley-Interscience, New York.

Johnson, M. L. 1992. Why, when, and how biochemists should use least squares. Anal. Biochem. **206:** 215-225.

Kaiser, M.S., P. L. Speckman, and J. R. Jones. 1994. J. Am. Stat. Assoc. **426:** 410-423.

Kameda, T., and J. Ishizaka. 2005. Size-fractionated primary production estimated by a two-phytoplankton community model applicable to ocean color remote sensing. J. Oceanogr. **61:** 663-672.

Kiørboe, T. 1997. Population regulation and role of mesozooplankton in shaping marine pelagic food webs. Hydrobiologia **363:** 13-27.

Kirk, J. T. O. 1994. Light and Photosynthesis in Aquatic Ecosystems. Cambridge University Press, Cambridge.

Kleiber, M. 1947. Body size and metabolic rate. Physiol. Rev. **27:** 511-541.

Koenker, R., and G. Bassett. 1978. Regression quantiles. Econometrica **46:** 33-50.

Koenker, R., and V. d'Orey. 1987. Computing regression quantiles. Applied Statistics **36:** 383-393.

Koenker, R., and J. A. F. Machado. 1999. Goodness of fit and related inference processes for quantile regression. J. Am. Stat. Assoc. **94:** 1296-1310.

Koenker, R. 2006. quantreg: Quantile Regression. R package version 4.01. http://www.r-project.org

Krogh, A. 1914. The quantitative relation between temperature and standard metabolism in animals. Int. Z. Phys. Chem. Biol. **1:** 491-508.

Lalli, C. M., and T. R. Parsons. 2002. Biological Oceanography an Introduction. Butterworth-Heinemann, Oxford.

Landry, M. R., J. Constantinou, M. Latasa, S. L. Brown, R. R. Bidigare, and M. E. Ondrusek. 2000. Biological response to iron fertilization in the eastern equatorial Pacific (IronEx II). III. Dynamics of phytoplankton growth and microzooplankton grazing. Mar. Ecol. Prog. Ser. **201:** 57-72.

Lee, H.-W., S. Ban, T. Ikeda, and T. Matsuishi. 2003. Effect of temperature on development, growth and reproduction in the marine copepod Pseudocalanus newmani at satiating food condition. J. Plankton Res. **25:** 261-271.

Levins, R. 1966. Strategy of model building in population biology. Am. Sci. **54:** 421-431.

Li, W. K. W., and P. M. Dickie. 1987. Temperature characteristics of photosynthetic and heterotrophic activities: seasonal variations in temperate microbial plankton. App. Env. Microbiol. **53:** 2282-2295.

Litchman, E., C. A. Klausmeier, O. M. Schofield, and P. G. Falkowski. 2007. The role of functional traits and trade-offs in structuring phytoplankton communities: scaling from cellular to ecosystem level. Ecol. Lett. **10:** 1170-1181.

López-Urrutia, Á., E. San Martin, R. P. Harris, and X. Irigoien. 2006. Scaling the metabolic balance of the oceans. Proc. Natl. Acad. Sci. USA **103:** 8739-8744.

May, R. M. 1976. Estimating *r*. a pedagogical note. Am. Nat. **110:** 496-499.

McClain, C.R., and M. A. Rex. 2001. The relationship between dissolved oxygen concentration and maximum size in deep-sea turrid gastropods: an application of quantile regression. Mar. Biol. **139:** 681-685.

Menard, F., C. Labrune, Y. J. Shin, A. S. Asine, and F. X. Bard. 2006. Opportunistic predation in tuna: a size-based approach. Mar. Ecol. Prog. Ser. **323:** 223-231.

Moisan, J. R., T. A. Moisan, and M. R. Abbott. 2002. Modelling the effect of temperature on the maximum growth rates of phytoplankton populations. Ecol. Model. **153:** 197-215.

Montagnes, D. J. S. 1996. Growth responses of planktonic ciliates in the genera *Strobilidium* and *Strombidium*. Mar. Ecol. Prog. Ser. **130:** 241-254.

Montagnes, D. J. S., and D. J. Franklin. 2001. Effect of temperature on diatom volume, growth rate, and carbon and nitrogen content: Reconsidering some paradigms. Limnol. Oceanogr. **46:** 2008-2018.

Montagnes, D. J. S., S. A. Kimmance, and D. Atkinson. 2003. Using Q_{10}: Can growth rates increase linearly with temperature? Aquat. Microb. Ecol. **32:** 307-313.

Montagnes, D. J. S., and J. A. Berges. 2004. Determining parameters of the numerical response. Microbial Ecol. **48:** 139-144.

Montagnes, D. J. S., G. Morgan, J. E. Bissinger, D. Atkinson, and T. Weisse. 2008. Short-term temperature change may impact freshwater carbon flux: a microbial perspective. Global Change Biol. **14:** 1-16.

Motulsky, H., and A. Christopoulos. 2004. Fitting Models to Biological Data Using Linear and Non-Linear Regression. A Practical Guide to Curve Fitting. Oxford University Press, Oxford.

Paasche, E. 1967. Marine plankton algae grown with light-dark cycles I *Coccolithus huxleyi*. Physiol. Plant. **20:** 946-955.

Parsons, T. R., M. Takahashi, and B, Hargrave1977. Biological Oceanographic Processes, 2nd ed.. Pergamon Press, Oxford.

Raven, J. A., and R. J. Geider. 1988. Temperature and algal growth. New Phytol. **110:** 441-461.

Reynolds, C. S. 2006. Ecology of Phytoplankton. Cambridge University Press, Cambridge.

Robinson, W. R., R. H. Peters, and J. Zimmermann. 1983. The effects of body size and temperature on metabolic rate of organisms. Can. J. Zool. **61:** 281-288.

Rogers, W. H. 1992. Quantile regression standard errors. Stata Technical Bulletin **9:** 16-19.

Rose, J. M., and D. A. Caron. 2007. Does low temperature constrain the growth rates of heterotrophic protists? Evidence and implications for algal blooms in cold waters. Limnol. Oceanogr. **52:** 886-895.

Rothhaupt, K. O. 1990. Population growth rates of two closely related rotifer species: Effects of food quantity, particle size, and nutritional quality. Freshw. Biol. **23:** 561-570.

Ryther, J. H. 1969. Photosynthesis and fish production in the sea. Science. **166:** 72-76.

Savage, V. M., J. F. Gillooly, J. H. Brown, G. B. West, and E. L. Charnov. 2004a. Effects of body size and temperature on population growth. Am. Nat. **163:** 429-441.

Savage, V. M., J. F. Gillooly, W. H. Woodruff, G. B. West, A. P. Allen, B.J. Enquist, J. H. Brown. 2004b. The predominance of quarter-power scaling in biology. Funct. Ecol. **18:** 257-282.

Scharf, F. S., F. Juanes, and M. Sutherland. 1998. Inferring ecological relationships from the edges of scatter diagrams; comparison of regression techniques. Ecology **79:** 448-460.

Schoolfield, R. M., P. J. H. Sharpe, and C. E. Magnuson. 1981. Non-linear regression of biological temperature-dependent rate models based on absolute reaction-rate theory. J. Theor. Biol. **88:** 719-731.

Sharpe, P. J. H., and D. W. DeMichele. 1977. Reaction kinetics of poikilotherm development. J. Theor. Biol. **64:** 649-670.

Sharples, J., O. N. Ross, B. E. Scott, S. P. R. Greenstreet, and H. Fraser. 2006. Inter-annual variability in the timing of stratification and the spring bloom in the North-western North Sea. Cont. Shelf Res. **26:** 733-751.

Sicko-Goad, L., and N. A. Andresen. 1991. Effect of growth and light/dark cycles on diatom lipid content and composition. J. Phycol. **27:** 710-718.

Sokal, R. R., and F. J. Rohlf. 1995. Biometry: The Principles and Practices of Statistics in Biological Research. Freeman & Co. New York.

Sommer, U. 1989. Maximal growth rates of Antarctic phytoplankton: Only weak dependence on cell size. Limnol. Oceanogr. **34:** 1109-1112.

Sommer, U. 1994. The impact of light intensity and daylength on silicate and nitrate competition among marine phytoplankton. Limnol. Oceanogr. **39:** 1680-1688.

Stanistreet, M. 1996. Writing your thesis. Suggestions for planning and writing theses and dissertations in science-based disciplines. University of Liverpool.

Stevenson, R. J. 1996. An introduction to algal ecology in freshwater benthic habitats, p. 3-30. *In* R. J. Stevenson, Bothwell, M. and Lowe, R. [ed.], Algal Ecology. Academic Press, San Diego.

Tang, E. P. Y. 1995. The allometry of algal growth rates. J. Plankton Res. **17:** 1325: 1335.

Tang, E. P. Y., and W. F. Vincent. 2000. Effects of daylength and temperature on the growth and photosynthesis of an Arctic cyanobacterium, *Schizothrix calcicola* (Oscillatoriaceae). Eur. J. Phycol. **35:** 263-272.

Tett, P., S. I. Heaney, and M. R. Droop. 1985. The Redfield ratio and phytoplankton growth rate. J. Mar. Biol. Assoc. U.K. **65:** 487-504.

Thompson, P. 1999. Response of growth and biochemical composition to variations in daylength, temperature, and irradiance in the marine diatom *Thalassiosira pseudonana* (Bacillariophyceae). J. Phycol. **35:** 1215-1223.

Trudgill, D. L., A. Honek, D. Li, and N. M. Van Straalen. 2005. Thermal time - concepts and utility. Annal. Appl. Biol. **146:** 1-14.

van der Have, T. M. 2008. Slaves to the Eyring equation: Temperature Dependence of Life-History Characters in Developing Ectotherms. PhD Thesis. University of Wageningen.

Van't Hoff, J. H. 1884. Études de dynamique chimique. Muller.

Verity, P. G. 1982. Effects of temperature, irradiance, and daylength on the marine diatom *Leptocylindrus danicus* Cleve. IV. Growth. J. Exp. Mar. Biol. Ecol. **60:** 209-222.

Wagner, T.L., H. Wu., P.J.H. Sharpe., R. M. Schoolfield., and R.N. Coulson. 1984. Modeling insect development rates: a literature review and application of a biophysical model. Ann. Entomol. Soc. Am. **77:** 208:255.

White, C. R., P. Cassey, and T. M. Blackburn. 2007. Allometric exponents do not support a universal metabolic allometry. Ecology **88:** 315-323.

Yoder, J. A. 1979. Effect of temperature on light-limited growth and chemical composition of *Skeletonema costatum* (Bacillariophyceae). J. Phycol. **15:** 362-370.

Zar, J. H. 1999. Biostatistical Analysis. 4th ed. Prentice-Hall, New Jersey.

APPENDIX 1

Taxa and data sources used in the Liverpool phytoplankton database (*n* represents number of data points).

species/strain	source	temp (°C)	*n*
	Bacillariophyta		
Chaetoceros affinis	Braarud (1945)	10	1
Chaetoceros constrictus	Braarud (1945)	10	1
Coscinosira polychorda	Braarud (1945)	10	1
Eucampia zoodiacus	Braarud (1945)	10	1
Lauderia borealis	Braarud (1945)	10	1
Leptocylindrus danicus	Braarud (1945)	10	1
Skeletonema costatum	Braarud (1945)	10	1
Thalassiosira decipiens	Braarud (1945)	10	1
Thalassiosira nitzschioides	Braarud (1945)	10	1
Asterionella glacialis	Brand & Guillard (1981)	24	8
Bacteriastrum delicatulum	Brand & Guillard (1981)	24	8
Biddulphia sp.	Brand & Guillard (1981)	24	6
Corethron criophilum	Brand & Guillard (1981)	24	8
Coscinodiscus sp.	Brand & Guillard (1981)	24	8
Ditylum brightwellii	Brand & Guillard (1981)	24	7
Hemiaulus hauckii	Brand & Guillard (1981)	24	7
Streptotheca tamesis	Brand & Guillard (1981)	24	5
Thalassiosira pseudonana	Brand & Guillard (1981)	24	8
Thalassiosira sp.	Brand & Guillard (1981)	24	5
Thalassiosira pseudonana	Brand et al. (1981)	11.9-23.8	4
Skeletonema costatum	Curl & Mcleod (1961)	15-30	3
Skeletonema costatum	Davis et al. (1973)	18	1
Thalassiosira nordenskiöldii	Durbin (1974)	0-15	48
Coscinodiscus asteromphalus	Eppley & Sloan (1966)	20	1
Coscinodiscus wailesii	Eppley & Sloan (1966)	20	1
Cyclotella nana	Eppley & Sloan (1966)	21	1
Ditylum brightwellii	Eppley & Sloan (1966)	21	1
Skeletonema costatum	Eppley & Sloan (1966)	21	1
Thalassiosira fluviatilis	Eppley & Sloan (1966)	20	1
Thalassiosira rotula	Eppley & Sloan (1966)	21	1
Phaeodactylum tricornutum	Fawley (1984)	14.1-24.9	30
Chaetoceros curvisetum	Furnas (1978)	15-25	3
Skeletonema costatum	Gallagher (1982)	10-20	3
Skeletonema costatum	Gao et al. (2000)	5-25	3
Amphiprora sp.	Gilstad & Sakshaug (1990)	-0.5	26
Chaetoceros furcellatus	Gilstad & Sakshaug (1990)	-0.5	27
Nitzschia delicatissima	Gilstad & Sakshaug (1990)	-0.5	27
Nitzschia grunowii	Gilstad & Sakshaug (1990)	-0.5	27
Nitzschia vanhoeffenii	Gilstad & Sakshaug (1990)	-0.5	28
Porosira glacialis	Gilstad & Sakshaug (1990)	-0.5	26
Thalassiosira antarctica var. *borealis*	Gilstad & Sakshaug (1990)	-0.5	25
Thalassiosira bioculata	Gilstad & Sakshaug (1990)	-0.5	23
Thalassiosira bulbosa	Gilstad & Sakshaug (1990)	-0.5	26
Thalassiosira nordenskiöldii	Gilstad & Sakshaug (1990)	-0.5	26
Thalassiosira pseudonana	Goldman & McCarthy (1978)	18	1
Cyclotella nana	Guillard & Myklestad (1970)	20	1
Cyclotella nana	Guillard & Ryther (1962)	4-25	15
Detonula confervacea	Guillard & Ryther (1962)	4.1-14.5	3
Thalassiosira fluviatilis	Hobson (1974)	15-25	9
Skeletonema tropicum	Hulburt & Guilllard (1968)	16-31	9
Thalassiosira rotula	Krawiec (1982)	5-25	20
Phaeodactylum tricornutum	Kudo et al. (2000)	10-20	2
Skeletonema costatum	Langdon (1987)	15	11
Skeletonema costatum	Langdon (1988)	5-25	7
Phaeodactylum tricornutum	Li & Morris (1982)	4.8-24.4	6
Nitzschia americana	Miller & Kamykowski (1986)	25.1-30	4
Chaetoceros simplex var. *calcitrans*	Montagnes & Franklin (2001)	13-25	12
Coscinodiscus sp.	Montagnes & Franklin (2001)	8-16.5	9
Cyclotella cryptica	Montagnes & Franklin (2001)	10-25	15
Ditylum brightwellii	Montagnes & Franklin (2001)	9-20	15
Phaeodactylum tricornutum	Montagnes & Franklin (2001)	8-20	15

Skeletonema costatum	Montagnes & Franklin (2001)	9-20	12
Phaeodactylum tricornutum	Morris & Glover (1974)	7-18	3
Nitzschia closterium	Morris & Glover (1974)	7-12	2
Skeletonema costatum	Mortain-Bertrand et al. (1988)	13-18	3
Ditylum brightwellii	Paasche (1968)	3.8-33	38
Nitzschia turgidula	Paasche (1968)	20	20
Thalassiosira pseudonana	Parkhill et al. 2001	20	9
Thalassiosira curviseriata	Popovich & Gayoso (1999)	5-20	19
Porosira pseudodenticulata	Rivkin & Putt (1987)	-1	5
Thalassiosira scotia	Rivkin & Putt (1987)	-1	6
Skeletonema costatum	Sakshaug & Andresen (1986)	15	42
Skeletonema costatum	Sakshaug & Holm-Hansen (1977)	18	1
Chaetoceros pseudocurvisetum	Suzuki & Takahashi (1995)	14.9-35	11
Chaetoceros sp.	Suzuki & Takahashi (1995)	-0.1-10.1	10
Detonula confervacea	Suzuki & Takahashi (1995)	-1.9-10.3	31
Nitzschia frigida	Suzuki & Takahashi (1995)	0-6.5	11
Skeletonema costatum	Suzuki & Takahashi (1995)	2.1-30	31
Thalassiosira nordenskiöldii	Suzuki & Takahashi (1995)	-1-19.9	20
Chaetoceros sp.	Thomas (1966)	10.2-40.6	24
Chaetoceros gracilis	Thomas & Dodson (1975)	22	1
Leptocylindrus sp.	Thomas & Dodson (1975)	22	1
Chaetoceros calcitrans	Thompson et al. (1992)	10-24.9	16
Chaetoceros gracilis	Thompson et al. (1992)	12-25	16
Chaetoceros simplex	Thompson et al. (1992)	10.2-25	13
Phaeodactylum tricornutum	Thompson et al. (1992)	9.9-24.6	13
Thalassiosira pseudonana	Thompson et al. (1992)	0.2-25.9	15
Leptocylindrus danicus	Verity (1982)	5-20	49
Skeletonema costatum	Yoder (1979)	0-22	11
	Chlorophyta		
Pyramimonas sp.	Buma et al. (1993)	1	11
Asteromonas gracilis	Eppley (1963)	27	1
Asteromonas sp.	Eppley (1963)	27	1
Chlamydomonas sp.	Eppley (1963)	27	1
Dunaliella primolecta	Eppley (1963)	33.5	1
Dunaliella sp.	Eppley (1963)	25	1
Dunaliella sp.	Eppley (1963)	26	1
Dunaliella tertiolecta	Eppley (1963)	33.5	1
Tetraselmis tetrathele	Eppley (1963)	26	1
Dunaliella tertiolecta	Eppley & Sloan (1966)	12.3-25	6
Tetraselmis chui	Meseck et al. (2005)	18	12
Dunaliella tertiolecta	Morris & Glover (1974)	12-24	3
Dunaliella salina	Parsons et al. (1961)	18	1
Tetraselmis maculata	Parsons et al. (1961)	18	1
Dunaliella tertiolecta	Sosik & Mitchell (1994)	12-28	8
Nannochloris sp.	Thomas (1966)	14.9-36	22
Dunaliella tertiolecta	Thompson et al. (1992)	9.9-25.1	15
Micromonas pusilla	Throndsen (1976)	7.8-24.8	8
Pyramimonas disomata	Throndsen (1976)	14.8-28.6	3
	Cryptophyta		
Cryptomonas sp.	Buma et al. (1993)	1	11
Chroomonas salina	Hobson (1974)	10-25	12
Rhodomonas salina	Montagnes & Franklin (2001)	9-16	9
Cryptomonas sp.	Throndsen (1976)	15.1-25	3
	Haptophyta		
Emiliania huxleyi	Brand & Guillard (1981)	24	8
Gephyrocapsa oceanica	Brand & Guillard (1981)	24	8
Hymenomonas carterae	Brand & Guillard (1981)	24	8
Coccolithus huxleyi	Eppley & Sloan (1966)	21	1
Cricosphaera elongata	Eppley & Sloan (1966)	21	1
Isochrysis sp.	Hobson (1974)	10-25	12
Phaeocystis antarctica	Hong et al. (1997)	4	3
Isochrysis galbana	Montagnes & Franklin (2001)	13-25	12
Coccolithus huxleyi	Paasche (1968)	3.2-28.5	43
Monochrysis lutheri	Parsons et al. (1961)	18	1
Syracosphaera carterae	Parsons et al. (1961)	18	1
Pavlova lutheri	Sakshaug & Holm-Hansen (1977)	18	1
Isochrysis aff. *galbana*	Thompson et al. (1992)	9.8-25	12

Pavlova lutheri	Thompson et al. (1992)	10-24.9	14
Pavlova sp.	Throndsen (1976)	8-24.8	4
	Myzozoa		
Heterocapsa triquetra	Aelion & Chisholm (1985)	8-21.1	5
Ceratium candelabrum	Brand & Guillard (1981)	24	2
Ceratium platycorne	Brand & Guillard (1981)	24	6
Ceratium ranipes	Brand & Guillard (1981)	24	3
Dissodinium lunula	Brand & Guillard (1981)	24	6
Gonyaulax polyedra	Brand & Guillard (1981)	24	4
Prorocentrum micans	Brand & Guillard (1981)	24	8
Thoracosphaera heimii	Brand & Guillard (1981)	24	8
Gymnodinium catenatum	Bravo & Anderson (1994)	9.9-29	13
Peridinium trochoideum	Eppley & Sloan (1966)	21	1
Alexandrium monilatum	Juhl (2005)	20-31	3
Cochlodinium polykrikoides	Kim et al. (2004)	12.5-25	4
Gonyaulax tamarensis	Langdon (1987)	15	7
Gonyaulax tamarensis	Langdon (1988)	5-20	6
Ceratium furca	Meeson & Sweeney (1982)	10-20	24
Gonyaulax polyedra	Meeson & Sweeney (1982)	10-20	22
Amphidinium carteri	Parsons et al. (1961)	18	1
Exuviaella sp.	Parsons et al. (1961)	18	1
Gymnodinium sp.	Thomas (1966)	15.1-33.3	23
Gyrodinium estuariale	Throndsen (1976)	7.8-28.6	4
Katodinium rotundatum	Throndsen (1976)	7.9-25	4
Amphidinium carteri	Throndsen (1976)	5-29	5
	Ochrophyta		
Olisthodiscus luteus	Langdon (1987)	15	7
Olisthodiscus luteus	Langdon (1988)	10-20	6
Apedinella spinifera	Throndsen (1976)	10.1-25.1	4
Heteromastix pyriformis	Throndsen (1976)	7.9-28.7	4
Ochromonas minima	Throndsen (1976)	7.8-27.9	4
Olisthodiscus luteus	Throndsen (1976)	5.1-20	4
Pseudopedinella pyriforme	Throndsen (1976)	5-25.2	4
	Cyanobacteria		
Synechococcus bacillaris	Brand & Guillard (1981)	24	8
	Euglenozoa		
Eutreptiella gymnastica	Throndsen (1976)	5-29	6
Eutreptiella sp.	Throndsen (1976)	8-20	3

APPENDIX 2

Taxa, specific growth rates (μ, d^{-1}), daylengths (h), and data sources used in the analysis of the general microalgal growth response to daylength (n = 242). Specific growth rates marked * represent the mortality data not included in the initial model selection procedure.

species/strain	source	specific growth rate (μ, d^{-1})	μ as a proportion of that at 24h	daylength (h)
Thalassiosira nordenskiöldii	Baars (1981)	0.370	0.440	6
Thalassiosira nordenskiöldii	Baars (1981)	0.640	0.762	10
Thalassiosira nordenskiöldii	Baars (1981)	0.750	0.893	14
Thalassiosira nordenskiöldii	Baars (1981)	0.730	0.869	18
Thalassiosira nordenskiöldii	Baars (1981)	0.840	1.000	24
Cryptomonas sp.	Bissinger unpld.	-0.803*	-1.09	0
Cryptomonas sp.	Bissinger unpld.	-0.083*	-0.112	0.5
Cryptomonas sp.	Bissinger unpld.	-0.118*	-0.161	1
Cryptomonas sp.	Bissinger unpld.	0.070	0.095	2
Cryptomonas sp.	Bissinger unpld.	0.166	0.225	4
Cryptomonas sp.	Bissinger unpld.	0.297	0.403	6
Cryptomonas sp.	Bissinger unpld.	0.354	0.481	8
Cryptomonas sp.	Bissinger unpld.	0.571	0.776	10
Cryptomonas sp.	Bissinger unpld.	0.574	0.779	12
Cryptomonas sp.	Bissinger unpld.	0.644	0.875	14
Cryptomonas sp.	Bissinger unpld.	0.653	0.887	16
Cryptomonas sp.	Bissinger unpld.	0.662	0.899	18
Cryptomonas sp.	Bissinger unpld.	0.681	0.925	20
Cryptomonas sp.	Bissinger unpld.	0.681	0.925	22
Cryptomonas sp.	Bissinger unpld.	0.737	1.000	24
Thalassiosira antarctica var. *borealis*	Gilstad & Sakshaug (1990)	0.140	0.233	4
Thalassiosira antarctica var. *borealis*	Gilstad & Sakshaug (1990)	0.310	0.517	10
Thalassiosira antarctica var. *borealis*	Gilstad & Sakshaug (1990)	0.460	0.767	19
Thalassiosira antarctica var. *borealis*	Gilstad & Sakshaug (1990)	0.600	1.000	24
Thalassiosira antarctica var. *borealis*	Gilstad & Sakshaug (1990)	0.160	0.271	4
Thalassiosira antarctica var. *borealis*	Gilstad & Sakshaug (1990)	0.310	0.525	10
Thalassiosira antarctica var. *borealis*	Gilstad & Sakshaug (1990)	0.520	0.881	19
Thalassiosira antarctica var. *borealis*	Gilstad & Sakshaug (1990)	0.590	1.000	24
Thalassiosira antarctica var. *borealis*	Gilstad & Sakshaug (1990)	0.200	0.345	4
Thalassiosira antarctica var. *borealis*	Gilstad & Sakshaug (1990)	0.330	0.569	10
Thalassiosira antarctica var. *borealis*	Gilstad & Sakshaug (1990)	0.530	0.914	19
Thalassiosira antarctica var. *borealis*	Gilstad & Sakshaug (1990)	0.580	1.000	24
Thalassiosira antarctica var. *borealis*	Gilstad & Sakshaug (1990)	0.160	0.314	4
Thalassiosira antarctica var. *borealis*	Gilstad & Sakshaug (1990)	0.330	0.647	10
Thalassiosira antarctica var. *borealis*	Gilstad & Sakshaug (1990)	0.300	0.588	19
Thalassiosira antarctica var. *borealis*	Gilstad & Sakshaug (1990)	0.510	1.000	24
Thalassiosira nordenskiöldii	Gilstad & Sakshaug (1990)	0.110	0.196	4
Thalassiosira nordenskiöldii	Gilstad & Sakshaug (1990)	0.310	0.554	10
Thalassiosira nordenskiöldii	Gilstad & Sakshaug (1990)	0.290	0.518	19
Thalassiosira nordenskiöldii	Gilstad & Sakshaug (1990)	0.560	1.000	24
Thalassiosira nordenskiöldii	Gilstad & Sakshaug (1990)	0.120	0.261	4
Thalassiosira nordenskiöldii	Gilstad & Sakshaug (1990)	0.340	0.739	10
Thalassiosira nordenskiöldii	Gilstad & Sakshaug (1990)	0.270	0.587	19
Thalassiosira nordenskiöldii	Gilstad & Sakshaug (1990)	0.460	1.000	24

Thalassiosira nordenskiöldii	Gilstad & Sakshaug (1990)	0.130	0.260	4
Thalassiosira nordenskiöldii	Gilstad & Sakshaug (1990)	0.310	0.620	10
Thalassiosira nordenskiöldii	Gilstad & Sakshaug (1990)	0.390	0.780	19
Thalassiosira nordenskiöldii	Gilstad & Sakshaug (1990)	0.500	1.000	24
Thalassiosira nordenskiöldii	Gilstad & Sakshaug (1990)	0.200	0.345	4
Thalassiosira nordenskiöldii	Gilstad & Sakshaug (1990)	0.300	0.517	10
Thalassiosira nordenskiöldii	Gilstad & Sakshaug (1990)	0.440	0.759	19
Thalassiosira nordenskiöldii	Gilstad & Sakshaug (1990)	0.580	1.000	24
Thalassiosira nordenskiöldii	Gilstad & Sakshaug (1990)	0.130	0.250	4
Thalassiosira nordenskiöldii	Gilstad & Sakshaug (1990)	0.330	0.635	10
Thalassiosira nordenskiöldii	Gilstad & Sakshaug (1990)	0.430	0.827	19
Thalassiosira nordenskiöldii	Gilstad & Sakshaug (1990)	0.520	1.000	24
Porosira glacialis	Gilstad & Sakshaug (1990)	0.050	0.125	4
Porosira glacialis	Gilstad & Sakshaug (1990)	0.300	0.750	10
Porosira glacialis	Gilstad & Sakshaug (1990)	0.250	0.625	19
Porosira glacialis	Gilstad & Sakshaug (1990)	0.400	1.000	24
Porosira glacialis	Gilstad & Sakshaug (1990)	0.130	0.342	4
Porosira glacialis	Gilstad & Sakshaug (1990)	0.270	0.711	10
Porosira glacialis	Gilstad & Sakshaug (1990)	0.190	0.500	19
Porosira glacialis	Gilstad & Sakshaug (1990)	0.380	1.000	24
Porosira glacialis	Gilstad & Sakshaug (1990)	0.150	0.429	4
Porosira glacialis	Gilstad & Sakshaug (1990)	0.260	0.743	10
Porosira glacialis	Gilstad & Sakshaug (1990)	0.250	0.714	19
Porosira glacialis	Gilstad & Sakshaug (1990)	0.350	1.000	24
Nitzschia delicatissima	Gilstad & Sakshaug (1990)	0.100	0.278	4
Nitzschia delicatissima	Gilstad & Sakshaug (1990)	0.120	0.333	10
Nitzschia delicatissima	Gilstad & Sakshaug (1990)	0.350	0.972	19
Nitzschia delicatissima	Gilstad & Sakshaug (1990)	0.360	1.000	24
Nitzschia delicatissima	Gilstad & Sakshaug (1990)	0.060	0.120	4
Nitzschia delicatissima	Gilstad & Sakshaug (1990)	0.110	0.220	10
Nitzschia delicatissima	Gilstad & Sakshaug (1990)	0.420	0.840	19
Nitzschia delicatissima	Gilstad & Sakshaug (1990)	0.500	1.000	24
Nitzschia delicatissima	Gilstad & Sakshaug (1990)	0.010	0.022	4
Nitzschia delicatissima	Gilstad & Sakshaug (1990)	0.290	0.630	10
Nitzschia delicatissima	Gilstad & Sakshaug (1990)	0.340	0.739	19
Nitzschia delicatissima	Gilstad & Sakshaug (1990)	0.460	1.000	24
Nitzschia delicatissima	Gilstad & Sakshaug (1990)	0.110	0.306	4
Nitzschia delicatissima	Gilstad & Sakshaug (1990)	0.050	0.139	10
Nitzschia delicatissima	Gilstad & Sakshaug (1990)	0.300	0.833	19
Nitzschia delicatissima	Gilstad & Sakshaug (1990)	0.360	1.000	24
Thalassiosira bulbosa	Gilstad & Sakshaug (1990)	0.070	0.119	4
Thalassiosira bulbosa	Gilstad & Sakshaug (1990)	0.310	0.525	10
Thalassiosira bulbosa	Gilstad & Sakshaug (1990)	0.430	0.729	19
Thalassiosira bulbosa	Gilstad & Sakshaug (1990)	0.590	1.000	24
Thalassiosira bulbosa	Gilstad & Sakshaug (1990)	0.070	0.119	4
Thalassiosira bulbosa	Gilstad & Sakshaug (1990)	0.380	0.644	10
Thalassiosira bulbosa	Gilstad & Sakshaug (1990)	0.450	0.763	19
Thalassiosira bulbosa	Gilstad & Sakshaug (1990)	0.590	1.000	24
Thalassiosira bulbosa	Gilstad & Sakshaug (1990)	0.200	0.333	4
Thalassiosira bulbosa	Gilstad & Sakshaug (1990)	0.340	0.567	10
Thalassiosira bulbosa	Gilstad & Sakshaug (1990)	0.460	0.767	19
Thalassiosira bulbosa	Gilstad & Sakshaug (1990)	0.600	1.000	24
Thalassiosira bulbosa	Gilstad & Sakshaug (1990)	0.000	0.000	4
Thalassiosira bulbosa	Gilstad & Sakshaug (1990)	0.320	0.696	10
Thalassiosira bulbosa	Gilstad & Sakshaug (1990)	0.300	0.652	19
Thalassiosira bulbosa	Gilstad & Sakshaug (1990)	0.460	1.000	24
Thalassiosira bulbosa	Gilstad & Sakshaug (1990)	0.120	0.222	4
Thalassiosira bulbosa	Gilstad & Sakshaug (1990)	0.320	0.593	10
Thalassiosira bulbosa	Gilstad & Sakshaug (1990)	0.440	0.815	19
Thalassiosira bulbosa	Gilstad & Sakshaug (1990)	0.540	1.000	24
Thalassiosira bioculata	Gilstad & Sakshaug (1990)	0.000	0.000	4
Thalassiosira bioculata	Gilstad & Sakshaug (1990)	0.160	0.381	10
Thalassiosira bioculata	Gilstad & Sakshaug (1990)	0.290	0.690	19
Thalassiosira bioculata	Gilstad & Sakshaug (1990)	0.420	1.000	24
Thalassiosira bioculata	Gilstad & Sakshaug (1990)	0.000	0.000	4
Thalassiosira bioculata	Gilstad & Sakshaug (1990)	0.150	0.375	10
Thalassiosira bioculata	Gilstad & Sakshaug (1990)	0.330	0.825	19
Thalassiosira bioculata	Gilstad & Sakshaug (1990)	0.400	1.000	24
Thalassiosira bioculata	Gilstad & Sakshaug (1990)	0.120	0.279	4
Thalassiosira bioculata	Gilstad & Sakshaug (1990)	0.230	0.535	10

Thalassiosira bioculata	Gilstad & Sakshaug (1990)	0.300	0.698	19
Thalassiosira bioculata	Gilstad & Sakshaug (1990)	0.430	1.000	24
Chaetoceros furcellatus	Gilstad & Sakshaug (1990)	0.150	0.357	4
Chaetoceros furcellatus	Gilstad & Sakshaug (1990)	0.370	0.881	10
Chaetoceros furcellatus	Gilstad & Sakshaug (1990)	0.280	0.667	19
Chaetoceros furcellatus	Gilstad & Sakshaug (1990)	0.420	1.000	24
Chaetoceros furcellatus	Gilstad & Sakshaug (1990)	0.160	0.372	4
Chaetoceros furcellatus	Gilstad & Sakshaug (1990)	0.370	0.860	10
Chaetoceros furcellatus	Gilstad & Sakshaug (1990)	0.330	0.767	19
Chaetoceros furcellatus	Gilstad & Sakshaug (1990)	0.430	1.000	24
Nitzschia vanhoeffenii	Gilstad & Sakshaug (1990)	0.130	0.255	4
Nitzschia vanhoeffenii	Gilstad & Sakshaug (1990)	0.340	0.667	10
Nitzschia vanhoeffenii	Gilstad & Sakshaug (1990)	0.420	0.824	19
Nitzschia vanhoeffenii	Gilstad & Sakshaug (1990)	0.510	1.000	24
Nitzschia grunowii	Gilstad & Sakshaug (1990)	0.100	0.182	4
Nitzschia grunowii	Gilstad & Sakshaug (1990)	0.340	0.618	10
Nitzschia grunowii	Gilstad & Sakshaug (1990)	0.440	0.800	19
Nitzschia grunowii	Gilstad & Sakshaug (1990)	0.550	1.000	24
Nitzschia grunowii	Gilstad & Sakshaug (1990)	0.030	0.055	4
Nitzschia grunowii	Gilstad & Sakshaug (1990)	0.310	0.564	10
Nitzschia grunowii	Gilstad & Sakshaug (1990)	0.430	0.782	19
Nitzschia grunowii	Gilstad & Sakshaug (1990)	0.550	1.000	24
Nitzschia grunowii	Gilstad & Sakshaug (1990)	0.160	0.286	4
Nitzschia grunowii	Gilstad & Sakshaug (1990)	0.330	0.589	10
Nitzschia grunowii	Gilstad & Sakshaug (1990)	0.450	0.804	19
Nitzschia grunowii	Gilstad & Sakshaug (1990)	0.560	1.000	24
Tetraselmis chui	Meseck et al. (2005)	0.094	0.273	8
Tetraselmis chui	Meseck et al. (2005)	0.213	0.619	13
Tetraselmis chui	Meseck et al. (2005)	0.231	0.669	19
Tetraselmis chui	Meseck et al. (2005)	0.345	1.000	24
Tetraselmis chui	Meseck et al. (2005)	0.138	0.311	8
Tetraselmis chui	Meseck et al. (2005)	0.244	0.552	13
Tetraselmis chui	Meseck et al. (2005)	0.315	0.713	19
Tetraselmis chui	Meseck et al. (2005)	0.442	1.000	24
Tetraselmis chui	Meseck et al. (2005)	0.217	0.440	8
Tetraselmis chui	Meseck et al. (2005)	0.410	0.832	13
Tetraselmis chui	Meseck et al. (2005)	0.491	0.996	19
Tetraselmis chui	Meseck et al. (2005)	0.493	1.000	24
Coccolithus huxleyi	Paasche (1968)	0.074	0.187	6
Coccolithus huxleyi	Paasche (1968)	0.173	0.435	10
Coccolithus huxleyi	Paasche (1968)	0.331	0.830	16
Coccolithus huxleyi	Paasche (1968)	0.398	1.000	24
Coccolithus huxleyi	Paasche (1968)	0.213	0.270	6
Coccolithus huxleyi	Paasche (1968)	0.466	0.590	10
Coccolithus huxleyi	Paasche (1968)	0.691	0.875	16
Coccolithus huxleyi	Paasche (1968)	0.790	1.000	24
Coccolithus huxleyi	Paasche (1968)	0.552	0.448	6
Coccolithus huxleyi	Paasche (1968)	0.921	0.748	10
Coccolithus huxleyi	Paasche (1968)	1.227	0.997	16
Coccolithus huxleyi	Paasche (1968)	1.232	1.000	24
Coccolithus huxleyi	Paasche (1968)	0.208	0.310	6
Coccolithus huxleyi	Paasche (1968)	0.414	0.619	10
Coccolithus huxleyi	Paasche (1968)	0.610	0.911	16
Coccolithus huxleyi	Paasche (1968)	0.670	1.000	24
Coccolithus huxleyi	Paasche (1968)	0.389	0.390	6
Coccolithus huxleyi	Paasche (1968)	0.682	0.684	10
Coccolithus huxleyi	Paasche (1968)	0.970	0.973	16
Coccolithus huxleyi	Paasche (1968)	0.997	1.000	24
Coccolithus huxleyi	Paasche (1968)	0.540	0.441	6
Coccolithus huxleyi	Paasche (1968)	0.909	0.743	10
Coccolithus huxleyi	Paasche (1968)	1.214	0.991	16
Coccolithus huxleyi	Paasche (1968)	1.225	1.000	24
Coccolithus huxleyi	Paasche (1968)	0.588	0.448	6
Coccolithus huxleyi	Paasche (1968)	0.860	0.656	10
Coccolithus huxleyi	Paasche (1968)	1.104	0.842	16
Coccolithus huxleyi	Paasche (1968)	1.311	1.000	24
Nitzschia turgidula	Paasche (1968)	0.095	0.196	6
Nitzschia turgidula	Paasche (1968)	0.264	0.545	10
Nitzschia turgidula	Paasche (1968)	0.396	0.818	16
Nitzschia turgidula	Paasche (1968)	0.484	1.000	24

Nitzschia turgidula	Paasche (1968)	0.241	0.243	6
Nitzschia turgidula	Paasche (1968)	0.520	0.525	10
Nitzschia turgidula	Paasche (1968)	0.844	0.853	16
Nitzschia turgidula	Paasche (1968)	0.990	1.000	24
Nitzschia turgidula	Paasche (1968)	0.512	0.354	6
Nitzschia turgidula	Paasche (1968)	1.055	0.730	10
Nitzschia turgidula	Paasche (1968)	1.467	1.015	16
Nitzschia turgidula	Paasche (1968)	1.445	1.000	24
Nitzschia turgidula	Paasche (1968)	0.788	0.478	6
Nitzschia turgidula	Paasche (1968)	1.302	0.791	10
Nitzschia turgidula	Paasche (1968)	1.596	0.969	16
Nitzschia turgidula	Paasche (1968)	1.647	1.000	24
Skeletonema costatum	Sakshaug & Andresen (1986)	0.043	0.069	4
Skeletonema costatum	Sakshaug & Andresen (1986)	0.155	0.250	6
Skeletonema costatum	Sakshaug & Andresen (1986)	0.271	0.436	10
Skeletonema costatum	Sakshaug & Andresen (1986)	0.334	0.539	14
Skeletonema costatum	Sakshaug & Andresen (1986)	0.360	0.581	19
Skeletonema costatum	Sakshaug & Andresen (1986)	0.621	1.000	24
Skeletonema costatum	Sakshaug & Andresen (1986)	0.266	0.235	4
Skeletonema costatum	Sakshaug & Andresen (1986)	0.478	0.421	6
Skeletonema costatum	Sakshaug & Andresen (1986)	0.630	0.555	10
Skeletonema costatum	Sakshaug & Andresen (1986)	0.849	0.748	14
Skeletonema costatum	Sakshaug & Andresen (1986)	1.026	0.904	19
Skeletonema costatum	Sakshaug & Andresen (1986)	1.136	1.000	24
Skeletonema costatum	Sakshaug & Andresen (1986)	0.469	0.331	4
Skeletonema costatum	Sakshaug & Andresen (1986)	0.597	0.422	6
Skeletonema costatum	Sakshaug & Andresen (1986)	0.932	0.658	10
Skeletonema costatum	Sakshaug & Andresen (1986)	1.167	0.824	14
Skeletonema costatum	Sakshaug & Andresen (1986)	1.349	0.952	19
Skeletonema costatum	Sakshaug & Andresen (1986)	1.417	1.000	24
Skeletonema costatum	Sakshaug & Andresen (1986)	0.750	0.438	4
Skeletonema costatum	Sakshaug & Andresen (1986)	0.826	0.482	6
Skeletonema costatum	Sakshaug & Andresen (1986)	0.978	0.571	10
Skeletonema costatum	Sakshaug & Andresen (1986)	1.302	0.760	14
Skeletonema costatum	Sakshaug & Andresen (1986)	1.697	0.991	19
Skeletonema costatum	Sakshaug & Andresen (1986)	1.713	1.000	24
Skeletonema costatum	Sakshaug & Andresen (1986)	0.574	0.419	4
Skeletonema costatum	Sakshaug & Andresen (1986)	0.722	0.527	6
Skeletonema costatum	Sakshaug & Andresen (1986)	0.900	0.657	10
Skeletonema costatum	Sakshaug & Andresen (1986)	1.370	1.000	14
Skeletonema costatum	Sakshaug & Andresen (1986)	1.328	0.970	19
Skeletonema costatum	Sakshaug & Andresen (1986)	1.370	1.000	24
Skeletonema costatum	Sakshaug & Andresen (1986)	0.449	0.538	4
Skeletonema costatum	Sakshaug & Andresen (1986)	0.608	0.729	6
Skeletonema costatum	Sakshaug & Andresen (1986)	0.713	0.855	10
Skeletonema costatum	Sakshaug & Andresen (1986)	0.761	0.913	14
Skeletonema costatum	Sakshaug & Andresen (1986)	0.730	0.875	19
Skeletonema costatum	Sakshaug & Andresen (1986)	0.834	1.000	24
Schizothrix calcicola	Tang & Vincent (2000)	0.034	0.273	8
Schizothrix calcicola	Tang & Vincent (2000)	0.063	0.510	12
Schizothrix calcicola	Tang & Vincent (2000)	0.085	0.687	16
Schizothrix calcicola	Tang & Vincent (2000)	0.087	0.702	20
Schizothrix calcicola	Tang & Vincent (2000)	0.124	1.000	24
Schizothrix calcicola	Tang & Vincent (2000)	0.146	0.549	8
Schizothrix calcicola	Tang & Vincent (2000)	0.218	0.819	12
Schizothrix calcicola	Tang & Vincent (2000)	0.265	0.995	16
Schizothrix calcicola	Tang & Vincent (2000)	0.264	0.993	20
Schizothrix calcicola	Tang & Vincent (2000)	0.266	1.000	24

APPENDIX 3

Taxa, daylength, photon flux density (PFD), and sources of data used in the meta-analysis of microalgal μ_{max} as a function of PFD and daylength (n = 2178). (n represents the number of data points used).

species/strain	source	daylength (h)	PFD (μmol photons m^{-2} s^{-1})	n
	marine			
	pelagic			
Actinocyclus octonarius	Baars (1981)	6-14	18.6-46.5	4
Actinoptychus senarius	Baars (1981)	6-14	15.5-133	6
Amphidinium carteri	Parsons et al. (1961)	24	128	1
Amphiprora sp.	Gilstad & Sakshaug (1990)	4-24	3-200	19
Asterionella glacialis	Baars (1981)	14	36	1
Asterionella glacialis	Brand & Guillard (1981)	14-24	45.2-110.4	4
Asterionella kariana	Baars (1981)	6-14	18.6-46.5	3
Bacteriastrum delicatulum	Brand & Guillard (1981)	14-24	48.4-117.1	4
Bellerochea malleus	Baars (1981)	14	36	1
Biddulphia aurita	Baars (1981)	6-18	3.06-133	27
Biddulphia regia	Baars (1981)	6-14	18.6-46.5	6
Biddulphia sinensis	Baars (1981)	6-14	18.6-46.5	4
Biddulphia sp.	Brand & Guillard (1981)	14-24	43.0-100.0	3
Cerataulina bergonii	Baars (1981)	12	21	1
Ceratium candelabrum	Brand & Guillard (1981)	14	41.9-100.4	2
Ceratium furca	Meeson & Sweeney (1982)	12	4.9-191.0	22
Ceratium platycorne	Brand & Guillard (1981)	14-24	39.6-109.7	4
Ceratium ranipes	Brand & Guillard (1981)	14-24	106.9	2
Chaetoceros calcitrans	Thompson et al. (1992)	24	220	16
Chaetoceros curvisetum	Furnas (1978)	12	73.6-83.2	3
Chaetoceros debilis	Baars (1981)	6-14	12-46.5	5
Chaetoceros decipiens	Baars (1981)	18-24	26-133	3
Chaetoceros densus	Baars (1981)	18	26	1
Chaetoceros diadema	Baars (1981)	14-24	26-133	8
Chaetoceros didymus	Baars (1981)	9-14	36-53	3
Chaetoceros furcellatus	Gilstad & Sakshaug (1990)	4-24	3-200	19
Chaetoceros gracilis	Thomas & Dodson (1975)	24	156	1
Chaetoceros gracilis	Thompson et al. (1992)	24	220	16
Chaetoceros pseudocurvisetum	Suzuki & Takahashi (1995)	24	200-211.4	5
Chaetoceros simplex	Thompson et al. (1992)	24	220	13
Chaetoceros simplex var. *calcitrans*	Montagnes & Franklin (2001)	14	50	12
Chaetoceros sp.	Suzuki & Takahashi (1995)	24	50.1-201.5	10
Chaetoceros sp.	Thomas (1966)	24	168-203	9
Chaetoceros teres	Baars (1981)	14-18	3.06-146	11
Chaetoceros tortissimus	Baars (1981)	14	36	1
Coccolithus huxleyi	Eppley & Sloan (1966)	24	224	1
Coccolithus huxleyi	Paasche (1968)	6-24	17.9-224	31
Cochlodinium polykrikoides	Kim et al. (2004)	12	130	4
Corethron criophilum	Brand & Guillard (1981)	14-24	51.0-113.6	4
Coscinodiscus asteromphalus	Eppley & Sloan (1966)	24	224	1
Coscinodiscus centralis	Baars (1981)	14	4.65-146	6
Coscinodiscus concinnus	Baars (1981)	6-24	3.06-133	28
Coscinodiscus granii	Baars (1981)	6-18	18.6-133.0	6
Coscinodiscus jonesianus var. *commutata*	Baars (1981)	6-14	18.6-46.5	3
Coscinodiscus pavillardii	Baars (1981)	9-14	36-46.5	2
Coscinodiscus radiatus	Baars (1981)	6-14	15.5-46.5	5
Coscinodiscus sp.	Montagnes & Franklin (2001)	14	50	9
Coscinodiscus sp.	Brand & Guillard (1981)	14-24	42.8-108.8	4
Coscinodiscus wailesii	Eppley & Sloan (1966)	24	224	1
Cricosphaera elongata	Eppley & Sloan (1966)	24	224	1
Cryptomonas sp.	Buma et al. (1993)	12-24	4-50	10
Cyclotella cryptica	Montagnes & Franklin (2001)	14	50	15
Cyclotella nana	Guillard & Myklestad (1970)	14	60	1
Cyclotella nana	Eppley & Sloan (1966)	24	224	1
Cyclotella nana	Guillard & Ryther (1962)	24	58.5	15
Detonula confervacea	Guillard & Ryther (1962)	24	143	3
Detonula confervacea	Suzuki & Takahashi (1995)	24	3.97-208.5	27

Dissodinium lunula	Brand & Guillard (1981)	14-24	39.6-110.3	4
Ditylum brightwellii	Brand & Guillard (1981)	14-24	39.6-108.0	4
Ditylum brightwellii	Baars (1981)	6-14	18.6-53	9
Ditylum brightwellii	Montagnes & Franklin (2001)	14	50	15
Ditylum brightwellii	Paasche (1968)	6-24	13-114.1	12
Ditylum brightwellii	Eppley & Sloan (1966)	24	224	1
Dunaliella salina	Parsons et al. (1961)	24	128	1
Dunaliella tertiolecta	Eppley & Sloan (1966)	24	224	6
Dunaliella tertiolecta	Sosik & Mitchell (1994)	24	165	8
Dunaliella tertiolecta	Thompson et al. (1992)	24	220	15
Emiliania huxleyi	Brand & Guillard (1981)	14-24	46.6-108.8	4
Eucampia zoodiacus	Baars (1981)	14-18	26-36	2
Exuviaella sp.	Parsons et al. (1961)	24	128	1
Gephyrocapsa oceanica	Brand & Guillard (1981)	14-24	44.0-112.1	4
Gonyaulax polyedra	Meeson & Sweeney (1982)	12	11.1-191.1	19
Gonyaulax tamarensis	Langdon (1987)	14	32-199	4
Guinardia flaccida	Baars (1981)	6-14	26-46.5	5
Gymnodinium sp.	Thomas (1966)	24	165-224	12
Hemiaulus hauckii	Brand & Guillard (1981)	14-24	39.5-108.5	4
Heterocapsa triquetra	Aelion & Chisholm (1985)	14	100	5
Hymenomonas carterae	Brand & Guillard (1981)	14-24	41.9-112.5	4
Isochrysis aff. *galbana*	Thompson et al. (1992)	24	220	12
Isochrysis galbana	Montagnes & Franklin (2001)	14	50	12
Koliella antarctica	Vona et al. (2004)	24	130	3
Lauderia annulata	Baars (1981)	6-18	18.6-99.7	8
Leptocylindrus danicus	Verity (1982)	9-15	4.9-120.4	49
Leptocylindrus danicus	Baars (1981)	14	36	1
Leptocylindrus sp.	Thomas & Dodson (1975)	24	156	1
Lithodesmium undulatum	Baars (1981)	14	36	1
Melosira moniliformis	Baars (1981)	10-14	36-53	2
Melosira nummuloides	Baars (1981)	14	26	2
Monochrysis lutheri	Parsons et al. (1961)	24	128	1
Nannochloris sp.	Thomas (1966)	24	154-203	11
Nitzschia americana	Miller & Kamykowski (1986)	12	140	3
Nitzschia delicatissima	Gilstad & Sakshaug (1990)	4-24	3-200	19
Nitzschia frigida	Suzuki & Takahashi (1995)	24	7.2-207.2	9
Nitzschia grunowii	Gilstad & Sakshaug (1990)	4-24	3-200	19
Nitzschia turgidula	Paasche (1968)	6-24	16-112	12
Nitzschia vanhoeffenii	Gilstad & Sakshaug (1990)	4-24	3-200	20
Olisthodiscus luteus	Langdon (1987)	14	16-195	6
Pavlova lutheri	Thompson et al. (1992)	24	220	14
Peridinium trochoideum	Eppley & Sloan (1966)	24	224	1
Phaeocystis antarctica	Hong et al. (1997)	12	15-100	3
Phaeodactylum tricornutum	Montagnes & Franklin (2001)	14	50	15
Phaeodactylum tricornutum	Kudo et al. (2000)	24	85	2
Phaeodactylum tricornutum	Fawley (1984)	14	7-208	30
Phaeodactylum tricornutum	Thompson et al. (1992)	24	220	13
Porosira glacialis	Gilstad & Sakshaug (1990)	4-24	3-200	18
Prorocentrum micans	Brand & Guillard (1981)	14-24	46.1-115.3	4
Pyramimonas sp.	Buma et al. (1993)	12-24	4-50	10
Rhizosolenia alata f. *indica*	Baars (1981)	6-14	15.5-46.5	4
Rhizosolenia imbricata	Baars (1981)	6-9	18.6-46.5	2
Rhizosolenia robusta	Baars (1981)	6-14	15.5-46.5	6
Rhizosolenia setigera	Baars (1981)	6-14	18.6-46.5	8
Rhizosolenia stolterfothii	Baars (1981)	6-14	15.5-46.5	5
Rhodomonas salina	Montagnes & Franklin (2001)	14	50	9
Skeletonema costatum	Montagnes & Franklin (2001)	14	50	12
Skeletonema costatum	Gao et al. (2000)	12	150	3
Skeletonema costatum	Langdon (1987)	14	5-195	8
Skeletonema costatum	Suzuki & Takahashi (1995)	24	50.5-203.6	20
Skeletonema costatum	Yoder (1979)	9-15	11-60	11
Skeletonema costatum	Sakshaug & Andresen (1986)	4-24	12-100	24
Skeletonema costatum	Gallagher (1982)	14	180	3
Skeletonema costatum	Mortain-Bertrand et al. (1988)	24	40-120	3
Skeletonema costatum	Eppley & Sloan (1966)	24	224	1
Skeletonema costatum	Baars (1981)	6-14	18.6-36	3
Stephanopyxis palmeriana	Baars (1981)	6-14	15.5-46.5	6
Streptotheca tamesis	Brand & Guillard (1981)	14	43.0-106.0	2
Synechococcus bacillaris	Brand & Guillard (1981)	14-24	43.0-112.0	4
Synedra tabulata	Baars (1981)	9-14	36-46.5	2

Syracosphaera carterae	Parsons et al. (1961)	24	128	1
Tetraselmis chui	Meseck et al. (2005)	8-24	73-220	12
Tetraselmis maculata	Parsons et al. (1961)	24	128	1
Thalassiosira antarctica var. *borealis*	Gilstad & Sakshaug (1990)	4-24	3-200	17
Thalassiosira bioculata	Gilstad & Sakshaug (1990)	4-24	3-200	15
Thalassiosira bulbosa	Gilstad & Sakshaug (1990)	4-24	3-200	19
Thalassiosira curviseriata	Popovich & Gayoso (1999)	12	5.0-100.0	19
Thalassiosira decipiens	Baars (1981)	6-24	26.0-61.0	12
Thalassiosira eccentrica	Baars (1981)	6-18	4.7-146.0	21
Thalassiosira fluviatilis	Eppley & Sloan (1966)	24	138	1
Thalassiosira hendeyi	Baars (1981)	6-14	18.6-99.7	7
Thalassiosira levanderi	Baars (1981)	6-18	26-36	6
Thalassiosira nordenskiöldii	Suzuki & Takahashi (1995)	24	13.7-208.0	17
Thalassiosira nordenskiöldii	Gilstad & Sakshaug (1990)	4-24	3-200	18
Thalassiosira nordenskiöldii	Baars (1981)	6-24	12.0-133.0	35
Thalassiosira nordenskiöldii	Durbin (1974)	9-15	35.2-211.2	36
Thalassiosira polychorda	Baars (1981)	14	3.1-93.0	7
Thalassiosira pseudonana	Thompson et al. (1992)	24	220	15
Thalassiosira pseudonana	Brand & Guillard (1981)	14-24	42.5-108.2	4
Thalassiosira pseudonana	Parkhill et al. (2001)	12	9.0-200.0	7
Thalassiosira rotula	Krawiec (1982)	12	18.7-217.3	15
Thalassiosira rotula	Baars (1981)	6-24	22.4-133.0	37
Thalassiosira rotula	Eppley & Sloan (1966)	24	224	1
Thalassiosira sp.	Brand & Guillard (1981)	14-24	51.0	2
Thoracosphaera heimii	Brand & Guillard (1981)	14-24	42.2-106.9	4
Triceratium alternans	Baars (1981)	14	36.0	1
	benthic			
Achnanthes longipes	Lewis et al. (2002)	12	65	6
Achnanthes sp.	Waring unpld.	14	87	20
Amphiprora sp.	Admiraal (1977)	16	85	6
Bacillaria paxillifer	Baars (1981)	14	15.5-36.0	3
Cylindrotheca closterium	Mühlig-Hofmann unpld.	14	139	38
Cylindrotheca closterium	Waring unpld.	14	87	17
Navicula arenaria	Admiraal (1977)	16	85	6
Navicula comoides	Baars (1981)	9-14	36.0-46.5	4
Nitzschia ovalis	Saks (1982)	16	60	7
Nitzschia seriata	Smith et al. (1994)	24	25	8
Nitzschia sigma	Admiraal (1977)	16	85	6
Nitzschia sp.	Admiraal (1977)	16	85	6
Plagiotropis sp.	Mühlig-Hofmann unpld.	14	139	47
	brackish/estuarine			
	pelagic			
Agmenellum quadruplicatum	Parsons et al. (1961)	24	128	1
Alexandrium ostenfeldii	Jensen & Moestrup (1997)	16	45	6
Chaetoceros sp.	Renaud et al. (2002)	12	80	2
Chaetoceros sp.	Parsons et al. (1961)	24	128	1
Chaetoceros sp.	Lomas & Gilbert (1999)	14	180	3
Chlorella sorokiniana	Vona et al. (2004)	24	130	2
Coscinodiscus sp.	Parsons et al. (1961)	24	128	1
Cryptomonas sp.	Renaud et al. (2002)	12	80	2
Detonula confervacea	Smayda (1969)	24	28-168	9
Gonyaulax tamarensis	Watras et al. (1982)	14	170	25
Gyrodinium uncatenum	Lomas & Gilbert (1999)	14	180	2
Isochrysis sp.	Renaud et al. (2002)	12	80	2
Phaeodactylum tricornutum	Parsons et al. (1961)	24	128	1
Prorocentrum minimum	Lomas & Gilbert (1999)	14	180	3
Pseudo-nitzschia pseudodelicatissima	Lundholm et al. (1997)	16	55	6
Rhizosolenia fragilissima	Ignatiades & Smayda (1970)	24	28-168	12
Rhodomonas sp.	Renaud et al. (2002)	12	80	2
Skeletonema costatum	Parsons et al. (1961)	24	128	1
Thalassiosira weissflogii	Lomas & Gilbert (1999)	14	180	2
	freshwater			
	pelagic			
Asterionella formosa	Suzuki & Takahashi (1995)	24	102.1-204.9	15
Asterionella formosa	Butterwick et al. (2005)	24	100	8
Asterococcus superbus	Schlesinger et al. (1981)	24	9.2-55.2	8
Aulacoseira granulata var. *angustissima*	Coles & Jones (2000)	16	40	3

Aulacoseira subarctica	Foy & Gibson (1993)	3-18	7.8-173.2	20
Ceratium furcoides	Butterwick et al. (2005)	24	100	5
Chlamydomonas globosa	Seaburg et al. (1981)	24	75	7
Chlamydomonas intermedia	Seaburg et al. (1981)	24	75	8
Chlamydomonas subcaudata	Seaburg et al. (1981)	24	75	8
Chlorella vulgaris	Schlesinger et al. (1981)	24	9.2-55.2	8
Chlorella vulgaris	Dauta et al. (1990)	15	4.5-217.9	28
Chloromonas alpina	Seaburg et al. (1981)	24	75	8
Coelastrum microporum f. *astroidea*	Bouterfas et al. (2002)	15	225	2
Coelastrum microporum	Schlesinger et al. (1981)	24	9.2-55.2	8
Cosmarium subprotumidium	Bouterfas et al. (2002)	15	60	1
Cryptomonas erosa	Morgan & Kalff (1979)	24	3.2-128	4
Cryptomonas marssonii	Butterwick et al. (2005)	24	100	8
Cryptomonas ovata var. *palustris*	Cloern (1977)	15	13.1-153.1	14
Cryptomonas sp.	Bissinger (present study)	2-24	0.5-70	30
Cryptomonas sp.	Bissinger unpld.	24	9-138	57
Dinobryon divergens	Butterwick et al. (2005)	24	100	8
Fragilaria crotonensis	Dauta et al. (1990)	15	10.8-214.2	32
Limnothrix redekei	Nicklisch (1998)	4-12	56.3-183.0	4
Merismopedia tenuissima	Coles & Jones (2000)	16	40	3
Microcystis aeruginosa	Coles & Jones (2000)	16	40	3
Oscillatoria agardhii	Foy (1983)	3	6.6-190.3	19
Oscillatoria redekei	Foy (1983)	3	6.5-200.0	21
Oscillatoria redekei	Gibson & Foy (1983)	3-24	0.7-62.5	48
Oscillatoria sp.	Coles & Jones (2000)	16	40	3
Planktothrix agardhii	Nicklisch (1998)	4-24	61-160	3
Planktothrix agardhii	Nicklisch & Fietz (2001)	12	3.7-163.3	22
Scenedesmus acuminatus	Nicklisch (1998)	4-24	69.7-182.0	3
Scenedesmus armatus	Nicklisch (1998)	4-24	67.7-181.0	3
Selenastrum minutum	Bouterfas et al. (2002)	15	125-225	3
Staurastrum cingulum	Butterwick et al. (2005)	24	100	8
Staurastrum pingue	Dauta et al. (1990)	15	11.4-210.9	31
Stephanodiscus astraea	Foy & Gibson (1993)	3	15.3-156.8	14
Stephanodiscus hantzschii	Foy & Gibson (1993)	3	15.8-155.6	15
Stephanodiscus hantzschii	Suzuki & Takahashi (1995)	14	106.5-210.3	8
Stephanodiscus minutulus	Nicklisch (1998)	4-24	53.2-202.0	4
Stephanodiscus neoastraea	Nicklisch & Fietz (2001)	12	3.7-129.4	18
Synechocystis minima	Dauta et al. (1990)	15	11.2-220.1	23
Synedra acus	Nicklisch (1998)	4-24	60.7-203.0	
Tetraedron bitridens	Schlesinger et al. (1981)	24	9.2-55.2	8
Tribonema. Sp.	Butterwick et al. (2005)	24	100	8
Tychonema bourrellyi	Butterwick et al. (2005)	24	100	6
	freshwater			
	benthic			
Schizothrix calcicola	Tang & Vincent (2000)	8-24	225	15

APPENDIX 4 Taxa and data sources used in analyses of the temperature dependency of microalgal μ_{max}

4A) Taxa and data sources used in the within-species microalgal μ_{max} analysis and the across-species analysis of microalgal μ_{max} using quantile regression. Taxa: 1 = Bacillariophyta, 2 = Chlorophyta, 3 = Cryptophyta, 4 = Haptophyta, 5 = Myzozoa, 6 = Cyanobacteria, 7 = Charophyta.

pecies/strain	source	data points	taxa	temp (°C)	specific growth rate (μ, d^{-1})	activation energy (eV)
Heterocapsa triquetra	Aelion & Chisholm (1985)	5	5	8.0-21.1	0.300-0.625	0.3572
Cryptomonas sp.	Bissinger unpld.	9	3	7.9-21.2	0.054-0.546	0.5359
Thalassiosira pseudonana	Brand et al. (1981)	4	1	11.9-23.8	1.132-3.206	0.4725
Asterionella formosa	Butterwick et al. (2005)	6	1	2.0-17.0	0.277-0.998	0.4674
Staurastrum cingulum	Butterwick et al. (2005)	9	7	2.0-30.0	0.055-0.402	0.3821
Cryptomonas marssonii	Butterwick et al. (2005)	4	3	2.0-11.0	0.146-0.561	0.4544
Aulacoseira granulata var. angustissima	Coles & Jones (2000)	3	1	20.0-30.0	0.715-0.870	0.1515
Microcystis aeruginosa	Coles & Jones (2000)	3	6	15.0-25.0	0.174-0.910	0.4752
Dunaliella tertiolecta	Eppley & Sloan (1966)	6	2	12.3-25.0	0.444-1.608	0.5781
Aulacoseira subarctica	Foy & Gibson (1993)	3	1	3.9-12.1	0.048-0.130	0.4536
Stephanodiscus astraea	Foy & Gibson (1993)	4	1	4.0-16.0	0.125-0.331	0.4617
Cyclotella nana	Guillard & Ryther (1962)	4	1	4.0-19.7	0.374-1.792	0.4612
Phaeodactylum tricornutum	Li & Morris (1982)	5	1	4.8-19.1	0.275-1.178	0.6913
Ditylum brightwellii	Montagnes & Franklin (2001)	3	1	9.0-16.0	0.409-0.693	0.4580
Cyclotella cryptica	Montagnes & Franklin (2001)	5	1	10.0-25.0	0.447-0.775	0.2288
Isochrysis galbana	Montagnes & Franklin (2001)	3	4	16.0-25.0	0.677-0.719	0.0495
Plagiotropis sp.	Mühlig-Hofmann unpld.	5	1	5.5-19.5	0.416-2.603	0.8451
Gymnodinium galatheanum	Nielsen (1996)	4	5	7.0-20.0	0.170-0.570	0.4664
Coccolithus huxleyi	Paasche (1967)	3	4	3.3-16.5	0.398-1.232	0.4634
Merismopedia tenuissima	Coles & Jones (2000)	3	6	20.0-30.0	0.589-0.686	0.1179
Thalassiosira nordenskiöldii	Suzuki & Takahashi (1995)	5	1	0.1-14.9	0.548-0.921	0.2330
Detonula confervaceae	Suzuki & Takahashi (1995)	4	1	0.0-10.3	0.579-0.874	0.2647
Stephanodiscus hantzschii	Suzuki & Takahashi (1995)	4	1	10.0-25.0	0.478-1.344	0.5815
Skeletonema costatum	Suzuki & Takahashi (1995)	4	1	5.1-19.7	0.209-1.296	0.4647
Chaetoceros gracilis	Thompson et al. (1992)	4	1	10.1-20.6	0.518-1.602	0.4671
Isochrysis aff. galbana	Thompson et al. (1992)	5	4	9.9-24.9	0.414-1.760	0.5187
Eutreptiella gymnastica	Throndsen (1976)	3	9	5.0-14.9	0.651-1.529	0.4522
Cylindrotheca closterium	Waring unpld.	6	1	7.0-20.0	0.102-1.356	0.8657
Achnanthes sp.	Waring unpld.	6	1	7.0-20.0	0.276-0.939	0.4639
Gonyaulax tamarensis	Watras et al. (1982)	6	5	8.5-20.0	0.187-0.444	0.4258

4B) Taxa and data sources used in the analyses of: the within-species thermal sensitivity of diatom μ_{max}; the across-species thermal sensitivity of diatom μ_{max} using quantile regression; and the across-species thermal sensitivity of diatom μ_{max} using peak growth at T_{opt}.

species/strain	source	data points	temp (°C)	specific growth rate (μ, d^{-1})	activation energy (eV)
Plagiotropis sp.	Mühlig-Hofmann unpld.	5	5.5-19.5	0.416-2.603	0.8451
Cylindrotheca closterium	Waring unpld.	6	7.0-20.0	0.102-1.356	0.8657
Achnanthes sp.	Waring unpld.	6	7.0-20.0	0.276-0.939	0.4639
Thalassiosira nordenskiöldii	Suzuki & Takahashi (1995)	5	0.1-14.9	0.548-0.9214	0.2330
Detonula confervaceae	Suzuki & Takahashi (1995)	4	0.0-10.3	0.579-0.874	0.2647
Stephanodiscus hantzschii	Suzuki & Takahashi (1995)	4	10.0-25.0	0.478-1.344	0.5815
Skeletonema costatum	Suzuki & Takahashi (1995)	4	5.1-19.7	0.209-1.296	0.4647
Phaeodactylum tricornutum	Li & Morris (1982)	5	4.8-19.1	0.275-1.178	0.6913
Asterionella formosa	Butterwick et al. (2005)	6	2.0-17.0	0.277-0.998	0.4674
Aulacoseira subarctica	Foy & Gibson (1993)	3	3.9-12.1	0.048-0.130	0.4536
Stephanodiscus astraea	Foy & Gibson (1993)	4	4.0-16.0	0.125-0.331	0.4617

4C) Taxa and data sources used in the across-species thermal sensitivity of microalgal μ_{max} using peak growth at T_{opt} analysis. Taxa: 1 = Bacillariophyta, 2 = Chlorophyta, 3 = Cryptophyta, 4 = Haptophyta, 5 = Myzozoa, 6 = Cyanobacteria, 7 = Charophyta, 8 = Euglenozoa.

species/strain	source	data points	*Topt* temp(°C)	specific growth rate at *Topt* (μ,d^{-1})	taxa
Cryptomonas.sp	Bissinger unpld.	12	21	0.759	3
Asterionella formosa	Butterwick et al. (2005)	9	17	1.109	1
Cryptomonas marssonii	Butterwick et al. (2005)	9	11	0.561	3
Staurastrum cingulum	Butterwick et al. (2005)	10	30	0.658	7
Aulacoseira subarctica	Foy & Gibson (1993)	6	15.9	0.149	1
Stephanodiscus astraea	Foy & Gibson (1993)	6	16	0.331	1
Phaeodactylum tricornutum	Li & Morris (1982)	7	19.1	1.178	1
Plagiotropis sp.	Mühlig-Hofmann unpld.	6	19.5	2.603	1
Coccolithus huxleyi	Paasche (1967)	6	19.7	1.158	4
Thalassiosira nordenskiöldii	Suzuki & Takahashi (1995)	7	14.9	0.921	1
Skeletonema costatum	Suzuki & Takahashi (1995)	8	25.1	1.480	1
Stephanodiscus hantzschii	Suzuki & Takahashi (1995)	7	24.9	1.344	1
Detonula confervaceae	Suzuki & Takahashi (1995)	6	10.3	0.874	1
Eutreptiella gymnastica	Throndsen (1976)	6	20	1.616	8
Cylindrotheca closterium	Waring unpld.	7	20	1.356	1
Achnanthes sp.	Waring unpld.	7	20	0.939	1

APPENDIX 5 Taxa and data sources used in the microalgal growth rate thermal response analyses.

5A) Taxa and data sources used in the within-species microalgal growth rate thermal response analyses.

species /strain	source	most-likely model with no temperature inhibition	data points with no temperature inhibition	most-likely model with temperature inhibition	data points with temperature inhibition
Amphiprora sp.	Admiraal (1977)	Sharpe-Schoolfield	6	Flinn	7
Navicula arenaria	Admiraal (1977)			Gaussian	6
Nitzschia sigma	Admiraal (1977)	exponential	6		
Nitzschia sp.	Admiraal (1977)	Sharpe-Schoolfield	5		
Heterocapsa triquetra	Aelion & Chisholm (1985)	power	5		
Cryptomonas sp.	Bissinger unpld.	exponential	8	Flinn	13
Cryptomonas sp.	Bissinger unpld.	exponential/ Sharpe-Schoolfield	9	modified Gaussian	14
Cryptomonas sp.	Montagnes et al. (2008)	power	8	Flinn	15
Cryptomonas sp.	Bissinger unpld.	linear	8	modified Gaussian	12
Cosmarium subprotumidium	Bouterfas et al. (2002)	linear	5		
Selenastrum minutum	Bouterfas et al. (2002)	linear	5		
Gymnodinium catenatum	Bravo & Anderson (1994)			modified Gaussian	13
Asterionella formosa	Butterwick et al. (2005)	exponential/ Sharpe-Schoolfield	5	Hinshelwood	9
Ceratium furcoides	Butterwick et al. (2005)	linear	5	Gaussian	7
Cryptomonas marssonii	Butterwick et al. (2005)			quadratic	9
Dinobryon divergens	Butterwick et al. (2005)	linear	5	quadratic	9
Staurastrum cingulum	Butterwick et al. (2005)	Sharpe-Schoolfield	5	Hinshelwood	10
Tribonema Sp.	Butterwick et al. (2005)	power	5	quadratic	9
Tychonema bourrellyi	Butterwick et al. (2005)			Gaussian	6
Dunaliella tertiolecta	Eppley & Sloan (1966)	linear	6		
Haematococcus pluvialis	Fan et al. (1994)			quadratic	6
Phaeodactylum tricornutum	Fawley (1984)	power	5	Flinn	6
Phaeodactylum tricornutum	Fawley (1984)			Flinn	6
Phaeodactylum tricornutum	Fawley (1984)			quadratic	6
Phaeodactylum tricornutum	Fawley (1984)			quadratic	6
Aulacoseira subarctica	Foy & Gibson (1993)			Gaussian	6
Stephanodiscus astraea	Foy & Gibson (1993)			Flinn	6
Stephanodiscus hantzschii	Foy & Gibson (1993)			Gaussian/ quadratic	6
Skeletonema tropicum	Hulburt & Guillard (1968)	linear	6	quadratic	7
Skeletonema tropicum	Hulburt & Guilllard (1968)			quadratic	6
Skeletonema costatum	Langdon (1988)	linear	5		
Achnanthes longipes	Lewis et al. (2002)			quadratic	7
Phaeodactylum tricornutum	Li & Morris (1982)	Sharpe-Schoolfield	5	Gaussian	7
Pseudo-nitzschia pseudodelicatissima	Lundholm et al. (1997)	power	6		

Cyclotella cryptica	Montagnes & Franklin (2001)	power	5		
Amphidinium klebsii	Morton et al. (1992)	linear	6	Gaussian	11
Coolia monotis	Morton et al. (1992)	Sharpe-Schoolfield/ exponential/ Arrnenius/ power	5	Flinn	8
Gambierdiscus toxicus	Morton et al. (1992)	linear	6	Gaussian	9
Ostreopsis heptagona	Morton et al. (1992)	linear	5	Gaussian	8
Ostreopsis siamensis	Morton et al. (1992)	linear	5	Gaussian	9
Prorocentrum concavum	Morton et al. (1992)	Sharpe-Schoolfield/ exponential/ Arrhenius/ power	5	Flinn	8
Prorocentrum lima	Morton et al. (1992)			Gaussian	9
Prorocentrum mexicanum	Morton et al. (1992)			Gaussian	8
Cylindrotheca closterium	Mühlig-Hofmann unpld.	exponential	5		
Plagiotropis sp.	Mühlig - Hofmann unpld.	power	5	Flinn	6
Coccolithus huxleyi	Paasche (1967)			Flinn	6
Coccolithus huxleyi	Paasche (1967)			Gaussian	6
Coccolithus huxleyi	Paasche (1967)			Gaussian	6
Nitzschia ovalis	Saks (1982)	linear	7	Gaussian	12
Chlamydomonas globosa	Seaburg et al. (1981)	exponential	6	quadratic	8
Chlamydomonas intermedia	Seaburg et al. (1981)	Arrhenius	7	Schoolfield	9
Chlamydomonas subcaudata	Seaburg et al. (1981)	linear	6	Schoolfield	9
Chloromonas alpina	Seaburg et al. (1981)	Sharpe-Schoolfield/ Arrhenius/	6	Schoolfield	9
Nitzschia seriata	Smith et al. (1994)			Flinn	8
Asterionella formosa	Suzuki & Takahashi (1995)			quadratic	7
Detonula confervaceae	Suzuki &Takahashi (1995)			quadratic	6
Skeletonema costatum	Suzuki & Takahashi (1995)	linear	6	Gaussian	8
Stephanodiscus hantzschii	Suzuki & Takahashi (1995)	linear	5	quadratic	7
Thalassiosira nordenskiöldii	Suzuki & Takahashi (1995)			quadratic	7
Chaetoceros sp.	Thomas (1966)	linear	6		
Chaetoceros sp.	Thomas (1966)			quadratic	6
Chaetoceros sp.	Thomas (1966)			quadratic	6
Gymnodinium sp.	Thomas (1966)			quadratic	6
Gymnodinium sp.	Thomas (1966)			quadratic	6
Gymnodinium sp.	Thomas (1966)			quadratic	6
Nannochloris sp.	Thomas (1966)	linear	5	quadratic	6
Nannochloris sp.	Thomas (1966)	linear	6		
Nannochloris sp.	Thomas (1966)	power	6		
Nannochloris sp.	Thomas (1966)			quadratic	6
Chaetoceros calcitrans	Thompson et al. (1992)	power	5		
Chaetoceros simplex	Thompson et al. (1992)	linear	5		
Dunaliella tertiolecta	Thompson et al. (1992)	linear	5		
Isochrysis aff. Galbana	Thompson et al. (1992)	exponential	5		
Pavlova lutheri	Thompson et al. (1992)	exponential	5		
Phaeodactylum tricornutum	Thompson et al. (1992)	power	5		
Thalassiosira pseudonana	Thompson et al. (1992)	linear	5		
Eutreptiella gymnastica	Throndsen (1976)			quadratic	6

Achnanthes sp.	Waring unpld.	power/linear	6	Flinn	7
Cylindrotheca closterium	Waring unpld.	power	6	Gaussian	7
Gonyaulax tamarensis	Watras et al. (1982)	power	6		

5B) Taxa and data sources used in the across-species μ_{max} analysis with no high temperature inhibition

species/strain	source	temp °C	μ (d^{-1})
Amphiprora sp.	Admiraal (1977)	4.0-24.8	0.259-1.904
Navicula arenaria	Admiraal (1977)	3.9-25.0	0.149-0.958
Nitzschia sigma	Admiraal (1977)	4.0-25.0	0.146-0.416
Nitzschia sp.	Admiraal (1977)	4.0-25.0	0.243-1.726
Heterocapsa triquetra	Aelion & Chisholm (1985)	8.0-21.1	0.300-0.625
Actinocyclus octonarius	Baars (1981)	12.0-26.0	0.140-0.540
Actinoptychus senarius	Baars (1981)	6.0-20.0	0.090-0.570
Asterionella glacialis	Baars (1981)	12.0	1.150
Asterionella kariana.	Baars (1981)	12.0-20.0	0.210-0.360
Bacillaria paxillifer	Baars (1981)	12.0-16.0	0.410-0.560
Bellerochea malleus	Baars (1981)	12.0	0.260
Biddulphia aurita	Baars (1981)	-1.5-20.0	0.100-0.960
Biddulphia regia	Baars (1981)	6.0-26.0	0.130-0.680
Biddulphia sinensis	Baars (1981)	12.0-20.0	0.270-0.620
Cerataulina bergonii	Baars (1981)	18.0	0.710
Chaetoceros debilis	Baars (1981)	6.0-20.0	0.380-1.140
Chaetoceros decipiens	Baars (1981)	6.0	0.510-0.740
Chaetoceros densus	Baars (1981)	6.0	0.310
Chaetoceros diadema.	Baars (1981)	-1.5-6.0	0.270-0.950
Chaetoceros didymus	Baars (1981)	6.0-16.0	0.310-1.070
Chaetoceros teres	Baars (1981)	0.0-12.0	0.170-1.210
Chaetoceros tortissimus	Baars (1981)	12.0	0.980
Coscinodiscus centralis	Baars (1981)	12.0	0.160-0.740
Coscinodiscus concinnus	Baars (1981)	-1.5-16.0	0.090-0.590
Coscinodiscus granii	Baars (1981)	6.0-26.0	0.140-0.600
Coscinodiscus jonesianus var. commutata	Baars (1981)	12.0-26.0	0.140-0.340
Coscinodiscus pavillardii	Baars (1981)	12.0-20.0	0.530-0.680
Coscinodiscus radiatus	Baars (1981)	16.0-26.0	0.120-0.610
Ditylum brightwellii	Baars (1981)	0.0-26.0	0.150-1.050
Eucampia zoodiacus	Baars (1981)	6.0-12.0	0.350-0.950
Guinardia flaccida	Baars (1981)	6.0-20.0	0.240-0.660
Lauderia annulata	Baars (1981)	6.0-26.0	0.280-1.710
Leptocylindrus danicus	Baars (1981)	12.0	0.910
Lithodesmium undulatum	Baars (1981)	12.0	0.690
Melosira moniliformis	Baars (1981)	6.0-12.0	0.480-0.820
Melosira nummuloides	Baars (1981)	0.0-6.0	0.120-0.430
Navicula comoides	Baars (1981)	12.0-20.0	0.775-0.795
Rhizosolenia alata f. indica	Baars (1981)	16.0-26.0	0.250-0.700
Rhizosolenia imbricata	Baars (1981)	20.0	0.240-0.680
Rhizosolenia robusta	Baars (1981)	12.0-26.0	0.220-0.640
Rhizosolenia setigera	Baars (1981)	-1.5-20.0	0.140-0.830
Rhizosolenia stolterfothii	Baars (1981)	12.0-20.0	0.240-0.970
Skeletonema costatum	Baars (1981)	0.0-20.0	0.350-1.200
Stephanopyxis palmeriana	Baars (1981)	12.0-26.0	0.210-0.790
Synedra tabulata	Baars (1981)	12.0-20.0	0.370-0.410
Thalassiosira decipiens	Baars (1981)	0.0-20.0	0.110-1.080
Thalassiosira eccentrica	Baars (1981)	6.0-26.0	0.110-1.00
Thalassiosira hendeyi	Baars (1981)	12.0-20.0	0.260-0.710
Thalassiosira levanderi	Baars (1981)	0.0-12.0	0.350-1.130
Thalassiosira nordenskiöldii	Baars (1981)	-1.5-18.0	0.170-1.120
Thalassiosira polychorda	Baars (1981)	12.0	0.110-1.160
Thalassiosira rotula	Baars (1981)	-1.0-26.0	0.050-2.130
Triceratium alternans	Baars (1981)	12.0	0.740

Cryptomonas sp.	Montagnes et al. (2008)	9.7-27.3	0.057-0.759
Cryptomonas sp.	Bissinger unpld.	7.5-27.3	0.054-0.546
Cryptomonas sp.	Bissinger unpld.	16.0	0.015-0.769
Coelastrum microporum f. astroidea	Bouterfas et al. (2002)	15.1-25.2	0.467-1.162
Cosmarium subprotumidium	Bouterfas et al. (2002)	15.1-25.2	0.035-0.730
Selenastrum minutum	Bouterfas et al. (2002)	15.2-25.3	0.755-1.364
Chaetoceros affinis	Braarud (1945)	10.0	0.970
Chaetoceros constrictus	Braarud (1945)	10.0	1.248
Coscinosira polychorda	Braarud (1945)	10.0	0.693
Eucampia zoodiacus	Braarud (1945)	10.0	0.555
Lauderia borealis	Braarud (1945)	10.0	0.624
Leptocylindrus danicus	Braarud (1945)	10.0	0.347
Skeletonema costatum	Braarud (1945)	10.0	1.802
Thalassiosira decipiens	Braarud (1945)	10.0	0.901
Thalassiosira nitzschioides	Braarud (1945)	10.0	0.832
Asterionella glacialis	Brand & Guillard (1981)	24.0	0.859-3.669
Bacteriastrum delicatulum	Brand & Guillard (1981)	24.0	0.335-2.543
Biddulphia sp.	Brand & Guillard (1981)	24.0	0.000-1.690
Ceratium candelabrum	Brand & Guillard (1981)	24.0	0.106-0.087
Ceratium platycorne	Brand & Guillard (1981)	24.0	0.116-0.498
Ceratium ranipes	Brand & Guillard (1981)	24.0	0.330-0.369
Corethron criophilum	Brand & Guillard (1981)	24.0	0.660-2.203
Coscinodiscus sp.	Brand & Guillard (1981)	24.0	0.459-1.080
Dissodinium lunula	Brand & Guillard (1981)	24.0	0.166-0.260
Ditylum brightwellii	Brand & Guillard (1981)	24.0	0.227-1.267
Emiliania huxleyi	Brand & Guillard (1981)	24.0	0.774-1.932
Gephyrocapsa oceanica	Brand & Guillard (1981)	24.0	0.735-1.649
Gonyaulax polyedra	Brand & Guillard (1981)	24.0	0.417-0.693
Hemiaulus hauckii	Brand & Guillard (1981)	24.0	0.230-2.683
Hymenomonas carterae	Brand & Guillard (1981)	24.0	0.798-1.738
Prorocentrum micans	Brand & Guillard (1981)	24.0	0.281-0.863
Streptotheca tamesis	Brand & Guillard (1981)	24.0	0.008-1.575
Synechococcus bacillaris	Brand & Guillard (1981)	24.0	0.637-1.437
Thalassiosira pseudonana	Brand & Guillard (1981)	24.0	0.836-3.367
Thalassiosira sp.	Brand & Guillard (1981)	24.0	0.800-1.856
Thalassiosira pseudonana	Brand et al. (1981)	11.9-23.8	1.132-3.206
Gymnodinium catenatum	Bravo & Anderson (1994)	9.9-29.0	0.001-0.369
Cryptomonas sp.	Buma et al.(1993)	1.0	0.083-0.499
Asterionella formosa	Butterwick et al. (2005)	2.0-25.0	0.277-1.109
Ceratium furcoides	Butterwick et al. (2005)	11.0-25.0	0.042-0.201
Dinobryon divergens	Butterwick et al. (2005)	2.0-25.0	0.139-0.482
Staurastrum cingulum	Butterwick et al. (2005)	2.0-25.0	0.055-0.603
Tribonema. sp	Butterwick et al. (2005)	2.0-25.0	0.042-0.381
Tychonema bourrellyi	Butterwick et al. (2005)	8.0-25.0	0.201-0.658
Cryptomonas ovata var. palustris	Cloern (1977)	8.0-26.0	0.041-0.597
Aulacoseira granulata var. angustissima	Coles & Jones (2000)	15.0-25.0	0.418-0.779
Merismopedia tenuissima	Coles & Jones (2000)	15.0-25.0	0.186-0.626
Microcystis aeruginosa	Coles & Jones (2000)	15.0-25.0	0.174-0.910
Oscillatoria sp.	Coles & Jones (2000)	15.0-25.0	0.557-1.112
Skeletonema costatum	Curl & Mcleod (1961)	15.0-20.0	2.197-2.967
Chlorella vulgaris	Dauta et al. (1990)	10.0-25.0	0.007-1.048
Fragilaria crotonensis	Dauta et al. (1990)	10.0-25.0	0.002-0.585
Staurastrum pingue	Dauta et al. (1990)	10.0-25.0	0.030-0.736
Synechocystis minima	Dauta et al. (1990)	10.0-25.0	0.037-0.833
Skeletonema costatum	Dauta et al. (1990)	18.0	3.024
Thalassiosira nordenskiöldii	Durbin (1974)	0.0-15.0	0.020-1.250
Coccolithus huxleyi	Eppley & Sloan (1966)	21.0	1.282
Coscinodiscus asteromphalus	Eppley & Sloan (1966)	20.0	0.360
Coscinodiscus wailesii	Eppley & Sloan (1966)	20.0	0.482
Cricosphaera elongata	Eppley & Sloan (1966)	21.0	1.560
Cyclotella nana	Eppley & Sloan (1966)	21.0	1.296
Ditylum brightwellii	Eppley & Sloan (1966)	21.0	0.762
Dunaliella tertiolecta	Eppley & Sloan (1966)	12.3-25.0	0.444-1.608
Peridinium trochoideum	Eppley & Sloan (1966)	21.0	0.887
Skeletonema costatum	Eppley & Sloan (1966)	21.0	1.456
Thalassiosira fluviatilis	Eppley & Sloan (1966)	20.0	1.123

Thalassiosira rotula	Eppley & Sloan (1966)	21.0	1.192
Asteromonas gracilis	Eppley (1963)	27.0	1.250
Asteromonas sp.	Eppley (1963)	27.0	1.040
Chlamydomonas sp.	Eppley (1963)	27.0	0.760
Dunaliella sp.	Eppley (1963)	25.0-26.0	0.620-0.900
Tetraselmis tetrathele	Eppley (1963)	26.0	3.050
Haematococcus pluvialis	Fan et al. (1994)	20.1-27.9	0.906-1.301
Phaeodactylum tricornutum	Fawley (1984)	14.1-24.9	0.155-1.507
Aulacoseira subarctica	Foy & Gibson (1993)	3.9-24.1	0.022-0.286
Stephanodiscus astraea	Foy & Gibson (1993)	4.0-23.9	0.056-0.331
Stephanodiscus hantzschii	Foy & Gibson (1993)	4.1-24.2	0.051-0.402
Oscillatoria agardhii	Foy (1983)	5.0-23.0	0.010-0.203
Oscillatoria redekei	Foy (1983)	5.0-23.0	0.016-0.198
Chaetoceros curvisetum	Furnas (1978)	15.0-25.0	1.109-1.268
Skeletonema costatum	Gallagher (1982)	10.0-20.0	0.555-3.466
Skeletonema costatum	Gao et al. (2000)	5.0-25.0	0.490-1.700
Oscillatoria redekei van	Gibson & Foy (1983)	5.0-23.0	0.015-1.076
Amphiprora sp.	Gilstad & Sakshaug (1990)	-0.5	0.040-0.410
Chaetoceros furcellatus	Gilstad & Sakshaug (1990)	-0.5	0.050-0.490
Nitzschia delicatissima	Gilstad & Sakshaug (1990)	-0.5	0.010-0.500
Nitzschia grunowii	Gilstad & Sakshaug (1990)	-0.5	0.030-0.560
Nitzschia vanhoeffenii	Gilstad & Sakshaug (1990)	-0.5	0.020-0.510
Porosira glacialis	Gilstad & Sakshaug (1990)	-0.5	0.040-0.420
Thalassiosira antarctica var. borealis	Gilstad & Sakshaug (1990)	-0.5	0.010-0.600
Thalassiosira bioculata	Gilstad & Sakshaug (1990)	-0.5	0.010-0.430
Thalassiosira bulbosa	Gilstad & Sakshaug (1990)	-0.5	0.020-0.600
Thalassiosira nordenskiöldii	Gilstad & Sakshaug (1990)	-0.5	0.020-0.580
Thalassiosira pseudonana	Goldman & McCarthy (1978)	18.0	3.020
Cyclotella nana	Guillard & Ryther (1962)	4.0-25.0	0.143-1.986
Detonula confervacea	Guillard & Ryther (1962)	4.1-14.5	0.547-0.964
Chroomonas salina	Hobson (1974)	10.0-25.0	0.374-1.594
Isochrysis sp.	Hobson (1974)	10.0-25.0	0.402-2.426
Thalassiosira fluviatilis	Hobson (1974)	15.0-25.0	0.485-2.495
Phaeocystis antarctica	Hong et al. (1997)	4.0	1.019-1.144
Skeletonema tropicum	Hulburt & Guilllard (1968)	19.0-27.0	0.208-2.079
Rhizosolenia fragilissima	Ignatiades & Smayda (1970)	9.0-25.0	0.430-0.846
Alexandrium ostenfeldii	Jensen & Moestrup (1997)	11.3-20.6	0.055-0.222
Skeletonema costatum	Jȼrgensen (1968)	7.0-20.0	0.693-1.594
Alexandrium monilatum	Juhl (2005)	20.0-25.0	0.255-0.643
Cochlodinium polykrikoides	Kim et al.(2004)	12.5-25.0	0.100-0.410
Thalassiosira rotula	Krawiec (1982)	5.0-25.0	0.056-2.008
Phaeodactylum tricornutum	Kudo et al.(2000)	10.0-20.0	1.070-1.700
Gonyaulax tamarensis	Langdon (1987)	15.0	0.016-0.416
Olisthodiscus luteus	Langdon (1987)	15.0	0.039-0.610
Skeletonema costatum	Langdon (1987)	15.0	0.039-1.691
Gonyaulax tamarensis	Langdon (1988)	5.0-20.0	0.146-0.520
Olisthodiscus luteus	Langdon (1988)	15.0-25.0	0.277-1.033
Skeletonema costatum	Langdon (1988)	5.0-25.0	0.700-2.793
Achnanthes longipes	Lewis et al.(2002)	8.0-29.0	0.280-0.834
Phaeodactylum tricornutum	Li & Morris (1982)	4.8-24.4	0.275-1.178
Chaetoceros sp.	Lomas & Gilbert (1999)	4.0-20.0	0.420-1.220
Prorocentrum minimum	Lomas & Glibert (1999)	4.0-20.0	0.250-0.950
Gyrodinium uncatenum	Lomas & Glibert (1999)	15.0-20.0	0.080-0.580
Thalassiosira weissflogii	Lomas & Glibert (1999)	10.0-20.0	0.430-1.060
Pseudo-nitzschia pseudodelicatissima	Lundholm et al. (1997)	5.0-25.0	0.146-2.357
Ceratium furca	Meeson & Sweeney (1982)	10.0-20.0	0.004-0.291
Gonyaulax polyedra	Meeson & Sweeney (1982)	10.0-20.0	0.003-0.258
Tetraselmis chui	Meseck et al. (2005)	18.0	0.094-0.493
Nitzschia americana	Miller & Kamykowski (1986)	15.0-25.1	1.038-1.904
Chaetoceros simplex var. calcitrans	Montagnes & Franklin (2001)	13.0-25.0	0.399-0.697
Coscinodiscus sp.	Montagnes & Franklin (2001)	8.0-16.5	0.136-0.332
Cyclotella cryptica	Montagnes & Franklin (2001)	10.0-25.0	0.447-0.775
Ditylum brightwellii	Montagnes & Franklin (2001)	9.0-20.0	0.409-0.722
Isochrysis galbana	Montagnes & Franklin (2001)	13.0-25.0	0.624-0.719
Phaeodactylum tricornutum	Montagnes & Franklin (2001)	8.0-20.0	0.424-0.992
Rhodomonas salina	Montagnes & Franklin (2001)	9.0-16.0	0.476-0.896

Skeletonema costatum	Montagnes & Franklin (2001)	9.0-20.0	0.448-0.880
Cryptomonas erosa	Morgan & Kalff (1979)	1.0-23.5	0.017-0.853
Phaeodactylum tricornutum	Morris et al. (1974)	7.0-18.0	0.530-1.159
Dunaliella tertiolecta	Morris & Glover (1974)	12.0-24.0	0.493-1.180
Nitzschia closterium	Morris & Glover (1974)	7.0-12.0	0.263-0.491
Skeletonema costatum	Mortain-Bertrand et al. (1988)	3.0-18.0	0.402-1.386
Amphidinium klebsii	Morton et al. (1992)	19.0-29.0	0.048-0.294
Coolia monotis	Morton et al. (1992)	21.0-29.0	0.003-0.204
Gambierdiscus toxicus	Morton et al. (1992)	18.9-28.9	0.004-0.153
Ostreopsis heptagona	Morton et al. (1992)	16.0-28.9	0.002-0.160
Ostreopsis siamensis	Morton et al. (1992)	16.0-29.0	0.003-0.206
Prorocentrum concavum	Morton et al. (1992)	19.1-29.1	0.003-0.191
Prorocentrum lima	Morton et al. (1992)	21.1-28.9	0.046-0.206
Prorocentrum mexicanum	Morton et al. (1992)	21.1-28.8	0.002-0.171
Cylindrotheca closterium	Mühlig-Hofmann unpld.	5.5-23.0	0.028-2.195
Plagiotropis sp.	Mühlig-Hofmann unpld.	5.5-23.0	0.416-2.603
Planktothrix agardhii	Nicklisch & Fietz (2001)	20.0	0.051-0.535
Stephanodiscus neoastraea	Nicklisch & Fietz (2001)	20.0	0.067-1.067
Limnothrix redekei	Nicklisch (1998)	20.0	0.282-1.106
Planktothrix agardhii	Nicklisch (1998)	20.0	0.295-0.656
Scenedesmus acuminatus	Nicklisch (1998)	20.0	0.429-0.913
Scenedesmus armatus	Nicklisch (1998)	20.0	0.507-1.221
Stephanodiscus minutulus	Nicklisch (1998)	20.0	0.580-1.242
Synedra acus	Nicklisch (1998)	20.0	0.361-1.061
Gymnodinium galatheanum	Nielsen (1996)	7.0-24.0	0.170-0.570
Coccolithus huxleyi	Paasche (1967)	3.2-28.5	0.009-1.311
Ditylum brightwellii	Paasche (1968)	3.8-24.4	0.038-1.734
Nitzschia turgidula	Paasche (1968)	20.0	0.095-1.776
Thalassiosira pseudonana	Paasche (1973)	20.0	0.050-2.780
Agmenellum quadruplicatum	Parsons et al. (1961)	18.0	1.109
Amphidinium carteri	Parsons et al. (1961)	18.0	1.848
Chaetoceros sp.	Parsons et al. (1961)	18.0	0.979
Coscinodiscus sp.	Parsons et al. (1961)	18.0	0.462
Dunaliella salina	Parsons et al. (1961)	18.0	1.188
Exuviaella sp.	Parsons et al. (1961)	18.0	0.504
Monochrysis lutheri	Parsons et al. (1961)	18.0	0.875
Phaeodactylum tricornutum	Parsons et al. (1961)	18.0	0.723
Skeletonema costatum	Parsons et al. (1961)	18.0	1.280
Syracosphaera carterae	Parsons et al. (1961)	18.0	0.832
Tetraselmis maculata	Parsons et al. (1961)	18.0	2.079
Thalassiosira curviseriata	Popovich & Gayoso (1999)	5.0-20.0	0.142-1.407
Chaetoceros sp.	Renaud et al. (2002)	25.0-27.0	0.330-0.840
Isochrysis sp.	Renaud et al. (2002)	25.0-27.0	0.810-0.970
Rhodomonas sp.	Renaud et al. (2002)	25.0-27.0	0.300-0.350
Amphiprora antarctica	Rivkin & Putt (1987)	-1.0	0.102-0.281
Porosira pseudodenticulata	Rivkin & Putt (1987)	-1.0	0.433-0.487
Thalassiosira scotia	Rivkin & Putt (1987)	-1.0	0.285-0.688
Trachyneis aspera	Rivkin & Putt (1987)	-1.0	0.063-0.228
Nitzschia ovalis	Saks (1982)	15.0-27.5	0.076-1.275
Skeletonema costatum	Sakshaug et al. (1989)	15.0	0.043-1.713
Pavlova lutheri	Sakshaug & Holm-Hansen (1977)	18.0	1.317
Skeletonema costatum	Sakshaug & Holm-Hansen (1977)	18.0	2.426
Asterococcus superbus	Schlesinger et al. (1981)	16.0-26.0	0.142-0.530
Chlorella vulgaris	Schlesinger & Molot (1981)	16.0-26.0	0.151-0.864
Coelastrum microporum	Schlesinger & Molot (1981)	16.0-26.0	0.178-1.433
Tetraedron bitridens	Schlesinger & Molot (1981)	16.0-26.0	0.142-0.826
Chlamydomonas globosa	Seaburg et al. (1981)	5.0-20.0	0.534-1.262
Chlamydomonas intermedia	Seaburg et al. (1981)	-1.0-18.0	0.333-1.095
Chlamydomonas subcaudata	Seaburg et al. (1981)	-1.0-18.0	0.139-0.936
Chloromonas alpina	Seaburg et al. (1981)	-1.0-18.0	0.055-0.984
Detonula confervacea	Smayda (1969)	2.0-12.0	0.305-1.074
Nitzschia seriata	Smith et al. (1994)	-0.5-12.0	0.260-0.567
Dunaliella tertiolecta	Sosik & Mitchell (1994)	12.0-28.0	0.477-2.240
Asterionella formosa	Suzuki & Takahashi (1995)	2.1-25.0	0.003-1.315

Chaetoceros pseudocurvisetum	Suzuki & Takahashi (1995)	14.9-25.0	0.011-1.642
Chaetoceros sp.	Suzuki & Takahashi (1995)	-0.1-10.1	0.221-0.614
Detonula confervaceae	Suzuki & Takahashi (1995)	-1.9-10.3	0.048-0.911
Nitzschia frigida	Suzuki & Takahashi (1995)	0.0-6.5	0.010-0.403
Skeletonema costatum	Suzuki & Takahashi (1995)	2.1-25.1	0.009-1.480
Stephanodiscus hantzschii	Suzuki & Takahashi (1995)	5.2-25.0	0.006-1.344
Thalassiosira nordenskiöldii	Suzuki & Takahashi (1995)	-1.0-19.9	0.006-0.970
Cricosphaera elongata	Swift & Taylor (1966)	18.0	0.527
Schizothrix calcicola	Tang & Vincent (2000)	5.0-25.0	0.034-0.280
Chaetoceros gracilis	Thomas & Dodson (1975)	22.0	2.225
Leptocylindrus sp.	Thomas & Dodson (1975)	22.0	3.493
Chaetoceros sp.	Thomas (1966)	10.2-29.3	0.028-4.373
Gymnodinium sp.	Thomas (1966)	15.1-28.5	0.001-1.140
Nannochloris sp.	Thomas (1966)	14.9-29.0	0.280-2.556
Chaetoceros calcitrans	Thompson et al. (1992)	10.0-24.9	0.524-2.912
Chaetoceros gracilis	Thompson et al. (1992)	10.1-24.9	0.518-1.602
Chaetoceros simplex	Thompson et al. (1992)	10.2-25.0	0.367-2.184
Dunaliella tertiolecta	Thompson et al. (1992)	9.9-25.1	0.204-1.662
Isochrysis aff. Galbana	Thompson et al. (1992)	9.9-24.9	0.414-1.760
Pavlova lutheri	Thompson et al. (1992)	9.9-24.8	0.557-1.966
Phaeodactylum tricornutum	Thompson et al. (1992)	9.9-24.5	0.666-1.602
Thalassiosira pseudonana	Thompson et al. (1992)	9.8-24.7	0.594-1.842
Apedinella spinifera	Throndsen (1976)	10.1-25.1	0.478-1.202
Cryptomonas sp.	Throndsen (1976)	15.1-25.0	0.586-0.949
Eutreptiella gymnastica	Throndsen (1976)	5.0-29.0	0.148-1.616
Eutreptiella sp.	Throndsen (1976)	8.0-20.0	0.203-0.947
Gyrodinium estuariale	Throndsen (1976)	7.8-28.6	0.130-0.547
Heteromastix pyriformis	Throndsen (1976)	7.9-28.7	0.002-1.297
Katodinium rotundatum	Throndsen (1976)	7.9-25.0	0.593-1.023
Micromonas pusilla	Throndsen (1976)	7.8-27.8	0.474-2.857
Ochromonas minima	Throndsen (1976)	7.8-27.9	0.462-1.959
Olisthodiscus luteus	Throndsen (1976)	5.1-20.0	0.279-0.836
Pavlova sp.	Throndsen (1976)	8.0-24.8	0.690-1.187
Pseudopedinella pyriforme	Throndsen (1976)	5.0-25.2	0.147-0.978
Pyramimonas disomata	Throndsen (1976)	14.8-28.6	0.002-1.089
Amphidinium carteri	Throndsen (1976)	5.0-29.0	0.138-1.533
Leptocylindrus danicus	Verity (1982)	5.0-20.0	0.053-1.943
Chlorella sorokiniana	Vona et al. (2004)	20.0-25.0	1.040-2.450
Koliella antarctica SAG2030	Vona et al. (2004)	5.0-15.0	0.120-0.300
Achnanthes sp.	Waring unpld.	7.0-25.0	0.276-0.939
Cylindrotheca closterium	Waring unpld.	7.0-20.0	0.102-1.356
Gonyaulax tamarensis	Watras et al. (1982)	8.5-20.0	0.187-0.444
Skeletonema costatum	Yoder (1979)	0.0-22.0	0.326-2.641

5C) Additional data used in μ_{max} analysis including high temperature inhibition

species/strain	source	temp °C	μ (d^{-1})
Amphiprora sp.	Admiraal (1977)	29.9	1.641
Chaetoceros pseudocurvisetum	Suzuki & Takahashi (1995)	30.0-35.1	0.020-1.073
Stephanodiscus hantzschii	Suzuki & Takahashi (1995)	30.0	0.846
Skeletonema costatum	Suzuki & Takahashi (1995)	29.9-30.0	0.010-0.879
Nitzschia americana	Miller & Kamykowski (1986)	30.0	1.839
Amphidinium klebsii	Morton et al. (1992)	31.0-35.0	0.047-0.187
Coolia monotis	Morton et al. (1992)	31.1-35.1	0.006-0.140
Ostreopsis siamensis	Morton et al. (1992)	31.1-32.9	0.002-0.034
Prorocentrum concavum	Morton et al. (1992)	31.0-33.1	0.003-0.116
Prorocentrum lima	Morton et al. (1992)	31.0-33.1	0.038-0.113
Prorocentrum mexicanum	Morton et al. (1992)	30.9-32.9	0.064-0.094
Gambierdiscus toxicus	Morton et al. (1992)	30.9-35.0	0.002-0.085
Ostreopsis heptagona	Morton et al. (1992)	30.9	0.004
Aulacoseira granulata var. angustissima	Coles & Jones (2000)	30.0	0.870
Microcystis aeruginosa	Coles & Jones (2000)	30.0	1.096
Merismopedia tenuissima	Coles & Jones (2000)	30.0	0.686
Oscillatoria sp.	Coles & Jones (2000)	30.0	1.098
Achnanthes longipes	Lewis et al. (2002)	32.1	0.273
Selenastrum minutum	Bouterfas et al. (2002)	30.3-35.3	1.557-1.749
Coelastrum microporum f. astroidea	Bouterfas et al. (2002)	30.0-35.1	1.602-1.650
Cosmarium subprotumidium	Bouterfas et al. (2002)	30.2-35.2	0.880-1.010
Chaetoceros sp.	Renaud et al. (2002)	30.0-35.0	0.760-0.870
Cryptomonas sp.	Renaud et al. (2002)	30.0	0.270
Rhodomonas sp.	Renaud et al. (2002)	30.0-33.0	0.150-0.230
Isochrysis sp.	Renaud et al. (2002)	30.0-33.0	0.680-0.890
Alexandrium monilatum	Juhl (2005)	31.0	0.653
Skeletonema costatum	Curl & Mcleod 1961	30.0	2.967
Staurastrum cingulum	Butterwick et al. (2005)	30.0	0.658
Nitzschia ovalis	Saks (1982)	30.0-36.0	0.132-0.776
Chlorella sorokiniana	Vona et al. (2004)	30.0-35.0	2.880-3.180
Chlorella vulgaris	Dauta et al. (1990)	30.0-35.0	0.277-1.171
Fragilaria crotonensis	Dauta et al. (1990)	30.0-35.0	0.004-0.435
Staurastrum pingue	Dauta et al. (1990)	30.0-35.0	0.008-0.710
Synechocystis minima	Dauta et al. (1990)	30.0-35.0	0.455-1.180
Ditylum brightwellii	Paasche (1968)	29.8-33.0	0.006-1.295
Haematococcus pluvialis	Fan et al. (1994)	30.9-32.8	0.046-0.705
Rhizosolenia fragilissima	Ignatiades & Smayda (1970)	30.0	0.631
Dunaliella tertiolecta	Eppley (1963)	33.5	3.470
Dunaliella primolecta	Eppley (1963)	33.5	3.120
Skeletonema tropicum	Hulburt & Guilllard (1968)	31.0	1.664
Gymnodinium sp.	Thomas (1966)	30.2-31.7	0.006-0.830
Chaetoceros sp.	Thomas (1966)	29.4-40.6	0.011-3.883
Nannochloris sp.	Thomas (1966)	30.0-36.0	1.660-2.999
Actinocyclus octonarius	Baars (1981)	30.0	0.790
Actinoptychus senarius	Baars (1981)	30.0	0.730
Biddulphia sinensis	Baars (1981)	30.0	0.990
Coscinodiscus granii	Baars (1981)	30.0	0.700
Coscinodiscus jonesianus var. commutata	Baars (1981)	30.0	0.740
Coscinodiscus pavillardii	Baars (1981)	30.0	0.880
Coscinodiscus radiatus	Baars (1981)	30.0	0.830
Ditylum brightwellii	Baars (1981)	30.0	1.080
Rhizosolenia imbricata	Baars (1981)	30.0	1.080
Thalassiosira eccentrica	Baars (1981)	30.0	0.810

References

Admiraal, N. 1977. Influence of light and temperature on the growth rate of estuarine benthic diatoms in culture. Mar. Biol. **39:** 1-9.

Aelion, C. M., and S. W. Chisholm. 1985. Effect of temperature on growth and ingestion rates of *Favella* sp. J. Plankton. Res. **7:** 821-830.

Baars, J. W. M. 1981. Autecological investigations on marine diatoms 2. Generation times of 50 species. Hydrobiol. Bull. **18:** 137-151.

Bouterfas, R., M. Belkoura, and A. Dauta. 2002. Light and temperature effects on the growth rate of three freshwater algae isolated from a eutrophic lake. Hydrobiologia **489:** 207-217.

Braarud, T. 1945. Experimental studies on marine plankton diatoms. Avh. Norske Vidensk.-Akad. Oslo. 1. Mat.-Naturv. Kl. 1944 **10:** 3-16.

Brand, L. E., and R. R. L. Guillard. 1981. The effects of continuous light and light intensity on the reproduction rates of twenty-two species of marine phytoplankton. J. Exp. Mar. Biol. Ecol. **50:** 119-132.

Brand, L. E., L. S. Murphy, R. R. L. Guillard, and H.-T. Lee. 1981. Genetic variability and differentiation in the temperature niche component of the diatom *Thalassiosira pseudonana*. Mar. Biol. **62:** 103-110.

Bravo, I., and D. M. Anderson. 1994. The effects of temperature, growth medium and darkness on excystment and growth of the toxic dinoflagellate *Gymnodium catenatum* from northwest Spain. J. Plankton Res. **16:** 513-525.

Buma, A. G. J., A. A. M. Noordeloos, and J. Larsen. 1993. Strategies and kinetics of photoacclimation in three Antarctic nanophytoflagellates. J. Phycol. **29:** 407-417.

Butterwick, C., S. I. Heaney, and J. F. Talling. 2005. Diversity in the influence of temperature on the growth rates of freshwater algae, and its ecological significance. Freshwater Biol. **50:** 291-300.

Cloern, J. E. 1977. Effects of light intensity and temperature on *Cryptomonas Ovata* (Cryptophyceae) growth and nutrient uptake rates. J. Phycol **13:** 389-395.

Coles, J. F., and R. C. Jones 2000. Effect of temperature on photosynthesis-light response and growth of four phytoplankton species isolated from a tidal freshwater river. J. Phycol. **36:** 7-16.

Curl, H. J., and G. C. Mcleod. 1961. The physiological ecology of a marine diatom *Skeletonema costatum* (Grev.) Cleve. J. Mar. Res. **19:** 70-88.

Dauta, A., J. Devaux, F. Piquemal, and L. Boumnich. 1990. Growth rate of four freshwater algae in relation to light and temperature. Hydrobiologia **207:** 221-226.

Davis, C. O., P. J. Harrison., and R. C. Dugdale. 1973. Continuous culture of marine diatoms under silicate limitation. I. Synchronized life cycle of *Skeletonema costatum*. J. Phycol. **9:** 175-180.

Durbin, E. G. 1974. Studies on the autecology of the marine diatom *Thalassiosira nordenskiöldii* Cleve.1. The influence of daylength, light intensity, and temperature on growth. J. Phycol. **10:** 220-225.

Eppley, R. W. 1963. Evaluation of certain marine algal flagellates for mass culture. Tech. Doc. Rep. No. SAM-TDR-63-91. USAF School of Aerospace Medicine. Brooks Air Force Base, Tex.

Eppley, R. W., and P. R. Sloan. 1966. Growth rates of marine phytoplankton: correlation with light absorption by cell chlorophyll *a*. Physiol. Plant. **19:** 47-59.

Fan, L., A. Vonshak, and S. Boussiba. 1994. Effect of temperature and irradiance on growth of *Haematococcus pluvialis* (Chlorophyceae). J. Phycol. **30:** 829-833.

Fawley, M. W. 1984. Effects of light Intensity and temperature interactions on growth characteristics of *Phaeodactylum tricornutum* (Bacillariophyceae). J. Phycol. **20:** 67-72.

Foy, R. H. 1983. Interaction of temperature and light on the growth rates of two planktonic *Oscillatoria* species under a short photoperiod regime. Br. Phycol. J. **18:** 267-273.

Foy, R. H., and C. E. Gibson. 1993. The influence of irradiance, photoperiod and temperature on the growth kinetics of three planktonic diatoms. Eur. J. Phycol. **28:** 203-212.

Furnas, M. J. 1978. Influence of temperature and cell size on the division rate and chemical content of the diatom *Chaetoceros curvisetum* Cleve. J. Exp. Mar. Biol. Ecol. **34:** 97-109.

Gallagher, J. C. 1982. Physiological variation and electrophoretic banding patterns of genetically different seasonal populations of *Skeletonema costatum* (Bacillariophyceae). J. Phycol. **18:** 148-162.

Gao, Y., G. J. Smith, and R. S. Alberte. 2000. Temperature dependence of nitrate reductase activity in marine phytoplankton: biochemical analysis and ecological implications. J. Phycol. **36:** 304-313.

Gibson, C. E., and R. H. Foy. 1983. The photosynthesis and growth efficiency of a planktonic blue-green alga, *Oscillatoria redekei*. Br. phycol. J. **18:** 39-45.

Gilstad, M., and E. Sakshaug. 1990. Growth rates of ten diatom species from the Barents Sea at different irradiances and day lengths. Mar. Ecol. Prog. Ser. **64:** 169-173.

Goldman, J. C., and J. J. Mccarthy. 1978. Steady state growth and ammonium uptake of a fast-growing marine diatom. Limnol. Oceanogr. **23:** 695-703.

Guillard, R. R. L., and J. H. Ryther. 1962. Studies of marine planktonic diatoms .1. *Cyclotella Nana* Hustedt, and *Detonula confervacea* (Cleve) Gran. Can. J. Microbiol. **8:** 229-239.

Guillard, R. R. L., and S. Myklestad. 1970. Osmotic and ionic requirements of the marine centric diatom *Cyclotella nana*. Helgoländer wiss. Meersunters. **20:** 104-110.

Hobson, L. A. 1974. Effects of interactions of irradiance, daylength, and temperature on division rates of three species of marine unicellular algae. J. Fish. Res. Bd. Can. **31:** 391-395.

Hong, Y., W. O. Smith, and A-M. White. 1997. Studies on transparent exopolymer particles (TEP) produced in the Ross Sea (Antarctica) and by *Phaeocystis antarctica* (Prymnesiophyceae). J. Phycol. **33:** 368-376.

Hulburt, E. M., and R. R. L. Guillard. 1968. Relationship of the distribution of the diatom *Skeletonema tropicum* to temperature. Ecology **49:** 337-339.

Ignatiades, L., and T. J. Smayda. Autecological studies on the marine diatom *Rhizosolenia fragilissima* Bergon. I The influence of light, temperature, and salinity. J. Phycol. **6:** 332-339.

Jensen, M. Ø., and Ø. Moestrup. 1997. Autecology of the toxic dinoflagellate *Alexandrium ostenfeldii*: life history and growth at different temperatures and salinities. Eur. J. Phycol. **32:** 9-18.

Jȼrgensen, E. 1968. Adaptation of plankton algae .2. Aspects of temperature adaptation of *Skeletonema costatum*. Physiol. Plant. **21:** 423-427.

Juhl, A. R. 2005. Growth rates and elemental composition of *Alexandrium monilatum*, a red-tide dinoflagellate. Harmful Algae **4:** 287-295.

Kim, D.-I., Y. Matsuyama, S. Nagasoe, M. Yamaguchi, Y-H. Yoon, Y. Oshima, N. Imada, and T. Honjo. 2004. Effects of temperature, salinity and irradiance on the growth of the harmful red tide dinoflagellate *Cochlodinium polykrikoides* Margalef (Dinophyceae). J. Plankton Res. **26:** 61-66.

Krawiec, R. W. 1982. Autecology and clonal variability of the marine centric diatom *Thalassiosira rotula* (Bacillariophyceae) in response to light, temperature and salinity. Mar. Biol. **69:** 79-89.

Kudo, I., M. Miyamoto, Y. Noiri, and Y. Maita. 2000. Combined effects of temperature and iron on the growth and physiology of the marine diatom *Phaeodactylum tricornutum* (Bacillariophyceae). J. Phycol. **36:** 1096-1102.

Langdon, C. 1987. On the causes of interspecific differences in the growth irradiance relationship for phytoplankton .1. A comparative study of the growth irradiance relationship of 3 marine phytoplankton species - *Skeletonema costatum*, *Olisthodiscus luteus* and *Gonyaulax tamarensis*. J. Plankton Res. **9:** 459-482.

---. 1988. On the causes of interspecific differences in the growth-irradiance relationship for phytoplankton. II. A general review. J. Plankton Res. **10:** 1291-1312.

Lewis, R. L., L. M. Johnson, and K. D. Hoagland. 2002. Effects of cell density, temperature, and light intensity on growth and stalk production in the biofouling diatom *Achnanthes longipes* (Bacillariophyceae). J. Phycol. **38:** 1125-1131.

Li, W. K. W., and I. Morris. 1982. Temperature adaptation in *Phaeodactylum tricornutum* Bohlin: Photosynthetic rate compensation and capacity. J. Exp. Mar. Biol. Ecol **58:** 135-150.

Lomas, M. W., and P. M. Gilbert. 1999. Interactions between NH_4^+ and NO_3^- uptake and assimilation: comparison of diatoms and dinoflagellates at several growth temperatures. Mar. Biol. **133:** 541-551.

Lundholm, N., J. Skov, R. Pocklington, and Ø. Moestrup. 1997. Studies on the marine planktonic diatom *Pseudo-nitzschia*. 2. Autecology of *P. pseudodelicatissima* based on isolates from Danish waters. Phycologia **36:** 381-388.

Meeson, B. W., and B. M. Sweeney. 1982. Adaptation of *Ceratium furca* and *Gonyaulax polyedra* (Dinophyceae) to different temperatures and irradiances: growth rates and cell volumes. J. Phycol. **18:** 241-245.

Meseck, S. L., J. H. Alix, and G. H. Wikfors. 2005. Photoperiod and light intensity effects on growth and utilization of nutrients by the aquaculture feed microalga, *Tetreselmis chui* (PLY429). Aquaculture **246:** 393-404.

Miller, R. L., and D. L. Kamykowski. 1986. Effects of temperature, salinity, irradiance and diurnal periodicity on growth and photosynthesis in the diatom *Nitzschia americana*: light-saturated growth. J. Phycol. **22:** 339-348.

Montagnes, D. J. S., and D. J. Franklin. 2001. Effect of temperature on diatom volume, growth rate, and carbon and nitrogen content: Reconsidering some paradigms. Limnol. Oceanogr. **46:** 2008-2018.

Montagnes, D. J. S., G. Morgan, J. E. Bissinger, D. Atkinson, and T. Weisse. 2008. Short-term temperature change may impact freshwater carbon flux: a microbial perspective. Global Change Biol. **14:** 1-16.

Morgan, K. C., and J. Kalff. 1979. Effect of light and temperature interactions on growth of *Cryptomonas erosa* (Cryptophyceae). J. Phycol. **15:** 127-134.

Morris, I., and H. E. Glover. 1974. Questions on the mechanism of temperature adaptation in marine phytoplankton. Mar. Biol. **24:** 147-154.

Mortain-Bertrand, A., C. Descolas-Gros, and H. Jupin. 1988. Growth, photosynthesis and carbon metabolism in the temperate marine diatom *Skeletonema costatum* adapted to low temperature and low photon-flux density. Mar. Biol. **100:** 135-141.

Morton, S. L., D. R. Norris, and B. J. W. 1992. Effect of temperature, salinity and light intensity on the growth and seasonality of toxic dinoflagellates associated with ciguetera. J. Exp. Mar. Biol. Ecol. **157:** 79-90.

Nicklisch, A. 1998. Growth and light absorption of some planktonic cyanobacteria, diatoms and Chlorophyceae under simulated natural light fluctuations. J. Plankton Res. **20:** 105-119.

Nicklisch, A., and S. Fietz. 2001. The influence of light fluctuations on growth and photosynthesis of *Stephanodiscus neaostraea* (diatom) and *Planktothrix agardhii* (cyanobacterium). Arch. Hydrobiol. **151:** 141-156.

Nielsen, M. V. 1996. Growth and chemical composition of the toxic dinoflagellate *Gymnodinium galatheanum* in relation to irradiance, temperature and salinity. Mar. Ecol. Prog. Ser. **136:** 205-211.

Paasche, E. 1967. Marine plankton algae grown with light-dark cycles I. *Coccolithus huxleyi*. Physiol. Plant. **20:** 946-955.

---. 1968. Marine plankton algae grown with light-dark cycles. II. *Ditylum brightwellii* and *Nitzschia turgidula*. Physiol. Plant. **21:** 66-77.

---. 1973. Silicon and ecology of marine plankton diatoms .1. *Thalassiosira pseudonana* (*Cyclotella nana*) grown in a chemostat with silicate as limiting nutrient. Mar. Biol. **19:** 117-126.

Parkhill, J-P., G. Maillet., and J. J. Cullen. 2001. Fluorescence-based maximal quantum yield for PSII as a diagnostic of nutrient stress. J. Phycol. **37:** 517-529.

Parsons, T. R., K. Stephens, and J. D. H. Strickland. 1961. On the chemical composition of eleven species of marine phytoplankters. J. Fish. Res. Bd. Can. **18:** 1001-1016.

Popovich, C. A., and A. M. Gayoso. 1999. Effect of irradiance and temperature on the growth rate of *Thalassiosira curviseriata* Takano (Bacillariophyceae), a bloom diatom in Bahía Blanca estuary (Argentina). J. Plankton Res. **21:** 1101-1110.

Renaud, S. M., L.-V. Thinh, G. Lambrinidis, and D. L. Parry. 2002. Effect of temperature on growth, chemical composition and fatty acid composition of tropical Australian microalgae grown in batch cultures. Aquaculture **211:** 195-214.

Rivkin, R. B., and M. Putt. 1987. Photosynthesis and cell division by antarctic microalgae: comparison of benthic, planktonic and ice algae. J. Phycol. **23:** 223-229.

Saks, N. M. 1982. Temperature, salinity and ultraviolet irradiation effects on the growth of strains of *Nitzschia ovalis*. Mar. Biol. **68:** 175-179.

Sakshaug, E., K. Anderson, and D. A. Kiefer. 1989. A steady state description of growth and light absorption in the marine planktonic diatom *Skeletonema costatum*. Limnol. Oceanogr. **34:** 198-205.

Sakshaug, E., and K. Andresen. 1986. Effect of light regime upon growth rate and chemical composition of a clone of *Skeletonema costatum* from the Trondheimsfjord, Norway. J. Plankton Res. **8:** 619-637.

Sakshaug, E., and O. Holm-hansen. 1977. Chemical composition of *Skeletonema costatum* (Grev.) Cleve and *Pavlova* (*Monochrysis*) *lutheri* (Droop) Green as a function of nitrate-, phosphate-, and iron-limited growth. J. Exp. Mar. Biol. Ecol. **29:** 1-34.

Schlesinger, D. A., L. A. Molot, and B. J. Shuter. 1981. Specific growth rates of freshwater algae in relation to cell size and light intensity. Can. J. Fish. Aquat. Sci. **38:** 1052-1058.

Seaburg, K. G., B. C. Parker, R. A. Wharton Jr., and G. M. Simmons Jr. 1981. Temperature-growth responses of algal isolates from Antarctic oases. J. Phycol. **17:** 353-360.

Smayda, T. J. 1969. Experimental observations on the influence of temperature, light, and salinity on cell division of the marine diatom, *Detonula confervacea* (Cleve) Gran. J. Phycol. **5:** 150-157.

Smith, R. E. H., L. C. Stapleford, and R. S. Ridings. 1994. The acclimated response of growth, photosynthesis, composition and carbon balance to temperature in the psychrophilic ice diatom *Nitzschia seriata*. J. Phycol. **30:** 8-16.

Sosik, H. M., and B. G. Mitchell. 1994. Effects of temperature on growth, light absorption, and quantum yield in *Dunaliella tertiolecta* (Chlorophyceae). J. Phycol. **30:** 833-840.

Suzuki, Y., and M. Takahashi. 1995. Growth responses of several diatom species isolated from various environments to temperature. J. Phycol. **31:** 880-888.

Swift, E., and W. R. Taylor. 1966. Effect of pH on the division rate of the coccolithophorid *Cricosphaera elongata*. J. Phycol. **2:** 121-125.

Tang, E. P. Y., and W. F. Vincent. 2000. Effects of daylength and temperature on the growth and photosynthesis of an Arctic cyanobacterium, *Schizothrix calcicola* (Oscillatoriaceae). Eur. J. Phycol. **35:** 263-272.

Thomas, W. H. 1966. Effects of temperature and illuminance on cell division rates of three species of tropical oceanic phytoplankton. J. Phycol. **2:** 17-22.

Thomas, W. H., and A. N. Dodson. 1975. On silicic acid limitation of diatoms in near-surface waters of the eastern tropical Pacific Ocean. Deep-Sea Res. **22:** 671-677.

Thompson, P. A., M. Guo, and P. J. Harrison. 1992. Effects of variation in temperature. I. On the biochemical composition of eight species of marine phytoplankton. J. Phycol. **28:** 481-488.

Throndsen, J. 1976. Occurrence and productivity of small marine flagellates. Norw. J. Bot. **23:** 269-293

Verity, P. G. 1982. Effects of temperature, irradiance, and daylength on the marine diatom *Leptocylindrus danicus* Cleve. IV. Growth. J. Exp. Mar. Biol. Ecol. **60:** 209-222.

Vona, V., V. Di. M. Rigano, O. Lobosco, S. Carfagna, S. Esposito, and C. Rigano. 2004. Temperature responses of growth, photosynthesis, respiration and NADH: nitrate reductase in cryophilic and mesophilic algae. New Phytol. **163:** 325-331.

Watras, C. J., S. W. Chisholm, and D. M. Anderson. 1982. Regulation of growth in an estuarine clone of *Gonyaulax tamarensis* Lebour: salinity-dependent temperature responses. J. Exp. Mar. Biol. Ecol. **62:** 25-37.

Yoder, J. A. 1979. Effect of temperature on light-limited growth and chemical composition of *Skeletonema costatum* (Bacillariophyceae). J. Phycol. **15:** 362-370.

APPENDIX 6

Two papers that have arisen directly (Bissinger et al. 2008) or indirectly (Montagnes et al. 2008) from this thesis.

Limnol. Oceanogr., 53(2), 2008, 487–493

Predicting marine phytoplankton maximum growth rates from temperature: Improving on the Eppley curve using quantile regression

Jan E. Bissinger[1] *and David J. S. Montagnes*
School of Biological Sciences, University of Liverpool, Crown Street, Biosciences Building, Liverpool L69 7ZB, UK

Jonathan Sharples
Proudman Oceanographic Laboratory, 6 Brownlow Street, Liverpool L3 5DA, UK

David Atkinson[2]
School of Biological Sciences, University of Liverpool, Crown Street, Biosciences Building, Liverpool L69 7ZB, UK

Abstract

The Eppley curve describes an exponential function that defines the maximum attainable daily growth rate of marine phytoplankton as a function of temperature. The curve was originally fitted by eye as the upper envelope of a data set, and despite its wide use, the reliability of this function has not been statistically tested. Our analysis of the data using quantile regression indicates that while the curve appears to be a good estimate of the edge of the data, it may not be reliable because the data set is small (n = 162). We construct a contemporary, comprehensive data set (n = 1,501) and apply an objective approach, quantile regression, to estimate its upper edge (99th quantile). This analysis yields a new predictive equation, $\mu_{max} = 0.81e^{0.0631T}$, that describes the maximum specific growth rates (μ_{max}, d^{-1}) of marine phytoplankton as a function of temperature (T, °C). The Liverpool phytoplankton database (LPD) curve is higher than the Eppley curve across all temperatures, and at temperatures below 19°C, the Eppley curve falls below the lower 95% confidence interval of the LPD curve. However, the LPD Q_{10} value (1.88) is identical to that of the Eppley curve and thus supports the use of models that incorporate this as an estimate of phytoplankton growth-rate response to temperature change. To assess the potential effect of the LPD curve on primary production, we embedded the LPD function into a one-dimensional numerical model of a temperate, pelagic ecosystem. This analysis suggests that models using the Eppley function will underestimate primary production by as much as 30%.

Models of aquatic primary production are useful tools to predict global biogeochemical fluxes and better inform those involved in aquatic resource management. Marine phytoplankton are a key component of many of these models both because of their carbon assimilation (Behrenfeld et al. 2001) and because of their effect on other ecosystem components (Ryther 1969). Because the utility of such models hinges on the quality of the parameters, we need to be confident in their reliability. Thus, here we apply a statistical technique to assess the reliability of a parameter that relates phytoplankton maximum growth rates to temperature, which is a key component of numerous aquatic production models (e.g., Tett et al. 1985). Furthermore, the difference between this relationship and the growth-rate response of heterotrophic protists to temperature has been implicated in the formation of algal blooms in high-latitude ecosystems (Rose and Caron 2007). Thus, the consequences of correctly interpreting the data are considerable.

In dynamic ecosystem production models, a temperature function is often used to set the upper limit of phytoplankton growth rates. From this theoretical maximum, growth rates are then reduced by applying coefficients relating to environmental limiting factors such as day length, photon flux density, and nutrients (Bowie et al. 1985). One temperature function commonly used is that developed by Eppley (1972):

$$\mu_{max} = 0.59e^{0.0633T} \quad (1)$$

This exponential relationship defines the maximum attainable daily growth rate (μ_{max}, d^{-1}) of phytoplankton as a function of temperature (T, °C) and has the advantage over more complex functions of being able to generate predictions in the absence of other data, such as community composition or phytoplankton size. The relationship was formulated from a compilation of data from laboratory culture studies in which light and nutrients were considered replete. Eppley (1972) indicated that the data fell within an upper envelope and drew a line by eye that defined the maximum expected growth at any given temperature between 0°C and 40°C (Fig. 1).

The citation history (>800) of Eppley (1972) suggests that its strong influence is as pronounced today as it was

[1] Corresponding author (j.bissinger@liverpool.ac.uk).
[2] Contact for or Liverpool phytoplankton database enquiries.

Acknowledgments

We thank Roger Koenker for his assistance with various aspects of the quantile regression procedure, and one anonymous reviewer for valuable suggestions that have improved the manuscript. This work was partially funded by Natural Environment Research Council grant NER/S/A/2004/12818.

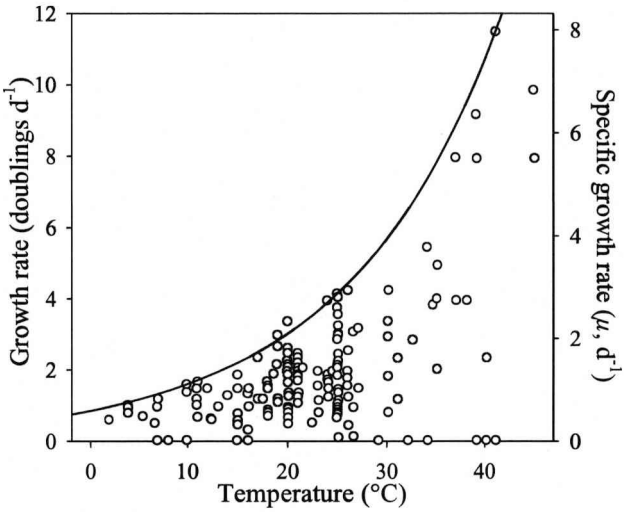

Fig. 1. Variation in the specific growth rate, μ, of photoautotrophic unicellular algae with temperature (redrawn from Figure 1 of Eppley 1972).

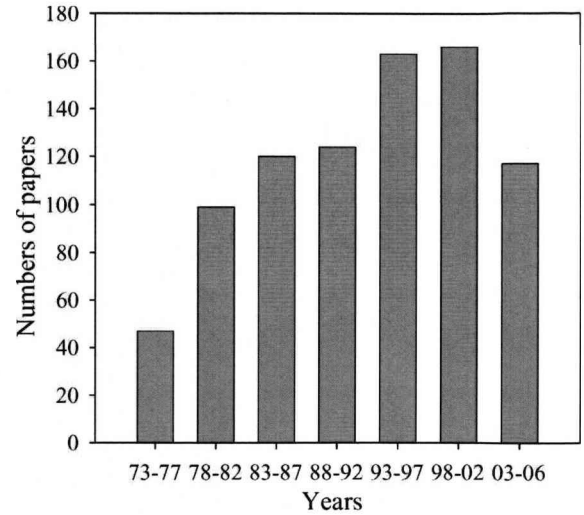

Fig. 2. Citation history (http://wok.mimas.ac.uk/) of "Temperature and phytoplankton growth in the sea" (Eppley 1972). Total number of citations = 835.

over 30 yr ago (Fig. 2). In a sample of 450 papers that cite Eppley (1972), 103 incorporate some aspect of the Eppley formulation in a model, i.e., either the function itself (e.g., Cugier et al. 2005) or the Q_{10} of 1.88 derived from the Eppley function (e.g., Tett et al. 1985). Another 85 studies compare their results to the theoretical maximum expected from the curve (e.g., Durbin 1974; Admiraal 1977); of these, 62 had results similar to or below the curve, and 15 had results that exceeded the theoretical maximum (e.g., Brush et al. 2002). In addition, some studies suggest that an exponential function is not the most appropriate model of the relationship across a wide range of temperatures (Moisan et al. 2002). Recognition of these discrepancies throws doubt on the applicability of the Eppley function and thus also on predictions of aquatic primary production.

Here, we focus on the exponential portion of the response, as Eppley (1972) did, and explore the outcome of a statistical approach that objectively defines the upper edge of a scatter graph, providing a quantitative measure of the reliability of the estimate obtained. Problems with fitting a line of maximum growth by eye include the subjectivity of the method, especially the risk that the relationship may be disproportionately affected by outliers, and the impossibility of quantitatively measuring the precision of the model parameter estimates. In the Eppley (1972) function, an estimate of μ_{max} was inferred from a small sample (n = 162) without any measure of the confidence in that estimate. Furthermore, since Eppley (1972) produced his curve, numerous growth-rate studies have been published with data suitable for incorporation into a new analysis. Therefore, if we plan to use Eppley-like functions in modern aquatic ecosystem models, a quantitative assessment of the reliability of this relationship is needed.

Quantile regression (Koenker and Bassett 1978) can be used to infer relationships from the edges of scatter graphs (e.g., the upper edge of the Eppley [1972] data set; Fig. 1); for example, the 99th quantile describes a line below which are found 99% of the observations. This approach has already been applied to other problems in the aquatic sciences (e.g., the study of maximum bathymetric body-size gradients in gastropods carried out by McClain and Rex [2001], and the investigation of opportunistic predation in tuna by Menard et al. [2006]). Briefly, quantile regression is based on least absolute deviations (LAD) regression, which uses the median rather than the mean, and it is therefore less sensitive to extreme outlying values than ordinary least squares (OLS) regression. The quantile of interest (τ) is estimated using an optimization function that minimizes the sum of weighted absolute deviations (Koenker and Bassett 1978; Koenker and d'Orey 1987), and the solution to the minimization problem is achieved using an algorithm such as the simplex method (Cade and Noon 2003). Typically, like most modern statistics, these algorithms are available in software packages, for example, *R* (http://www.r-project.org).

Regression quantiles, unlike OLS regression, make no assumptions about the error distribution in the model and retain their statistical properties under any linear or nonlinear monotonic transformation (Cade and Noon 2003). Consequently, this method has the added benefit that it is possible to use a nonlinear transformation (e.g., logarithmic) to estimate the regression quantiles and then back-transform the estimates without loss of information (Cade and Noon 2003). Furthermore, estimation of the edges of scatter graphs using quantile regression is not burdened by arbitrary decisions about data partitioning and the numbers of size classes (Scharf et al. 1998), as is the case when binning approaches are used (e.g., Blackburn et al. 1992; Rose and Caron 2007). Since calculation of the standard error for the quantile of interest is dependent on variance in the sample distribution around this quantile (Cade et al. 1999), it is not possible to calculate an upper

confidence interval (CI) for a 100% quantile ($\tau = 1.0$). Therefore, the most reliable estimate of the edge of the data is that defined by the highest (i.e., nearest to 100%) quantile regression line with confidence intervals that do not include zero (Cade et al. 1999). Thus, in this type of analysis, there is often a trade-off between the maximum regression quantile (τ) that can be estimated and the confidence in that estimate.

In this study, five issues are addressed: we analyze the data compiled by Eppley (1972) using quantile regression and examine the statistics associated with the 99th quantile; we follow the approach of Eppley (1972) and obtain all suitable available data to construct a new, large (n = 1,501) database (Liverpool phytoplankton database, LPD) and then use quantile regression to establish a new predictive equation; we investigate if our new, comprehensive database produces a biased response due to a larger proportion of diatoms, since diatoms tend to exhibit high specific growth rates (Furnas 1990); we calculate and compare the Q_{10} of the observed responses, since Q_{10} is used regularly to predict primary production (e.g., Tett et al. 1985; Doney et al. 1996); and finally, we investigate if the quantile regression parameter estimates are influenced by growth-rate data at high temperatures, since there are indications that the growth-rate response should deviate from an exponential response at higher temperatures (Behrenfeld and Falkowski 1997).

Materials and methods

Quantile regression—We use quantile regression to estimate the maximum growth rates of phytoplankton at different temperatures together with a quantitative measure of the confidence in that estimate. Because linear quantile regression provides estimates of standard errors and confidence intervals (CI), the data were linearized by logarithmic transformation. However, log-transformation of the data to accommodate zero and negative growth values (e.g., $\log y + 1$) prevented direct comparison with the Eppley equation, so these few data (<1% of the LPD and ~5% of the Eppley data set) were not included. Quantiles and associated statistics were calculated using the "quantreg" (Koenker 2006) package in *R*, which employs a variant of the Barrodale and Roberts (1974) simplex algorithm (Koenker and d'Orey 1987).

When estimating extreme quantiles with confidence, a large sample size is required to provide a reasonable density of observations near the edge of the data (Cade et al. 1999). To ensure reliable estimates, Rogers (1992) suggested $n > 5/(1 - q)$ (where n is the sample size, and q is the quantile of interest); so, to estimate the 99th quantile, $n > 500$. In this study, the most reliable estimate of the edge of each data set was taken to be the highest possible quantile that complied with the sample size : quantile recommendation of Rogers (1992) and had a slope with 95% CI that excluded zero. In the following analyses, data sets are identified with subscripts, where (E) signifies the Eppley data, (LPD) signifies the Liverpool phytoplankton database, and (43% D) signifies the subset of the LPD data where diatoms constitute 43% of the total (the same proportion as in the Eppley [1972] data set).

Reanalyzing Eppley's data—Eppley (1972) compiled phytoplankton growth-rate data from both primary and secondary sources and only included data from cultures that were grown in nutrient-replete conditions under continuous illumination, or at optimum day-length where a continuous photoperiod was detrimental to growth. Data points (n = 153 after zero values were removed) from Fig. 1 of Eppley (1972) were digitized using Grab It! data-capture software and converted from doublings per day to specific growth rates (μ, d^{-1}; Fig. 1). The $99^{th}_{(E)}$ quantile was calculated as described previously and visually compared to the Eppley curve (Fig. 3A), since the sample size was too small for further analysis.

Analyzing the Liverpool phytoplankton database—The Liverpool phytoplankton database (LPD, n = 1,501 growth rates of marine taxa) only includes laboratory studies from the primary literature, i.e., field-based observations and compilations of growth-rate studies were not included. Data presented graphically were digitized using Grab It!, and growth rates expressed as doublings or divisions per day were converted to specific growth rates (μ, d^{-1}). Data from species that were originally isolated from the benthos were not included, and where experiments varied in salinity, only those growth rates with salinities ≥30 were included. Thus, the LPD is composed of studies that measured growth rates at only one temperature and those that collected growth rates over a number of different temperatures, in batch, continuous, and chemostat experiments, and for various day-length and photon flux density combinations. Consequently, the LPD includes data where conditions were not always replete and maximum growth rates were not always achieved. The LPD was compiled from 51 publications, is ~10 times larger than Eppley's data set, and is composed of 92 species or strains from 62 genera (*see* Web Appendix 1, www.aslo.org/lo/toc/vol_53/issue_2/0493a1.pdf).

The influence of the percentage of diatoms in the data—Because regression quantiles are based on the percentage of data above or below the specified quantile, and the fast growth rates of diatoms (Furnas 1990) may mean that there is a greater percentage close to the upper envelope, we investigated whether the larger proportion of diatoms in the LPD (68% compared to ~43% in the Eppley data set) biased our analysis. We did so by randomly subsampling (n = 828) the LPD to create 30 subsets, where diatoms constituted 43% of the total in each subset. For each subset, we then calculated the $99^{th}_{(43\%\ D)}$ quantile with ±95% CI, and the mean of these was then compared to the Eppley curve and $99^{th}_{(LPD)}$ quantile. To determine if differences existed between the slopes and intercepts of the log-transformed Eppley curve, $99^{th}_{(LPD)}$, and $99^{th}_{(43\%\ D)}$ quantiles (i.e., three comparisons), t-tests were applied. To be conservative, these tests were Bonferroni corrected (Sokal and Rohlf 1995), giving an α value of 0.01.

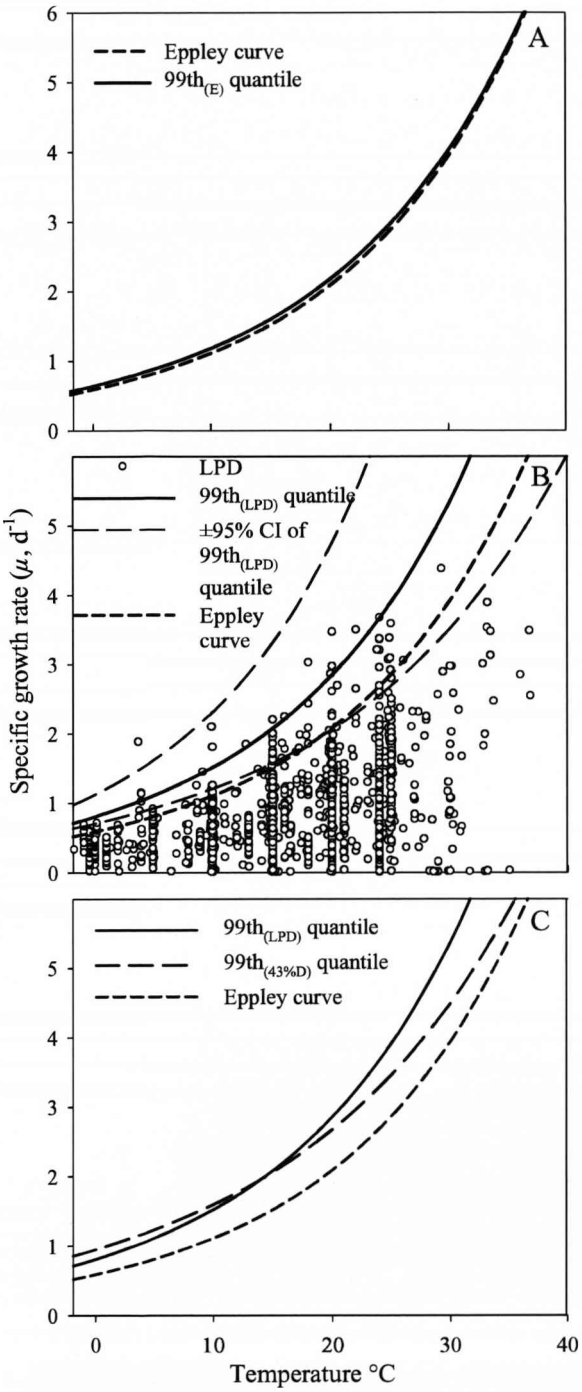

Fig. 3. Marine phytoplankton maximum growth rates (μ_{max}) as a function of temperature. (A) A comparison of the two methodologies used to estimate the upper edge of Eppley's data. The Eppley curve, which was drawn by eye, is compared to the $99^{th}_{(E)}$ regression quantile calculated from Eppley's digitized data (n = 153). (B) The $99^{th}_{(LPD)}$ quantile and associated ±95% confidence intervals calculated from the Liverpool phytoplankton database (LPD) (n = 1,501). The Eppley curve is shown for comparison. (C) Normalization of the LPD data to account for differences in the percentage of diatoms in the data. Lines show the $99^{th}_{(LPD)}$ and $99^{th}_{(43\%\ D)}$ (n = 828) quantiles, with the Eppley curve shown for comparison.

Calculating the Q_{10} value—We calculated the Q_{10} value of the LPD μ_{max} and that derived from the subsets with 43% diatoms using the Q_{10} model of Van't Hoff (1884). Assumptions included an exponential response and no inhibition of growth rate at high temperatures, following the approach of Eppley (1972).

The influence of growth rates at high temperatures—At higher temperatures (>29°C, Fig. 3B), data points were fewer and appeared to have maxima below the calculated 99^{th} quantile. So, to alleviate any concerns that these high-temperature data may unduly influence the parameter estimates from the quantile regression analysis, a reduced data set was created that excluded growth-rate data at temperatures >29°C. To determine if there were differences between the log-transformed regression parameters from the full and reduced data sets, t-tests were applied.

Results

Analysis of Eppley's data—Qualitatively, the $99^{th}_{(E)}$ quantile appears to be similar to the Eppley curve (Fig. 3A). However, as only one positive residual point occurs above the $99^{th}_{(E)}$ quantile, it was not possible to statistically analyze the differences between the $99^{th}_{(E)}$ quantile and the Eppley curve. Thus, error estimates were not obtained for the Eppley curve using quantile regression.

Analysis of Liverpool phytoplankton database—Since the ±95% CI of the $99^{th}_{(LPD)}$ quantile slope estimate excluded zero and complied with the minimum size recommended by Rogers (1992) (Table 1), this quantile provided the most reliable estimate of the edge of the LPD data set. Back-transformation of the parameters from the $99^{th}_{(LPD)}$ quantile yields:

$$\mu_{max} = 0.81e^{0.0631T} \quad (2)$$

A comparison of the log-transformed quantile parameters to those of the Eppley curve indicates that the intercept of the $99^{th}_{(LPD)}$ quantile is significantly greater than that of the Eppley curve (t = 3.20, df = 1,499, $p < 0.01$). Furthermore, at temperatures below 19°C, the Eppley curve falls below the lower 95% CI associated with the $99^{th}_{(LPD)}$ quantile (Fig. 3B). However, the slope of the $99^{th}_{(LPD)}$ quantile is not significantly different from that of the Eppley curve (t = 0.53, df = 1,499, $p > 0.01$). The slope and intercept of the $99^{th}_{(43\%\ D)}$ quantile are not significantly different from those of the Eppley curve (t = 1.05, df = 826, $p > 0.01$, and t = 2.08, df = 826, $p > 0.01$, respectively), or the $99^{th}_{(LPD)}$ quantile (t = 0.97, df = 2325, $p > 0.01$, and t = 0.66, df = 2325, $p > 0.01$, respectively).

The Q_{10} value of the $99^{th}_{(LPD)}$ quantile (1.88) is identical to that of the Eppley curve, whereas the Q_{10} value of the $99^{th}_{(43\%\ D)}$ quantile is 1.68. The log-transformed slope and intercept parameter estimates of the reduced (≤29°C) data set are not significantly different (t = 0.24, df = 2953, $p > 0.01$, and t = 0.18, df = 2953, $p > 0.01$, respectively) from those of the full data set.

Table 1. 99th regression quantile slope parameter estimates and associated statistics for the Liverpool phytoplankton (LPD) data sets. The parameter values are calculated to a confidence level of $\alpha = 0.05$, and $n > 5/(1 - q)$ represents the minimum recommended sample size at the specified quantile (Rogers 1992). Note that the 43% D slope estimate and ±95% CI represent the mean value of 30 subsamples.

Data set	n	$n>5/(1-q)$	Estimate	−95% CI	+95% CI
LPD	1,501	500	0.0631	0.0535	0.0721
43% D	828	500	0.0518	0.0259	0.0668

Discussion

Using quantile regression, we recognized that the Eppley curve could be improved upon. To this end, we derived a new exponential function for marine phytoplankton growth rates as a function of temperature using the Liverpool phytoplankton database (LPD), and we compared it to that derived by Eppley (1972). However, the data set compiled by Eppley (1972) did not fulfil the minimum size recommendations of Rogers (1992) for calculating the 99th quantile with confidence. Calculating extreme quantiles with a small sample size may lead to a limited number of residuals, which renders methods for calculating standard errors unreliable (R. Koenker pers. comm.). Consequently, it was not possible to provide error estimates for the Eppley curve using quantile regression. Nevertheless, the visual fit of the $99^{th}_{(E)}$ quantile to the original Eppley (1972) curve (Fig. 3A) suggests that the Eppley curve is a good estimate of the edge of the data. Furthermore, there is no significant difference between the log-transformed slopes of the LPD and the Eppley curve, indicating equivalence in Q_{10} values (1.88) and suggesting that the Eppley curve has been an appropriate estimate of the thermal sensitivity of phytoplankton growth rates. This result supports and complements studies that demonstrate fundamental differences in growth-rate thermal sensitivity between heterotrophs and phototrophs (Allen et al. 2005; López-Urrutia et al. 2006; Rose and Caron 2007), and it should also reassure those who have used the Q_{10} value of 1.88 in models over the last 35 yr.

The significant difference between the intercept of the log-transformed $99^{th}_{(LPD)}$ and the Eppley curve supports studies that suggest that the Eppley curve is too low (e.g., Brush et al. 2002). However, in our new relationship (Eq. 2), the intercept value (0.81) is lower than the value (0.97) derived by Brush et al. (2002). We suggest that this discrepancy is due to the different methodologies adopted in defining the edge of the upper envelope. In their analysis, Brush et al. (2002) adopted the same slope value as Eppley (1972) and determined the upper edge of their data by eye. As discussed earlier, in relation to Eppley (1972), there are possible problems with this approach, e.g., the subjectivity involved and the lack of quantitative measures of reliability.

Construction of the LPD subset containing 43% diatoms, i.e., an equivalent proportion to that of Eppley (1972), allowed us to further investigate whether differences between the LPD envelope and the Eppley curve could be attributed to the greater percentage of diatoms in the LPD, since diatoms typically have disproportionately high growth rates (Furnas 1990). However, because there were no significant differences between the intercepts of the $99^{th}_{(43\%\ D)}$ quantile and the $99^{th}_{(LPD)}$ quantile, the dissimilarities between the Eppley curve and the $99^{th}_{(LPD)}$ quantile cannot be solely attributable to differing proportions of diatoms in the two data sets. Consequently, the LPD function (Eq. 2) is an appropriate model when a single theoretical maximum function is required, e.g., when the only data available are biomass, or Chl *a* and temperature.

A good example of where a single temperature function has been repeatedly employed is in pelagic ecosystem models (e.g., Balch and Byrne 1994; Antoine et al. 1996; Sharples et al. 2006). To assess the extent to which our function may alter model results, we compared the output of one temperate shelf–sea ecosystem model (Sharples et al. 2006) using our new function and that of Eppley (1972). This simple analysis suggests that models that incorporate the Eppley function may underestimate primary production in cooler temperate waters by ~30%. This underestimate applied to both the $99^{th}_{(LPD)}$ quantile and the $99^{th}_{(43\%\ D)}$ quantile, since these two responses are similar at lower temperatures (Fig. 3C). Consequently, assessments of the thermal influence of primary production on ecosystem services such as oxygen production, carbon sequestration, and biogeochemical cycling may also require revision.

Our analysis of the influence of diatom percentage abundance on the upper envelope, and, in particular, the differences in slope parameter estimates between the $99^{th}_{(43\%D)}$ quantile and the $99^{th}_{(LPD)}$ quantile (Table 1), indicates how other variables may be incorporated into a more accurate model. Size (Savage et al. 2004) and taxonomic affiliation (Banse 1982), for example, may explain much of the remaining variation in μ_{max} among phytoplankton. Building on our revised general growth rate–temperature relationship, we are currently developing new predictive models, using the LPD, that incorporate these and other variables, such as community composition and habitat.

Finally, in this study, we concentrated on producing a relationship that is directly comparable to the Eppley curve, but we acknowledge that there are limitations with the applicability of this function in warm or oligotrophic oceanic areas, where the maximum growth rates of phytoplankton may always be limited by factors other

han temperature. Furthermore, this analysis has highlighted two issues that need to be addressed in the future. First, while our analysis of the reduced data set (≤29°C) indicates hat the use of the full data set to determine the upper nvelope is valid, we note that the relationship is not xponential at very high temperatures. We will address the hape of the maximum envelope in future models, and we aution against using our existing model (Eq. 2) at emperatures >29°C. Second, a $Q_{10\ \text{value}}$ of 1.88 is omewhat higher than predicted by the metabolic theory f ecology (Brown et al. 2004; Allen et al. 2005), which ives a Q_{10} value of between 1.62 (for 0–10°C) and 1.52 (for 0–30°C), derived from a predicted activation energy of .32eV for rates controlled by photosynthesis. This liscrepancy clearly merits further scrutiny.

In conclusion, while recognizing the utility and robustness of the Eppley curve over the last 35 yr, the quantitative measures of reliability associated with our LPD function (Eq. 2) should give users greater confidence in its value and suitability in situations where a single exponential growth-rate relationship is sought.

References

ADMIRAAL, N. 1977. Influence of light and temperature on the growth rate of estuarine diatoms in culture. Mar. Biol. **39:** 1–9.

ALLEN, A. P., J. F. GILLOOLY, AND J. H. BROWN. 2005. Linking the global carbon cycle to individual metabolism. Funct. Ecol. **19:** 202–213.

ANTOINE, D., J.-M. ANDRÉ, AND A. MOREL. 1996. Oceanic primary production. Estimation and global scale from satellite (coastal zone colour scanner) chlorophyll. Glob. Biogeochem. Cyc. **10:** 57–69.

BALCH, W. M., AND C. F. BYRNE. 1994. Factors affecting the estimate of primary production from space. J. Geophys. Res. **99:** 7555–7570.

BANSE, K. 1982. Cell volumes, maximal growth rates of unicellular algae and ciliates and the role of ciliates in the marine pelagial. Limnol. Oceanogr. **27:** 1059–1071.

BARRODALE, I., AND F. ROBERTS. 1974. Solution of an over determined system of equations in the l_1 norm. Commun. ACM **17:** 319–320.

BEHRENFELD, M. J., AND P. G. FALKOWSKI. 1997. A consumer's guide to primary productivity models. Limnol. Oceanogr. **42:** 1479–1491.

———, J. T. RANDERSON, C. R. MCCLAIN, G. C. FELDMAN, S. O. LOS, C. J. TUCKER, P. G. FALKOWSKI, C. B. FIELD, R. FROUIN, W. E. ESAIAS, D. D. KOLBER, AND N. H. POLLACK. 2001. Biospheric primary production during an ENSO transition. Science **291:** 2594–2597.

BLACKBURN, T. M., J. H. LAWTON, AND J. N. PERRY. 1992. A method of estimating the slope of upper bounds of plots of body size and abundance in natural animal assemblages. Oikos **65:** 107–112.

BOWIE, G. L., W. B. MILLS, D. B. PORCELLA, C. L. CAMPBELL, J. R. PAGENKOPF, G. L. RUPP, K. M. JOHNSON, P. W. H. CHAN, AND S. A. GEHRINI. 1985. Rates, constants, and kinetics formulations in surface water quality modelling, 2nd ed. U.S. EPA Environmental Research Laboratory.

BROWN, J. H., J. F. GILLOOLY, A. P. ALLEN, V. M. SAVAGE, AND G. B. WEST. 2004. Toward a metabolic theory of ecology. Ecology **85:** 1771–1789.

BRUSH, M. J., J. W. BRAWLEY, S. W. NIXON, AND J. N. KREMER. 2002. Modelling phytoplankton production: Problems with the Eppley curve and an empirical alternative. Mar. Ecol. Prog. Ser. **238:** 31–45.

CADE, B. S., AND B. R. NOON. 2003. A gentle introduction to quantile regression for ecologists. Front. Ecol. Environ. **1:** 412–420.

———, J. W. TERREL, AND R. L. SCHROEDER. 1999. Estimating effects of limiting factors with regression quantiles. Ecology **80:** 311–323.

CUGIER, P., A. MÉNESGUEN, AND F. D. GUILLAUD. 2005. Three dimensional (3D) ecological modelling of the Bay of Seine (English Channel, France). J. Sea Res. **54:** 104–124.

DONEY, S. C., D. M. GLOVER, AND R. G. NAJJAR. 1996. A new coupled, one-dimensional biological-physical model for the upper ocean: Applications to the JGOFS Bermuda Atlantic time-series study (BATS) site. Deep-Sea Res. Pt. II. **43:** 591–694.

DURBIN, E. G. 1974. Studies on the autecology of the marine diatom *Thalassiosira nordenskioeldii* Cleve.1. The influence of day length, light intensity, and temperature on growth. J. Phycol. **10:** 220–225.

EPPLEY, R. W. 1972. Temperature and phytoplankton growth in the sea. Fish. Bull. **70:** 1063–1085.

FURNAS, M. J. 1990. In situ growth rates of marine phytoplankton: Approaches to measurement, community and species growth rates. J. Plankton. Res. **12:** 1117–1151.

KOENKER, R. 2006. Quantreg: Quantile regression R software version 4.02.

———, AND G. BASSETT. 1978. Regression quantiles. Econometrica **46:** 33–50.

———, AND V. D'OREY. 1987. Computing regression quantiles. Appl. Stat. **36:** 383–393.

LÓPEZ-URRUTIA, Á., E. SAN MARTIN, R. P. HARRIS, AND X. IRIGOIEN. 2006. Scaling the metabolic balance of the oceans. Proc. Natl. Acad. Sci. USA **103:** 8739–8744.

MCCLAIN, C. R., AND M. A. REX. 2001. The relationship between dissolved oxygen concentration and maximum size in deep-sea turrid gastropods: An application of quantile regression. Mar. Biol. **139:** 681–685.

MENARD, F., C. LABRUNE, Y. J. SHIN, A. S. ASINE, AND F. X. BARD. 2006. Opportunistic predation in tuna: A size-based approach. Mar. Ecol. Prog. Ser. **323:** 223–231.

MOISAN, J. R., T. A. MOISAN, AND M. R. ABBOTT. 2002. Modelling the effect of temperature on the maximum growth rates of phytoplankton populations. Ecol. Model. **153:** 197–215.

ROGERS, W. H. 1992. Quantile regression standard errors. Stata Technical Bulletin **9:** 16–19.

ROSE, J. M., AND D. A. CARON. 2007. Does low temperature constrain the growth rates of heterotrophic protists? Evidence and implications for algal blooms in cold waters. Limnol. Oceanogr. **52:** 886–895.

RYTHER, J. H. 1969. Photosynthesis and fish production in the sea. Science **166:** 72–76.

SAVAGE, V. M., J. F. GILLOOLY, J. H. BROWN, G. B. WEST, AND E. L. CHARNOV. 2004. Effects of body size and temperature on population growth. The Am. Nat. **163:** 429–441.

SCHARF, F. S., F. JUANES, AND M. SUTHERLAND. 1998. Inferring ecological relationships from the edges of scatter diagrams; comparison of regression techniques. Ecology **79:** 448–460.

SHARPLES, J., O. N. ROSS, B. E. SCOTT, S. P. R. GREENSTREET, AND H. FRASER. 2006. Inter-annual variability in the timing of stratification and the spring bloom in the north-western North Sea. Cont. Shelf Res. **26:** 733–751.

SOKAL, R. R., AND F. J. ROHLF. 1995. Biometry: The principles and practices of statistics in biological research., Freeman & Co.

TETT, P., S. I. HEANEY, AND M. R. DROOP. 1985. The Redfield ratio and phytoplankton growth rate. J. Mar. Biol. Assoc. U.K. **65:** 487–504.

VAN'T HOFF, J. H. 1884. Études de dynamique chimique. Muller.

Received: 19 June 2007
Accepted: 24 October 2007
Amended: 4 December 2007

Global Change Biology (2008) **14**, 1–16, doi: 10.1111/j.1365-2486.2008.01700.x

Short-term temperature change may impact freshwater carbon flux: a microbial perspective

DAVID J. S. MONTAGNES*, GARETH MORGAN*, JAN E. BISSINGER*, DAVID ATKINSON* and THOMAS WEISSE†

School of Biological Sciences, BioSciences Building, University of Liverpool, Liverpool L69 7ZB, UK, †Institute for Limnology of the Austrian Academy of Sciences, Mondseestr. 9, A-5310 Mondsee, Austria

Abstract

Small freshwater bodies are abundant and economically and ecologically important on a global scale. Within these, protozoa play an important role in structuring planktonic food webs and sequestering CO_2. We hypothesized that short-term (~20 days) fluctuations, of 2–10 °C, will significantly alter carbon flux associated with predator–prey interactions within the microbial planktonic food web. We examined the model ciliate, *Urotricha farcta*, which is abundant and common; it was fed the autotrophic flagellate *Cryptomonas* sp., which is also common. Laboratory experiments were conducted over relevant ranges: 8–24 °C; 0–2 × 10^5 prey mL^{-1}. Mechanistic-phenomenological multiple regressions were developed and fit to the data to obtain relationships for (1) growth rate and volume changes of the flagellate vs. temperature and (2) growth rates, grazing, and cell volume change of the ciliate vs. temperature and prey concentration. Responses revealed interaction between temperature and prey levels on all ciliate parameters, indicating it is inappropriate to apply simple temperature corrections (e.g. Q_{10}) to such functions. The potential impact of such temperature changes on carbon flux was illustrated using a simple ciliate–flagellate predator–prey model, with and without the top grazer, *Daphnia*, added. The model indicated that predator–prey pulses occurred over 20 days, with the ciliate controlling the prey population. For ciliates and prey, carbon production peaked at 20 °C and rapidly decreased above and below this maximum; differences between minimum and maximum were approximately fourfold, for both prey and ciliate, with low levels at 25–30 °C and 10–15 °C. Including literature data to parameterize, the influence of the grazer *Daphnia* did not alter the prediction that the ciliate may control short-term flagellate pulses and temperature will influence these in a nonintuitive fashion.

Keywords: episodic shift, microbial food web plankton

Received 5 March 2008; revised version received 21 May 2008 and accepted 22 May 2008

Introduction

Because of their high productivity, freshwaters, globally and locally, can play a significant role in processing and sequestering atmospheric carbon (e.g. Schindler, 1978; O'Sullivan & Reynolds, 2003). Specifically, in these systems, the pelagic food web influences carbon flux by fixing and releasing water column CO_2 and mediating carbon losses through sedimentation and respiration (Flanagan *et al.*, 2006). Such freshwaters represent ~3% of the terrestrial surface (Downing *et al.*, 2006), with much higher contributions in some regions (e.g. northern temperate North America and Europe), and it is noteworthy that >7.2 million of these water bodies are small, having a surface of 0.01–0.1 km^2 (Reynolds, 2003). As many of these will have substantial economic and social importance and are an intimate link to wetland and terrestrial ecosystems (Moss, 1998; O'Sullivan & Reynolds, 2003), there is strong impetus to study them.

Climate change will raise the average temperature of small water bodies, following predicted long-term increases (3–6 °C over the next century; Houghton, 2005), but of more immediate impact is the predicted increase in intensity and frequency of short-term varia-

Correspondence: David J. S. Montagnes, e-mail: dmontag@liv.ac.uk

tions, due to global warming (Houghton, 2005). Furthermore, short-term warming events caused by other global processes such as the North Atlantic Oscillation will alter the temperature of small water bodies (e.g. Gerten & Adrian, 2000). Thus, large lakes are likely to change slowly, but for small water bodies and the productive shallow regions of larger lakes, temperatures will respond rapidly to air temperature (Carpenter *et al.*, 1992), and episodic changes in water temperature by $>5\,^{\circ}C$ over 1–2 weeks may be more common (see McKee *et al.*, 2000 for an example of the present prevalence of $>5\,^{\circ}C$ pulses in temperate small water bodies). In response to this prediction, we have hypothesized that short-term fluctuations, on the order of 2–10 °C, will substantially influence population dynamics and carbon flux in a major component of the biota of small water bodies: predator–prey interactions within the microbial planktonic food web.

Freshwater ecosystem studies have tended to focus on the classical food web: the link between primary production and zooplankton, such as *Daphnia* (Jürgens, 1994). There is, however, a growing recognition that the microbial food web, often dominated by protozooplankton grazers, plays a significant role in these systems (e.g. Riemann & Christoffersen, 1993; Jürgens, 1994; Weisse, 2003); through it much of the organic matter produced by phytoplankton passes to flagellates and ciliates (Azam *et al.*, 1983; Porter *et al.*, 1988), with ciliates having a key role in shaping food web structure (Zingel *et al.*, 2007). Unlike most metazooplankton, ciliates have inherently rapid growth rates, often exceeding those of their prey (Weisse, 2006). There is good evidence that many of the planktonic ciliates respond rapidly to increases in prey abundance (e.g. Montagnes, 1996), and short-term pulses of a few similar species (or virtually monospecific pulses) can occur, when prey become abundant (e.g. Müller *et al.*, 1991; Wilson, 2002, see 'Discussion'). Such rapid increases may occur when prey populations are stimulated to grow (e.g. by brief increases in temperature). This component of the microbial food web may then be linked to the classical food web through zooplankton grazers such as *Daphnia* (Jürgens, 1994), as localized increases in protozoa may act as discrete regions of improved nutritional resource.

As growth of the protistan component of food webs will respond more rapidly than the metazoan components to temperature change, it seems prudent to consider localized protistan predator–prey dynamics when assessing temperature-induced changes in aquatic carbon flux, especially if these temperature effects are extreme and sufficiently short-term to not propagate up the food web. In general, we know temperature has a number of pronounced effects on protists. Their cell size (and presumably carbon content; see Menden-Deuer & Lessard, 2000) decreases with increasing temperature by ~2.5% of their size at 15 °C for an increase of 1 °C (i.e. cell carbon content may decrease by 25% over 10 °C; Atkinson *et al.*, 2003). Temperature and prey concentrations also have unexpected, interactive effects on the growth, production, and population dynamics of protozoa and their prey (Weisse *et al.*, 2002; Kimmance *et al.*, 2006), placing into question the typical application of Q_{10} as a parameter to independently predict thermal sensitivities (Montagnes & Lessard, 1999; Montagnes *et al.*, 2003; Kimmance *et al.*, 2006). Here, we extend these works by taking an inductive approach and establish a series of carefully determined responses for a single highly relevant species that is a 'typical' freshwater protozoan (Foissner *et al.*, 1999). Then to illustrate the potential importance of these monospecific pulses, following the example of others (e.g. Davidson, 1996; Shertzer *et al.*, 2002; Fulton *et al.*, 2003), we apply our responses to an exploration of predator–prey dynamics, using a focused, minimized model. Clearly, the impact of these changes may eventually propagate through the food web and alter population and community dynamics and carbon flux. However, constructing a full food web model is not our intent, instead we apply a predator–prey model to emphasize, at a general level, that including these dynamics will significantly alter estimates of carbon flux; then we discuss the use and limitations of our responses as a predictive tool. Such integration of laboratory work and fundamental population modelling is uncommon in a single study; here we illustrate how it can be an important, iterative step before developing more complex food web models.

Specifically, in the laboratory we examined responses of the model ciliate, *Urotricha*, which occurs throughout the year, and is abundant, in oligotrophic to hypertrophic temperate, boreal, and subtropical ponds, lakes, and rivers (Foissner *et al.*, 1999; Weisse *et al.*, 2001). The ciliate was raised on the flagellate *Cryptomonas* sp., which is also common in a multitude of freshwater environments (Sommer, 1986; Dokulil, 1988; Pedrós-Alió *et al.*, 1995) and is used as a standard food in experiments with ciliates (Müller & Geller, 1993; Weisse & Montagnes, 1998; Müller & Schlegel, 1999; Montagnes & Weisse, 2000). Using these laboratory data we first develop and evaluate responses of how temperature and prey concentration influence the grazing, growth, and cell volume of the ciliate and then we use these responses to indicate how temperature may alter short-term (20 days) carbon flux in a ciliate–flagellate predator–prey model. Finally, recognizing that both *Urotricha* and *Cryptomonas* fit into the classical food web, and may be exposed to top-down control by metazooplankton (Weisse, 2003, 2006), we use literature parameters to explore the influence of adding the grazer

Daphnia to our model. Therefore, we have focused on an energetically important model system to provide insights by highlighting the temperature sensitivity of predator–prey dynamics within the microbial food web.

Materials and methods

Study organisms

The prostomatid ciliate *Urotricha farcta* (~25 μm) was isolated from the mesotrophic Lake Schöhsee, Germany (Weisse & Montagnes, 1998). The prey flagellate *Cryptomonas* sp. strain 26.80 (~10 μm) was obtained from the Culture Collection of Algae in Göttingen (Germany). Both the ciliate and prey were maintained in modified Woods Hole medium (MWC medium, Guillard & Lorenzen, 1972) at 15 ± 1 °C, throughout all experiments. Cultures were not axenic, but *U. farcta* does not feed on bacteria if suitable flagellates are abundant (Weisse *et al.*, 2001). For all experiments, both ciliate and flagellate cultures were harvested in exponential phase.

Phytoplankton (prey) response to temperature

To determine how temperature affected the prey-specific growth rate and cell volume, batch cultures were maintained at 12 temperatures (see Fig. 1) at a continuous irradiance of ~55 μmol photons $m^{-2} s^{-1}$; cultures were suspended in double glazed, cooled or heated water baths that maintained temperatures ± 1 °C. Before experiments, cultures were acclimated to the experimental conditions for eight generations. Then specific growth rate (μ_p, day^{-1}) was determined during exponential growth phase from measurements made over 3–5 days, from the slope of ln abundance vs. time; note population decline at low temperatures was assumed to be a *per capita* rate (i.e. in these cases $\mu_p < 0$; see Montagnes, 1996). Abundance was determined once per day from Lugol's fixed samples (2% v/v), enumerated in a Sedgewick–Rafter chamber. Cell volume was determined from length and width measurements of 30 live, exponential-phase cells, assuming a prolate spheroid shape. Prey cell volumes were converted to carbon (C) following C (pg) = $0.216V^{0.939}$, where V is cell live-volume (μm^3) (Menden-Deuer & Lessard, 2000).

Ciliate response to prey and temperature

Ciliate stock cultures were maintained at 15 °C. Over 5–7 days, ciliates and prey were step-wise (up to 3 °C day^{-1}) acclimated to experimental prey levels and six temperatures (see Fig. 2) at 70 μmol photons $m^{-2} s^{-1}$;

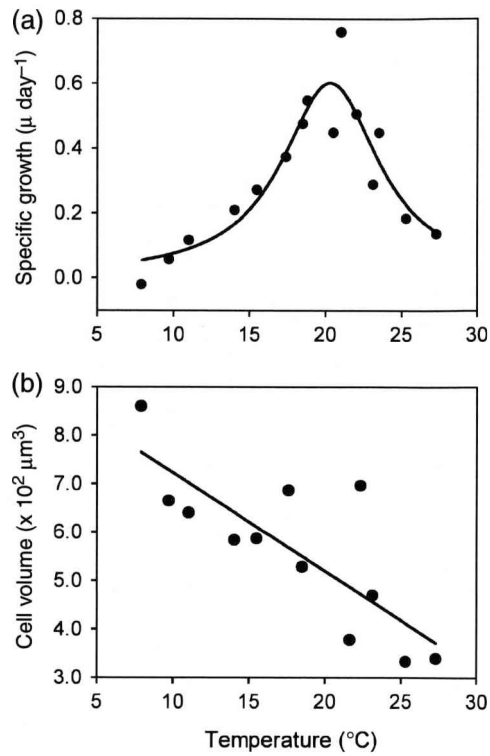

Fig. 1 The effect of temperature on specific growth rate (a) and cell volume (b) of the flagellate *Cryptomonas* sp. Points represent growth rate or cell volume measurements. The line is the fit of Eqn (4) (a) and a straight line (b) to the data; see Table 1 for the parameters of these fits and estimates of their error.

these experiments were run in incubators that maintained temperatures ± 0.5 °C. Prey levels were monitored with an electronic particle counter during the acclimation period, and ciliates were regularly fed to maintain food levels. Prey levels were maintained in exponential phase under the same temperature conditions as the ciliates.

After acclimation, ciliates were inoculated into flasks containing acclimated prey at concentrations ranging from 1.0×10^4 to 2.5×10^5 mL^{-1} at 70 μmol photons $m^{-2} s^{-1}$. Initial concentrations of ciliates ranged from 3.0×10^2 to 7.4×10^3 mL^{-1} but in most experiments were initiated at 5.0×10^2–1.0×10^3 mL^{-1}. Controls for prey growth, without ciliates, were run at prey and light levels identical to the ciliate–prey treatments. All cultures were maintained for 24 h at each temperature. After 12 and 24 h, prey numbers were adjusted with temperature-acclimated prey or medium alone if they deviated from the target levels by >20%. The experimental incubation began immediately after this re-adjustment of prey concentrations and lasted 24 h. Each treatment was run with three to five replicates.

 Global Change Biology, doi: 10.1111/j.1365-2486.2008.01700.x

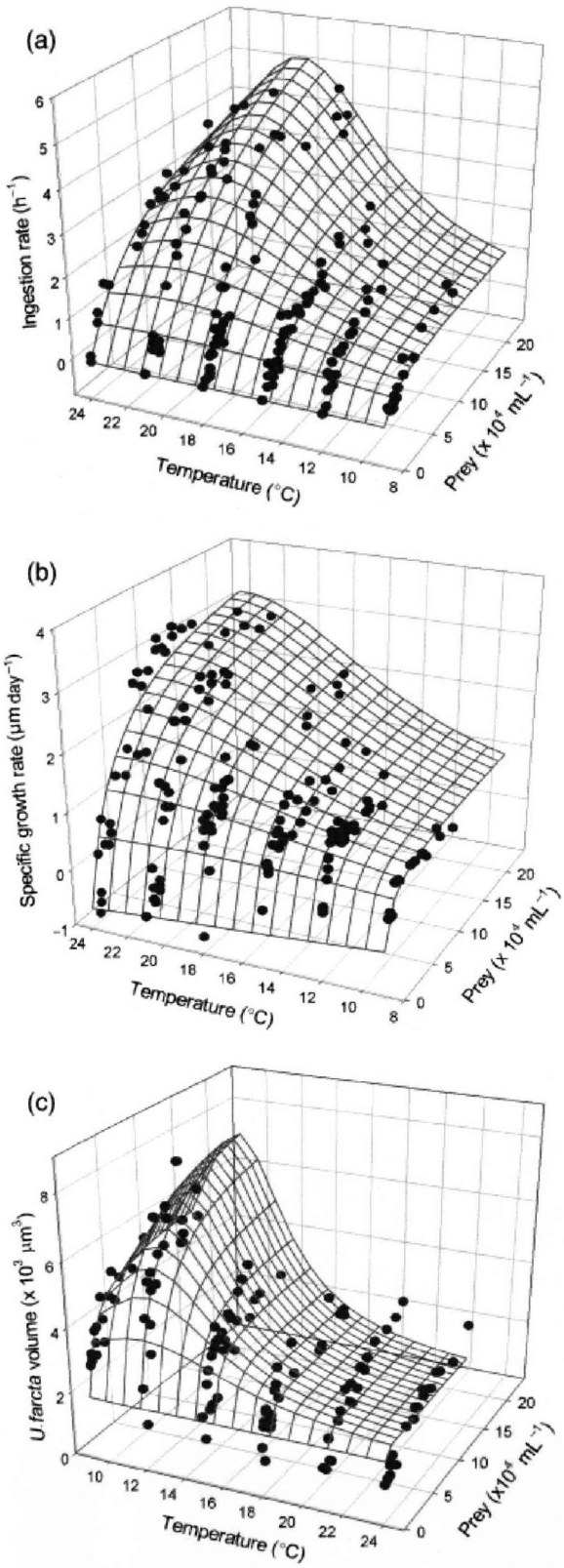

Samples were taken at 6–12 h intervals and fixed: for flow cytometric analyses samples were fixed with formalin (2% v/v); for microscopic analyses samples were fixed with acid Lugol's (as above). Prey and ciliate numbers were determined by flow cytometry according to our published protocols (Lindström *et al.*, 2002; Weisse *et al.*, 2002) or counted microscopically (as above).

Ciliate volumes were determined from length and width measurements, assuming a prolate spheroid shape, on >50 exponential phase ciliates obtained at the end of the experiment, from each treatment. Ciliate size measurements were made on Lugol's fixed material, which underestimates ciliate live volume by ~30% (Jerome *et al.*, 1993), and this was corrected for. Ciliate volumes were converted to carbon units using the conversion of Menden-Deuer & Lessard (2000); see above.

Ciliate grazing rate (prey ciliate^{-1} h^{-1}) was determined from changes in growth rate of prey observed in controls, without ciliates, minus prey growth rate measured in the experimental containers with predators present, following methods outlined in Weisse *et al.* (2001).

Developing response equations

For modelling purposes, we established functions that could be used to predict predator ingestion rate, specific growth rate, and cell volume in response to varying temperature and prey concentrations. We also established responses for prey-specific growth rate and volume changes to temperature alone. These responses are presented here and further evaluated in the 'Discussion'.

Predator (ciliate) ingestion rate (I_c, prey predator^{-1} h^{-1}) was assumed to vary with prey concentration (P, mL^{-1}), following the mechanistic, Holling Type II equation [Holling, 1959, Eqn (1)], where a and b are constants. Predator-specific growth rate (μ_c, day^{-1}) was assumed to follow a similar rectangular hyperbolic response, but with a nonzero intercept (P', mL^{-1}), determined by the predator's basal metabolic rate (Montagnes, 1996), where c and d are constants [Eqn (2)]. Predator cell volume (V, µm^3) was also assumed to

Fig. 2 The combined effect of temperature and prey (*Cryptomonas* sp.) abundance on *Urotricha farcta*: (a) ingestion, (b) specific growth, and (c) cell volume; note the temperature axis on the last panel (c) is reversed to adequately display the shape of this response. The grids are the fits of Eqns (5)–(7) to the data (see text for details); see Table 2 for the parameters of these fits and estimates of their error.

follow a rectangular hyperbolic response, but with a positive value at zero prey, assuming a minimal cell size [V', Montagnes & Lessard, 1999, Eqn (3)], where e and f are constants. Temperature (T, °C)-dependent responses (R) for predator and prey growth rate (μ_c and μ_p, respectively), predator ingestion rate (I_c), and predator volume (V) were assumed to increase exponentially to a maximum, plateau, and then decrease with changing temperatures, following a phenomenological model [Flinn, 1991, Eqn (4)], where g, h, and i are constants (see Appendix A). Flinn & Hagstrum (2002) and Menon *et al.* (2002) combined a Type II functional response with their temperature response, and we have followed this approach for ingestion, growth, and volume responses [Eqns (5)–(7)], where lower case, italicized letters represent constants, and α [Eqn (6)] has a value of unity and dimensions of T^{-1}. Prey volume was assumed to decrease linearly with temperature, following predictions of Atkinson *et al.* (2003).

$$I_c = \frac{aP}{1 + bP} \tag{1}$$

$$\mu_c = \frac{c(P - P')}{1 + d(P - P')} \tag{2}$$

$$V = \frac{eP}{1 + fP} + V' \tag{3}$$

$$R = \frac{1}{1 + (g - hT + iT^2)} \tag{4}$$

$$I_c = \frac{jP}{[1 + (k - lT + mT^2)]P} \tag{5}$$

$$\mu_c = \frac{n(P - T\alpha P')}{[1 + (o - qT + rT^2)](P - T\alpha P')} \tag{6}$$

$$V = \frac{uP}{[1 + (v - wT + xT^2)]P} + V'. \tag{7}$$

Ciliate growth, ingestion, and volume responses were related to the treatment temperature and average prey concentration (P); note, average P over incubations was determined following methods described by Frost (1972). The above equations [Eqns (5)–(7)] were, respectively, fit to the temperature-influenced numerical, functional, and volume response data using the Marquardt–Levenberg algorithm (SIGMAPLOT, SPSS Inc., Chicago, IL, USA); this algorithm is appropriate for describing such biological datasets (Berges *et al.*, 1994). Adjusted R^2 values for the responses and standard errors of the estimates were determined, using SIGMAPLOT, as indications of their goodness of fit.

Modelling

To illustrate the extent to which temperature change may impact carbon flux in this predator–prey system, a model was constructed using our experimental flagellate (prey) and ciliate responses (see 'Results') and responses for *Daphnia* from the literature (see below). In this system, flagellates grew exponentially (with no carrying capacity as maximal prey levels were always predator controlled) and were preyed upon strictly by ciliates or by both ciliates and *Daphnia* (predators); ciliate growth rate was prey dependent, and ciliate mortality was regulated either strictly by starvation below threshold levels or also by top-down control by the grazer (*Daphnia*); the following couplet of differential equations [Eqns (8) and (9)] describe the model:

$$\frac{dP}{dt} = \mu_p P - I_c C - I_{dp} D \tag{8}$$

$$\frac{dC}{dt} = \mu_c C - I_{dc} D, \tag{9}$$

where P is the flagellate abundance; μ_p is the temperature-dependent specific growth rate of the flagellate; I_c and μ_c are the temperature and the prey-dependent grazing and growth rates, respectively, of the ciliate; C is the ciliate abundance; I_{dp} and I_{dc} are the temperature and prey-dependent grazing rates of *Daphnia* on flagellates and ciliates, respectively; and D is *Daphnia* abundance. Flagellate and ciliate numbers were then converted to volumes using our predictive equations (see 'Results') and then to carbon, following the conversion of Menden-Deuer & Lessard (2000) (see above).

Daphnia grazing pressure was based on assuming: (1) a constant abundance (0.05 mL^{-1}) of generic, *Daphnia* (~0.8 mm long) being maintained over the simulations (Gilbert, 1988; Gliwicz, 2003); (2) specific filtration rates on the ciliate and prey being the same (Jürgens, 1994); and (3) the influence of temperature on filtration rate (F, mL^{-1} individual day^{-1}) followed Eqn (10), derived by Mourelatos & Lacroix (1990):

$$\log F = 2.07 \log L + 0.126T - 0.0024T^2 - 0.628, \tag{10}$$

where L is *Daphnia* length and T is temperature (Fig. 5f).

To assess the impact of the temperature-induced responses on ciliate–prey pulses, a 20-day simulation was used to represent the maximum period over which a single warming event might influence a small water body, without the influence of other abiotic (e.g. nutrient change) or biotic (e.g. *Daphnia* population growth)

factors substantially altering the predator–prey system. Furthermore, this period was sufficiently long to express one predator–prey cycle, given initial conditions of 4×10^3 prey and 10 predators mL^{-1} (the starting condition of all simulations of population dynamics); these initial abundances represent typical levels that occur in nature (Weisse *et al.*, 1990). Note, a range of initial concentrations of ciliate and prey, similar to those found in nature, produce cycles over 5–20 days (data not shown); we chose the above single set of initial levels as realistic examples, which is in concordance with the aims of our analysis. However, to illustrate the robustness of our analysis, we also assessed and present the impact of varying both initial flagellate (200–8×10^3 mL^{-1}) and ciliate (1–100 mL^{-1}) abundances on the respective total production over the 20-day simulation. All simulations were run for temperatures ranging from 8 to 30 °C, a range over which the prey and ciliate might be found (e.g. Foissner *et al.*, 1999).

Results

Phytoplankton (prey) response to temperature

Specific growth rate of *Cryptomonas* sp. increased from its lower temperature limit (cells did not survive at <8 °C; data not shown) to a maximum at ~20 °C and then subsequently decreased (Fig. 1a). A response was fit to the specific growth data following Eqn (4), where in this case R is prey-specific growth rate (μ_p, day^{-1}) (Table 1). Prey volume decreased linearly with temperature (Fig. 1b, Table 1).

Ciliate response to prey and temperature

Ciliate ingestion rate increased with increasing prey concentration; it also increased with increasing temperature to a maximum at ~22 °C and then decreased (Fig. 2a). A response was fit to the ingestion data following Eqn (5) (Table 2). Ciliate-specific growth rate increased with both increasing prey concentration and temperature (Fig. 2b). A response was fit to the growth data following Eqn (6) (Table 2). Ciliate volume increased with increasing prey concentration; it first increased with increasing temperature to a maximum at ~10–12 °C and then decreased (Fig. 2c). A response was fit to the volume data following Eqn (7) (Table 2).

Table 1 Parameters, error estimates (1 standard error, SE), adjusted R^2 for the specific growth (μ_p, day^{-1}) [Eqn (4)], and volume (V, μm^3) responses ($V = yT + z$) for *Cryptomonas* sp. to temperature (T, °C)

Parameters	Value	Units	SE	Adjusted R^2
Specific growth rate				
g	46.0	day	11.4	0.96
h	4.46	day $C^{\circ -1}$	1.13	
i	0.11	day $C^{\circ -2}$	0.28	
Volume				
y	−20.3	μm^3 $C^{\circ -1}$	4.87	0.60
z	926	μm^3	91.7	

The impact of temperature change on population dynamics and carbon flux

For the flagellate–ciliate simulations without top-down control by *Daphnia*, there was one prey and one predator peak over almost the entire range of temperatures examined (Fig. 3). An example, at 20 °C, illustrates the change in biomass of prey and predator, over time (Fig. 3a). A synthesis of the entire set of simulations is presented as predator and prey density plots, to indicate population dynamics over time, across the examined temperature range (Fig. 3b and c). Simulations indicated that the prey populations increased over several days, always peaked before that of the predator and then rapidly decreased, as they were grazed by the growing predator population. The predator population increased rapidly, once prey were abundant, and then decreased more gradually than that of the prey, as the former died due to starvation; this decrease became more rapid at higher temperatures, reflecting higher mortality rates at low prey concentrations and higher temperatures (Fig. 2b). Finally, at high and low temperatures, pulses were not pronounced and occurred near the end of the 20-day simulation, while at 20 °C the pulses reached the highest numbers (cf. Fig. 3a) and occurred early, between days 4 and 7 (Fig. 3a–c).

The biomass produced by the prey and predator (ciliate) (Fig. 3d and e) equates to the sequestered carbon from atmospheric CO_2, through primary production of the prey and its transfer to the consumer, the predator. Production of both predator and prey was greatest when simulations were initiated with few predators and prey (Fig. 4); in these cases reduced grazing pressure initially allowed the prey population to rise, but then there was a subsequent bloom of the ciliates, resulting in high production of both (population cycle, data not shown). In all cases, carbon production peaked at or near 20 °C and rapidly decreased above and below this maximum (Figs 3 and 4); this consistency of the distribution of this measurement of production illustrate the robustness of the model output over a range of prey and ciliate levels (Fig. 4). Differences between minimum and maximum production were on the order of 5–10-fold, for both prey and predator (Fig. 3d and e).

Table 2 Parameters, error estimates (1 standard error, SE), adjusted R^2 for *Urotricha farcta* ingestion rate (I_c, prey predator^{-1} h^{-1}) [Eqn (5)], specific growth rate (μ_c, day^{-1}) [Eqn (6)], and volume (V, μm^3) [Eqn (7)] response to changing prey (*Cryptomonas* sp.) and temperature

Parameters	Value	Units	SE	Adjusted R^2
Ingestion rate [Eqn (5)]				
j		prey predator^{-1} h^{-1}		0.90
	6.04×10^{-5}		4.06×10^{-6}	
k				
	1.68×10^{-4}		2.13×10^{-5}	
l		C$^{\circ -1}$		
	1.55×10^{-5}		2.05×10^{-6}	
m		C$^{\circ -2}$		
	3.77×10^{-7}		5.10×10^{-8}	
Specific growth rate [Eqn (6)]				
n		day^{-1}		0.71
	8.04×10^{-5}		1.02×10^{-5}	
P'		prey mL^{-1}		
	2.92×10^{2}		6.20×10	
o				
	1.77×10^{-4}		4.65×10^{-5}	
q		C$^{\circ -1}$		
	1.31×10^{-5}		4.27×10^{-6}	
r		C$^{\circ -2}$		
	2.76×10^{-7}		1.03×10^{-7}	
Volume [Eqn (7)]				
u		μm^3		0.77
	2.89×10^{-1}		5.37×10^{-2}	
V'		μm^3		
	1.92×10^{3}		1.36×10^{2}	
v				
	7.01×10^{-4}		2.00×10^{-4}	
w		C$^{\circ -1}$		
	-1.14×10^{-4}		2.42×10^{-5}	
x		C$^{\circ -2}$		
	4.89×10^{-6}		1.01×10^{-6}	

When *Daphnia* were introduced to the system, there is a clear indication of its grazing impact, but ciliate–phytoplankton pulses still occur over a limited range of temperatures (Fig. 5a–c), following patterns described above, indicating that the direct microbial link can remain active, even when a higher level predator exists, at typical levels. Maximum flagellate and ciliate production (at ~20 °C) over the 20-day period was altered compared with when *Daphnia* was absent, but not to a great extent; however, there was a pronounced effects of temperature on production at the upper and lower limits of the range (cf Figs 3b, c and 5b, c). The amount of carbon transferred to *Daphnia*, by grazing, was also influenced by temperature (Fig. 5g and h), indicating that temperature change could have larger scale impacts on more complex food web dynamics.

Discussion

Temperature response functions

There is a continuing need to parameterize pelagic ecosystem models (Anderson, 2005), especially components of the microbial food web, which can be pivotal in terms of freshwater pelagic carbon flux (Weisse *et al.*, 1990; Straile, 1998; Zingel *et al.*, 2007). Food levels, grazing pressures, and growth rates have typically been considered to be the primary influencing factors in planktonic ecosystem dynamics, and the last 20 years have seen a focus on establishing functional and numerical responses for protozooplankton species (e.g. Jonsson, 1986; Montagnes, 1996; Jürgens & Šimek, 2000; Gismervik, 2005), using methods and approaches similar to ours. However, with the recognition that

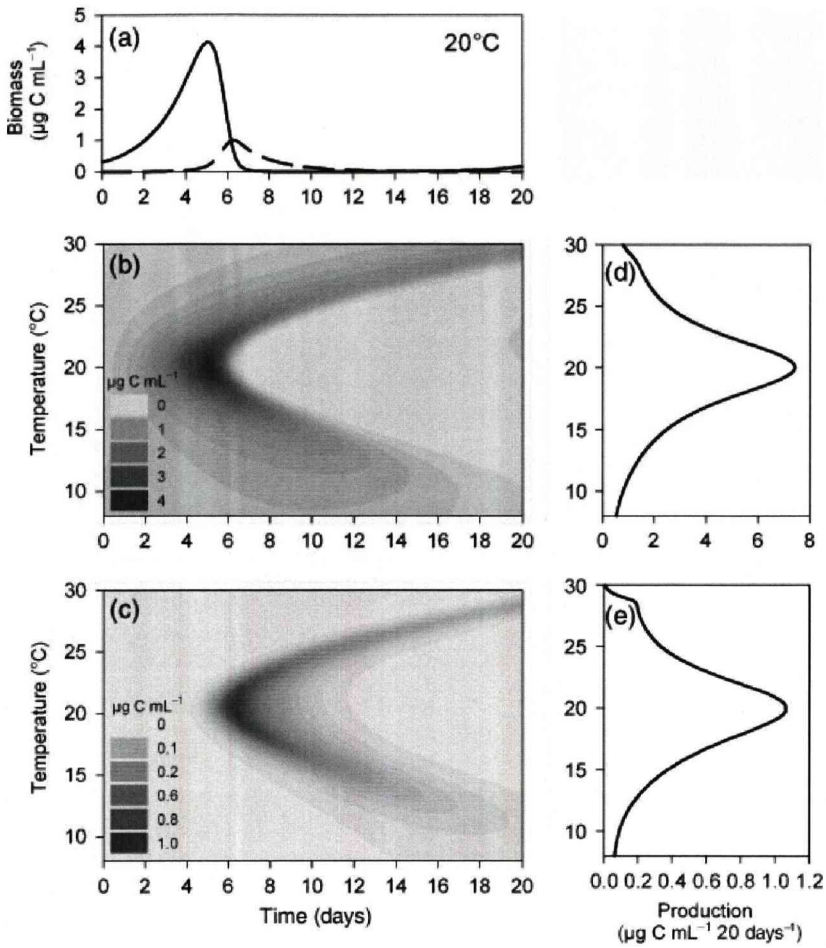

Fig. 3 Results from the model of predator (*Urotricha farcta*) and prey (*Cryptomonas* sp.) population dynamics over 20 days (see 'Materials and methods' for details of the model). Predator and prey are presented as $\mu g\,C\,mL^{-1}$. (a) An indication of the population dynamics over 20 days at one discrete temperature: 20 °C; prey (solid line), predator (dashed line). (b, c) Density plots of prey and predator population dynamics, respectively, at temperatures ranging from 8 to 30 °C, over 20 days. (d, e) An indication of the carbon produced by the prey and predator, respectively, over the 20 days; note this represents the total amount made, regardless of its fate.

climate change will both increase ambient temperature and change the intensity and frequency of warming events, there has been a commensurate effort to consider temperature responses in models of protozoan feeding and growth. Generally, the approach has been to impose a thermal function on existing protozoan rate processes (e.g. a simple or modified Q_{10} function; Blackford *et al.*, 2004), but this simplistic approach is likely inappropriate (e.g. Montagnes *et al.*, 2003; Kimmance *et al.*, 2006). The present study provides, to our knowledge, the first indication of how more complex, empirically derived temperature relationships can alter short-term carbon flux, influenced by predator–prey dynamics, within the freshwater microbial food web.

Our responses [Eqns (4)–(7), Tables 1 and 2] are based on a combination of mechanistic and phenomenological equations. There is good indication that functional [Eqn (1)] and numerical [Eqn (2)] responses are at least semimechanistic (Holling, 1959; Fenchel, 1986). In contrast, the quadratic function [Eqn (4)] employed by Flinn (1991) is a phenomenological model. We have compared this model to a number of mechanistic and phenomenological models using information theory (Burnham & Anderson, 2002), and it has proven consistently to be one of the best to describe thermal responses (Appendix A). We recognize that more complex, mechanistic functions may explain temperature responses (e.g. Schoolfield *et al.*, 1981), but to provide simple, predictive functions for modelling, we have followed the approach of others (e.g. Flinn & Hagstrum, 2002; Kimmance *et al.*, 2006) to combine mechanistic and phenomenological functions, to yield parsimonious equations.

 Global Change Biology, doi: 10.1111/j.1365-2486.2008.01700.x

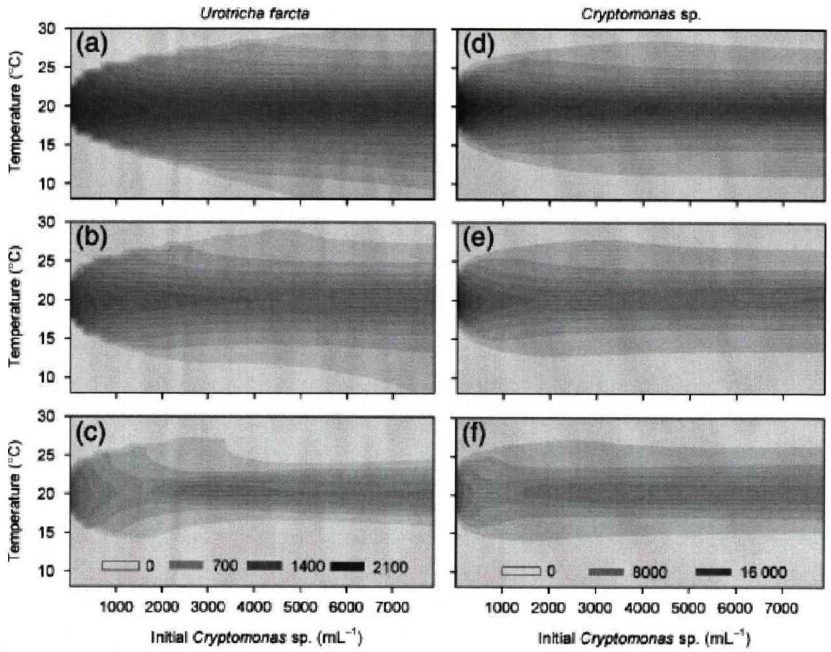

Fig. 4 The influence of initial ciliate and prey abundance on carbon production over a 20-day simulation, at temperatures ranging from 8 to 30 °C. (a–c) *Urotricha farcta* production; (d–f) *Cryptomonas* sp. production. Parts (a, d) were initiated with 1 *U. farcta* mL^{-1}; parts (b, d) were initiated with 10 *U. farcta* mL^{-1}; parts (c, f) were initiated with 100 *U. farcta* mL^{-1}. Values denoted by shading in bottom panels apply to all above panels and are in units of $\mu g\,C\,mL^{-1}\,20\,day^{-1}$.

Our main alteration to the model of Flinn & Hagstrum (2002) was to impose a temperature dependency on the threshold concentration [P'; Eqn (6)]; P' represents the prey concentration where sufficient food is available to allow the predator population to survive but not increase or decrease (Montagnes, 1996). The value of this parameter typically increases with temperature (Weisse *et al.*, 2002 and references within; Kimmance *et al.*, 2006), presumably as increased temperature raises metabolic needs. Including this modification provided a better fit to the data than responses that lacked the interaction (data not shown). We suggest that our response equations [Eqns (5)–(7)], if not their specific parameters (Tables 1 and 2), are a good method of assessing the protozoan contribution to carbon flux in models that examine thermal impacts; we illustrate this below.

How might temperature alter population dynamics and carbon flux?

Using a specific example, we indicate that temperature changes of 2–10 °C can impact protistan population dynamics and carbon flux (Figs 3–5). Assuming that ambient temperatures in temperate freshwaters is generally <20 °C, the model suggests that a rise towards 20 °C would increase the magnitude and occurrence of predator–prey pulses. Such increases in temperature on the order of 5 °C are not uncommon in small ~3000 L, temperate water bodies (see Mckee *et al.*, 2000), but as indicated above, climate change is predicted to increase the prevalence and the severity of these fluctuations (Carpenter *et al.*, 1992). The ensuing increase in pulses of ciliates and prey may then alter food web dynamics on a larger scale. However, because of their brief nature and likely local occurrence, it is, and will be, difficult to observe short-term pulses in routine sampling programs, and this may be why they are rarely carefully considered.

Our model output is, however, comparable to *in vitro* incubations: using the same taxa as we have examined, Weisse *et al.* (2001) presented time series data for predator–prey abundances, at 15 and 20 °C, over ~20 days; their data exhibit distinct predator–prey pulses over 10–15 days, which occurred earlier at the warmer temperature, supporting our arguments for the importance of this short-term phenomenon and the influence of temperature on the dynamics. A second approach to assess if predator–prey pulses occur is to regularly monitor communities in microcosms (i.e. large tanks populated with seminatural assemblages, simulating *in situ* conditions; e.g. McKee *et al.*, 2000). Although there have been several such studies to examine the impact of global warming on freshwater pelagic

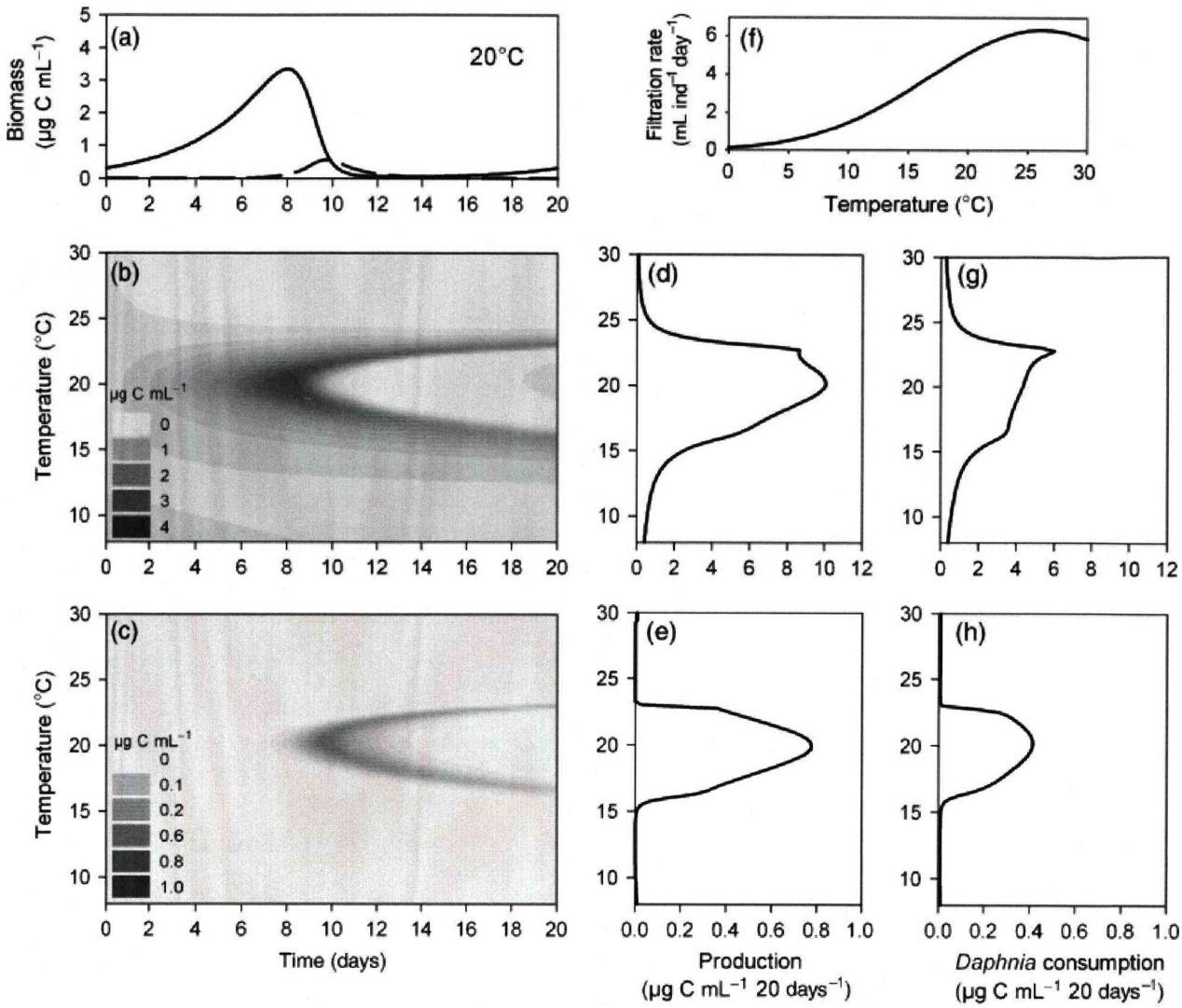

Fig. 5 Results from the model of predator (*Urotricha farcta*) and prey (*Cryptomonas* sp.) population dynamics over 20 days with the addition of *Daphnia* as a grazer (see 'Materials and methods' for details of the model). Predator and prey are presented as $\mu g\,C\,mL^{-1}$. (a) An indication of the population dynamics over 20 days at one discrete temperature: 20 °C; prey (solid line), predator (dashed line). (b, c) Density plots of prey and predator population dynamics, respectively, at temperatures ranging from 8 to 30 °C, over 20 days. (d, e) An indication of the carbon produced by the prey and predator, respectively, over the 20 days; note this represents the total amount made, regardless of its fate. (f) An illustration of the response of *Daphnia* filtration rate to changing temperature (see 'Materials and methods' for details of this response). (g, h) An indication of the prey and predator carbon, respectively, consumed by the upper level grazer, *Daphnia*, over the 20 days; note this represents the total amount grazed, regardless of its fate.

ecosystems (tanks maintained 3–5 °C above ambient levels; e.g. McKee *et al.*, 2002; Strecker *et al.*, 2004; Christoffersen *et al.*, 2006), to our knowledge only one has focused on protozooplankton, and specifically ciliates (Montagnes *et al.*, 2002; Wilson, 2002); in this study, there was an increased occurrence of ciliate species blooming when temperatures were raised 3 °C above ambient levels, and fish were included to remove crustacean grazers. Similarly, but less apparent, blooms of *Urotricha* spp. and other small ciliates occur in field observations (e.g. in Lake Constance in the summer when crustaceans, such as *Daphnia*, are not abundant; Müller *et al.*, 1991). These laboratory, microcosm, and field data suggest that our modelled predator–prey pulses, although difficult to observe, may be common in nature and suggest that warming may increase such pulses, increasing carbon flux through populations within the microbial food web. However, it is also instructive to note that we predict, in our specific case, an increase in temperature (>20 °C) will reduce the magnitude and period of the predator–prey dynamics and carbon flux.

 Global Change Biology, doi: 10.1111/j.1365-2486.2008.01700.x

Rarely, however, do simple predator–prey models, such as ours, accurately predict *in situ* or *in vitro* population dynamics, and this is not necessarily their intention, rather it is to explore and test hypotheses (see Turchin, 2003). A combination of uncharacterized stochasticity, under-parameterization of responses, and omission of deterministic variables can be attributed to the cause of the mismatch (Turchin, 2003). However, it is well accepted that although such models are rarely explicitly predictive, they reveal qualitative effects (e.g. Shertzer *et al.*, 2002; Fulton *et al.*, 2003). Thus, we propose that our fundamental premise that small, episodic, temperature changes, induced by climate change, will upset food web dynamics in an unexpected manner is well supported by our model results, and our analysis of production (Fig. 4) reveals that our predictions are robustly supported over a range of predator and prey levels. Furthermore, the analysis suggests that our responses [Eqns (5)–(7)] should provide researchers with data to further parameterize temperature effects on ciliates in existing pelagic ecosystem models. Possibly of greater impact though is our illustration that predators and prey will often have different thermal sensitivities, and these produce unintuitive, nonlinear results (May, 1986). Recently, it has been argued that planktonic autotrophs are less sensitive to temperature than planktonic heterotrophs (Rose & Caron, 2007), but our data suggest that the change in dynamics above and below ~20 °C are at least in part due to the rapid positive and negative autotrophic-prey response near 20 °C (Fig. 1), suggesting that in this case the thermal sensitivity of *Cryptomonas* sp. is driving the strong patterns in the system. These findings emphasize the more general recognition that different temperature dependencies of autotrophy and heterotrophy may significantly decouple existing plankton dynamics on local and global scales (e.g. López-Urrutia *et al.*, 2006).

Application, integration, and extension of this work

There are some caveats to our conclusions that are worth noting. First, our temperature responses (Fig. 2) are for genera that are ubiquitous in temperate freshwaters, but *U. farcta* strains can have different thermal sensitivities, as do different species within the genus *Urotricha* (Weisse & Montagnes, 1998). This is not surprizing, as regional adaptations of taxa to a variety of environmental variables, including temperature should be expected (e.g. Mitchell & Lampert, 2000) and was recently demonstrated for freshwater ciliates (Gächter & Weisse, 2006). Still, meta-analyses regarding protistan growth and volume responses to temperature (e.g. Atkinson *et al.*, 2003; Montagnes *et al.*, 2003; Bissinger *et al.*, 2008) suggest predictable similarities across taxa, and aggregation of species into functional groups is advocated for large-scale ecosystem models (Fulton *et al.*, 2003). Thus, although the specifics of our model output might not be repeated, the trends of population pulses and carbon flow might be similar, regardless of the taxa; as a case in point, our own study on a marine, heterotrophic flagellate supports our arguments for the temperature sensitivity of population dynamics (Kimmance *et al.*, 2006). Second, like most ecophysiological responses, our discrete measurements (i.e. points on Figs 1 and 2) were determined under constant temperatures. In shallow freshwater environments, ambient temperature will not be constant, possibly fluctuating hourly or daily by several degrees, and fluctuating ambient temperatures (on a daily regime) can alter *Urotricha* growth rates (both up or down) compared with constant temperatures (Montagnes & Weisse, 2000); such transient behaviour requires further parameterization before it is incorporated into models. These concerns, however, do not invalidate our parsimonious approach towards examining trends (which reflects that of most ecosystem and many population models) or the potential applicability of the responses provided, but they do indicate that a further degree of sensitivity analysis, related to the temperature optima of taxa and their response to fluctuating temperatures, would be appropriate in more complex modelling efforts.

Given the limitations of the study, how then does the model predict general patterns of carbon uptake and sequestration? At 20 °C, the phytoplankton prey produce ~7 $\mu g C mL^{-1}$ over 20 days (Fig. 3). However, some of this production is transferred to the ciliate, little of it remains phytoplankton biomass, and by the end of the 20 days, in virtually all cases, the ciliate standing-stock biomass is negligible (i.e. almost all ciliates die), indicating that this biomass is not sequestered; similar responses occur when the upper-level grazer, *Daphnia*, is added. Likely, this small protozoan, which has no hard parts, if not grazed, would die, rupture, and become part of the dissolved organic carbon pool; the biomass would then cycle through the microbial loop (Azam *et al.*, 1983; Montagnes, 1996). Consequently, little to none of the carbon would be sequestered on a seasonal or longer scale (e.g. in sediment), as might be the case when crustacean predators are present (see Flanagan *et al.*, 2006). Recognizing, and incorporating, this potential source of recycling will undoubtedly alter estimates of carbon sequestering in freshwater models; that is, the impact of short-term protozoa–phytoplankton pulses could potentially substantially reduce estimates of freshwater carbon sequestration.

The first scenario we have modelled (Fig. 3) may occur in freshwaters, when upper level zooplankton consumers are not abundant (e.g. when *Daphnia* are

consumed by fish; McKee *et al.*, 2002). However, when the keystone grazer *Daphnia* is present, it effectively consumes ciliates and their prey (Jürgens, 1994). The model also reveals a clear impact of *Daphnia* grazing on the system, but pronounced ciliate–phytoplankton pulses still occur over a range of temperatures (Fig. 5b and c), suggesting that the direct microbial link may remain active. Support for this conclusion was recently provided by a long-term data analysis from the spring to the clear-water phase development in Lake Constance (Tirok & Gaedke, 2006): although ciliates remained the most important algal grazers in spring, *Daphnia* benefited from increased temperature by 1–2 °C, substantially enhancing their grazing on small, prey such as *Cryptomonas* spp.

In our model, production over the 20-day period is also altered when *Daphnia* are added, but there is a more pronounced effect of temperature on the change in production (cf Figs 3b, c and 5b, c). The amount of carbon produced that is transferred to *Daphnia* is also influenced by temperature, supporting arguments that temperature change could have larger scale impacts on food web dynamics (Orcutt & Porter, 1984). We do, however, emphasize that our inclusion of *Daphnia* is based on realistic but limited information. Both prey level and temperature have nonlinear effects on *Daphnia* growth and grazing parameters (Kibby, 1971; Orcutt & Porter, 1984; Mourelatos & Lacroix, 1990; McKee, 1995; Giebelhausen & Lampert, 2001), and studies exist on interactive impacts of food and temperature on *Daphnia* feeding attributes (e.g. Orcutt & Porter, 1984; Giebelhausen & Lampert, 2001). However, none of the published functional responses provide sufficient detail to appropriately parameterize models (i.e. produce functions similar to those illustrated in Fig. 2a–c). These past works have focused on a few discrete temperatures and prey concentrations, replicating to test for treatment effects. We have taken a different approach in this work and others (e.g. Montagnes *et al.*, 2001; Kimmance *et al.*, 2006): to rigorously establish nonlinear responses appropriate for application in models, focus must be placed on spreading measurements along the independent variable(s), rather than replicating discrete treatments (Montagnes & Berges, 2004); this approach provides key information on the shape of responses. Given the importance of *Daphnia* in freshwater food webs, we propose that future work focuses on carefully parameterizing such temperature–prey responses.

Acknowledgements

This research was partially supported by a travel grant from the Royal Society awarded to DJSM and by a NERC studentship awarded to DJSM and DA for JB.

References

Anderson TR (2005) Plankton functional type modelling: running before we can walk? *Journal of Plankton Research*, **27**, 1073–1081.

Atkinson D, Ciotti BJ, Montagnes DJS (2003) Protists decrease in size linearly with temperature: ca. 2.5 °C^{-1}. *Proceedings of the Royal Society B*, **270**, 2605–2611.

Azam F, Fenchel T, Field JG, Gray JS, Meyer-Reil LA, Thingstad F (1983) The ecological role of water-column microbes in the sea. *Marine Ecology Progress Series*, **10**, 257–263.

Berges JA, Montagnes DJS, Hurd CL, Harrison PJ (1994) Fitting ecological and physiological data to rectangular hyperbolae: a comparison of methods using Monte Carlo simulations. *Marine Ecology Progress Series*, **114**, 175–183.

Bissinger JE, Montagnes DJS, Sharples J, Atkinson D (2008) Predicting marine phytoplankton maximum growth rates from temperature: improving on the Eppley curve using quantile regression. *Limnology and Oceanography*, **53**, 487–493.

Blackford JC, Allen JI, Gilbert FJ (2004) Ecosystem dynamics at six contrasting sites: a generic modelling study. *Journal of Marine Systems*, **52**, 191–215.

Burnham KP, Anderson DR (2002) *Model Selection and Multimodel Inference: A Practical Information-Theoretic Approach*. Springer, New York.

Carpenter SR, Fisher SG, Grimm NB, Kitchell JF (1992) Global change and freshwater ecosystems. *Annual Review of Ecology and Systematics*, **23**, 119–139.

Christoffersen K, Andersen N, Søndergaard M, Liboriussen L, Jeppesen E (2006) Implications of climate-enforced temperature increases on freshwater pico- and nanoplankton populations studied in artificial ponds during 16 months. *Hydrobiologia*, **560**, 259–266.

Davidson K (1996) Modelling microbial food webs. *Marine Ecology Progress Series*, **145**, 279–296.

Dokulil M (1988) Seasonal and spatial distribution of cryptophycean species in the deep, stratifying, alpine lake Mondsee and their role in the food web. *Hydrobiologia*, **161**, 185–201.

Downing JA, Prairie Y, Cole JJ *et al.* (2006) The global abundance and size distribution of lakes, ponds, and impoundments. *Limnology and Oceanography*, **51**, 2388–2397.

Fenchel T (1986) Protozoan filter feeding. In: *Progress in Protistology*, Vol. I (eds Corliss JO, Patterson DJ), pp. 65–113. Biopress, Bristol.

Flanagan KM, McCauley E, Wrona F (2006) Freshwater food webs control carbon dioxide saturation through sedimentation. *Global Change Biology*, **12**, 644–651.

Flinn PW (1991) Temperature-dependent functional response of the parasitoid *Cephalonomia waterstoni* (Gahan) (Hymenoptera: Bethylidae) attacking rusty grain beetle larvae (Coleoptera: Cucujidae). *Environmental Entomology*, **20**, 872–876.

Flinn PW, Hagstrum DW (2002) Temperature-mediated functional response of *Theocolax elegans* (Hymenoptera: Pteromalidae) parasitizing *Rhyzopertha dominica* (Coleoptera: Bostrichidae) in stored wheat. *Journal of Stored Product Research*, **38**, 185–190.

Foissner W, Berger H, Schaumburg J (1999) *Identification and ecology of limnetic plankton ciliates*. Informationsberichte des

Bayerischen Landesamtes für Wasserwirtschaft 3/99. Bayerisches Landesamt für Wasserwirtschaft.

Frost BW (1972) Effects of size and concentration of food particles on the feeding behavior of the marine planktonic copepod *Calanus pacificus*. *Limnology and Oceanography*, **17**, 805–815.

Fulton EA, Smith ADM, Johnson CR (2003) Effect of complexity on marine ecosystem models. *Marine Ecology Progress Series*, **253**, 1–16.

Gächter E, Weisse T (2006) Local adaptation among geographically distant clones of the cosmopolitan freshwater ciliate *Meseres corlissi*. I. Temperature response. *Aquatic Microbial Ecology*, **45**, 291–300.

Gerten D, Adrian R (2000) Climate-driven changes in spring plankton dynamics and the sensitivity of shallow polymictic lakes to the North Atlantic Oscillation. *Limnology and Oceanography*, **45**, 1058–1066.

Giebelhausen B, Lampert W (2001) Temperature reaction norms of *Daphnia magna*: the effect of food concentration. *Freshwater Biology*, **46**, 281–289.

Gilbert JJ (1988) Suppression of rotifer populations by *Daphna*: a review of the evidence, the mechanisms, and the effects on zooplankton community structure. *Limnology and Oceanography*, **33**, 1286–1303.

Gismervik I (2005) Numerical and functional responses of choreo- and oligotrich planktonic ciliates. *Aquatic Microbial Ecology*, **40**, 163–173.

Gliwicz ZM (2003) Zooplankton. In: *The Lakes Handbook – Limnology and Limnetic Ecology*, Vol. I (eds O'Sullivan PE, Reynolds CS), pp. 417–460. Blackwell Science Ltd, Malden, MA.

Guillard RL, Lorenzen CJ (1972) Yellow-green algae with chlorophyllide c. *Journal of Phycology*, **8**, 10–14.

Holling CS (1959) The components of predation as revealed by a study of small mammal predation of the European pine sawfly. *Canadian Entomologist*, **91**, 293–320.

Houghton J (2005) Global warming. *Reports on Progresses in Physics*, **68**, 1343–1403.

Jerome CA, Montagnes DJS, Taylor FJR (1993) The effect of the quantitative protargol stain and Lugol's and Bouin's fixatives on cell size: a more accurate estimate of ciliate species biomass. *Journal of Eukaryotic Microbiology*, **40**, 254–259.

Jonsson PR (1986) Particle size selection, feeding rates and growth dynamics of marine planktonic oligotrichous ciliates (Ciliophora: Oligotrichina). *Marine Ecology Progress Series*, **33**, 265–277.

Jürgens K (1994) Impact of *Daphnia* on planktonic microbial food webs – a review. *Marine Microbial Food Webs*, **8**, 295–324.

Jürgens K, Šimek K (2000) Functional response and particle size selection of *Halteria* cf. *grandinella*, a common freshwater oligotrichous ciliate. *Aquatic Microbial Ecology*, **22**, 57–68.

Kibby HV (1971) Effect of temperature on the feeding behaviour of *Daphnia rosa*. *Limnology and Oceanography*, **16**, 580–581.

Kimmance S, Atkinson D, Montagnes D (2006) Do temperature–food interactions matter? Responses of production and its components in the model heterotrophic flagellate *Oxyrrhis marina*. *Aquatic Microbial Ecology*, **42**, 63–73.

Lindström ES, Weisse T, Stadler P (2002) Enumeration of small ciliates in culture by flow cytometry and nucleic acid staining. *Journal of Microbial Methods*, **49**, 173–182.

López-Urrutia Á, Martin E, Harris RP, Irigoien W (2006) Scaling the metabolic balance of the oceans. *Proceedings of the National Academy of Science of the United States of America*, **103**, 8739–8744.

May RM (1986) When two and two do not make four: nonlinear phenomena in ecology. *Proceedings of the Royal Society London B*, **228**, 241–266.

McKee D (1995) Long-term temperature acclimation in *Daphnia magna*: effect on filtration rates. *Journal of Plankton Research*, **17**, 1095–1103.

McKee D, Atkinson D, Collings S *et al.* (2000) Heated aquatic microcosms for climate change experiments. *Freshwater Forum*, **14**, 51–58.

McKee D, Atkinson D, Collings S *et al.* (2002) Macro-zooplankter responses to simulated climate warming in experimental freshwater microcosms. *Freshwater Biology*, **47**, 1–14.

Menden-Deuer S, Lessard EJ (2000) Carbon to volume relationships for dinoflagellates, diatoms, and other protist plankton. *Limnology and Oceanography*, **45**, 569–579.

Menon A, Flinn PW, Dover BA (2002) Influence of temperature on the functional response of *Anisopteromalus calandrae* (Hymenoptera: Pteromalidae) parasitoid of *Rhyzopertha dominica* (Coleopteran: Bostrichidae). *Journal of Stored Product Research*, **38**, 463–469.

Mitchell SE, Lampert W (2000) Temperature adaptation in a geographically widespread zooplankter, *Daphnia magna*. *Journal of Evolutionary Biology*, **13**, 371–382.

Montagnes DJS (1996) Growth responses of planktonic ciliates in the genera *Strobilidium* and *Strombidium*. *Marine Ecology Progress Series*, **130**, 241–254.

Montagnes DJS, Berges JA (2004) Determining parameters of the numerical response. *Microbial Ecology*, **48**, 139–144.

Montagnes DJS, Kimmance SA, Atkinson D (2003) Using Q_{10}: can growth rates increase linearly with temperature? *Aquatic Microbial Ecology*, **32**, 307–313.

Montagnes DJS, Kimmance SA, Tsonunis G, Gumbs JC (2001) Combined effect of temperature and food concentration on the grazing rate of the rotifer *Brachionus plicatilis*. *Marine Biology*, **139**, 975–979.

Montagnes DJS, Kimmance SA, Wilson D (2002) *Effects of global and local temperature changes on free living, aquatic protists*. Conference Proceedings of the 14th International Conference on Comparative Physiology, Climate Changes: Effects on Plants, Animals, and Humans (eds Bolis CL, Keines R, Elia M *et al.*). Available on CD ROM (from the senior author).

Montagnes DJS, Lessard EJ (1999) Population dynamics of the marine planktonic ciliate *Strombidinopsis multiauris*: its potential to control phytoplankton blooms. *Aquatic Microbial Ecology*, **20**, 167–181.

Montagnes DJS, Weisse T (2000) Fluctuating temperatures affect growth and production rates of planktonic ciliates. *Aquatic Microbial Ecology*, **21**, 97–102.

Moss B (1998) *Ecology of Fresh Waters, Man and Medium, Past and Present* (pp. 572). Blackwell: Oxford, UK.

Mourelatos S, Lacroix G (1990) In situ filtering rates of cladocera: effect of body length, temperature, and food concentration. *Limnology and Oceanography*, **35**, 1101–1111.

Müller H, Geller W (1993) Maximum growth rates of aquatic ciliated protozoa: the dependence on body size and temperature reconsidered. *Archiv für Hydrobiologie*, **126**, 315–327.

Müller H, Schlegel A (1999) Responses of three freshwater planktonic ciliates with different feeding modes to cryptophyte and diatom prey. *Aquatic Microbial Ecology*, **17**, 49–60.

Müller H, Schöne A, Pinto-Coelho RM, Schweizer A, Weisse T (1991) Seasonal succession of ciliates in Lake Constance. *Microbial Ecology*, **21**, 119–138.

Orcutt JD, Porter KJ (1984) The synergistic effects of temperature and food concentration on life history parameters of *Daphnia*. *Oecologia*, **63**, 300–306.

O'Sullivan PE, Reynolds CS (2003) *The Lakes Handbook – Limnology and Limnetic Ecology*, Vol. 1 and 2. Blackwell Science Ltd, Malden, MA.

Pedrós-Alió C, Massana R, Latasa M, Garci-Cantizano J, Gasol JM (1995) Predation by ciliates on a metalimnic *Cryptomonas* population: feeding rates, impact and effects of vertical migration. *Journal of Plankton Research*, **17**, 2131–2154.

Porter KG, Paerl H, Hodson R, Pace M, Priscu J, Riemann B, Scavia D, Stockner J (1988) Microbial interactions in lake food webs. In: *Complex Interactions in Lake Communities* (ed. Carpenter SR), pp. 209–227. Springer-Verlag, New York.

Reynolds CS (2003) Lakes, limnology and limnetic ecology: towards a new synthesis. In: *The Lakes Handbook – Limnology and Limnetic Ecology*, Vol. 1 (eds O'Sullivan PE, Reynolds CS), pp. 1–7. Blackwell Science Ltd, Malden, MA.

Riemann B, Christoffersen K (1993) Microbial trophodynamics in temperate lakes. *Marine Microbial Food Webs*, **7**, 69–100.

Rose JM, Caron DA (2007) Does low temperature constrain the growth rates of heterotrophic protists? Evidence and implications for algal blooms in cold waters. *Limnology and Oceanography*, **52**, 886–895.

Schindler DW (1978) Factors regulating phytoplankton production and standing crop in the world's freshwaters. *Limnology and Oceanography*, **23**, 478–486.

Schoolfield RM, Sharpe PJ, Magnuson CE (1981) Non-linear regression of biological temperature-dependent rate models based on absolute reaction-rate theory. *Journal of Theoretical Biology*, **88**, 719–731.

Shertzer KW, Ellner SP, Fussmann GF, Hairston NG Jr (2002) Predator–prey cycles in an aquatic microcosm: testing hypotheses of mechanisms. *Journal of Animal Ecology*, **71**, 802–815.

Sommer U (1986) The periodicity of phytoplankton in Lake Constance (Bodensee) in comparison to other deep lakes in central Europe. *Hydrobiologia*, **138**, 1–7.

Straile D (1998) Biomass allocation and carbon flow in the pelagic food web of Lake Constance. *Archiv für Hydrobiologie, Special Issues Advances in Limnology*, **53**, 545–563.

Strecker AL, Cobb TP, Vinebrooke RD (2004) Effects of experimental greenhouse warming on phytoplankton and zooplankton communities in fishless alpine ponds. *Limnology and Oceanography*, **49**, 1182–1190.

Tirok K, Gaedke U (2006) Spring weather determines the relative importance of ciliates, rotifers and crustaceans for the initiation of the clear-water phase in a large, deep lake. *Journal of Plankton Research*, **28**, 361–373.

Turchin P (2003) *Complex Population Dynamics: A Theoretical Empirical Synthesis*. Princeton University Press, Princeton.

Weisse T (2003) Pelagic microbes – Protozoa and the microbial food web. In: *The Lakes Handbook – Limnology and Limnetic Ecology*, Vol. 1 (eds O'Sullivan PE, Reynolds CS), pp. 417–460. Blackwell Science Ltd, Malden, MA.

Weisse T (2006) Freshwater ciliates as ecophysiological model organisms – lessons from *Daphnia*, major achievements, and future perspectives. *Archiv für Hydrobiologie*, **167**, 371–402.

Weisse T, Karstens N, Meyer VCM, Janke L, Lettner S, Teichgräber K (2001) Niche separation in common prostome freshwater ciliates: the effect of food and temperature. *Aquatic Microbial Ecology*, **26**, 167–179.

Weisse T, Montagnes DJS (1998) Effect of temperature on inter- and intraspecific isolates of *Urotricha* (Prostomatida, Ciliophora). *Aquatic Microbial Ecology*, **15**, 285–291.

Weisse T, Müller H, Pinto-Coelho RM, Schweizer A, Springmann D, Baldringer G (1990) Response of the microbial loop to the phytoplankton spring bloom in a large prealpine lake. *Limnology and Oceanography*, **35**, 781–794.

Weisse T, Stadler P, Lindström ES, Kimmance SA, Montagnes DJS (2002) Interactive effect of temperature and food concentration on growth rate: a test case using the small freshwater ciliate *Urotricha farcta*. *Limnology and Oceanography*, **47**, 1447–1455.

Wilson D (2002) *The response of ciliates to simulated global warming, simulated argicultural run-off, and fish predation: a mesocosm experimemt*. PhD thesis, University of Liverpool, 81 pp.

Zingel P, Agasild H, Nõges T, Kisand V (2007) Ciliates are the dominant grazers on pico- and nanoplankton in a shallow, naturally highly eutrophic lake. *Microbial Ecology*, **53**, 134–142.

Appendix A

Determining the most likely model to describe the growth rate of *Cryptomonas* sp. as a function of temperature: an information-theoretic approach

Seven candidate models were identified that might describe the response of *Cryptomonas* sp. growth rate to temperature (Fig. A1, Table A1). From these the most likely was selected using an information-theoretic approach (Burnham & Anderson, 2002). The major advantage of this approach, as compared with simple measures of fit, such as r^2, is that it accounts for the model's complexity, that is the number of parameters (Angilletta, 2006). The first step in this procedure is to calculate the Akaike information criterion (AIC) for each candidate model. This provides an estimate of the relative distance between the fitted model and the unknown true mechanism; the most likely model is that with the lowest AIC, relative to those in the set of models (Burnham & Anderson, 2002).

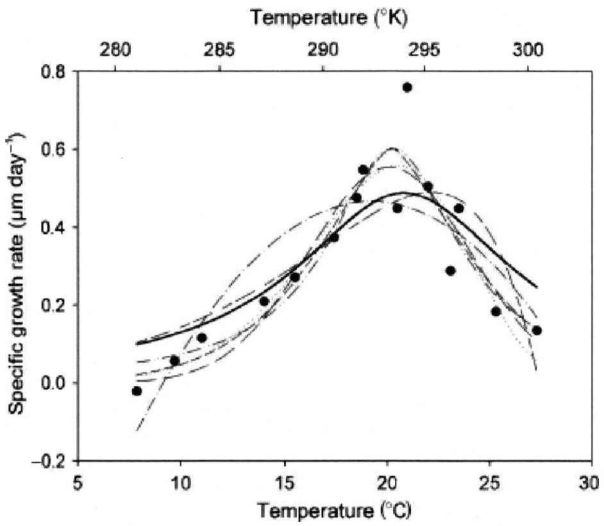

Fig. A1 Candidate models fit to *Cryptomonas* sp. growth data (see main text for details). Data points are growth rates (day^{-1}), and numbered lines are the following equations: (1) Gaussian, (2) quadratic, (3) modified Gaussian, (4) Weibull, (5) Schoolfield *et al.* (1981), (6) Hinshelwood (1947), and (7) Flinn (1991). Lines are formatted to facilitate following the path of each equation.

In this study, the candidate models (Table A1) were the four best performing thermal responses assessed by Angilletta (2006) (i.e. Gaussian, quadratic, modified Gaussian, Weibull) and three models that describe thermal rate responses of ectotherms (see Flinn, 1991; Hinshelwood, 1947; Schoolfield *et al.*, 1981). Of these models, only those presented by Schoolfield *et al.* (1981) and Hinshelwood (1947) have a mechanistic basis; the others are phenomenological.

Models were iteratively fit to response data using the Marquardt–Levenberg least squares algorithm (SIGMAPLOT), and parameters were determined. Then, using the residual sum of squares (RSS) from each fit, the maximized log-likelihood value (L) of the model [Eqn (A.1)] was determined (Burnham & Anderson, 2002); this was used to calculate the AIC_c (AIC corrected for small sample size) for each model [Eqn (A.2)]:

$$L = \log\left(\frac{RSS}{N}\right)\frac{-N}{2} \tag{A.1}$$

$$AIC_c = -2L + 2K + \frac{2K(K+1)}{N-K-1} \tag{A.2}$$

where N is the sample size and K is the number of parameters (including the error term). The Akaike weights [Eqn (A.4)] were calculated from the likelihood of each model [Eqn (A.3)], as a proportion of the total

Table A1 The candidate models used to describe the relationship between *Cryptomonas* sp. growth (μ, day^{-1}) and temperature (T, °C or K, depending on the model); italicized letters are constants

Equation/source	Function	K	AIC_c	Δ_i	w_i
Flinn (1991)	$\mu = \frac{1}{1+(a+bT+cT^2)}$	4	−65.40	0	0.61
Gaussian	$\mu = ae^{\left[-0.5\left(\frac{T-T_0}{b}\right)^2\right]}$	4	−63.43	1.97	0.23
Schoolfield *et al.* (1981)	$\mu_{(T)} = \frac{a\left(\frac{T}{293.15}\right)e^{\left[\frac{b}{R}\left(\frac{1}{293.15}-\frac{1}{T}\right)\right]}}{1+e^{\left[\frac{c}{R}\left(\frac{1}{d}-\frac{1}{T}\right)\right]}}$	5	−61.40	4.01	0.08
Modified Gaussian	$\mu = ae^{\left[-0.5\left(\frac{\lvert T-T_0\rvert}{b}\right)^c\right]}$	5	−60.36	5.05	0.05
Weibull	$\mu = a\left(\frac{d-1}{d}\right)^{1-d/d}\left[\frac{T-b}{c}+\left(\frac{d-1}{d}\right)^{1/d}\right]^{d-1} e^{-\left[\left(T-\frac{b}{c}\right)+\left(d-\frac{1}{d}\right)^{1/d}\right]^d}+\frac{d-1}{d}$	5	−59.66	5.74	0.03
Quadratic	$\mu = \mu_0 + aT + bT^2$	4	−53.61	11.8	0.00
Hinshelwood (1947)	$\mu = ae^{\left[\frac{-c}{RT}\right]} - be^{\left[\frac{-d}{RT}\right]}$	5	−47.57	17.8	0.00

AIC_c Akaike information criterion, K is the number of parameters in the model (including the error term), Δ_i is the difference between a given model's AIC_c and that of the lowest AIC_c, and w_i is the Akaike weight that is the normalized likelihood that the model is the best one in the set. In the Schoolfield *et al.* (1981) model, a is the growth rate at temperature T (K), b is the enthalpy of the activation of the reaction that is catalyzed by the limiting enzyme, c is the change in enthalpy associated with high-temperature inactivation of the limiting enzyme, d is the temperature (K) at which the enzyme is half active, and R is the universal gas constant (i.e. the Boltzmann constant, 8.617343×10^{-5} when expressed in eV). In the Hinshelwood (1947) model, a and b are the pre-exponential factors, c and d are activation energies, and R is the universal gas constant (i.e. the Boltzmann constant).

 Global Change Biology, doi: 10.1111/j.1365-2486.2008.01700.x

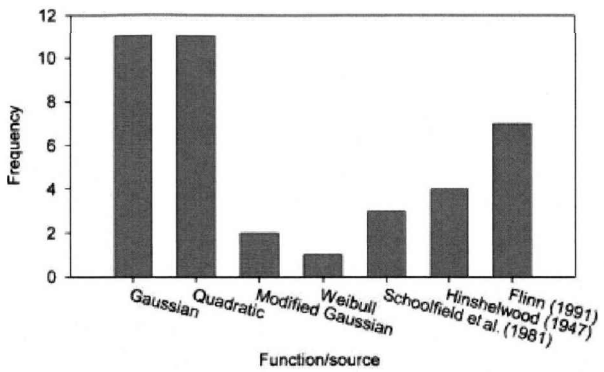

Fig. A2 The frequency that candidate functions were the best performing models when fit to 39 phytoplankton thermal response datasets.

likelihoods of all the candidate models.

$$\ell(g_i|x) \propto e\left(-\frac{1}{2}\Delta_i\right) \tag{A.3}$$

$$w_i = \frac{e\left(-\frac{1}{2}\Delta_i\right)}{\sum_{r=1}^{R} e\left(-\frac{1}{2}\Delta_r\right)} \tag{A.4}$$

where $\ell(g_i|x)$ is the likelihood of the model g_i, given the data x; Δ_i is the difference between a given model's AIC_c and that of the lowest AIC_c; and R is the set of candidate models.

Thermal response curves typically exhibit a left-sided skewness that plateaus at the optimal temperature, and then declines (e.g. as described in Montagnes *et al.*, 2003). Furthermore, the skewed portion of the response generally follows an exponential relationship (e.g. Eppley, 1972; Bissinger *et al.*, 2008). From the candidate models fitted to the *Cryptomonas* sp. data (Table A1), the quadratic model was unable to describe this initial exponential response (Fig. A1), and was therefore rejected. Of the remaining functions, the phenomenological model of Flinn (1991) had both the lowest AIC_c and highest Akaike weight. Thus, it was the most likely function of this set of models and was used to provide a predictive response in our modelling work.

A further assessment of this type of curve fitting on 39 phytoplankton thermal response datasets revealed that the Gaussian and quadratic functions were the most likely models (Fig. A2), with the Flinn (1991) function the third best performing model. However, as noted above, the quadratic function does not describe the exponential portion of the response; so for consistency we have used the Flinn (1991) function (Table A1) to structure all our temperature responses in this work on modelling the effects of temperature on protistan population dynamics.

Appendix references

Angilletta MJ (2006) Estimating and comparing thermal performance curves. *Journal of Thermal Biology*, **31**, 541–545.

Bissinger JE, Montagnes DJS, Sharples J, Atkinson D (2008) Predicting marine phytoplankton maximum growth rates from temperature: improving on the Eppley curve using quantile regression. *Limnology and Oceanography*, **53**, 487–493.

Burnham KP, Anderson DM (2002) *Model Selection and Multimodel Inference: A Practical Information-Theoretic Approach*, 2nd edn. Springer.

Eppley RW (1972) Temperature and phytoplankton growth in the sea. *Fishery Bulletin*, **70**, 1063–1085.

Flinn PW (1991) Temperature-dependent functional response of the parasitoid *Cephalonomia waterstoni* (Gahan) (Hymenoptera, Bethylidae) attacking rusty grain beetle larvae (Coleoptera, Cucujidae). *Environmental Entomology*, **20**, 872–876.

Hinshelwood CN (1947) *The Chemical Kinetics of the Bacterial Cell*. Oxford University Press.

Montagnes DJS, Kimmance SA, Atkinson D (2003) Using Q10: can growth rates increase linearly with temperature? *Aquatic Microbial Ecology*, **32**, 307–313.

Schoolfield RM, Sharpe PJH, Magnuson CE (1981) Nonlinear regression of biological temperature-dependent rate models based on absolute reaction-rate theory. *Journal of Theoretical Biology*, **88**, 719–731.

